"Medical Imaging Assisted Computational Bio-heat transfer Analysis of Magnetic Nanoparticles Induced Hyperthermia for Breast Cancer"

A

Thesis Dissertation Report

Submitted in partial fulfillment of the requirements

for the award of degree of

Master of Engineering

in

Thermal Engineering

Submitted by

Manpreet Singh

Registration No.: 801483015

Under the Supervision of

DR. S.K.MOHAPATRA (Supervisor)

(PROFESSOR & HEAD OF DEPARTMENT (M.E.),TU PATIALA)

&

DR.SANJEEV SONI(Co-Supervisor)

(SR.SCIENTIST, CSIO-CHANDIGARH)

&

DR.SATBIR SEHGAL(Co-Supervisor)

(PROFESSOR & DEAN RESEARCH, CU GHARUAN)

DEPARTMENT OF MECHANICAL ENGINEERING

THAPAR UNIVERSITY, PATIALA

(July,2014-July,2016)

CANDIDATE'S DECLARATION/CERTIFICATE

I, Manpreet Singh, do here by declare that this thesis dissertation report entitled **"Medical Imaging Assisted Computational Bio-heat transfer Analysis of magnetic nanoparticles induced hyperthermia for Breast Cancer"**, is an authentic record of my work submitted towards fulfillment of the requirements for the award of the degree of Master's **of Engineering** in **Thermal Engineering**, in **Mechanical Engineering Department of Thapar University, Patiala**, during July,2014 to July,2016. This document is entirely my own work and no part of the matter embodied in this report has been submitted to any other university or institute for the award of any degree.

Date: 12th July, 2016 **MANPREET SINGH**
Place: Patiala Postgraduate Research Scholar
ME-Thermal Engineering
Registration.No.-801483015
Thapar University, Patiala

This is to certify that above statement made by the candidate is correct and true to the best of our knowledge and belief.

DR.SATBIR SEHGAL
(Co-Supervisor)
PROFESSOR & DEAN RESEARCH
Department of Mechanical Engineering
Chandigarh University,Gharuan(Punjab)

DR.SANJEEV SONI
(Co-Supervisor)
SENIOR SCIENTIST
Department of Biomedical Instrumentation
CSIR-Central Scientific Instruments
Organisation,Sector-30C, Chandigarh

संजीव सोनी / Sanjeev Soni
वरिष्ठ वैज्ञानिक/Senior Scientist
Sector 30-C, Chandigarh

DR. SAROJ KUMAR MOHAPATRA
(Supervisor) 15/7/16
SENIOR PROFESSOR& H.O.D
Department of Mechanical Engineering,
Thapar University, Patiala (Punjab).

Countersigned by

DR. S.K. MOHAPATRA
HEAD,Mechanical Engineering, Department
Thapar University, Patiala-147004(Punjab).

PROF.S.S.BHATIA
DEAN OF ACADEMIC AFFAIRS
Thapar University, Patiala-147004(Punjab).

Dedicated to

My parents
Sh.Krishan Chand and Smt.Paramjeet Kaur,
Brother & Sister-in-law who motivated me to join the M.E. program at Thapar University, Patiala

ACKNOWLEDGEMENTS

I would like to acknowledge a number of people who, without their sincere help and support, this dissertation would have been impossible to accomplish.

First of all, I would like to express my grateful thanks and appreciation to my advisor Dr.S.K.Mohapatra and co-advisors, Dr.Satbir Sehgal and Dr.Sanjeev Soni. It is their guidance, patience, encouragement and support throughout my master's studies that helped me to emerge as a researcher andto come up with improvement over mycritical thinking abilities. The word "thanks" can even be smaller that they have accepted me as their student and ready to bestow their showers of knowledge on me to become my potential supervisors."*Research through Learning and Sharing"* is the fundamental been set into my quality traits and let me achieve beyond my expectation levels. Although I can confidently say they are my ideal supervisors.

First vote of thanks to Dr.Saroj Kumar Mohapatra who provides me wings to explore the oceans of knowledge to join CSIR-CSIO as M-tech trainee and to keep watch on my weekly work contributions.

The idea to work on medical domain program is truly a new approach for mechanical engineer like me but to formulate the problem as an important principle of thermal engineering science is credited towards my co-advisor Dr.Satbir Sehgal.

There is always a scope of opportunities that needs to be explored, and research can always be refined until the day we want to summarize. The key idea to approach towards problem and to work under such guidelines are by my co-advisor Dr.Sanjeev Soni who without his fructuous efforts and brainstorming sessions, this thesis cannot be a success. I am grateful to him to keep keen eyes on my work performance and to provide every conceptual support been required to make it feasible take the work into such heights.

I would also like to thank Dr.Tulika Singh(Department of Radiodiagnosis) and Dr.Karthik(Department of Radiodiagnosis)from PGIMER, Chandigarh who patiently took their time and gave requisite knowledge about Carcinoma and giving me insightful remarks about further refinement of current research. Data collection is one of the difficult task in medical domain related research to take appropriate permissions and to clear ethical clearance. This would have not been accomplished unless Dr. Jainy Sachdeva(Department of Electrical

Engineering,Thapar University) would put hard core efforts to complete the process of M.O.U with PGIMER, Chandigarh and Thapar University, Patiala.

I would also want to thank Dr.Harry Garg(Department of Optics,CSIR-CSIO) who gave me requisite permission to work into their lab for Comsol-Multiphysics simulation software licensed system. I am truly thankful to Mr.Negi(Doctorate student) who helped me a lot to come out from bugs,errors and for any concept refinement. I also want to thank the number of students of similar fields with whom I holds the brainstorming sessions to critically upgrade with my work. I would offer my special vote of thanks to Dr.Harry who permit me to work beyond lab hours to work on requisite software.

I would also want to convey my vote of thanks to Dr. V.K.Meena of Imaging processing lab (Department of Biomedical-Instrumentation, CSIR-CSIO), who permits me to work on their super-computer having 64GB Ram to have access to licensed software's MIMICS, 3-MATIC to develop the three dimensional model from two dimensional information of DICOM format data and to successfully complete my simulations. I would also like to pay my gratitude towards Mohit(Doctorate scholar,CSIR-CSIO), Vikram(ME scholar, NITTTR,Chandigarh), Rishi(ME scholar, NIT,Srinagar), Gagan(Research assistant, CSIR-CSIO).

I would also want to attribute my vote of thanks to some of the pioneers of bio-heat transfer Dr.Sarit Kumar Das (Director,IIT Ropar) and Dr.Soham Ghosh (Research Doctorate,University of Collarado, USA) who helped me to understand and clarify the doubts I have received while solving their research paper through emails.

I would also like to thank all those representatives of COMSOL who helped me resolve the issues via their support portal, to held workshops, and to send free trials extensions for completion of my work.

Last but not least, I would also like to acknowledge my parents who are been a true support in every sphere of my life and without their moral values,I might have not accomplished what I have achieved.

MANPREET SINGH

ABSTRACT

Due to the increased concerns and burden of cancer on the world, the computational related studies plays a very pivotal role. To assist the ongoing treatment modalities, it becomes an important part of interdisciplinary research to assist nanomedicine and theranostics(therapeutic-diagnostic). Patient-specific modeling is the major area which provides the desired outcomes before implementing the treatment modalities. For this various design engineers, researchers are putting their effortsto develop and compute such algorithms. In relation to this, number of computational softwares are available that provides the reliable results extracted from MRI/CT scan images of patients anatomy.

In the present work, the anatomical model of human(female) breast tissue is processed from large sets of Dicom-format(medical) images via Materialise Mimics-17.0 and 3-Matic. Three dimensional model is generated in Mimics and in 3-Matic tool desired surface layers are provided on the geometry to successfully employ boundary conditions. There is availability of sharing interface(import/export option) that save the model as mesh file(.mphtxt). For thermal analysis, this mesh file is imported into COMSOL-MULTIPHYSICS. Three dimensional model is generated from mesh file to define material(physiological) properties, initial and boundary conditions, mesh variations(grid independency test) to perform the thermal simulations. The concept of averaging of properties is used while defining material properties to nanoparticles loaded tumor to channelize the simulations and to approach towards correct results.Computational model is made by COMSOL-MULTIPHYSICS software to understand the physics behind microparticles/nanoparticles.In Comsol, two kinds of studies are performed by considering the problem study as Uncoupled analysis and One-way coupled analysis. Uncoupled analysis includes only Heat transfer module(Bio-heat transfer module) to compute temperature field distributions. While One-way coupled analysis includes the electromagnetic heating induced in particles via AC-DC module(magnetic fields with current) and Heat transfer module(Bio-heat transfer module).

MATLAB is used to account for calculations of Specific absorption Rate (S.A.R)/Specific Loss Power (S.L.P) via self-written algorithms/codes. It accounts for the effect of nanoparticles and magnetic heating principles to save the results which is an important heat input to Comsol-Multiphysics simulations. Two type of variations i.e. diameter of nanoparticles

and magnetic field tunable parameter frequency are performed to calculate S.A.R.The calculated value validate the results of Chin & Tse et al. under given conditions.Values comes out to be 2 x $10^5 W/m^3$ which matched with the value of 1.95 x $10^5 W/m^3$ for 19nm magnetite particle.

The iron-oxide particles(Magnetite) are essentially assumed to be spherical in shape and the aforementioned variables help to account for selection of effective size nanoparticles and particular frequency range at which the results will be optimum in relation to hyperthermia studies.The particles are uniformly distributed,monodispersed over the whole domain.Safe and tolerable conditions as reported by Atkinson, Brezovich, Hergt and confirmed by Pankhurst of human exposure to magnetic field through clinical trials are also put into consideration to verify computational simulation parameters.

For Cancerous tissue the objective function is to maximize the temperature between 41.5°C to 46.5°C in tumor region to maintain hyperthermia for effective necrosis to be used in conjunction with chemotherapy or radiotherapy. For hyperthermia to be used as monotherapy thermal ablation of tumors in temperature range of 50°C-70°C is also been studied. For all the simulations transient analysis is used to achieve the effective results.

In the present work, the first level of simulations are performed by defining computational geometry(regular geometry) which consist of two domains i.e cylindrical healthy tissue and ellipsoid cancerous tissue loaded with particles. The spatial-temporal distribution curves are generated in tissue along the horizontal and vertical axis passing through center of tumor. Multiple site intratumoral injections(homogeneous distribution and monodispersion of particles) are considered which is itself been the first effort to consider individually the temperature achieved in all injection sites. Temperature at center of tumor is also studied. Muscle tissue is considered in this analysis.

In realistic case, the geometrical domains are irregular in shape. To consider this aspect, the current model is extended towards realistic tumor model of irregular shape and similar analysis is performed to analyse the temperature distributions for breast tissue. For the current study bio-heat transfer module is used and different S.A.R values(heat quantization tunable parameter) are given as an input to study temperature distributions and effective necrosis plots.

The next level of study includes analytical calculations performed for tissues put under the magnetic field. It involves calculations for number of turns for coil under considerations of current and magnetic field strength. These analytical results computed for the geometry are

verified with computational results plotted for same set of inputs and conditions. This magnetic field computed from coil is sufficient to produce heating effects via relaxation phenomenon(Néel relaxation and Brownian motion) if magnetite particles or domain containing particles is concerned. Now, the heat parameter(S.A.R) is defined asan input to bioheat transfer module by magnetic fields with current module. The temperature and magnetic field distributions curves are plotted against vertical and horizontal axis passing through the center of tumor.

In this work, an extensive literature review is performed on magnetic nanoparticles(Magnetite,Maghemite,Iron-Platinum,Iron-Cobalt,Barium Ferrite, and Cobalt Ferrite) been studied till date to present all the key magnetic field parameters in single sheet and to quantify all for desired computational inputs.

Microscale/nanoscale heat transfer principles to malignant tumorsis done efficiently by simultaneously trying to achieve the temperature range of 41.5°C to 46.5°C to do apoptosis.

The choice of effective bio-compatible super-paramagnetic nanoparticle is proved to be an effective tool aided with other current means of Chemotherapy and radiotherapy. We propose magnetite material, an extensively studied particle for our simulations to study hyperthermia as monotherapy.For the present simulations the temperature achieved is 71°C which matched with the literature results of Hilger et al.,2001[28].

The heat quantization parameter needs to be tuned in order to select proper heat input value.Coupling between bioheat transfer module and magnetic field with current (frequency variations) are performed on muscle tissue for proper choice of magnetic nanoparticle diameter, SAR value is calculated via self written MATLAB codes and analytical calculation results are verified with literature.

IMPORTANT KEYWORDS

Computer Assisted Intervention(CAI), 3-D Medical Imaging, Segmentation, 3D-Reconstruction, Prior shape knowledge, Image based 3D Computer-aided design(CAD), Magnetic Fluid Hyperthermia(MFH), Nanothermotherapy, Magnetic Heating Treatment(MHT), Bio-heat transfer, Bio-electromagnetics, Tumor, Cancerous tissue, AC magnetic field, Finite Element Analysis(FEA), Superparamagnetic Iron-Oxide Nanoparticles(SPION's), Volumetric heating temperature, Cancer treatment, Image-based mesh generation, Materialise-MIMICS, 3-MATIC, COMSOL-MULTIPHYSICS, MATLAB, Magnetic Resonance Imaging(MRI), Specific Absorption Rate(SAR), Spherical nanoparticles, Penne's Bioheat Equation(PBHE), Thermal Simulations, Ferrofluid, Magnetite, Maghemite, Mathematical Modeling, Breast Cancer, Spatial-temporal distributions, Thermal ablation, Breast conserving therapy, Minimal-Invasive therapy, Saturation magnetization, Bio-compatibility, Magnetic fields with current module, Bio-heat transfer module, Non-interacting particles, Nano-scale heat transfer.

TABLE OF CONTENTS

LIST OF ILLUSTRATION

LIST OF TABLES

NOMENCLATURE

English Symbols	***Description***	***Units***
B	Magnetic Induction	T
C_P	Specific heat capacity	$\frac{J}{kg.K}$
F	Applied frequency	Hz
H_o	Applied magnetic field amplitude	$\frac{A}{m}$
k_B	Boltzmann's constant	$1.38\times10^{-23}\ \frac{J}{K}$
K	Magnetic anisotropy constant	$\frac{J}{m^3}$
M	Magnetization	$\frac{A}{m}$
σ	Saturation magnetization	$\frac{emu}{g}$
M_r	Remanent magnetization	$\frac{A}{m}$
M_s	Saturation magnetization	$\frac{A}{m}$
P	Volumetric power generation	$\frac{W}{m^3}$
SAR	Specific absorption rate	$\frac{W}{m^3}$
SAR_{Fe}	Specific absorption rate-iron	$\frac{W}{kg_{Fe}}$
SLP	Specific loss power	$\frac{W}{kg_{Fe}}$
T	Absolute temperature	K
T	Time	s
U	Internal energy	J
V_m	Magnetic volume of particle	m^3
V_H	Hydraulic volume	m^3
W	Magnetic work	J
r_n	Radius of nanoparticle	nm
A	Frequency factor	s^{-1}
E_a	Activation energy	$Jmol^{-1}$
h	Convection coefficient	$\frac{W}{m^2.K}$
k	Thermal conductivity	$\frac{W}{m.K}$

C_n	Concentration of nanoparticles	$\frac{kg}{m^3}$
Q_m	Metabolic heat generation	$\frac{W}{m^3}$
Q_s	External heat source	$\frac{W}{m^3}$
N	Avogadro's constant	$6.022 \times 10^{23}\, mole^{-1}$
T_B	Blocking temperature	K
M_n	Molecular weight of nanoparticle	[-]
D_n	Diameter of nanoparticle	nm
M_d	Domain magnetization	$\frac{A}{m}$

Greek Symbols	***Description***	***Units***
χ	Magnetic susceptibility	[-]
$\chi^{/}$	In-phase susceptibility	[-]
$\chi^{//}$	Out-of-phase susceptibility	[-]
χ_o	Static susceptibility	[-]
$\chi^{/}$	Intitial susceptibility	[-]
ϕ	Nanoparticle volume fraction	[-]
η	Fluid viscosity	$Pa\text{-}s$
μ_o	Permeability of free space	$4\pi \times 10^{-7}\, \frac{N}{A^2}$
ρ	Density	$\frac{kg}{m^3}$
τ_R	Effective relaxation time	s
τ_o	Attempt time or average relaxation time	s
τ_B	Brownian relaxation time	s
τ_N	Néelian relaxation time	s
ω	Blood perfusion rate	s^{-1}
δ	Ligand layer thickness	nm
Ω	Arrhenius integral	[-]
ξ	Parameter in langvein equation	[-]

Subscripts	***Description***
b	Blood

a	Artery
t	Tissue
n	Nanoparticle
air	Air
m	Magnetic
i	Initial
Fe	Iron
ambient	Ambient
ext	External
mix	Mixture
tissue	Tissue
met	Metabolic
avg	Average
max	Maximum
min	Minimum
o	Steady state

Superscripts	***Description***
*	Dimensionless

Acronyms	***Description***
SAR	Specific Absorption Rate
SLP	Specific Loss Power
MagMED	Magnetic Mediated Energy Delivery
MNP	Magnetic Nanoparticle
NP	Nanoparticle
IONP	Iron Oxide Nano-Particle
SPION	Super Paramagnetic Iron-Oxide Nano-Particle
3D	Three-dimensional
2D	Two-dimensional
CEM	Cumulative equivalent Minutes
MFH	Magnetic Fluid Hyperthermia
MHT	Magnetic Heating Treatment
FEA	Finite Element Analysis
CT	Computed tomography
MRI	Magnetic Resonance Imaging
CAD	Computer Aided Design
PD	Power Density
PBHE	Penne's Bio-Heat Equation
SWOT	Strengths, Weakness, Opportunities, Threats
SPM	Superparamagnetic
FM	Ferromagnetic

BV	Blood Vessel
MTS	Metastasis
TCHT	Thermo chemotherapy
HT	Hyperthermia

CHAPTER 1

INTRODUCTION

1.1 OVERVIEW

This chapter is an introductory note to build the interest of readers to gather all the important aspects of research. It is been elaborated into seven sections that briefs the problem statement of current technology. The first section starts with motivation for simulation with inclusion of rationales and research significance. The Research objectives and specific aims pertaining against proposed computational work of the study are also been presented in this chapter. The thesis outline is precisely split into three sub-sections that enlightens about application areas, research scope and importance of work with last section outlines the organization of the thesis. Design of experiment(DOE) and Time-Plan of the thesis dissertation is also been described.

This chapter primarily focused on "knowing" about cancer, its progression and development. Broader classification of tumors is presented via pictorial representation and the threat of newer cases that are likely to appear by keeping in preview present prevailing conditions of US. The burden of cancer on the world(US) with probable statistics is defined. Special concern is given in relation with breast cancer. The anatomy of breast tissue, with two methods of invasive breast cancer prognosis are also briefly explained with past, present, and future trends. Definition of risks that are associated with cancer is also been a part of discussion.

This chapter primarily focused on the current treatments been implemented to cure cancer or to treat cancer. Mostly clinically proven studies have emphasized on chemotherapy and radiotherapy to treat the cancers. In this view, we try to present the burden of cancer to medical science and the emergence of newer principles of engineering to aid this specific study. The contribution of nano-engineered particles to potentially target these carcinogenic cells is a new state of art and needs to be explored with magnetic principles and also to further extends its role to drag the particles to desired malignant site and the concept emerged to be "targeted hyperthermia". The role of principle researchers and engineers of interdisciplinary branches to

gather at one single platform to apply their domain knowledge to work towards complete eradication of this ill disease.

This chapter presents the brief review of the current practices, studies or modalities been practiced or near to be practiced are briefly discussed. The figures in relation to cancer via whole globe, particularly in India and also the statistics of PGIMER, Chandigarh. Since, the present thesis dissertation deals with the Breast Cancer, so more stress is given on this particular type of cancer only.

1.2 MOTIVATION FOR SIMULATION:

The main aim of advanced computers or smart computers or super computers operated studies is to channelize the results close to real time applicability to human beings. Advanced simulations being run on such machines are capable of been delivering the results to close proximity to the clinical trials. Simulations are been carried to realize the potential results of the operating modality well in advance and do necessary changes if required at later on stage.

Simulation is must need requirement because:

- Provide better heating through treatment preplanning.
- Optimize setups for treatment cases.
- Assist new applicator designs in the future.

The electromagnetic field and the thermal phenomenon needs to be computed at a speed suitable for clinical environment. Temperature limits needs to be defined appropriately to effectively quantify the amount of nanoparticle concentration. Upper bound must be imposed on temperature $T<T_{lim}$. Typical values for T_{lim} are 44°C for muscle, fat, and bone tissues and, 42°C for more sensitive organs such as bladder or intestine.(M.Weiser,2008[]).

1.3 THESIS OUTLINE

1.3.1 APPLICATION OF WORK

Computational advancement let the researchers to use the advanced tools of computation to account for the analysis(FEA) that are sufficient to produce results according to requirements. Research strategies are developed to address the issues with the aid of mathematical models, numerical analysis techniques, theoretical reviews with computational software packages.

In lieu concernof this, we attribute our efforts to assist the oncologists to pre-analyse the results after injection of nanoparticles into tumors and help realize the potential benefits, drawbacks, opportunities that can guide such level of approaches to near clinical acceptance and avoid the current used techniques of healing i.e chemotherapy and radiotherapy which are itself the initiators of second cancers caused due to multiple exposure and drug intake.

1.3.2 RESEARCH SCOPE OF THESIS

This study mainly focused on the efficiency of magnetic fluid hyperthermia or thermal ablation, which was evaluated in terms of magnetic field parameters and bio-heat transfer equation, successfully studying the breast tumor temperature variations and heat caused necrosis.

The study was carried out by using COMSOL software. Before implementing the COMSOL software, data collection for magnetic field related parameters, breast tissue and tumor volume were needed. Also, To introduce the medical imaging concepts, DICOM format data collection which is a pre-cursor to deduce 3D model is required. After data collection, Materialise's Interactive Medical Image Control System (MIMICS) image files were converted by using interface between MIMICS and COMSOL software. 3-Matic is used to define surface layers which are at later stage will help during material selection. After converting the image files, simulation was run by using COMSOL software. The accuracy of the model wholly depends upon the data been used, the refinement of data i.e number of sets of images been taken at the time of MRI/CT scan. The thickness defined by radiodiagnostic(definite protocols set by individual medical constituting bodies) at the time of scan helps to define the uniformity of model and exact shape and volume characteristics that will be of prime importance in real sense. The role of design(thermal engineers) comes into picture once the data is actually portrayed and gather by software. Moreover, image refinement comes with amount of contrast been injected into the patient's body. The simulation was conducted with identified independent variables (i.e. concentration of particles, deepness of tumor, temporal and spatial evaluation along the center line of given model and also along the radial direction, magnetic field tunable parameters). Simulation produced with different parameters was saved for further analyses. Graphs that relate the effect of SAR value or heat quantization parameter value at breast tumor were also developed. From the developed graphs, the association between the efficiency of hyperthermia and thermal ablation on realistic breast cancer patients given could be made feasible in clinical

areas to visualize the results actually before hyperthermic procedures and reduce the loads of surgical operations to assist the future scope of studies.

1.3.3 ORGANIZATION OF THESIS

This thesis is mainly delegated into ten different chapters. Every chapter initiates with a "Overview" section that will brief the reader about the contents.

In **first chapter**, the motivation for simulation, background of study, thesis outline elaborating application of work, scope of thesis, problem statement and problem formulation, objectives, and significance of dissertation are reviewed in order to list out the tasks and act as a guideline for this study. Based upon the key objectives, the design of experiment and plan of action is formulated to define the state of art of problem and in bifurcation of work.

The statistics of cancer and particularly for breast cancer patients, theoretical discussions includes classification of tumors, Prognosis for breast cancer, relative risks, current trends,treatments and some basic information related to the thesis title that will made the base to approach for computational related studies is detailed in this **chapter**.

Chapter 2 describes the theoretical background and underlying physics of magnetic nano particle induced hyperthermia. In this chapter, principles of hyperthermia stating temperature treatments for biological tissues, Classification, Challenges, and Important concepts are the prime terms of discussion. Important considerations in hyperthermia studies is also been enlightened. Discussion on nanoparticles is described with advantages, properties, factors influencing the extent of heating. Bio-heat transfer models(Pennes Bio-heat Continuum Model) with concepts of intravenous and intratumoral injections are discussed. Relevant magnetic principles defining safe exposure limits, mechanisms of heat generation and its parametric formulation with special emphasis on heat quantization parameter SAR/SLP value. Concept of Averaging of properties is defined that will be an input to material properties defined for geometrical domain. Lastly, we tried to approach hyperthermia from engineering(Design and Computation principles) view point and describes importance of Hyperthermia Treatment Planning(HTP) to assist computational work.

Chapter 3 presents the brief view of 3D-Medical Imaging. This chapter elaborates the medical imaging processing concepts, Imaging technology, Co-ordinate systems defined in medical terminology(Anatomical planes). The data conversion from stack of 2D images to generate 3D models. Softwares are extensively reviewed by keeping in preview the desired

computational requirements to process DICOM format data to three dimensional models. We found Materialise-MIMICS, 3-MATIC, COMSOL-MULTIPHYSICS17.0, are well suitable and licensed forms are been available at CSIR-CSIO.

Chapter 4 is dedicated to literature review. In this chapter, the major computational work been performed in relation to hyperthermia studies is presented in tabular format. This chapter aims at quantifying the parameters been selected by researchers to approach and satisfy the given temperature requirements. Elaborative literature review covers all aspects of computation related studies and in each reviewed article the very first column defines the type of work whether Numerical, Analytical, Experimental, Theoretical, Computational, Review study. Magnetic field related parameters collected from large number of research articles are been presented under one roof to use the respective value whenever required for given inputs to computational softwares. 40 research papers are well explained and easy for anyone to know the state-of-art of the concepts. Lastly, tissue properties are presented to account for particularly tissues.Each individually reviewed paper quantifies the inferences drawn to approach for research gaps will help to formulate the problem definition.

Chapter 5 presents the methodology used from the starting until the end of the study, which includes the computer machine or material or softwares used for completing the study, designing the simulation and how to run the simulation. An overview of overall methodology that designated in a flow chart as guideline for task sequences also included in this chapter. Research gaps are also been quantified to propose the work and define the objectives of work.

Chapter 6 is a representation of different model studies been incorporating in relation to finite element analysis to initially match the results with benchmark papers and propose newer concepts against the research gap findings. It covers all the things that a computational problem should consists of. It includes COMSOL MODELS, Insight to Image generation, geometry details, properties, governing equations, Initial and Boundary conditions, Time requirements by computational software for calculations, Mesh configurations, Grid Independency test and last but not least the type of solvers used to calculate the results for physics defined problems .

Chapter 7 shows the results obtained from the simulation. Several graphs made to preview the relationship between the temperature achieved and time i.e transient analysis, which were resulting from different parameters also presented. At the end of this chapter, Results and

discussion, some of findings and the sources of errors that affect the simulation outcomes are discussed in details.

Chapter 8 states the conclusions of the study, Closing remarks and also the future research directions(Recommendations) for improvement or extension of study in the future are also outlined in this chapter.

1.4 RATIONALES AND SIGNIFICANCE

This study had the significance to validate a new strategy on developing a more promising technology based on imaging to treat breast cancer. This study holds its importance for eliminating the side effects or toxicities caused by conventional drug therapies(chemotherapy), radiotherapy. This was replaced by the application of newer to implement technology, MNP's induced hyperthermia assisted with medical imaging. The other significance was including pre-estimating the necrosis plots that will induce desired changes in tumor physiology. Temperature based simulations plots provides estimates on the optimum nanoparticle dosage used for breast cancer treatment. It also reduced side effects and drug dosage use, thereby decreasing the cost of breast cancer treatment.This technique helps to provide better changes in micro-environment of tumor to minimize surgeries and exposure to radiations(radiotherapy procedures). Since, the results are realistic,thereby it provides more reliable results

1.5 PROBLEM STATEMENT AND PROBLEM FORMULATION

Magnetic fluid hyperthermia therapy can be used as a treatment for tumors. However, high temperatures induced by hyperthermia treatment can cause damage to surrounding cells. A COMSOL model of nanoparticles induced heating within a cancerous tumor, which couples the concentration profile to magnetic heating principles, can be used to optimize treatment time to maximize damage to tumor cells while minimizing damage to normal tissue.

- In COMSOL model, a tumor is approximated as sphere or ellipsoid surrounded by a cylindrical/Spherical normal healthy tissue.
- The transient temperature profile of the tissue will be evaluated to observe the extent of damage to both the tumor tissue and surrounding healthy tissue.
- Multiple site injections while considering uniform volume of particles to observe the effect of surface-area to volume ratio for requisite temperature profiles.

- Microparticles/nanoparticles heat production within the tumor during exposure to a magnetic field is proportional to the nanoparticle concentration.
- To adjust the model based upon the tumor size, geometry, and specific parameters such as density, as well as various types of nanoparticles used in clinical setting to determine optimal treatment prior to the beginning of hyperthermia treatment.

1.6 RESEARCH OBJECTIVES AND SPECIFIC AIMS AGAINST PROPOSED COMPUTATIONAL WORK

The aim of this study was to treat breast cancer by magnetic nanoparticles based heating and perform simulations first on simpler geometries and then once they are been validated, we approached towards final realistic breast model.This can be achieved by the following specific objectives:

- To convert Materialise's Interactive Medical Image Control System (MIMICS) image files into Comsol-Multiphysics advanced analysis software.
- To determine the effect of ferrofluid tumor loading for breast tissues.
- To investigate the relationship between alternating magnetic field parameters (Field Amplitude, Frequency) and effective nanoparticle concentrations.
- To study the effect of spatial and temporal distribution on temperature.
- Bio-heat transfer phenomenon in presence of magnetic field.
- Magnetic interaction of micro/nanoparticles (Study of heat Absorption /Dissipation pattern).
- Quantify the extent of tissue necrosis caused by the heating process.
- Optimize electromagnetic heating time to maximize tumor damage while minimizing damage to surrounding normal tissue based on specific tumor and nanoparticle properties.
- Verification & Validation: Verifying the results and validate the results obtained from computational work with respect to benchmark paper and the previous conducted experimental studies/clinical trials conducted on human tissues/animal models.

1.7 TIME-PLAN OF ACTION

The purpose of developing a time plan for a thesis project is to have a clear understanding of the relationship between important dates, thesis activities, and the time needed for each activity.

The time plan for this thesis is as below:

- Literature Survey and Problem Definition Jan 2016

- ❖ Learning Software's Jan 2016
- ❖ Design May 2016
- ❖ Data Collection May 2016
- ❖ Analysis and Result Comparison May 2016
- ❖ Thesis Report Writing and Submission July 2016

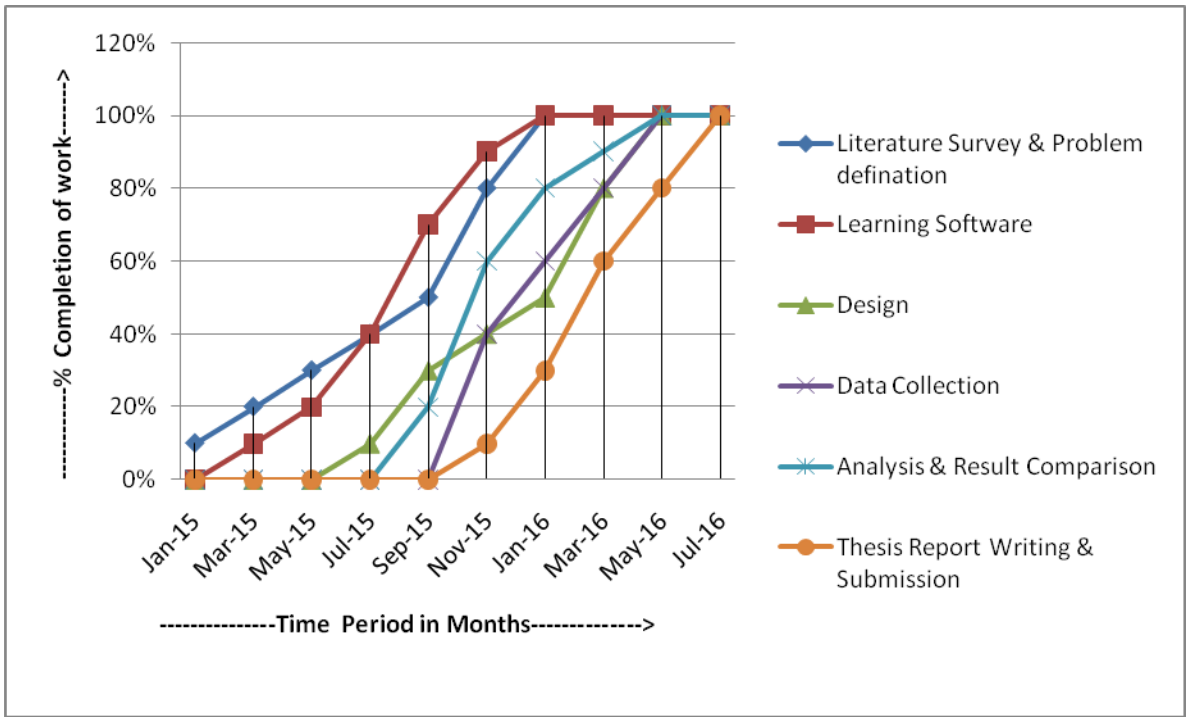

Figure 1.1: Time-plan of action representing %completion of work against time period in months

1.8 DESIGN OF EXPERIMENT (D.O.E)

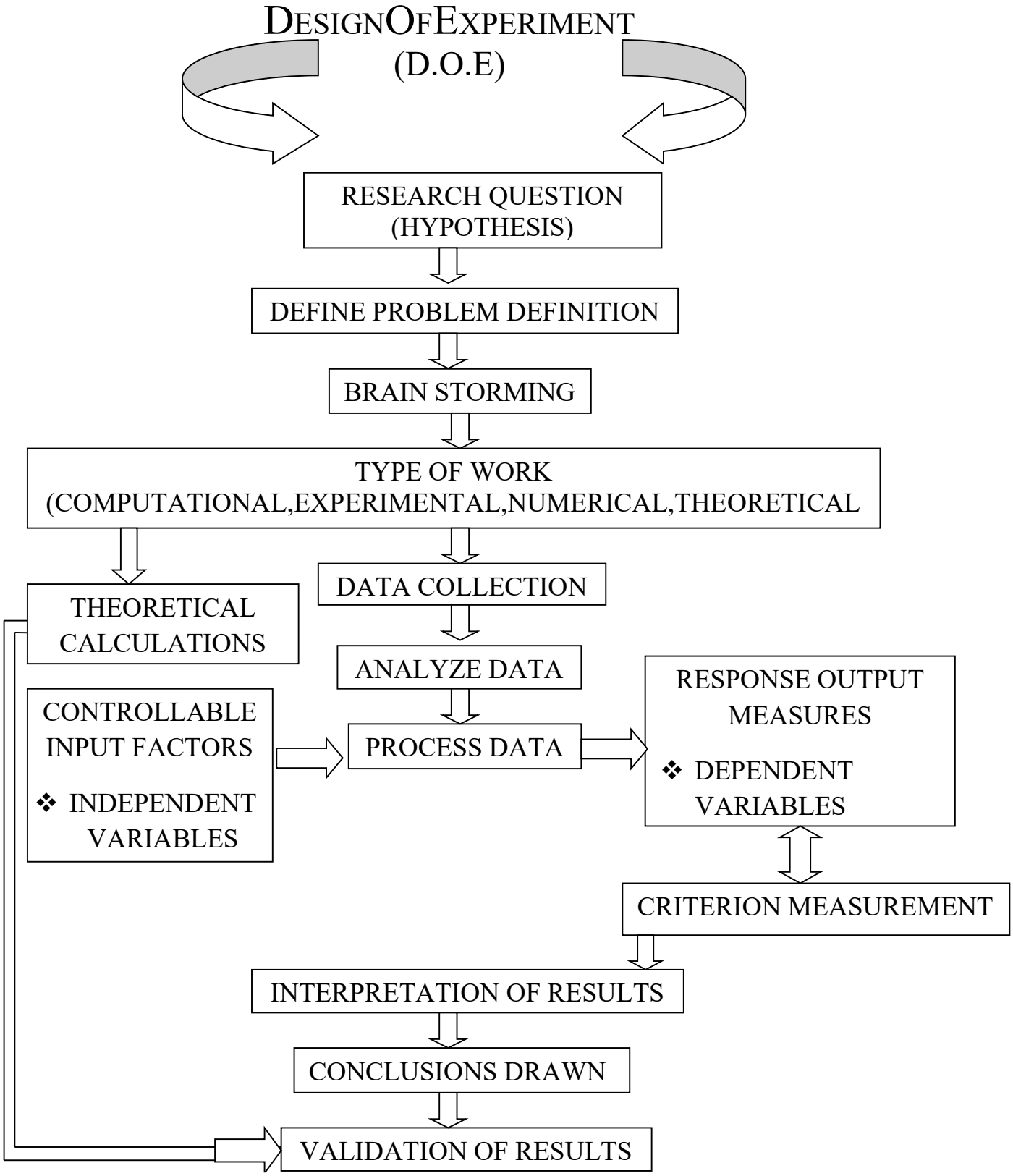

Figure 1.2:Design of Experiment for computational based problem

1.9 INTRODUCTION TO CANCER

According to the definition stated by the "*American Cancer Society,*"[W.5] "**Cancer**" may be defined as group of diseases characterized by uncontrolled growth and spread of abnormal cells that causes the cells in the body to change and make their own lymphatic drainage system. If the spread is not controlled, it can often results in death of patients. The blood carrying vessels are often leaky in nature. Most types of cancer cells eventually form a lump or mass called a **tumor**, and are often named after the part of the body where the tumor originates. If the spread of cancer is from one specific site(where it actually originates) to other organs, than it usually refers to as "**Metastasis**" and it is often referred to as advanced stage cancer.

There are both external as well as internal factors that contribute for the carcinoma. Cancer is caused by external factors, such as tobacco, infectious organisms, and an unhealthy diet, and internal factors, such as inherited genetic mutations, hormones, and immune conditions. These factors may act together or in sequence to cause cancer. In a study it is revealed that one cell often requires seven years of approximate time to grow and develop as a single unit that may inhibit pains to the patients and made its presence felt.

Treatments include surgery, radiation, chemotherapy, hormone therapy, immune therapy, and targeted therapy (drugs that interfere specifically with cancer cell growth). The new research fields made their existence felt after successful clinical trials on animals(rats, rabbits) and fewer on humans(breast cancer, prostate cancer, lung cancer) such as Magnetic Nanoparticles(MNPs) induced hyperthermic studies can be used as monotherapy or as an adjuvant to chemotherapy or radiotherapy. The nanotechnology assisted these nanocarriers can also be potentially recalled in "Nanomedicine" and addressed as a therapeutic and diagnostic tools often been studied as a newer field "Nano-theranostics."

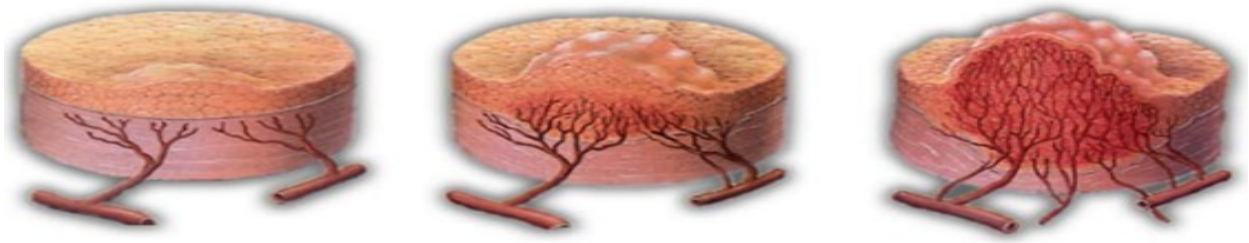

Figure 1.3: Cancer progression and development of network of tumor blood vessels (Adapted from Brusentsov et al.,2001[58]).

1.10 CLASSIFICATION OF TUMORS

The tumors may be benign or malignant depending upon the local conditions prevailing i.e the microenvironment and morphological structure of tumors. Most benign tumors are not harmful(non-cancerous) to human body, but some may press against nerves or blood vessels and cause pain or other negative effects. In the malignant tumor, the cells divide and grow uncontrollably invading surrounding tissues or spread to other organs(metastasis) through the lymphatic system or bloodstream. This kind of tumor is referred to "Cancer" and cause patient's death.

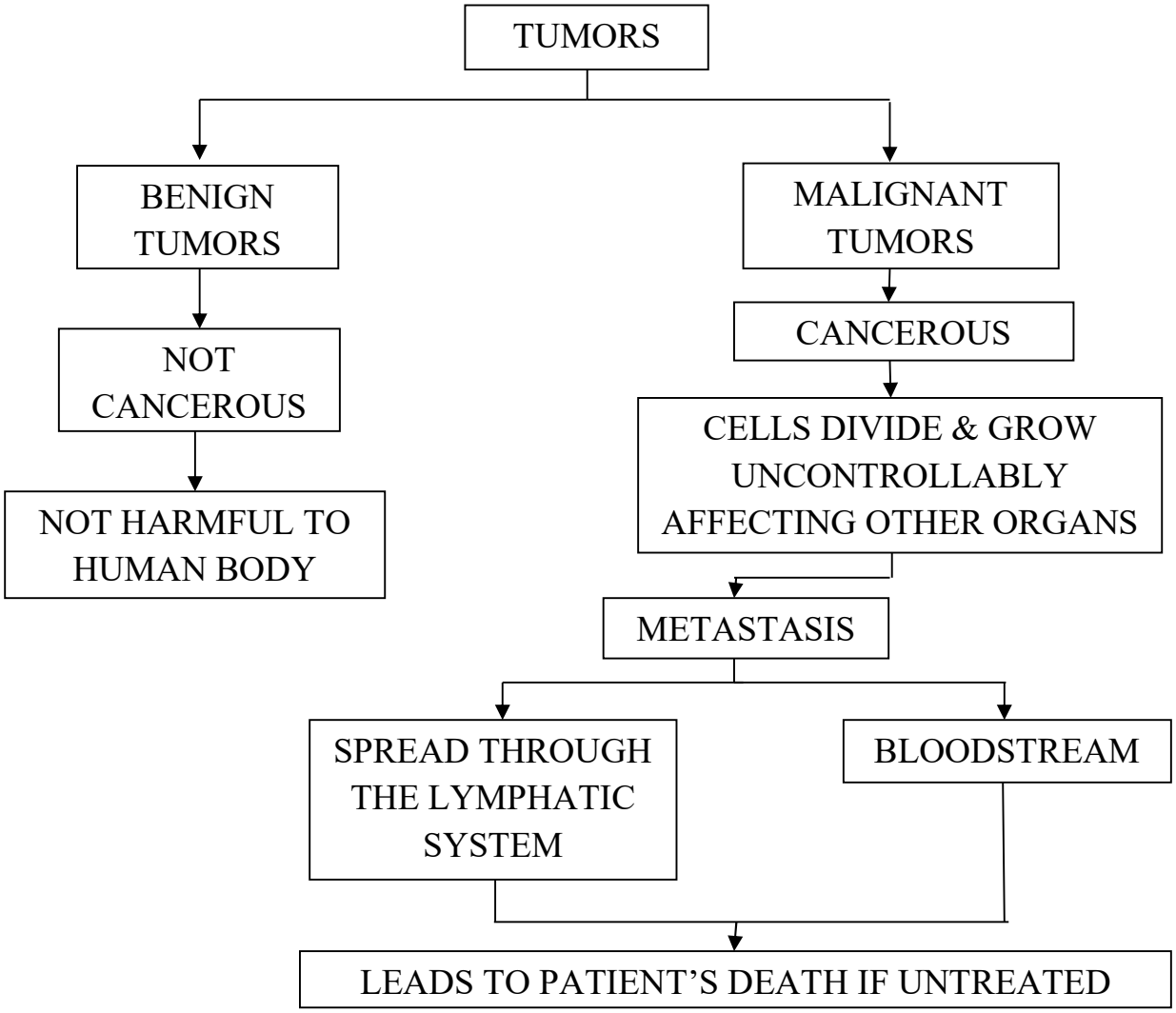

Figure 1.4: Tumors and its classification

1.11 CURRENT STATUS ON CANCER: NEW CASES AND DEATHS EXPECTATION

Cancer is the second most common cause of death in the USA, exceeded only by heart disease, and accounts for nearly 1 of every 4 deaths. About 1,685,210 new cancer cases are expected to be diagnosed in 2016 (Table 1.1). As per American Society of Cancer Research[W.5],About 5,95,690 Americans are expected to die of cancer in 2016, which translates to about 1,630 people per day(Table 1.1).

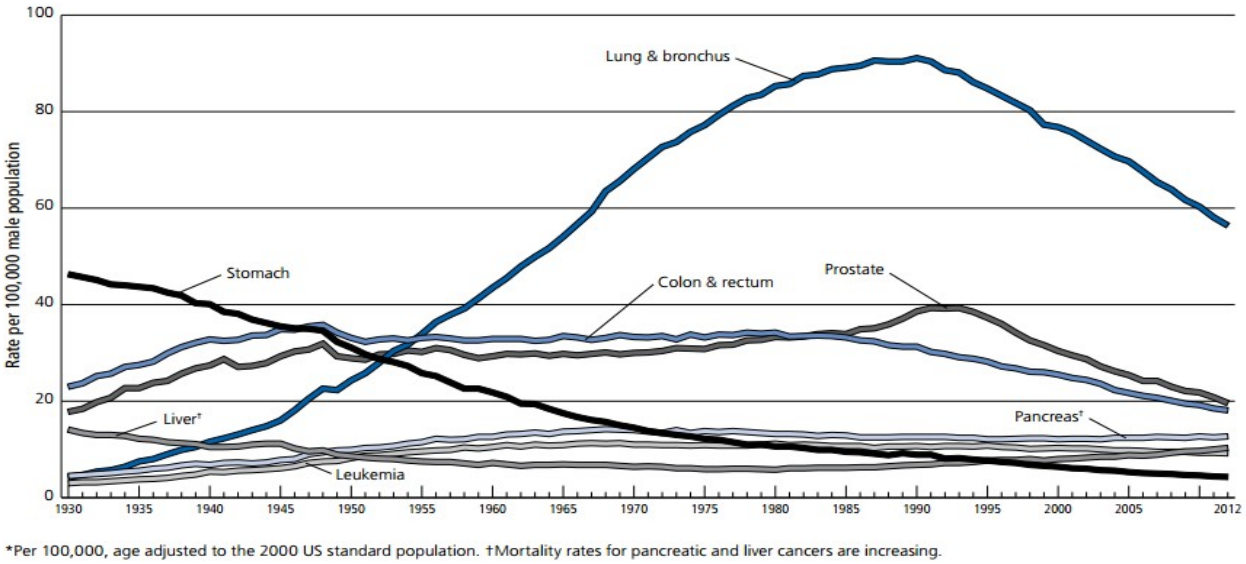

*Per 100,000, age adjusted to the 2000 US standard population. †Mortality rates for pancreatic and liver cancers are increasing.

Figure 1.5: Trends in Age-adjusted cancer death rates for males in US, 1930-2012,(Adapted from American Cancer Society,2016[W.5]).

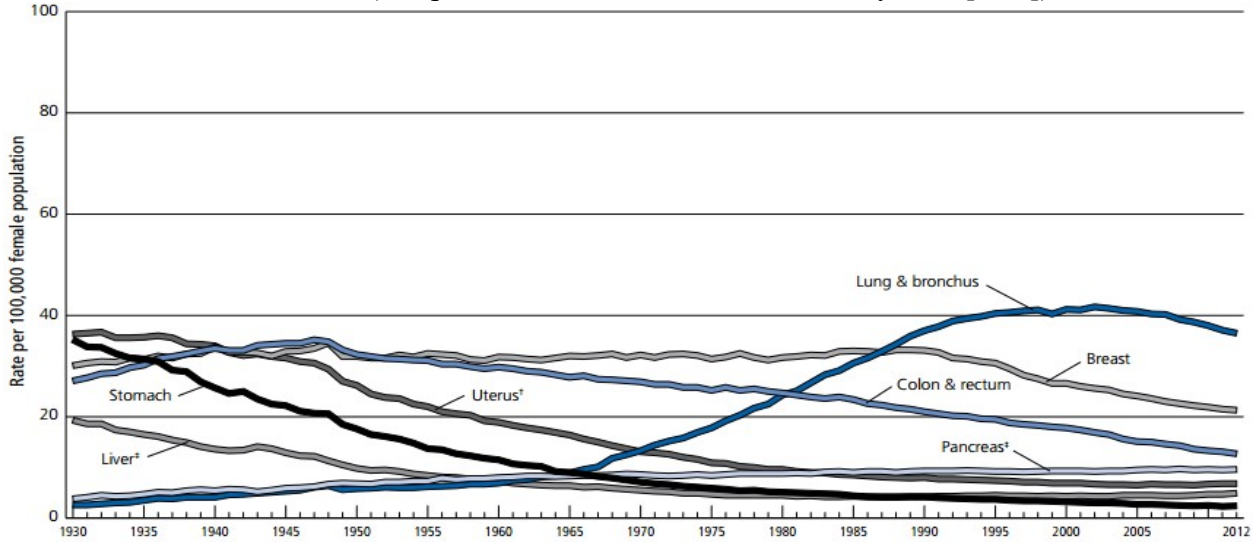

*Per 100,000, age adjusted to the 2000 US standard population. †Uterus refers to uterine cervix and uterine corpus combined. ‡Mortality rates for pancreatic and liver cancers are increasing.

Figure 1.6: Trends in Age-adjusted cancer death rates for females in US, 1930-2012,(Adapted from American Cancer Society,2016[W.5]).

Table 1.1: Estimated number of new cancer cases and deaths by sex, in USA,2016,(Adapted from American Cancer Society,2016[W.5]).

	Estimated New Cases			Estimated Deaths		
	Both sexes	Male	Female	Both sexes	Male	Female
All Sites	1,685,210	841,390	843,820	595,690	314,290	281,400
Oral cavity & pharynx	48,330	34,780	13,550	9,570	6,910	2,660
Tongue	16,100	11,700	4,400	2,290	1,570	720
Mouth	12,910	7,600	5,310	2,520	1,630	890
Pharynx	16,420	13,350	3,070	3,080	2,400	680
Other oral cavity	2,900	2,130	770	1,680	1,310	370
Digestive system	304,930	172,530	132,400	153,030	88,700	64,330
Esophagus	16,910	13,460	3,450	15,690	12,720	2,970
Stomach	26,370	16,480	9,890	10,730	6,540	4,190
Small intestine	10,090	5,390	4,700	1,330	710	620
Colon†	95,270	47,710	47,560	49,190	26,020	23,170
Rectum	39,220	23,110	16,110			
Anus, anal canal, & anorectum	8,080	2,920	5,160	1,080	440	640
Liver & intrahepatic bile duct	39,230	28,410	10,820	27,170	18,280	8,890
Gallbladder & other biliary	11,420	5,270	6,150	3,710	1,630	2,080
Pancreas	53,070	27,670	25,400	41,780	21,450	20,330
Other digestive organs	5,270	2,110	3,160	2,350	910	1,440
Respiratory system	243,820	132,620	111,200	162,510	89,320	73,190
Larynx	13,430	10,550	2,880	3,620	2,890	730
Lung & bronchus	224,390	117,920	106,470	158,080	85,920	72,160
Other respiratory organs	6,000	4,150	1,850	810	510	300
Bones & joints	3,300	1,850	1,450	1,490	860	630
Soft tissue (including heart)	12,310	6,980	5,330	4,990	2,680	2,310
Skin (excluding basal & squamous)	83,510	51,650	31,860	13,650	9,330	4,320
Melanoma of the skin	76,380	46,870	29,510	10,130	6,750	3,380
Other nonepithelial skin	7,130	4,780	2,350	3,520	2,580	940
Breast	249,260	2,600	246,660	40,890	440	40,450
Uterine corpus	60,050		60,050	10,470		10,470
Ovary	22,280		22,280	14,240		14,240
Vulva	5,950		5,950	1,110		1,110
Vagina & other genital, female	4,620		4,620	950		950
Prostate	180,890	180,890		26,120	26,120	
Testis	8,720	8,720		380	380	
Penis & other genital, male	2,030	2,030		340	340	
Urinary system	143,190	100,920	42,270	31,540	21,600	9,940
Urinary bladder	76,960	58,950	18,010	16,390	11,820	4,570
Kidney & renal pelvis	62,700	39,650	23,050	14,240	9,240	5,000
Ureter & other urinary organs	3,530	2,320	1,210	910	540	370
Eye & orbit	2,810	1,510	1,300	280	150	130
Brain & other nervous system	23,770	13,350	10,420	16,050	9,440	6,610
Endocrine system	66,730	16,200	50,530	2,940	1,400	1,540
Thyroid	64,300	14,950	49,350	1,980	910	1,070
Other endocrine	2,430	1,250	1,180	960	490	470
Lymphoma	81,080	44,960	36,120	21,270	12,160	9,110
Hodgkin lymphoma	8,500	4,790	3,710	1,120	640	480
Non-Hodgkin lymphoma	72,580	40,170	32,410	20,150	11,520	8,630
Myeloma	30,330	17,900	12,430	12,650	6,430	6,220
Leukemia	60,140	34,090	26,050	24,400	14,130	10,270
Acute lymphocytic leukemia	6,590	3,590	3,000	1,430	800	630
Chronic lymphocytic leukemia	18,960	10,830	8,130	4,660	2,880	1,780
Acute myeloid leukemia	19,950	11,130	8,820	10,430	5,950	4,480
Chronic myeloid leukemia	8,220	4,610	3,610	1,070	570	500
Other leukemia‡	6,420	3,930	2,490	6,810	3,930	2,880
Other & unspecified primary sites‡	34,170	17,810	16,360	42,700	23,900	18,800

1.12 TYPES OF CANCER

The chance of successful treatment depends on the stage of cancer development, response of patient's physiology to treatment. The cancer is named after the organ where it actually starts to grow and in advanced stages may invade the other organs also. The cancer that are been cured by hyperthermia are:

Sarcoma, Carcinoma, Melanoma, Head and Neck, Brain, Thyroid, Lung, Esophagus, Breast, Kidney, Bladder, Liver, Appendix, Stomach, Pancreas, Endometrial, Ovarian, Cervix, Peritoneal lining (Mesothelioma), Rectum.

1.13 DISCUSSION ON BREAST CANCER

The vast majority of breast cancers begin in the parts of the breast tissue that are made up of glands for milk production, called lobules, and ducts that connect the lobules to the nipple. The remainder of the breast is made up of fatty, connective, and lymphatic tissues.

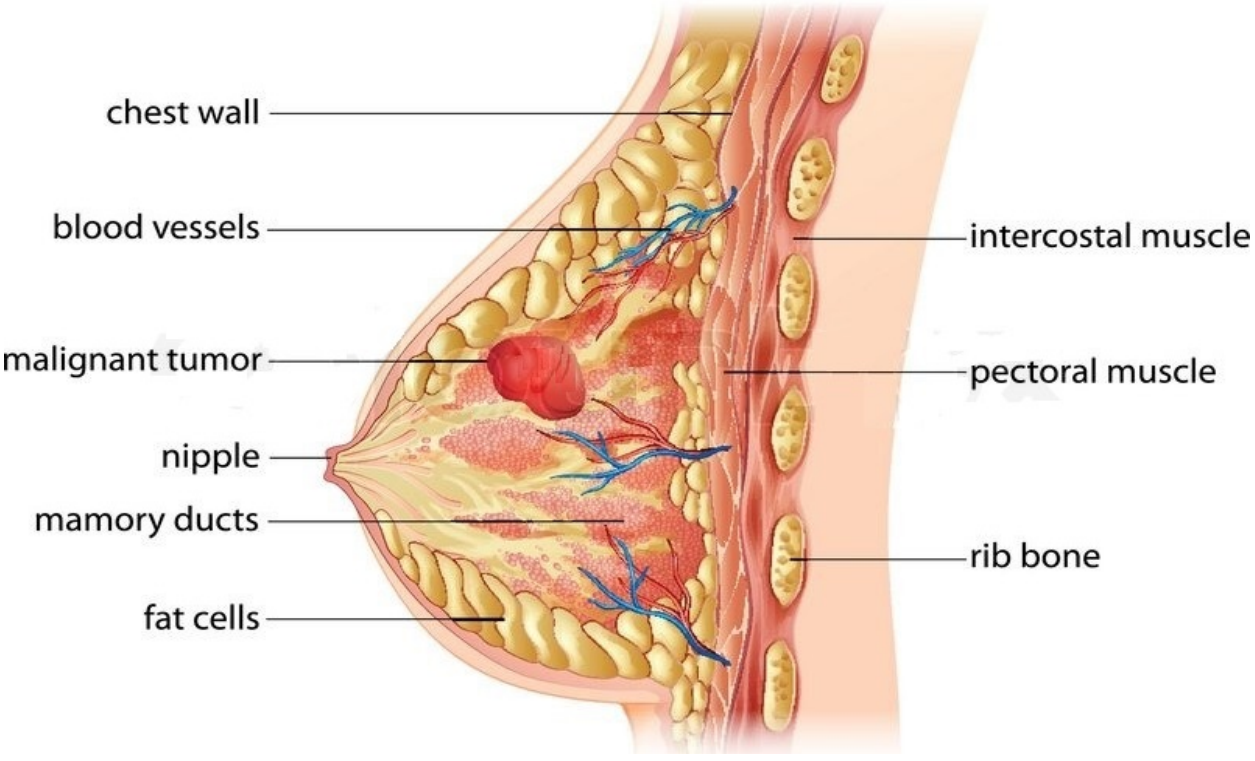

Figure 1.7: Illustration of the anatomy of breast with malignant tumor(Adapted from[]).

Breast cancer is typically detected either during a screening examination, before symptoms have developed, or after a woman notices a lump. Most masses seen on a mammogram and most breast lumps turn out to be benign; that is, they are

not cancerous, do not grow uncontrollably or spread, and are not life-threatening. When cancer is suspected, microscopic analysis of breast tissue is necessary for a definitive diagnosis and to determine the extent of spread (in situ or invasive) and characterize the type of the disease. The tissue for microscopic analysis can be obtained via a needle or surgical biopsy. Selection of the type of biopsy is based on individual patient clinical factors, availability of particular biopsy devices, and resources.Most breast cancers are invasive, or infiltrating.These cancers have broken through the walls of the glands or ducts where they originated and grown into surrounding breast tissue.

1.14 PROGNOSIS OF INVASIVE BREAST CANCER

The prognosis of invasive breast cancer is strongly influenced by the stage of the disease – that is, the extent or spread of the cancer when it is first diagnosed. There are two main staging systems for cancer.

2.7.1. The TNM Staging System

2.7.2. The Surveillance, Epidemiology, and End Results(SEER) Summary Stage System.

1.14.1 THE TNM(TISSUE, NODE, METASTASIS) STAGING SYSTEM:

The *TNM Staging System* is commonly used staging system in clinical settings. The TNM system assesses cancer growth(information on tumor size) and spread in 3 ways: extent of the primary tumor or spread within the organ(Breast) or to adjacent tissue(T), absence or presence of regional lymph node involvement or spread to nearby lymph nodes (N), and absence or presence of distant metastases(spread to distant organs) (M). Once the T, N, and M categories are determined, a stage of 0, I, II, III, or IV is assigned, with stage 0 being in situ, stage I being early stage invasive cancer, and stage IV being the most advanced disease. Some cancers (e.g., lymphoma) have alternative staging systems. As the biology of cancer has become better understood, additional tumor-specific features have been incorporated into treatment plans and/or stage for some cancers.

1.14.2 THE SEER(SURVEILLANCE, EPIDEMIOLOGY, AND END RESULTS) SUMMARY STAGE SYSTEM FOR BREAST CANCER:

According to *SEER Summary Staging System* , it defines three different stages as Local stage, Regional stage, Distant stage.

a.) Local stage: It refers to cancers that are confined to the breast(corresponding to stage I and some stage II cancers in the TNM staging system).

b.) Regional stage: It refers to tumors that have spread to surrounding tissue or nearby lymph nodes(generally corresponding to stage II or III cancers, depending on size and lymph node involvement).

c.) Distant stage: Distant stage refers to cancers that have metastasized (spread) to distant organs or lymph nodes above the collarbone(corresponding to some stage IIIc and all stage IV cancers).

1.14.3 BREAST CANCER CASES AND TRENDS

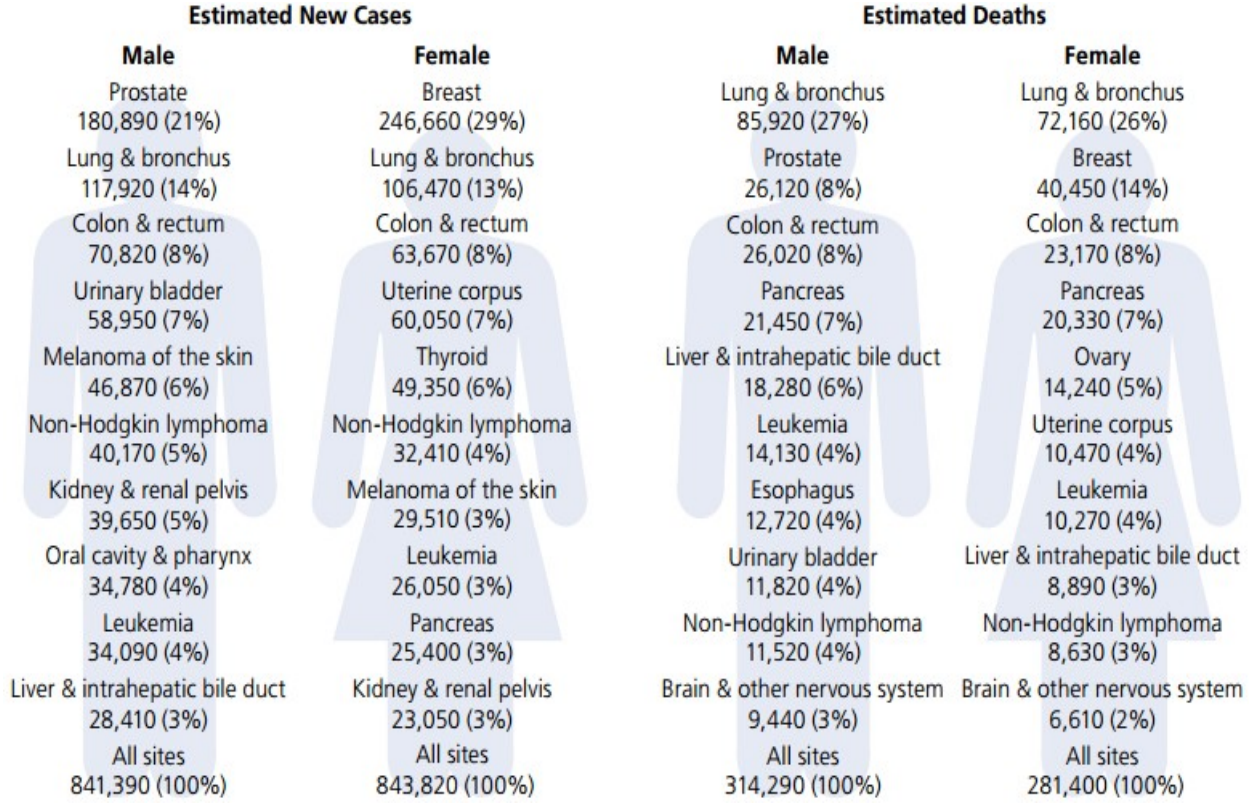

Figure 1.8: Leading sites of new cancer cases and deaths-2016 Estimates (Adapted from American Cancer Society, Inc.2016, [W.5]).

New Cases:

In 2016, invasive breast cancer will be diagnosed in about 2,46,660 women and 2,600 men. An additional 61,000 new cases of in situ breast cancer will be diagnosed in women. Breast cancer is the most frequently diagnosed cancer in women.

Deaths:

An estimated 40,890 breast cancer deaths(40,450 women,440 men) are expected in 2016. Breast cancer ranks second as a cause of cancer death in women.

Mortality trends:

From 2003 to 2012, breast cancer death rates decreased by 1.9% per year in white women and by 1.4% per year in black women. Overall, breast cancer death rates declined by 36% from 1989 to 2012 due to improvements in early detection and treatment, translating to the avoidance of approximately 249,000 breast cancer deaths.

Incidence trends:

From 2003 to 2012, the most recent 10 years for which data are available, breast cancer incidence rates were stable in white women and increased slightly (by 0.3% per year) in black women, resulting in the convergence of rates in blacks with those in whites.

Signs and symptoms:

The most common symptom of breast cancer is a lump or mass in the breast, which is often painless. Less common symptoms include other persistent changes to the breast, such as thickening, swelling, distortion, tenderness, skin irritation, redness, scaliness, nipple abnormalities, or spontaneous discharge. Breast pain is more likely to be caused by benign conditions and is not a common symptom of breast cancer.

1.15 DEFINING RISKS IN CANCER DEVELOPMENT

LIFETIME RISK:

Lifetime risk refers to the probability that an individual will develop or die from cancer over the course of a lifetime. In the US, the lifetime risk of developing cancer is 42% (1 in 2) in men and 38% (1 in 3) in women. These probabilities are estimated based on the overall experience of the

general population and may overestimate or underestimate individual risk because of differences in exposures.

RELATIVE RISK:

Relative risk is a measure of the strength of the relationship between a risk factor and cancer. It compares the risk of developing cancer in people with a certain exposure or trait to the risk in people who do not have this characteristic. For example, women who have a mother, sister, or daughter with a history of breast cancer are about twice as likely to develop breast cancer as women who do not have this family history; in other words, their relative risk is about 2.

1.16 TREATMENTS FOR CANCER

The main types of cancer treatments include as follows:

- Surgery
- Radiation Therapy
- Chemotherapy
- Immunotherapy
- Targeted Therapy
- Hormone Therapy
- Stem Cell Transplant
- Precision Medicine
- Treatments used in conjunction
- Hyperthermia heating systems i.e MNP's, Laser, High Intensity Focused Ultrasound(HIFU), Microwaves(MW), Radiofrequency(RF)

1.17 CASE STUDIES

Depending upon the indications, the hyperthermia treatment is given once or twice a week. Due to thermotolerance a general phenomenon pertaining to transient resistance to additional heat stress, it is impractical to apply two different HT sessions with an interval shorter than 48-72 hours, until the resistance decays to negligible level. Total number of sessions entirely depends upon the tumor characteristics and varies between 5 and 10 per patient. Chemotherapy is administered concurrently, radiation therapy must closely precede or follow the hyperthermia treatment by upto 120 minutes(Sardari et al.,2011[W.1]).

In a study involving 109 patients with superficial tumors, patients mostly suffering from breast wall recurrence due to mammary carcinoma, the enhancement effect of hyperthermia in combination with radiation therapy was demonstrated. Previously irradiated patients who underwent a second round of radiation therapy in conjunction with hyperthermia responded significantly better to this therapy. Complete remission was achieved in 68% of those treated with hyperthermia plus radiation while in the control group who did not receive hyperthermia, complete remission was received in only 24% of the patients.(E.Jones, 2005[111]).

CHAPTER 2

THEORETICAL BACKGROUND & UNDERLYING PHYSICS OF MAGNETIC NANOPARTICLES INDUCED HYPERTHERMIA

2.1 OVERVIEW

This chapter details about the theoretical background and underlying physics that establishes a very strong fundamental base to computational simulations. The chapter is discretized into twelve subsections that throws insight to concepts of hyperthermia, related terms, important definitions. Important considerations in hyperthermic studies details about noteable properties, parameters of nanoparticles, magnetic field concepts, Safe exposure and tolerable limits of humans to magnetic fields. The chapter is fully equipped and assisted with figures to explain the concepts there only. Mathematical model(Penne's Bio-heat Model) is explained with assumptions, advantages, drawbacks in relation to aid computational model. Relevant magnetic principles(Relaxation mechanisms) are well elaborated.Concept of averaging of properties after nanoparticles embedded into cancerous tissue is explained that will be an input to computational model. Lastly, an engineering approach to hyperthermia is discussed with hyperthermia treatment planning assisted with important role of simulations. Important heat quantization parameter is derived and defined in terms of (S.A.R)W/m^3 or (S.L.P)W/g_{Fe}.

2.2 PRINCIPLES OF HYPERTHERMIA

"Hyperthermia" comes from Greek word hyper("raise") and therme("heat").The clinical use of hyperthermia began in India around 3000years ago. It becomes part of a clinical protocol called "Panchkarma" that was used as a curative measure and preventive medicine. The first paper on hyperthermia was published in 1886 by Bush. Several clinical trials were developed in 1980's. Worldwide interest in hyperthermia is stated by the fact of initiation of first international conference on hyperthermic oncology in 1975 in Washington.

2.2.1 INTRODUCTION TO HYPERTHERMIA

Today, medical science is feeling helpless due to the loads of CANCER patients in the world, there is very urgent need to recall principle concepts of science and engineering to emerge at a one single platform to discuss this critical issuesand think for alternative proposals to tackle this critical issue. There is a foremost need that Microbiologists, Pharmacologists, Chemical engineers, Biomedical engineers, Radiodiagnosis experts, Doctors, Oncologists, Mechanical-thermal engineers should join their hands and provide a new technology base to address this unresolved problem. There is a keen need to create synergy in this direction and to increase the efforts to fourfold.

Hyperthermia is one of the techniques used in oncology that uses physical methods to heat certain tissue or organ by delivering an adequate temperature in an appropriate period of time(thermal dose), to the entire tumor volume for achieving optimal therapeutic results. The approach known as "magnetic fluid hyperthermia" is first proposed by Gilchrist et al.[103] to completely destroy the cancer cells in lymph nodes by injecting them with'particulate matter' of maghemite($\gamma - Fe_2O_3$) and observed the experimental observation after application of alternating magnetic field to induce 'selective inductive heating'. So far know since the nanotechnology based study grow by time, MFH has been approved in Europe for treatment of glioblastomamultiforme in a procedure that requires direct delivery of MNP's to cancer site.

Clinical trials are been performed byMagforce(Berlin,Germany based) to study the application of MFH for treating prostate and pancreatic cancer. This nanoparticle based therapy is of clinical interest and is also reported in a review study on MFH by Kozissnik et al.[104] as "magnetically mediated energy delivery"(MagMED).

The "intent of hyperthermia" is to raise the temperature of target tissue to alter its physiology and biology, and also at the same time to prime the tissue for greater response to be used as a standalone technique (monotherapy) or to be used in conjunction with other therapeutic modalities such as radiotherapy and chemotherapy. Thermal therapy in form of "Hyperthermia" involves long exposure times up to 30-60minutes with moderate temperature range achievement of 45°C is sufficient to do desired changes in tumor physiology. If the temperatures are further increased, a similar platform of heating is defined known as "Thermal ablation" which involves short exposure times up to 4minutes with high temperature range achievement of 50°C are very well studied and clinically proved modalities been studied by researchers, oncologists, engineers

as cancer healing treatment. The report of the European Society for Hyperthermic Oncology(ESHO) and the Committee for Concerted Action in Bio-Medical Engineering(COMAC BME) by Lagendijk et al., of 1992[102] was the first comprehensive document to summarize all available techniques and measurement data required for HTP(Hyperthermia Treatment Planning) and validation.

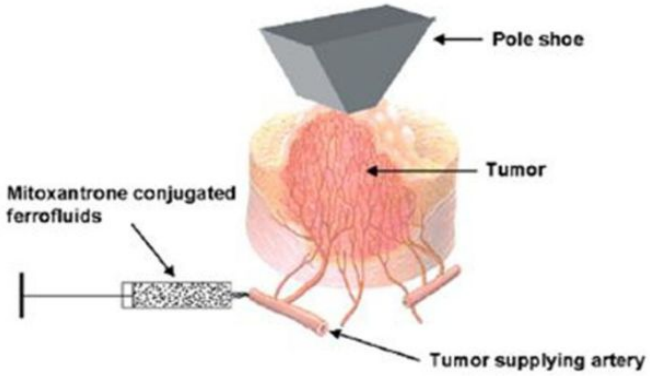

Figure 2.1:Supply of drug loaded ferrofluid to tumor supplying artery,[]

In the context of magnetic hyperthermia, the success of any new discoveries/ proposals/technologies/medicines/modalities depends upon the afterwards patient survival outcomes. The proof-of concept trials must show favourable results. R.Issels et al.,2016[] in their review article discussed about the six hallmarks of hyperthermia in driving the future of clinical hyperthermia as targeted therapy.1.Blocking cell survival 2.Inducing cellular stress response 3.Modulating immune response 4.Evading DNA repair 5.Changing tumor micro-environment, and 6.Sensitisation to radiation and chemotherapy. The hyperthermia used in addition to radiotherapy, chemotherapy, and surgery increases the *survival prognostic of patients.*

The most important feature is that the heat source is directly in contact with target cells. The factors which contributes towards the success of this therapy i.e. control of the deposition of nanoparticle dosages and the handling of the intratumoral distribution patterns.

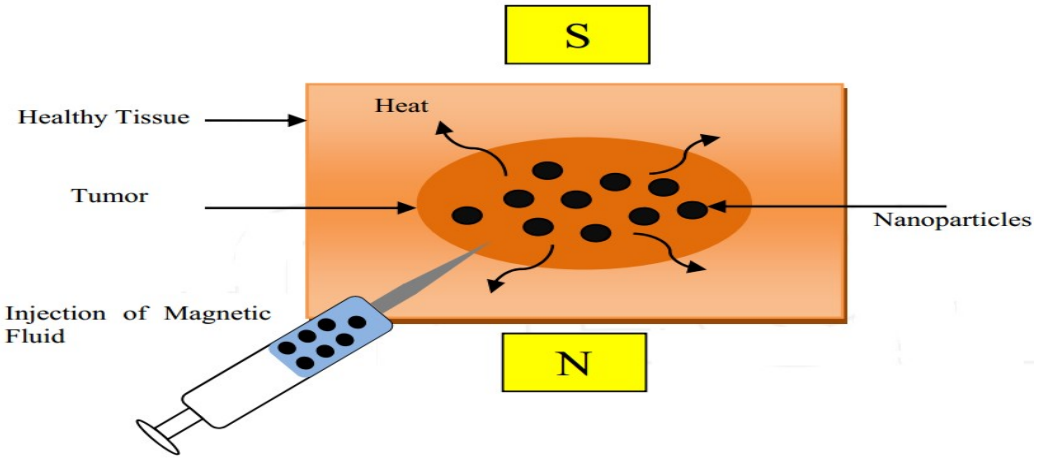

Figure2.2:Schematic of magnetic fluid hyperthermia process,(Reproduced from Lahonian M.et al.[W.4]).

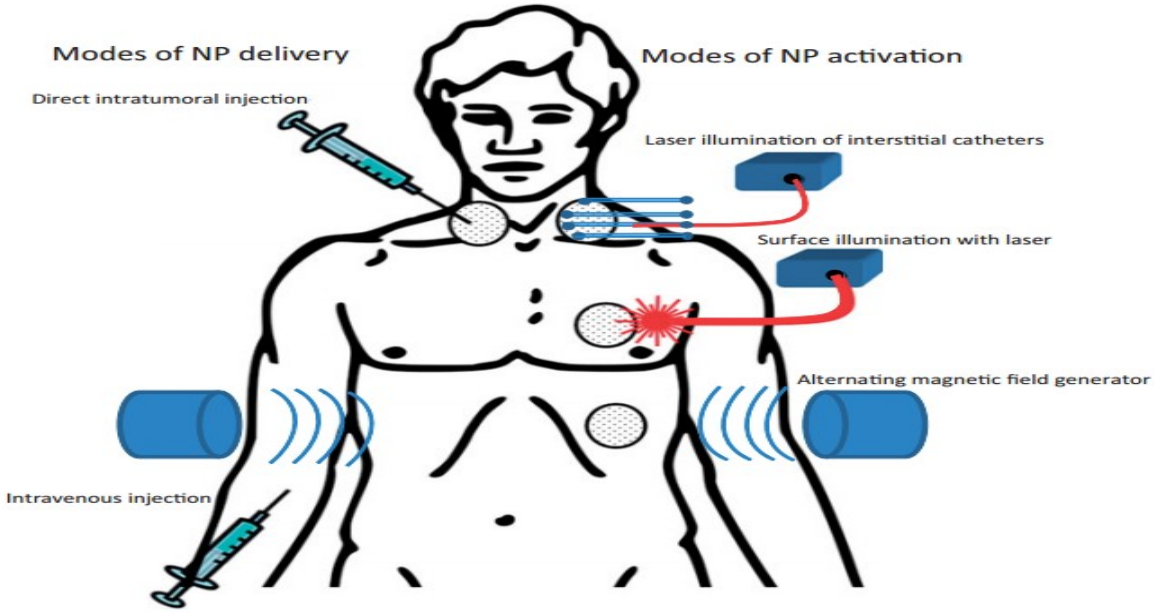

Figure2.3:Schematic illustration of modes of nanoparticle delivery and activation via mostly proposed modalities,(Adapted from Kaur et al.,2016[99])

2.2.2 TEMPERATURE TREATMENTS IN BIOLOGICAL TISSUES

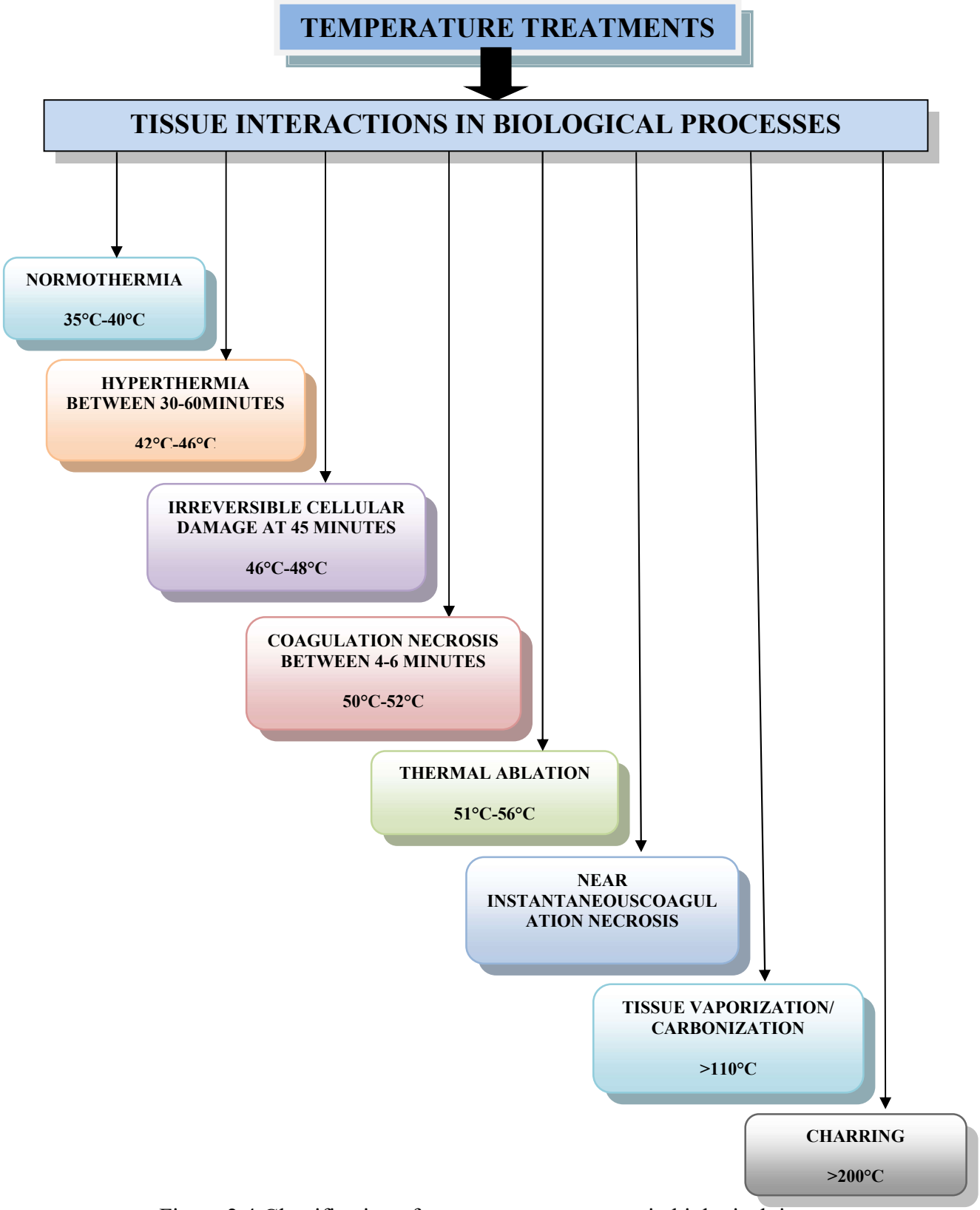

Figure 2.4:Classification of temperature treatments in biological tissues

2.2.3 CLASSIFICATION OF HYPERTHERMIA

- Local hyperthermia
  - External local hyperthermia
  - Intraluminal local hyperthermia
  - Interstitial local hyperthermia
- Regional hyperthermia
  - Deep regional hyperthermia
  - Regional perfusion hyperthermia
  - Other regional hyperthermic techniques
- Whole-body hyperthermia(WBH)
- Extracellular hyperthermia

Primary malignant tumors before occurrence of metastasis stage(Advanced Stage Cancer) are treated with local hyperthermia by superficial applicators(Energy sources may be RF, Microwave, HIFU).

External local/Superficial hyperthermia involves external applicators to be used to deliver the energy to the tumors below the skin for specific cell killing by the placement of intervening layer between them called “bolus”.

Intraluminal hyperthermia is used to treat tumors within or near body cavities(rectum or esophagus) by the placement of radiative probes inside cavity.

Interstitial hyperthermia is used to treat tumors deep within body(brain tumors) by the placement of probes or needles into the tumor to deliver energy along with pre-application of anesthesia.For large deeply seated, inoperable tumors, regional hyperthermia is used. It can be used to operate cervical and bladder cancers.

Regional perfusion hyperthermia is used to treat the cancers of legs and arms(eg. Melanoma).In this patient’s blood is removed, heated and then pumped or perfused back into the organ.

Whole body hyperthermia is achieved with either radiant heat or other technologies that can elevate the temperature of entire body to atleast at 41°C. Use of hot water blankets, inductive coils, or thermal chambers.

2.2.4 CHALLENGES IN HYPERTHERMIA

- Invasive method of generation of heat
- Difficulty in maintaining temperatures at desired levels
- Lack of monitoring and modeling
- Logistical hurdles with delivering and reimbursing this treatment
- Practical challenge of poor acceptance and adoption in clinic
- TECHNICAL CHALLENGE IN HYPERTHERMIA:

  The difficulty in limiting heating close to the tumor region without damaging the healthy tissue is a technical challenge in hyperthermia.

2.2.5 THERMO-NECROSIS OF EMBEDDED TISSUE

In order to examine the potential of hyperthermia as a viable candidate/alternative to chemotherapy and radiotherapy treatment, it is necessary to define what such a treatment would hope to accomplish.Temperatures in the range of 41°C -45°C are enough to slow or halt the growth of cancerous tissue,but such heating can also damage healthy cells.Ideal hyperthermia should sufficiently increase the temperature of tumor cells while maintaining the temperature of healthy tissue below 41°C.Ferrofluid based thermotherapy i.e thermo-ablation typically heats tissue upto 56°C.Ferrofluids are colloidal suspension of MNPs in a non-polar medium.

2.2.6 EPR EFFECT

Cellular uptake not only depends upon the cell type, but also on the size, shape, surface charge, and chemistry of the materials. Tumor vessels differs from normal ones particularly, because they are irregular in shape, leaky, defective(lack of basal membrane, endothelial cells poorly aligned) and dilated. An increased retention of the nanoparticles is attributed to the lack of lymphatic drainage in tumors. This effect is called Enhanced Permeability and Retention and Effect(EPR).

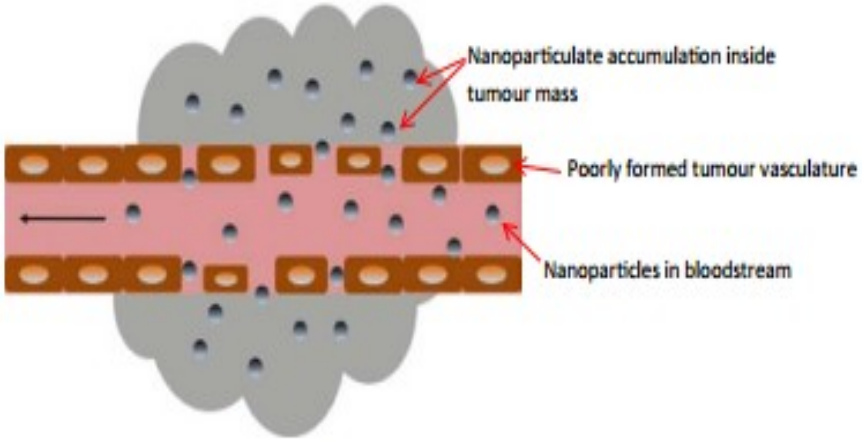

Figure 2.5:Schematic representation of the enhanced permeability and retention effect (Reproduced from Malekigorji M. et al.,2014[91])

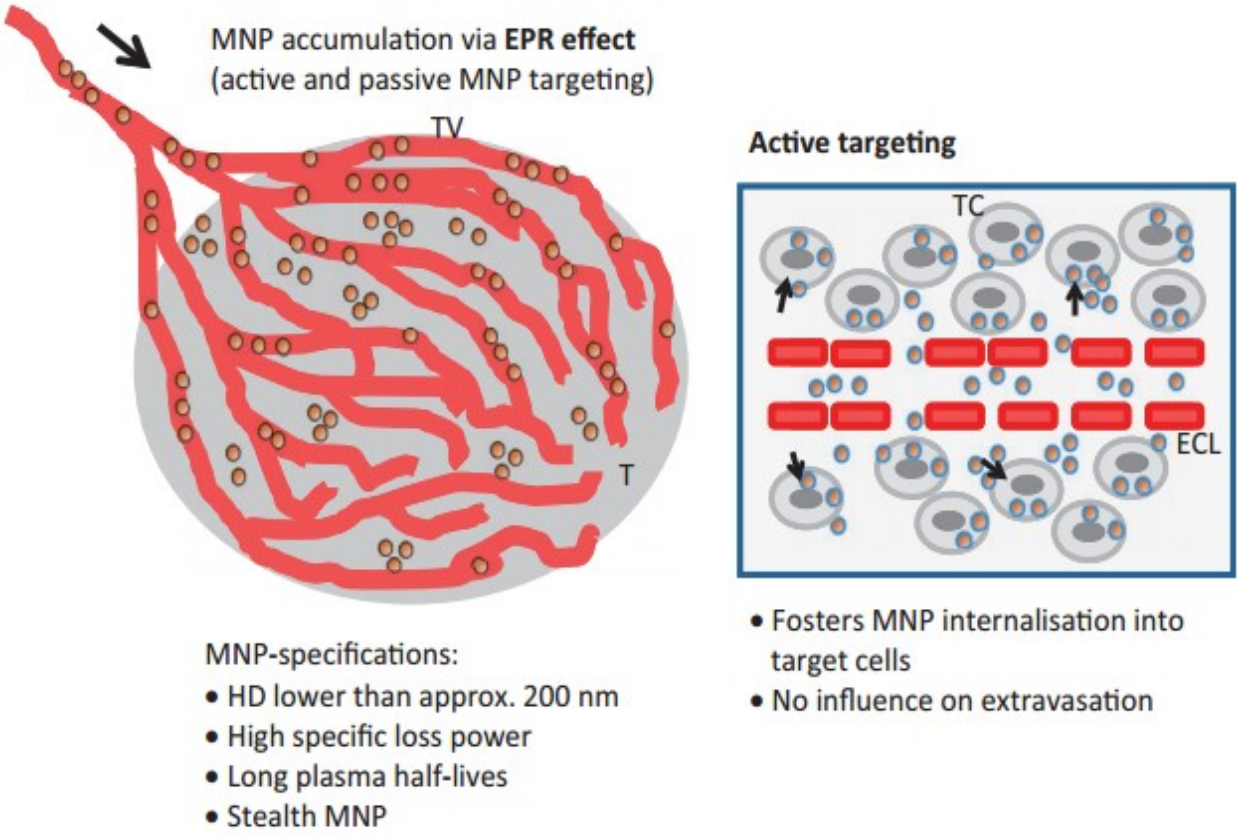

Figure 2.6:Rules governing active(internalization into target cells isaugmented) and passive targeting for magnetic hyperthermia based on EPR effect,(Adapted from Hilger et al.,2013[100]),where, ECL=Endothelial Cell Layer, MNP=Magnetic Nanoparticle HD=Hydrodynamic Diameter, TV=Tumor Vessel, T=Tumor TC=Tumor Cell

2.2.7 TUMOR/CANCER ANGIOGENESIS

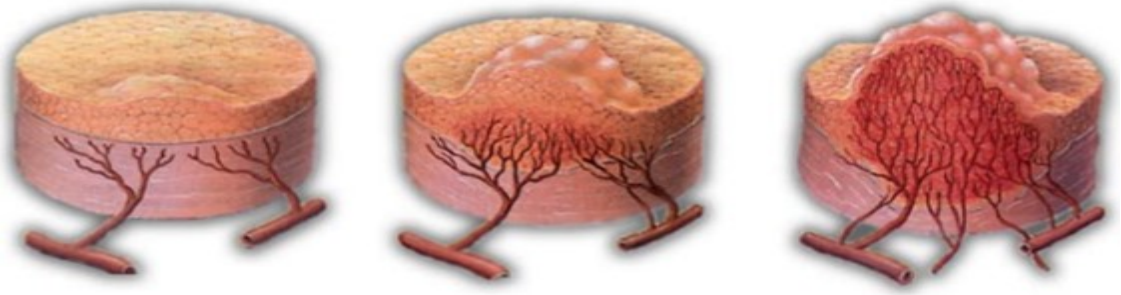

Figure 2.7:Depiction of growth of tumor: Tumor Angiogenesis (Adapted from Brusentsov et al.,2001[58]).

When a tumor reaches the size of a few cubic millimeters, it releases tumor angiogenic factors toward a neighboring vessel. “Tumor Angiogenesis” may be defined as process of formation of new blood vessels. Once the tumor gets the new supply of blood, it continues to grow until it spreads(metastasis) to other organs. Angiogenesis inhibitors may be used to restrict the spread but in context of hyperthermic studies, the best possible way is to load the tumor with nanoparticles and this blocking can restrict the particles to generate uniform heat by the application of magnetic fields. Magnetite and Maghemite are the two most promising particles that are studied by researchers and also found via clinical trials on animals(rats).

2.2.8 THERMAL ISO-EFFECTIVE DOSE:

The thermal iso-effect dose is an established quantity for assessing the therapeutic benefit of a treatment. As for now CEM 43°C T90 (cumulative equivalent minutes at a standard targeted treatment temperature of 43°C obtained within 90% of the tumour volume) appears to be the most useful dosimetric parameter in clinical research. Treatment planning based on the tumor cell survival has been proposed for thermoseedplacement , but up to now rather ad hoc cost functional based on the temperature distribution or on the absorption rate density have been used for regional hyperthermia(Overgaard et al.,2009[109]).

2.2.9 CONCEPT OF THERMOTOLERANCE:

The phenomena of thermotolerance complicates the practical application of this thermal isoeffect dose model. The dose modification caused by chronic thermotolerance which occurs during exposure at mild hyperthermic temperatures can be estimated by calculating the thermotolerance

dose ratio (TTDR) between the equivalent-minute dose calculated with and without a transition temperature at 43°C. The data suggest that the TTDR as a function of time can be mathematically described and used to correct for the dose modifying effect of thermotolerance. Using these results in a modification of the thermal isoeffect dose model causes a significant improvement in the fit for in vitro data below 43°C(Sapareto et al.,1984[110])

In magnetic nanoparticles(MNPs) induced hyperthermia,MNPs as the heat source the therapeutically optimal parameters are been determined and temperature distribution patterns are been discussed by the variants of most acceptable bio-heat transfer equation.Although this can be a demanding task, a planning tool greatly improves the medical treatment quality with a virtual experiment to model, simulate and optimize the therapy with high precision.

2.2.10 CLINICAL TRIAL

A clinical trial is an experiment that is used to assess the safety and efficacy of treatments or other interventions for human disease and health problems. Generally, participants receive either the state-of-the-art standard treatment or a new therapy that may offer improved survival and/or fewer side effects. Participation in clinical trials provides essential information on the effectiveness and risks of a new treatment.

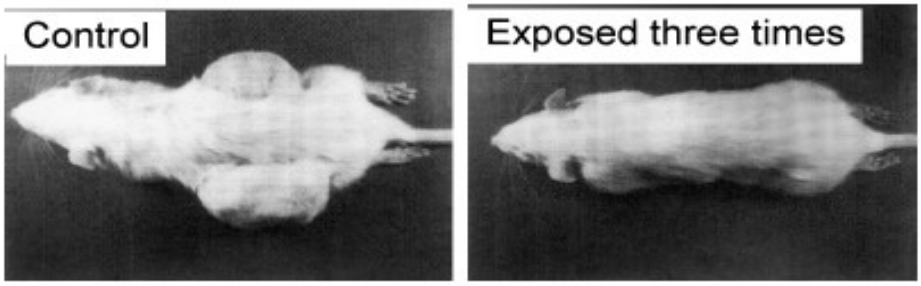

Figure 2.8:Preliminary clinical trials on rats,(Adapted from [96]).

2.2.11 SYNERGISTIC EFFECT

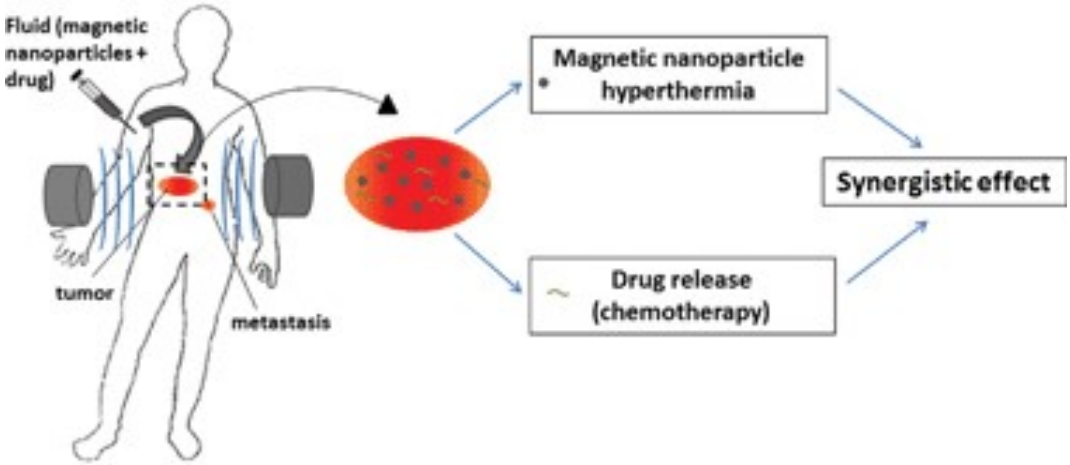

Figure 2.9:Hyperthermia in combination with other modalities:Synergistic effect,(Adapted from Wust et al.,2006[68])

2.3 TUMOR VASCULATURE

The architecture of the vasculature in the tumor is disorganized and abnormal compared to normal tissue(one of the main features being lower vessel density).In many cases, tumor blood flow remains greater than in the surrounding healthy tissues, especially in small tumors(tumor blood flow generally decreases with increasing tumor size). However, when hyperthermia, is applied at temperatures over 42°C, tumor blood flow tends to decrease while in normal tissue it significantly increases. This decreased blood flow results in a lower heat dissipation rate, and hence the temperature in the tumor will rise faster than in normal tissue. This difficulty in dissipating heat may cause cancer cells undergo apoptosis(programmed cell death).

Necrosis is a form of cellular damage that results in premature death of cells in body tissues and initiates an inflammatory response in the surrounding environment. Hyperthermia induced apoptosis is therefore preferable.

2.4 IMPORTANT CONSIDERATIONS IN HYPERTHERMIA STUDIES

(MNPs employed, Magnetic field exposure, Tissue under consideration)

Due to their small size and particularly due to their increasing surfacearea-to-volume ratio, the properties of nanosized materials will differ from the ones of bulk materials(i.e optic, catalytic, magnetic and electronic properties).

TYPE OF EVALUATION STUDIES/ANALYSIS INVOLVED

- Experimental
- Computational
- Analytical
- Theoretical
- Numerical
- Review

NANOPARTICLE RELATED

- Size
- Material
  - Iron(Magnetic and superparamagnetic)
  - Gold
- Shape
  - Nanospheres
  - Nanorods
  - Nanoshells
  - Agglomerates/Aggregation
- Surface coating
- Composition
- Concentration
- Saturation magnetization
- Magnetic anisotropy
- Particle distribution
  - Monodispersion
  - Polydispersity
- Nanoparticle properties
  - Thermal conductivity
  - Specific heat
  - Density

MEDIUM

- Suspending medium
- Viscosity
- Specific heat
- Volume fraction
- Ferrofluid concentration

HEATING MECHANISMS

- Relaxation mechanism
    - Néel relaxation
    - Brownian relaxation
- Hysteresis
- Eddy currents

MAGNETIC BEHAVIOR

- Superparamagnetic-Single domain
- Multi-domain
- Bulk material

EXCITATION SOURCE PROPERTIES

- Alternating magnetic fields
    - Applied frequency
    - Field strength/amplitude
    - Uniformity
    - Eddy currents
    - Time exposure
- Laser sources
    - Strength
    - Duration
    - Frequency

INJECTION RELATED

- Injection rate and amount
- Locations of injection sites

TISSUE RELATED

- INTRINSIC
  - Bio-heat transfer
    - Specific heat capacity of tissue and blood
    - Density of tissue and blood
    - Thermal conductivity of tissue
    - Blood perfusion rate
    - Arterial temperature
    - Metabolic heat generation and applied heat
    - Tissue Porosity and Tortuosity
  - Tumor shape and size
  - Heterogeneity
- pH of environment
- Nanoparticles in tissue
  - Concentration
  - Spatial distribution
  - Temporal distribution

HEAT MEASUREMENT MEASURE

- Specific absorption rate(S.A.R)
- Specific loss power(S.L.P)
- Intrinsic loss power(I.L.P)

S.A.R EVALUATION STUDY

- In-vitro studies
- In-vivo studies
- Phantom based studies

In nutshell, these are the important factors

- ❖ Duration of hyperthermia
- ❖ Homogeneity of temperature in tissue
- ❖ Tissue type
- ❖ Context of treatment

2.5 NANOPARTICLE ASSISTED THERMAL THERAPY: AN EVOLVING RESEARCH AREA

2.5.1 INTRODUCTION

A new entrant in the field of hyperthermia is Nanotechnology which capitalizes on locally injected or systemically administered nanoparticles that are activated by extrinsic energy sources. Nanoparticles interaction with the tissues is analysed to be a very interesting area of research where it is expected and envisioned to be "*future relies in nanoheat carriers*". These are the reliable sources to project their reach to deep seated regions. Once injected inside the body, they can successfully invade the tumor regions and enter through the leaky vasculature of tumors. One such proof-of-principle concept study is an assessment of in-vitro studies including tissue particle interaction to assist realistic in-vivo studies.MNPs are therefore recalled as promising candidates for CANCER related therapies.

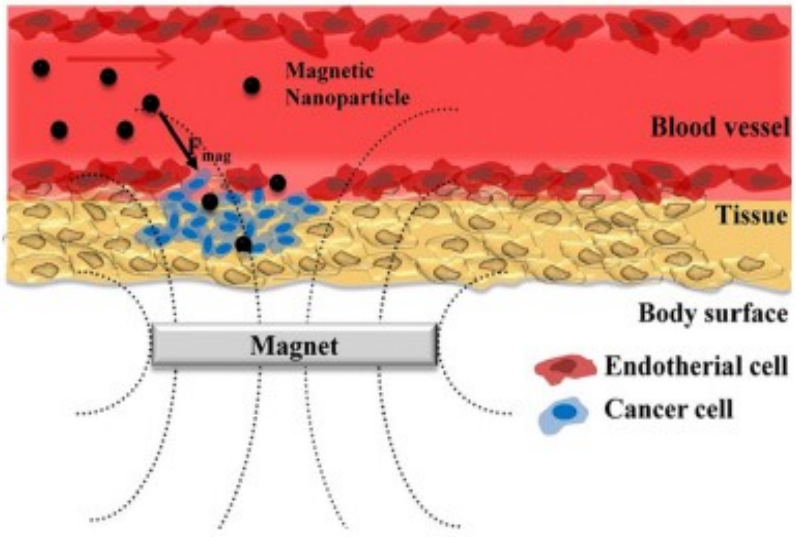

Figure 2.10: Representation of concept explanation of magnetic nanoparticles dragged into cancerous cells under the influence of external magnetic field.-(Adapted from Park et al., 2010[94]).

2.5.2 DEFINING NANOPARTICLES

"Nanoparticles" are traditionally defined as a class of smart materials whose scope of applicability is not only confined to engineering defined problems but to address the special issues of medical science which are been unresolved till date. Nanoparticles are simply particles in the nanosize range (10^{-9} m), usually,have their size dimensions less than 100nm, although the particles upto 1μm in size are also defined and lumped within this definition. Due to their small size and surface area characteristics, they exhibit unique electronic, optical, and magnetic properties that can be exploited for drug delivery and heat interacted applications.When these metallic particles are considered as bulk materials, for interaction with surrounding molecules, they are found to be have greatest potential to invade the complex vasculature of human body to reach through very fine microchannels to establish their well defined base for medical oncology. They are also known as nanovectors in the field of targeted drug delivery(controlled release of drugs) because they can satisfy the two most important criteria for successful therapy, i.e, spatial placement and temporal delivery.These particles can induce the specific changes into the tumor pathophysiology which ultimately leads to apoptosis at elevated transient temperatures.The NPs are designed to combine several therapeutic functions(hyperthermia and drug delivery) or therapeutic and diagnostic functions(so-called theranostics).

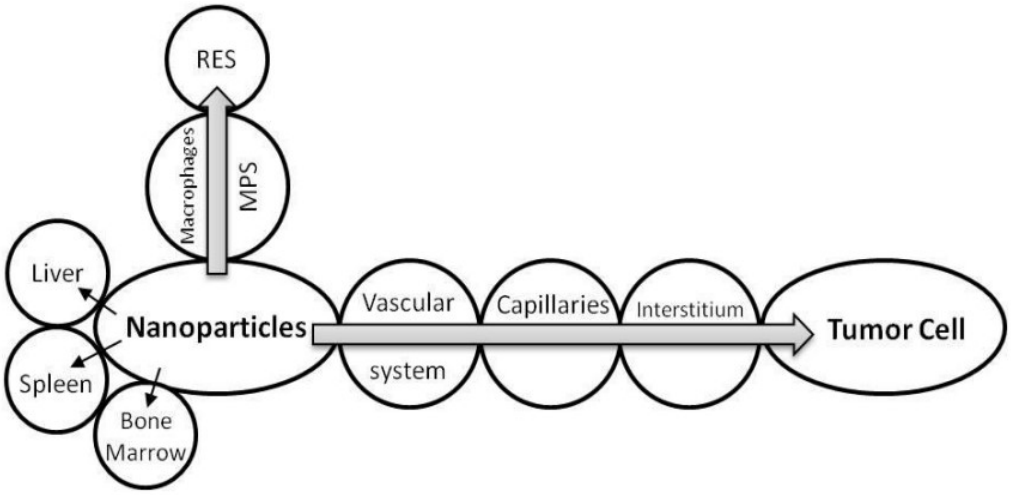

Figure 2.11:Different cases of distribution and the routes taken by nanoparticles after injection into the body for cancer therapy,(Adapted from ChallaS.S.R.Kumar, 2005[97]).

The magnetic nanoparticles/seeds are placed at the tumor locations to focus large amount of energy. When these nanoparticles are exposed to time varying magnetic field, specific magnetisation take place which induce magnetic hyperthermia.This nanoparticle assisted thermal

therapy referred to as “Magnetic Fluid Hyperthermia(MFH),” has found to bridge the gap of unresolved issues of medical science.A unique attribute of Nanoparticle-mediated hyperthermia is the potential for confinement of hyperthermia conformally to the tumor via active targeting of the nanoparticle to the tumour as a means of enhancing the*tumour-to normal tissue* ratio of *nanoparticle accumulation.*

Depending upon the morphological features of magnetic material i.e(nanoparticle size, nanoparticle shape, microstructure) different mechanisms are been quantified which are responsible for delivery of heating. The magnetic particles are been classified as multi-domain and single domain particles. In relation to multi-domain particles(size larger than >40nm depending upon magnetic field parameters), heating is delivered by displacements of the domain wall(hysteresis loss).In contrast, suspensions of nanoparticles with diameters lower than 40nm are called superparamagnetic nanoparticles which usually exhibit single domain wall and the process of heating is reorientation of the magnetisation in the magnetic field or frictional losses where the nanoparticle is able to rotate in surrounding medium.

2.5.3 ADVANTAGES OF NANOPARTICLES

- Excellent conductors of heat
- Can efficiently transmit heat generated within them to surrounding tissue
- Can accumulate preferentially in tumors via the enhanced permeability and retention effect(EPR effect) when administered via intravenous injection.
- Particles can extravasate from leaky, immature, chaotic tumor blood vessels due to tumor angiogenesis process.
- No adverse effect as per experimental investigations performed via clinical trials on mouse, rabbits, rats to efficiently clear the lymphatic drainage system.

2.5.4 PROPERTIES OF IRON-OXIDE PARTICLES

Iron –oxide MNPs are still the most studied magnetic material for hyperthermia applications due to their:

- Non-toxic
- Non-immunogenic
- Biocompatible
- Stable

- Possibly biodegradable
- Ease of synthesis
- Surface functionalisation

2.5.5 FACTORS INFLUENCING EXTENT OF HEATING

There are many factors that must be considered during heating of nanoparticles:

- Magnitude of AMF
- Size and characteristic of SPIONs
- Concentration of SPIONs in the tumor
- Depth of tumor within body
- High loading of SPIONs
- Efficient generation of heat
- Localization within the centre of the tumor

2.6 CONCEPT OF INJECTION AND ITS CLASSIFICATION

Nanoparticles can extravasate to tumor interstitium due to complex specific tumor vessel architecture. There are different methods of administering the nanoparticles into the site of tumor either via Direct injection(Inhomogeneous distribution but more concentration at the specific injection site, lesser time to invade the tumor) and Intravenous injection(Homogeneous distribution but less concentration of particles at the tumor location, more time to invade the tumor). Similarly, Active and Passive targeting are the further routes of reach to target tissues.

- Systemic Injection(Intravenous Injection)
  - Active targeting
  - Passive Targeting
- Direct Injection(Intratumoral Injection)

Prospects of Passive-targeting in magnetic hyperthermia:

Passive targeting is the local accumulation of nanoparticles as a result of particular physiology and anatomy of the tumor after intravenous application. Passive targeting of MNPs could be favourable in terms of improving a homogeneous distribution. Accumulation of particles at the target site can be controlled to a lesser extent compared to intratumoral application. This makes this methodology particularly challenging and is one of the reasons why it has not been as intensively pursued compared to intratumoral application of the magnetic material.

Intravenous injected nanoparticles will mainly accumulate in the liver and spleen and to comparatively lower extent in brain, heart, kidney, and lung. Therefore, to favour the accumulation of nanoparticles via passive targeting is the use of "stealth" MNPs with increased circulation time and a reduced uptake by MPS(monocyte phagocyte system).

Passive targeting tightly depends on the pathophysiology of the tumor such as vascularisation degree, interstitial pressure, lack of lymphatic drainage and the structural features of the magnetic material(Size, Surface, Coating).Passive targeting favours the homogeneous nanoparticle distribution pattern and therefore the therapeutic outcome of hyperthermia.

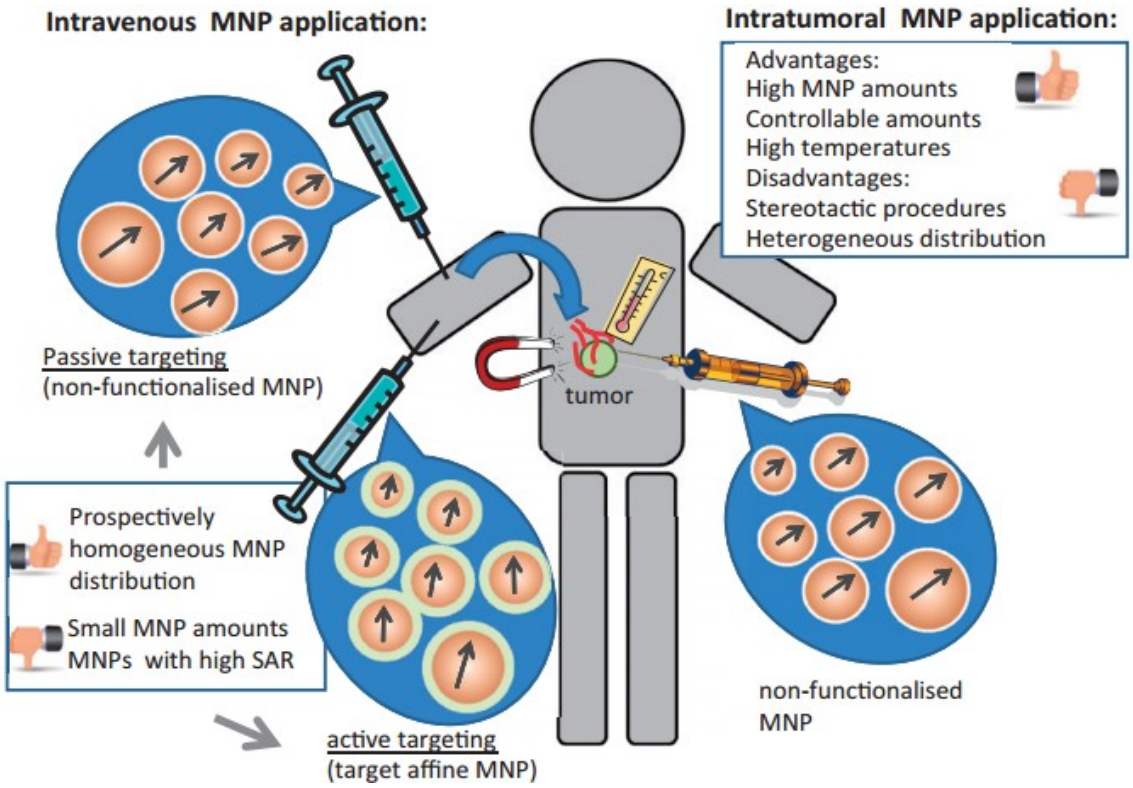

Figure 2.12: Different application routes of magnetic nanoparticles and their implication for magnetic hyperthermia(Adapted from Hilger etal.,2013[100]).

Prospects of Active-targeting magnetic hyperthermia:

Active targeting of MNPs for hyperthermia has ideally the advantage of a highly selective accumulation at cells within the tumor with a high affinity binding between the nano-particle surface and a selective target structure at the tumor region. The magnetic particles are sought to accumulate particularly at the tumor interstitium surrounding the hyper-vascularised areas of the tumor. However, upto now there are contradictory results on how active targeting can really

increase the nanoparticle accumulation in tumors which is been a topic of debate in scientific community.

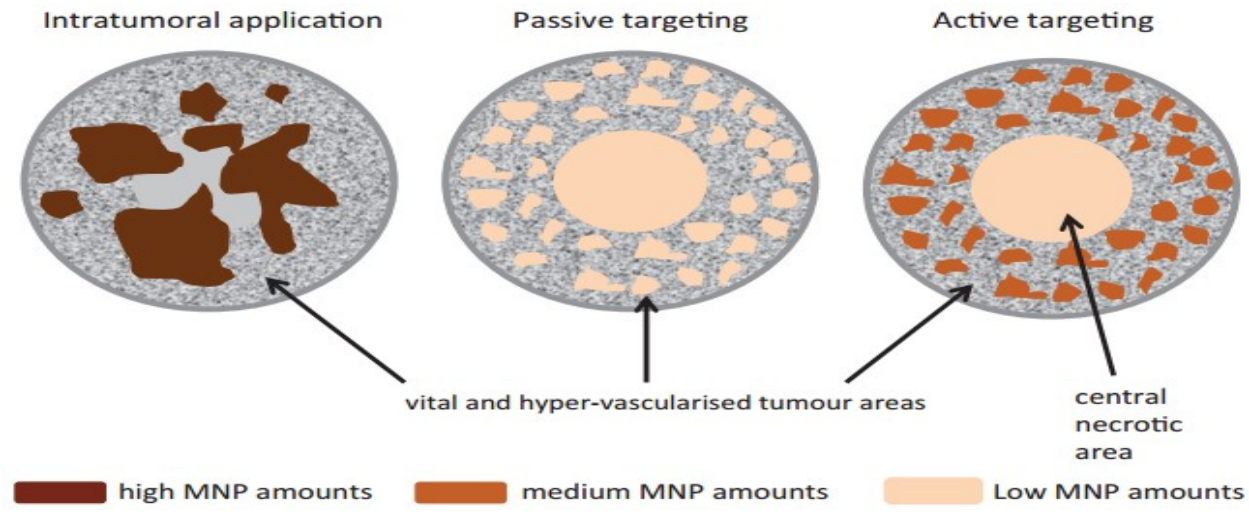

Figure 2.13 Concept stating Intratumoral and Intravenous(Active Targeting and passive targeting) injections and also the nanoparticle distribution patterns (Heterogeneous and Homogeneous distributions), (Adapted fromHilger et al.,2013[100]).

2.7 ISOTHERMS OF HUMAN BODY:

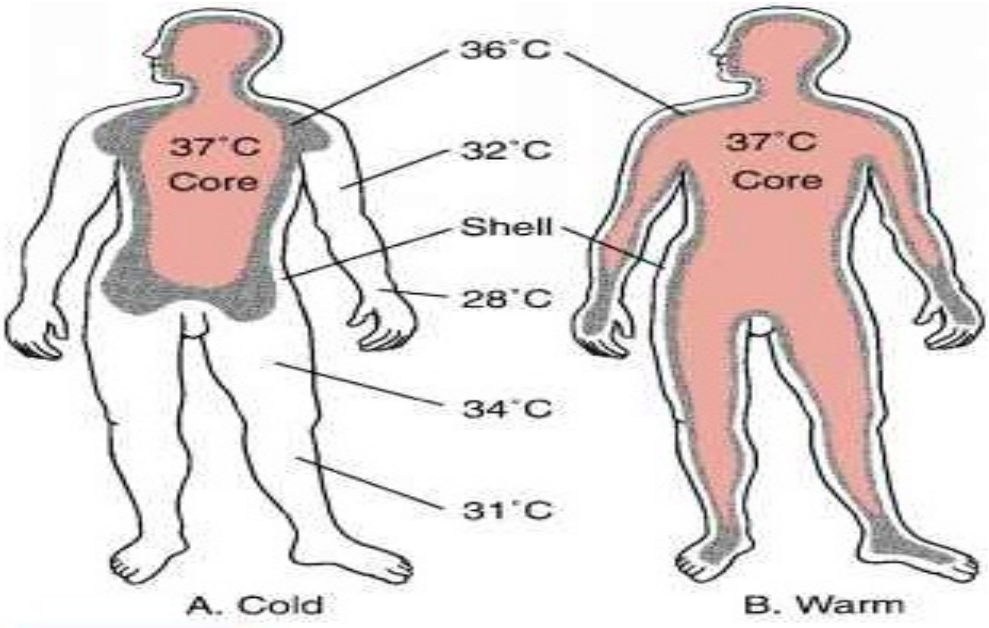

Figure 2.14:Temperatures isotherms within the human body in cold(A) and warm(B) surroundings [W.10]

Core Temperature of the Body(Homeothermic core):

It is been seen from the isotherms plots of human body that core temperature is 37°C which is also used as one of the important input parameter in our computational work.

2.8 PHENOMENON OF HEAT TRANSFER IN HUMAN BODY AND CONCEPT OF THERMOREGULATION:

Thermoregulation is the ability of an organism to keep its body temperature within certain boundaries, even when the surrounding temperature is very different.

Heat is been produced within all tissues of the human body but is lost due to the environment contact from nearby tissues predominantly from the skin and also from respiratory tract but to a lesser extent. There is an immense need to consider heat transfer within the body, especially

1.The heat transfer from major sites of heat production to the rest of the body,

2.The heat transfer taking place from the core to the skin.

Table 2.1:Significance of heat transfer modes involved in typical biological/biothermal systems

HEAT TRANSFER MODES	**BIO-THERMAL SYSTEMS**			
	TISSUES	BONES	BLOOD VESSELS	SKINS
Conduction	Significant	Significant	Less significant	Insignificant
Convection	Less significant	Insignificant	Significant	Significant
Radiation	Insignificant	Insignificant	Insignificant	Significant

Heat is transported within the body by two main means:

1.Heat transfer through Conduction phenomenon through the tissues

2.Heat transfer through Convection phenomenon by the blood i.e a process in which flowing blood carries heat from warmer tissues to cooler tissues.

Heat flow by conduction varies

1.Directly with the thermal conductivity of the tissues,

2.The change in temperature over the distance the heat travels,

3.The area (perpendicular to the direction of heat flow) through which the heat flows.

4.It varies inversely with the distance the heat must travel.It is been justified in literature that the tissues are rather poor heat conductors.

Heat flow by convection depends on

1.The rate of blood flow

2.The temperature difference between the tissue and the blood supplying to the tissue. Because the vessels of the microvasculature have thin walls, a large total surface area, the blood comes to the temperature of the surrounding tissue before it reaches the capillaries. Changes in skin blood flow in a cool environment change the thickness of the shell. When skin blood flow is reduced in the cold, the affected skin becomes cooler.

2.9 STRUCTURE OF BLOOD PERFUSED TISSUES

The biological tissues include the layers of skin, fat, muscle and bone. Skin is composed of two stratified layers: epidermis and dermis.

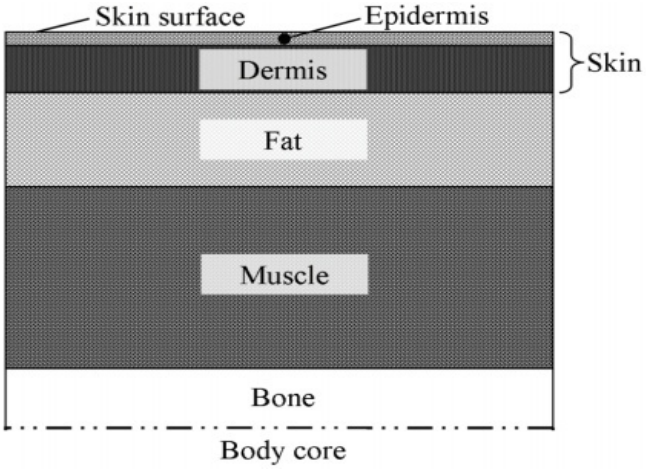

Figure 2.15:Schematic structure of blood perfused tissues(Adapted from Chapter by Zolfaghari A. *et al*[W.2]).

2.10 MATHEMATICAL MODELING

2.10.1 Classification of Bio-heat Models:

The effects of blood flow on heat transfer in living tissue is been quantified by various bio-heat transfer models which is based upon two noteable approaches i.e the continuum approach and the discrete vessel(vascular) approach.

In the continuum approach, the thermal impact of all blood vessels; models with a single global parameter. The effect of blood flow in the region of interest is averaged over a control volume. Thus, in the considered tissue region, there is no blood vessel present; however its effect is treated by either adding an additional term in the conduction equation for the tissue or changing some of the thermophysical parameters in the conduction equation.Continuum models cannot describe point-by-point temperature variations in blood. Blood vessels disappears. Still they are well studied and validated based on the fundamental heat transfer aspects.

In the vascular approach, the thermal impact of each blood vessel individually(Raaymakers et al.,2009[108]).Large blood vessels may significantly cool tissue volumes around them, making it very difficult to cover the whole tumor volume with therapeutic thermal exposure.

The bio-heat models which are been studied, commented and accepted models are provided in undermentioned table.

Table 2.2:Important Mathematical Models in hyperthermic studies.

MODEL	YEAR
Pennes Continuum Model	1948
Wulff Continuum Model	1974
Klinger Continuum Model	1974
Chen-Holmes(CH) Continuum Model	1980
Weinbaum, Jiji and Lemons(WJL) Bioheat Model	1984
Simplified Weinbaum-Jiji(WJ) Model	1985
Wissler Mathematical Whole Body Model	1985
Charny Evaluative and Reviewal of WJL model	1990
Baish Statistical Model	1994
Brinck and Werner Vascular Model	1994
Fu Mathematical Model	1995
Zhu Model	1996
Xuan and RoetzelVolume Averaging Model	1997
Weinbaum Model	1997
Roemer and Dutton Volume Averaging Model	1998
Zhu Model	2002
Salloum Theoretical Model	2005
Nakayama and KuwaharaVolume Averaging Model	2008
Shrivastava and Vaughan Volume Averaging Model	2009
Simplified Thermoregulatory Bioheat (STB)Model	2010
Pearce Theoretical Model	2013
Whitney Arrhenius Parameter based Model	2013
Prakash MathermaticalModel	2013
Chiang Computational Model	2013
Reddy Thermal Dose Model	2013
FahrenholtzPolynomial Chaos Method Model	2013

Kok's Discrete Blood Perfusion InclusionMathematical Model	2013
Paulides Simulation Model	2013

2.10.2 PENNE'S BIO-HEAT EQUATION: (Based on CONTINUUM MODEL)

PBHE(Penne's Bio-heat Equation) method is mostly used for thermal modeling of clinical applications. It models the effect of blood perfusion as a temperature- dependent heat source or sink term which is proportional to blood flow rate and the difference between the body core temperature and local tissue temperature i.e practically simulate convection heat transfer of blood. It is been assumed that the blood perfusion effect is homogeneous and isotropic, and that thermal equilibration occurs in the micro-circulatory capillary bed. Penne's also describes the effects of metabolism and blood perfusion on the energy balance within the tissues. $\rho_t c_t \frac{\partial T_t}{\partial t} + \nabla.(-k_t \nabla T_t) = Q_{blood} + Q_{metabolic} + Q_{source}$

(2.1)

$$Q_{blood} = \rho_b \omega_b c_b (T_b - T_t) \quad (2.2)$$

$$\rho_t c_t \frac{\partial T_t}{\partial t} + \nabla.(-k_t \nabla T_t) = \rho_b \omega_b c_b (T_b - T_t) + Q_{metabolic} + Q_{source} \text{where,} \quad (2.3)$$

ρ_t =Density of tissue

c_t =Specific heat capacity of tissue

T_t =Temperature variations of tissue with time t

t =Exposure time duration

k_t =Thermal conductivity of tissue

Q_{blood} =Contribution of blood perfusion rate

ρ_b =Density of blood

ω_b =Blood perfusion rate

c_b =Specific heat capacity of blood

T_b =Arterial blood temperature

$Q_{metabolic}$ =Amount of energy generated by metabolic processes or volumetric rate of metabolic heat generation

Q_{source} =Heat generation by loss power or Power generated per unit volume of nanoparticle or distributed volumetric heat generation due to spatial heating

Assumptions:

1. The model properties such as mass density, heat capacity, and thermal conductivity of tissue as well as metabolic heat parameter are constant.
2. The rate of heat transfer from blood to tissue is proportional to the temperature difference between tissue and blood in arteries.
3. The volumetric blood perfusion rate and arterial blood temperature are constant throughout the tissue.
4. Large blood vessels in the vicinity of capillary beds play no role in the energy exchange between tissue and capillary blood.
5. Blood is assumed to reach the arterioles supplying the capillary bed at the body core temperature. It instantaneously exchanges energy and equilibrates with the local tissue temperature.
6. The flow of blood in small capillaries is assumed to be isotropic. This neglects the effect of blood flow directionality.

Advantages:

1.It leads to reasonable estimates within the known uncertainty of tissue properties.
2.It can be applied without the inclusion of accurate vascular trees, which are computationally unmanageable for large tissue regions.

Drawbacks:

1. Tissue heterogeneity was not considered and the perfusion term in the equation is a scalar, thus non-directional.
2.Penne's equation is unable to take into account thermal effects of large vessels in the tissue domain of interesti.e the model doesn't considers local vascular geometry.
3. Directionality of blood perfusion is not considered that accounts for exchange of energy between vessels and tissues.

2.11 RELEVANT MAGNETIC PRINCIPLES

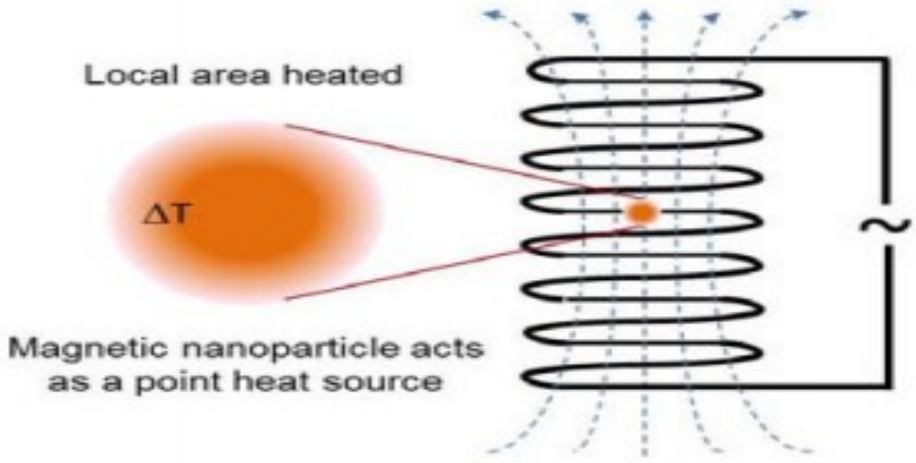

Figure 2.16:Schematic of mechanism of hyperthermia induction inside magnetic field (Reproduced from Malekigorji M. et al.,2014[91]).

2.11.1 SAFE& TOLERABLE LIMITS OF EXPOSURE OF HUMAN BEINGS TO AC MAGNETIC FIELDS

The field frequency and amplitude used to generate the heating area are limited by biomedical reasons.Brezovichet al.[105]concluded that the safe exposure to magnetic fields as $H.f \leq 4.85\times10^{8}\ Am^{-1}s^{-1}$ which has also been confirmed by Pankhurst[106]. Hergt[107] further defined the weaker criterion with C=5 x $10^{9}Am^{-1}s^{-1}$, where H.f<C.

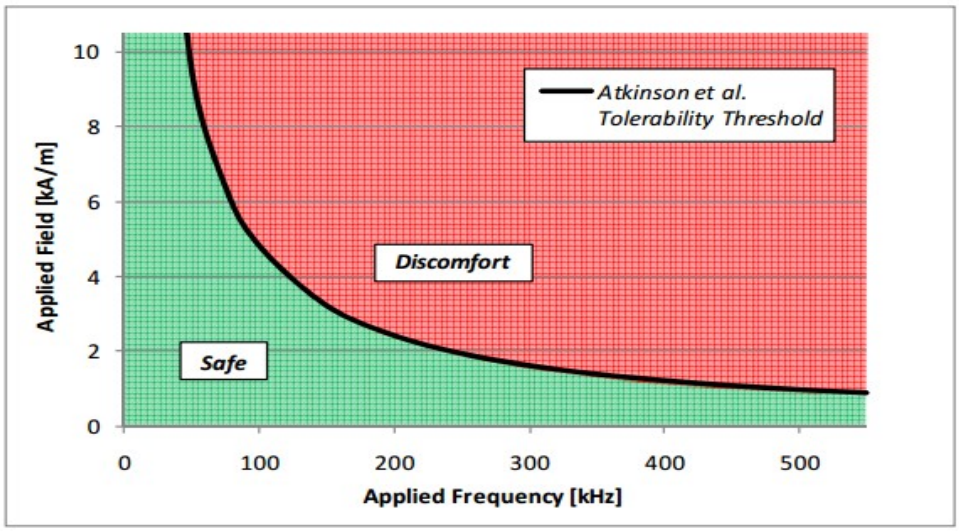

Figure 2.17:Clinical limits of AC magnetic field parameters proposed by Atkinson *et al.*, 2007 [92].

2.11.2 PHYSICAL MECHANISMS OF HEAT GENERATIONS

The heating mechanism for magnetic nanoparticle fluids has been detailed by Rosensweig[20] by using the Debye's model for dielectric dispersion in polar fluids.

Mechanism of heat:

The conversion from magnetic energy to thermal energy in MNPs subjected to AC magnetic field can be due to several mechanisms. The heating of magnetic nanoparticles arise due to magnetization reversal in the particle system. At larger sizes there exists multi-domain ground state leading to narrow hysteresis loop as it exploits relatively less field energy to make the domain walls move. When an external magnetic field is applied, the magnetic domains tends to align themselves in the same direction as the applied field. The saturation magnetisation is reached as soon as each moment of each domain is aligned towards this direction.In smaller particles there existsthe individual a single domain ground state leading to broad hysteresis loop. At even smaller sizes they show superparamagnetism where the M-H curve is sigmoidal but non-hysteretic. In this state, the magnetic moment of the particle is a whole free to fluctuate in response to radiative energy maintaining the individual atomic moments in their ordered state relative to each other. At small sizes the energy barrier for magnetization reversal also decreases and thus thermal fluctuations leads to relaxation phenomenon. This is the principal heating source for magnetic particles.

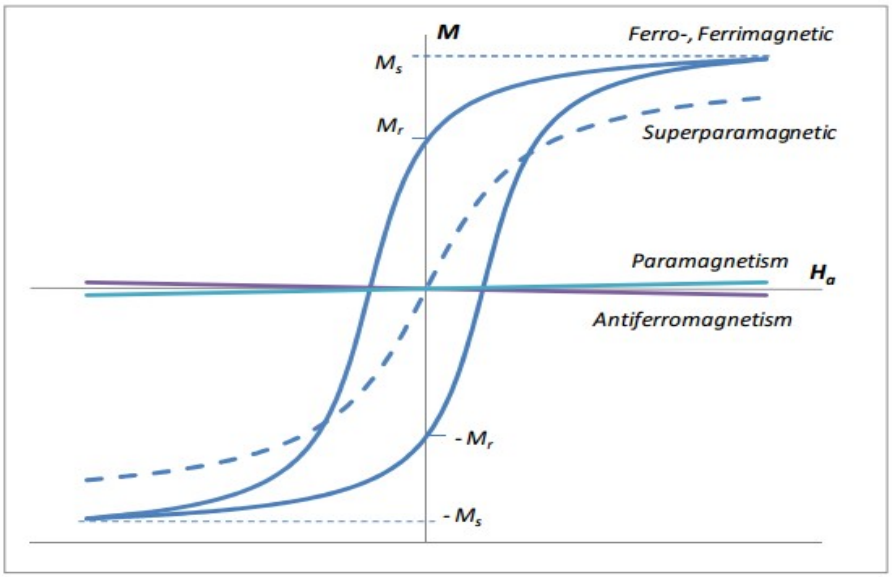

Figure 2.18: Characteristic response to an applied field for various types of Magnetism (Adapted from [W.3]).

Remanent magnetization:

When the applied field is removed, the magnetization doesn't revert back to zero, and this is called remanent magnetization.

Coercivity/Coercive field: In order to reduce the magnetization to zero again, a magnetic field with a precise intensity needs to be applied, and it is called coercivity.

Superparamagnetism is a form of magnetism that occurs in ferromagnetic or ferrimagnetic materials when they are in the form of sufficiently small NPs.

Bulk materials basically contain multiple magnetic domains due to their large size. However, small enough NPs are single domain particles which can be regarded as one giant magnetic moment composed of all magnetic moments of the atoms forming the NPs. Super-paramagnetic NPs are preferred over ferri- and ferromagnetic NPs for biomedical applications, because they don't retain any magnetization once the magnetic field is removed. Single-domain NPs dissipate heat through relaxation losses which fall under two modes: Néel relaxation and Brownian relaxation. The mechanism of relaxation depends on the size of NPs but also on the magnetic material (due to its anisotropy constant).Néel relaxation comes from the reorientation of the magnetic moment in the same direction as the applied magnetic field with each field oscillation.

RELAXATION MECHANISMS: SUPERPARAMAGNETIC NANOPARTICLES
RELAXATION MODES

Depending on the size of MNP's the particles can be found in following magnetic states i.esuperparamagnetic, single domain or multi-domain ferro or ferromagnetic. Due to these states ,the heat generation within the tissue is mainly attributed to three types of loss processes. These are classified as:

1. Hysteresis losses(Ferromagnetic(FM), multi-domain behavior of particle)
2. Relaxation losses(Heat generation in superparamagnetic (SPM) regime, single domain particles)
   2.1 Brownian relaxation
   2.2 Néel relaxation
3. Resonance losses(Occurs at higher frequency range and is unsuitable for MFH therapy and can be neglected).
4.Eddy current loss in bulk magnetic materials

On application of the magnetic field the domain walls in ferromagnetic materials are washed away and aligned to the direction of the magnetic field. Whereas, in a superparamagneticmaterials usually defined as the single domain structure has no domain walls, but magnetic moments align to the direction of the applied external magnetic field.

In the first case, the hysteresis losses($L.P_{FM}$= Loss power for Ferromagnetic(FM) particles) are equal to the area of hysteresis loop multiplied by frequency.

$$L.P_{FM} = \mu_O f \oint H.dM \text{ where,} \tag{2.4}$$

Permeability, $\mu_O = 4\pi \times 10^{-7} H/m$

Superparamagnetic MNP with small size(less than 20nm for magnetite) are the single domain MNP that have no hysteretic behavior butsuperparamagneticbehavior.These materials have zero remanence and transforms the energy of the magnetic field into heat through kinds of power loss mechanisms namely Hysteresis and Relaxation loss. The efficiency of the transformation of energy is strongly dependent on the strength and frequency of the magnetic field and also the properties of magnetic particles. When the external magnetic field applied to ferrofluid is reduced to zero, its magnetization decreases to zero due to ambient thermal energy; the relaxation mechanisms occurs rapidly as AMF varies between positive and negative values of its maximum amplitude.

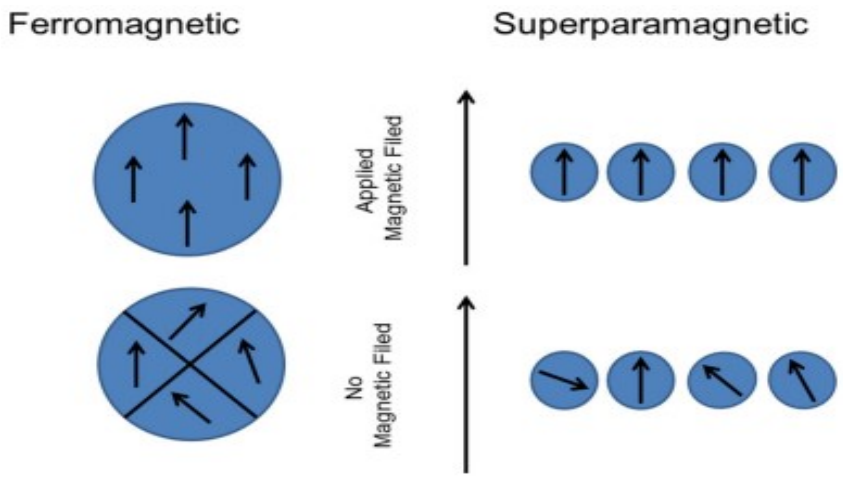

Figure 2.19: Representation of magnetic moment in both ferromagnetic and superparamagnetic materials. The domain structure of the magnetic materials has been drawn for simplicity.-(Reproduced from Mody et al.,2013[95]).

In particles with a superparamagnetic behavior, losses may occur either through Brownian or Néel relaxations. When a time varying magnetic field H_o is applied to ferrofluid,

nanoparticles itself or their individual magnetic moments align with the changing magnetic fields.

In Néel relaxation, the magnetic moment of the particle rotates internally to align with the field and power dissipation is caused by friction while in Brownian relaxation, the particle physically rotates in the viscous medium to align the moment with the field. The relaxation processes are further characterized by relaxation times. For Brownian relaxation, the relaxation time, τ_B and for Néel relaxation, the relaxation time is τ_N .The loss power(L.P) due to relaxation losses ($L.P_{SPM}$ =L.P for SPM particles) may thus be expressed by heat quantization parameter defined under article2.11.5 as S.A.R(Specific Absorption Rate) or S.L.P(Specific Loss Power) as

$$L.P_{SPM} = \pi\mu_O\chi_O f H_O^2 \frac{2\pi f\tau_R}{1+(2\pi f\tau_R)^2} \tag{2.5}$$

$$\text{where, } \chi_O = \frac{\mu_O M_S^2 V_m}{k_B T} \tag{2.6}$$

where,

M_S= is the saturation magnetization

V_M=is the magnetic nanoparticle volume

Also, Hergt[107] defined maximum theoretical value of L.P(Loss Power) as

$$L.P_{SPM-\max} = \frac{\pi\mu_O\chi_O C^2\tau_R}{\left[1+\left(\frac{C^2\tau_R^2}{H_O^2}\right)\right]}; \text{ wherein, } C = 5\times10^9\, Am^{-1}s^{-1} \tag{2.7}$$

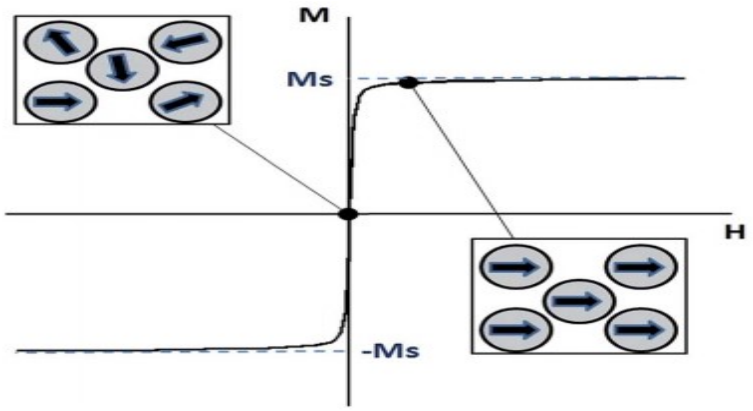

Figure 2.20: Typical curve for a superparamagnetic material(Squares showing the orientation of the moment of single-domain nanoparticles with increasing field strength)-(Reproduced from Hervault A. et al.,2014[93]).

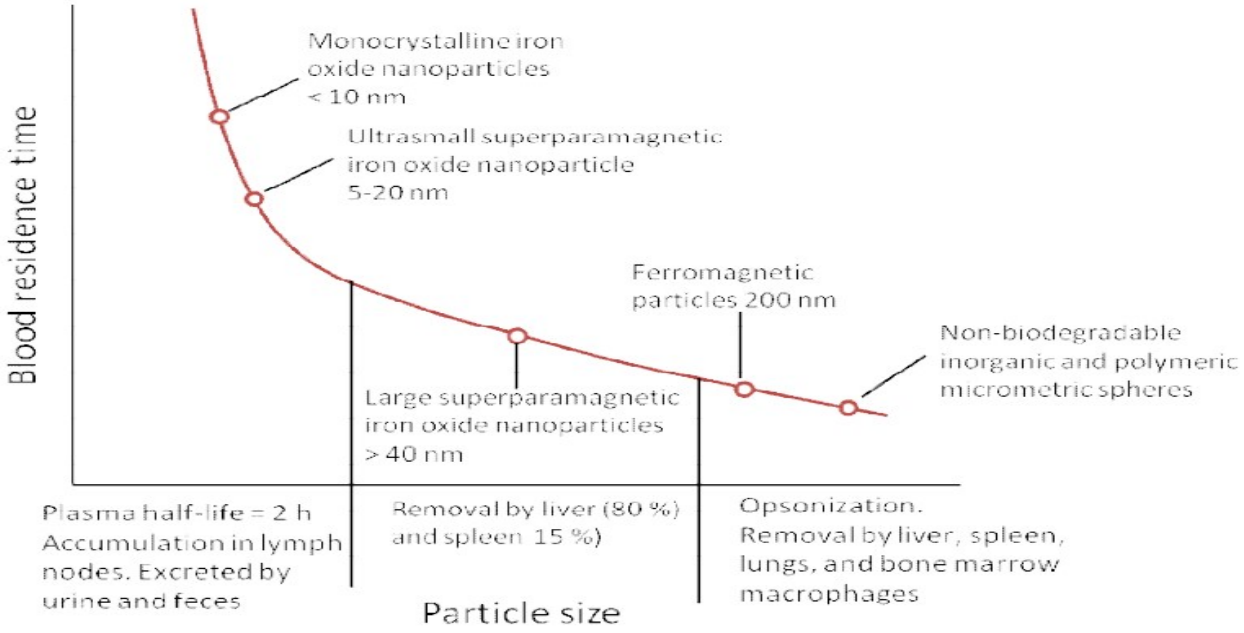

Figure 2.21:Dependence of blood residence time of NPs on their size,(Adapted from Arruebo Manuel, 2007[98])

2.11.3 PARAMETRIC FORMULATION OF MAGNETIC HEAT GENERATION:

POWER DISSIPATION FOR SUPERPARAMAGNETIC NANOPARTICLE HEATING

From the first law of thermodynamics,

$$\delta Q = \delta U + \delta W \tag{2.8}$$

where,

U is the internal energy

Q is the heat added

W is the magnetic work done on the system (taken as negative)

$$\therefore , \delta Q = \delta U - \delta W \tag{2.9}$$

Since, for an adiabatic process, $\delta Q = 0$;

$$=> \delta U = \delta W \tag{2.10}$$

Differential magnetic work can be written as, $\delta W = H.dB$

$$\Rightarrow \quad \delta U = H.dB \tag{2.11}$$

Where,

$$B = \mu_o (H + M) \tag{2.12}$$

H is the magnetic field intensity

B is the induction

μ_O is the permeability of free space

M is the material magnetization, which is a function of applied field and magnetic susceptibility

$$\delta U = -\mu_O \oint M dH \tag{2.13}$$

When magnetization lags the field, integration yields positive results indicating conversion of magnetic work into internal energy.

Expressing magnetization in terms of complex ferrofluid susceptibility,

$$\chi = \chi^{/} + i\chi^{//} \tag{2.14}$$

$\chi^{/}$ = In-phase component of χ

$\chi^{//}$ = Out of phase component of χ (Term relates to material parameters of ferrofluid)

$$H(t) = H_o Cos\,\omega t = \mathrm{Re}[H_o e^{i\omega t}] \tag{2.15}$$

$e^{i\omega t} = Cos\omega t + iSin\omega t$

= Real part + Imaginary part

$$M(t) = \mathrm{Re}[\chi H_o e^{i\omega t}] = H_o[\chi^{/} Cos\,\omega t + \chi^{//} Sin\,\omega t] \tag{2.16}$$

$$\delta U = 2\mu_o H_o^2 \chi^{//} \int_0^{2\pi/\omega} Sin^2 \omega t$$

(2.17)

$\chi^{//}$ =Loss component

$\omega = 2\pi f$

$=> f = \dfrac{\omega}{2\pi}$

Volumetric power dissipation, $P = f.\delta U = \pi\mu_o f H_o^2 \chi^{//}$ (2.18)

Writing equation for motionless fluid in oscillatory field as;

$$\frac{\partial M(t)}{\partial t} = \frac{1}{\tau_R}(M_o(t) - M(t)) \tag{2.19}$$

=>Equilibrium Magnetization, $M_o = \chi_o H_o Cos\omega t = \mathrm{Re}(\chi_o H_o e^{i\omega t})$ (2.20)

=>Complex Susceptibility in terms of equilibrium susceptibility, $\chi = \frac{\chi_o}{1 + i\omega\tau_R}$

Complex Susceptibility depends upon frequency and effective relaxation time.

$$\chi^{/} = \frac{\chi_o}{1 + (\omega\tau_R)^2} = \frac{\chi_o}{1 + (2\pi f\tau_R)^2} \tag{2.21}$$

$$\chi^{//} = \frac{\omega\tau_R}{1 + (\omega\tau_R)^2}\cdot\chi_o = \frac{2\pi f\tau_R}{1 + (2\pi f\tau_R)^2}\cdot\chi_o \tag{2.22}$$

Reinvoking, Volumetric power dissipation,

$$\begin{aligned} P &= \pi\mu_o f H_o^2 \chi^{//} \\ &= \pi\mu_o f H_o^2 \left(\frac{2\pi f\tau_R}{1 + (2\pi f\tau_R)^2}\cdot\chi_o \right) \\ &= \pi\mu_o \chi_o H_o^2 f \left(\frac{2\pi f\tau_R}{1 + (2\pi f\tau_R)^2} \right) \end{aligned} \tag{2.23}$$

This expression is equivalent to SAR in watts per cubic meter of fluid(or tissue) (i.e SAR=P). This can be easily converted into more standard units of cubic centimeters or grams tissue. In addition, absorption for magnetic nanoparticles is often expressed in terms of watts per mass iron, which is obtained by dividing this expression by the product of bulk density of iron in the nanoparticles(ρ_{Fe}) and the nanoparticle volume fraction($\phi or \upsilon$).This value is often termed as SAR_{Fe} or S.L.P(Specific Loss Power).

S.A.R=Units(W/m^3)

$$S.L.P = \frac{S.A.R}{\rho_{Fe}.\phi} \tag{2.24}$$

where, ϕ denotesferrofluid volume fraction~Units(W/g_{Fe}).

$S.A.R_{Fe}$or S.L.P is independent of nanoparticle concentration(assuming non-interacting particles).These relations are commonly expressed for monodisperesed particles.

2.11.4 CALCULATION OF POWER LOSS OF SUPERPARAMAGNETIC MATERIALS:PARAMETER OF QUANTIZATION OF HEAT INPUTS: S.A.R(S.L.P)

The heating potential of nanoparticles(Specific Absorption Rate) is an important parameter which dictates the relationship between therapeutic dosage and region to which they are been targeted. It defines the amount of heating delivered per unit mass and time as a consequence of the exposure of nanoparticles to an alternating magnetic field.

Higher the SAR, lower is the MNP concentration needed to achieve the temperature range for full therapeutic efficacy, which is crucial as a too high NP concentration may have significant toxicity.Lower the polydispersity, higher the SAR value, will be no matter what the NP size.

Loss power should be less than 7.5 x 10^9W/m^3 values that corresponds to field amplitude less than 7kA/m and field frequency less than 250kHz when the nanoparticles size is 18nm in diameter with a superparamagnetic behavior and to a field amplitude and frequency less than 15kA/m and respectively 500kHz for particles that describes the hysteretic behavior(Pavel M. and Stancu,2009[1]). Magnetite and Maghemite are the well studied iron-oxide particles which are been extensively studied for hyperthermia applications. The optimum loss power for MFH therapy was obtained for magnetite for frequencies between 500kHz-550kHz using a field amplitude of 6.5kA/m and particle radius of 9-10nm(diameter of 19nm). By increasing the value of amplitude, there is must requirement to reduce the frequency to keep the product in safe limits as defined under article2.11.1.By considering, field amplitude of 13.5kA/m frequency range between 160-180kHz For further increase of field amplitude the frequency must be less than 90kHzFor the particles under ferromagnetic regime, biocompatible values of H and f are less than 20kA/m and 600kHz.(Pavel M.,2008[3]).

Specific Loss Power(S.L.P) or Specific Absorption Rate(S.A.R) or Q_{gen} (Heat Generation Term):

$$\text{S.L.P}spm = \pi\mu_o\chi_o H_o^2 f \frac{2\pi f\tau_R}{1+(2\pi f\tau_R)^2} \tag{2.25}$$

Where,

μ_o = is the permeability of free space= $4\pi\times10^{-7} Tm/A$

χ_o = is the equilibrium susceptibility

H_o = is the AMF(Alternating Magnetic Field) strength

f = is the AMF(Alternating Magnetic Field) frequency

τ_R = is the effective relaxation time

The effective relaxation time is given as:

$$\frac{1}{\tau_R} = \frac{1}{\tau_B} + \frac{1}{\tau_N} \tag{2.26}$$

Or

$$\tau_R = \frac{(\tau_N . \tau_B)}{(\tau_N + \tau_B)} \tag{2.27}$$

Where,

τ_B = is the Brownian relaxation time

$$\tau_B = \frac{3\eta V_H}{k_B T} \tag{2.28}$$

Where,

η = is the viscosity of the fluid/medium

T = is the temperature

V_H = is the hydrodynamic volume of the magnetic nanoparticles

$$V_H = \frac{\pi (D + 2\delta)^3}{6} \tag{2.29}$$

Where,

D = is the diameter of magnetic nanoparticles

δ = is the ligand layer thickness

k_B = is the boltzmann's constant= $1.38 \times 10^{-23} JK^{-1}$

$\tau_N =$ is the Néel relaxation time

$$\tau_N = \frac{\sqrt{\pi}}{2}\tau_o \frac{\exp\left(\frac{KV_M}{k_B T}\right)}{\sqrt{\frac{KV_M}{k_B T}}} \tag{2.30}$$

Or

$\tau_N =$ The Néel relaxation time of the system is determined by the ratio of anisotropy energy to thermal energy.

$$\tau_N = \tau_o \exp\left(\frac{KV_M}{k_B T}\right) \tag{2.31}$$

Where,

$K =$ is the magneto-crystalline anisotropy constant

$V_M =$ is the magnetic volume or volume of magnetic nanoparticles

$$V_M = \frac{\pi D^3}{6} \tag{2.32}$$

Where,

$D =$ is the diameter of magnetic nanoparticles

$\delta =$ is the ligand layer thickness

$\tau_o =$ Attempt period or the average relaxation time in response to thermal fluctuation = 10^{-9} sec or 10^{-11} sec

χ_o can be calculated from the following expressions:

$$\chi_o = \chi_i \frac{3}{\xi}\left(\coth\xi - \frac{1}{\xi}\right) \tag{2.33}$$

$$\chi_i = \frac{\mu_o \phi M_d^2 V_M}{3k_B T} \tag{2.34}$$

$$\xi = \frac{\mu_o M_d H_o V_M}{k_B T} \tag{2.35}$$

$$M_s = \phi M_d \tag{2.36}$$

Where,

$\phi =$ is the volume fraction of nanoparticles in the ferrofluid

$M_d =$ is the domain magnetization of the nanoparticle

$M_s =$ is the bulk saturation magnetization

Experimentally, heat generation from magnetic particles is given by the specific absorption rate which can be calculated as:

$$SAR = C\left(\frac{\Delta T}{\Delta t}\right)\frac{mass_{ferrofluid}}{mass_{nanoparticles}} \tag{2.37}$$

Where,

$C =$ mass weighted heat capacity of the ferrofluid

$\left(\frac{\Delta T}{\Delta t}\right)$ = is the slope of the initial section of the temperature versus time curve

Also, χ_O, can be calculated from

$$\chi_O = \frac{\mu_O M_S^2 V_m}{k_B T} \tag{2.38}$$

Where,
M_S= is the saturation magnetization
V_M=is the magnetic nanoparticle volume

2.11.5 CONCEPT OF AVERAGING OF PROPERTIES FOR COMPUTATIONAL ANALYSIS

The mean value of specific heat, density, and thermal conductivity for cancerous tissues with embedded nanoparticles can be approximated by a serial arrangement of two materials with two volume proportions.

$$\rho_{composite} = \phi\rho_{ferrofluid} + (1-\phi)\rho_{tumor} \tag{2.39}$$

$$C_{composite} = \phi C_{ferrofluid} + (1-\phi)C_{tumor} \tag{2.40}$$

$$\frac{1}{k_{composite}} = \frac{\phi}{k_{ferrofluid}} + \frac{1-\phi}{k_{tumor}} \tag{2.41}$$

where,
ϕ is the volume fraction

2.12 AN ENGINEERING APPROACH TO HUMAN SUBJECTS

Due to varying tumor location and geometry and different size and shape of patients, individual therapy planning is necessary. The first step of hyperthermia treatment planning(HTP) is the generation of a patient model by segmentation of images from computerized tomography (CT) or magnetic resonance imaging (MRI) scans. In some cases, online parameter identification based on MRI is performed. Depending upon the type of the applicator used,thissegmentation is used to calculate the power absorption (PA, [W/m3]) or specific absorption rate (SAR, [W/kg]) distribution in the patient by electromagnetic models.

A temperature distribution in the patient can be calculated from the power absorption distribution by applying Pennes' bio-heat equation (PBHE), or from more elaborative algorithms including the blood vessel network, i.e.discrete vasculature (DIVA) models, down to vessel sizes in the millimeter range.

The main problems with these thermal methods are long time-requirements for the generation of a vessel network and the large, poorly-predictable, variations in thermal properties of tissues.The target in treatment planning is to heat a particular tumor and delivering at least 43°C to 90% of its volume for cumulative in multiple treatments for longer than 10 minutes corresponds to doubling of the probability for complete response and duration of response to hyperthermia and radiotherapy versus radiotherapy alone (*Oleson et al. 1993*).

2.12.1 ENGINEERING ASPECTS OF HYPERTHERMIA

Cancerous cells typically have diameters of 10 to 100 micrometers.This has produced the motivation to use MNP to penetrate into a cell.Energy absorption in cancerous tissues provides the heat required for temperature increase. Predominantly, electromagnetic heating of nanoparticles in various frequency ranges are elaborated by keeping in preview the criterion of safe exposure of human body as proposed by Atkinson, Brezovich, Hergt and validated by Pankhurst. Maxwell's equations are solved for the specific geometry with estimated electrical and magnetic properties at the given anatomy. This computation process leads to SAR calculations in Watts per unit mass of tissue.

SAR is directly related with applied field amplitude and frequency as well as geometrical(size, shape) and structural features of the particle. High SAR values limits the MNP concentration as low and biocompatibility issues restricts the materials choice. An alternate route towards larger SAR values is expected to be the enhancement of magnetic moment per particle. Then, heat transfer equation must be solved to reproduce the temperature distribution in cancerous tissue and the adjacent healthy tissue. In contrast to RF ablation and focused ultrasound therapies, electrical and thermal properties of tissue don't change significantly over 37-45°C temperature range. For this very reason, these values are assumed as constants depending upon the tissue type. Successful production of model from patient's anatomy needs a dedicated computer in clinical lab having extensive graphical processing unit. Superparamagnetic nanoparticles are ideal candidates for hyperthermia cancer treatment as they can well operate between frequencies in tens to hundreds(kHz and MHz). Magnetic nanoparticles agitate in magnetic field and can spatially adjust the power absorption requirements by cancerous tissue.

2.12.2 HYPERTHERMIA TREATMENT PLANNING (HTP) & SIMULATION

Simulations for HTP can be grouped into four distinct important tasks:

1. Generation of patient model based upon the accuracy of obtained MRI/CT Scan to generate more uniform computational domain(Geometry).
2. Pre-calculations for the distribution of power deposition in the tissue under analysis.

3. Spatial and Temporal Thermal distribution patterns i.e resulting temperature distributions in the tissue.
4. Type of Analysis: Steady State Analysis and Transient Analysis defined to analyze the type of behavior with respect to the tissue geometry.

Explanatory notes:
Initially, the geometry and tissue properties of the involved tissue region must be carefully identified and defined as far as the selection of individual geometrical subsections(subparts) are concerned. For improving the accuracy of the model, *"Patient Specific Modelling"*is performed by segmenting tissues using computed tomography(CT) or magnetic resonance imaging(MRI) of the actual subject.Next, the specific absorption rate(S.A.R) or more specifically the power density(P.D), distribution is determined by EM, US, NPs, related modeling approaches. Once, the PD pattern is established, the temperature(T) distribution can be predicted based upon the thermal redistribution of energy within the heated region with special consideration of the impact of physiological aspects such as blood perfusion and core temperature. So, we have tried to incorporate the features such as patient anatomy, tissue interfaces, and tissue properties to precisely model in computational software comsol. Although there are specific assumptions in this study like homogeneous distribution of particles which is normally not the case. Therefore attempts needs to be made to increase the accuracy as well as the computational speed. The simulation tools and techniques developed for clinical hyperthermia assists the realization of path from *"model"* to *"clinic"*.

2.12.3 COMPUTATIONAL ANALYSIS AND ROLE OF SIMULATIONS

1.Simulations are very much helpful for assessing treatment risks to the patient, for example the afterwards effects of nanoparticles and its behavior in magnetic fields or other metallic implants.
2.The main strength of simulations is to effectively judge different scenario's before the hyperthermia session to help in selection of treatment approach, specific power excitation planning, and clinical outcome prediction.
3.Simulation tools can also assist enhanced treatment approaches or retrospectively to analyze and enhance treatment quality.
4.To better understand the uncertainties and the impact of individual parameters.

5.Treatment plans opens scope of opportunities for interdisciplinary discussions and also acts as an excellent venue for improvements in hyperthermia therapy.

2.12.4 PROSPECTS

- Hyperthermia may find additional applications in gene therapy, stem cell purging, targeted drug delivery.
- Physical process of field interference and heat distribution inside very heterogeneous human body is very complex
- Reliability of mathematical models depends on vascular geometry information obtained via various clinical trials and largely vary depending upon patient's comfort/discomfort levels. In particular, physiological parameters are individually varying to significant amount such that a priori models are subject to significant modeling errors.
- Heating deep seated tumors effectively still remains an unsolved technical problem and needs to be updated as per the methodology proposed by author to assist the hyperthermia study with computer assisted interventions by using the concept of medical imaging in near future studies.

CHAPTER 3

3D-MEDICAL IMAGING

3.1 OVERVIEW:

This chapter deals with the medical images extension to thermal modeling of soft tissues especially attention is keen towards breast tissues. All needed working steps such as image import, segmentation, 3D-model generation, modeling of cancerous tissues and effective temperature rise and necrosis states are examined. Evaluation tool which is been used is Mimics as main software package. Surface layers are processed by Materialise 3-Matic software to define initial and boundary conditions. The interface between three software's are an important aspect which is also briefly reviewed. The detailed discussions about the co-ordinate systems of medical anatomy i.e Anatomical planes are also briefly reviewed. DICOM data processing includes import and applying subsequent operations to generate model from two dimensional images.

3.2 INTRODUCTION

Medical Imaging is the technique/process of creation of visual representations of the interior of a body for **medical** intervention and clinical analysis. **Medical imaging** seeks to reveal internal structures hidden by the skin and bones, as well as to diagnose and treat disease.

Medical Imaging(2D/3D scans) is an assistive tool that helps the doctors/clinical surgeons to locate the exact position of tumors/cancerous diseased tissue, to know the exact size of solid lesion that can be investigated on later stage as benign or malignant depending upon the properties been observed after interventions. Generation of 3D model from 2D slices helps the physicians to analyze the volumetric size of tumors and the proper treatments that best suits to it depending upon the stage of development.Moreover,3D medical imaging helps to extract information from image files to create 3D model.

The high resolution images produced by the modern imaging modalities offered to the medical doctors with multi-orientation views and much more details, considerably assisting the clinical diagnosis and the treatment that follows. The first step of processing these images is to segment the desired organs or structures from image series. Usually, to perform the manual segmentation medical technicians need to sketch the contours slice by slice using pointing devices such as a mouse or a trackball. This procedure is very time-consuming and the results may suffer from intra- or inter-observer variability. In the past few decades, many algorithms have been proposed to perform the computer-aided segmentation. The incorporations of modern mathematical and physical techniques have greatly enhanced the accuracy of the segmentation results.

Based upon the computed tomography images or magnetic resonance images of the subjects in breast cancer patients and the software for performing analyzing of medical images, three dimensional models were generated. Geometrical reconstruction of the soft tissues was realized and the(Fibro-glandular tissues, Skin tissues, Fat tissues & also the blood carrying vessels etc can be obtained with maximum contrast agents as prescribed) and the finite element models were meshed.

3.3 TYPES OF MEDICAL IMAGING / DIGITAL IMAGING MODALITIES:

1. Imaging using X-rays

1.1 Conventional X-ray scan

1.2 Computed Tomography scan(CT-scan)

1.3 Mammography

2. Molecular Imaging

3. Other types of Medical Imaging

3.1 Magnetic Resonance Imaging(MRI-scan)

3.2 Ultrasound Imaging(Ultrasonography)

3.3 Positron Emission Tomography/Computed Tomography(PET/CT-scan)

3.4 Positron Emission Tomography/Magnetic Resonance Imaging(PET/MRI)

3.4 IMAGING TECHNOLOGY:

Computer processing is used to generate a three dimensional image of the human body from a large series of two-dimensional images. There are various modalities commonly used today in medical imaging, two of them are Computed Tomography (CT) and Magnetic Resonance Imaging (MRI).CT image is ideal for use when scanning objects have different density, depending upon absorption coefficient. However, CT image is not efficient at distinguishing between different soft tissues, the image quality will be poor. So, MRI allows the excellent soft-tissue contrast. So CT and MRI are sensitive to different tissue properties, the appearance of the images obtained with the two techniques differ markedly.

3.4.1 BREAST MAGNETIC RESONANCE IMAGING:

Magnetic Resonance Imaging of Breast is a promising tool for use in diagnosing breast conditions. It is highly sensitive, although not specific test and serves as an adjunct to mammography. A coil is placed around the breast, and the patient is placed inside the MRI machine for about 2 minutes. An injection of gadolinium, a contrast dye, is given intravenously.MRI of the breast can be helpful in determining the exact size of a lesion or the presence of multiple foci more precisely than mammography. It can also determine more precisely than a CT scan if a lesion is fixed to the chest wall. Other uses include identifying occult(undetectable) breast cancer, determining the tumor's response to chemotherapy, and determining the integrity of saline or silicone breast implants. The cost of breast MRI, however, is high; therefore, it is not currently used for routine screening. However, the sensitivity of the MRI may be beneficial for cancer detection in higher-risk women, and the results from preliminary studies are encouraging,(Schnall et al.2001,Medical Surgical Nursing by Suzanne C.Smeltzer,[101]).

BREAST CANCER MRI-SCAN OPERATING PROCEDURES:

Figure 3.1: Breast MRI Scan Preview by GE Health care(Reproduced from John Hopkin's University,[W.7])

For a breast MRI, the woman usually lies face down, with her breasts positioned through openings in the table. In order to check breast positioning, the technologist watches the MRI through a window while monitoring for any potential movement.A breast MRI usually requires the use of contrast that is injected into a vein in the arm before or during the procedure. The dye may help create clearer images that outline abnormalities more easily.

MRI, used with mammography and breast ultrasound, can be a useful diagnostic tool. Recent research has found that MRI can locate some small breast lesions sometimes missed by mammography. It can also help detect breast cancer in women with breast implants and in younger women who tend to have dense breast tissue. Mammography may not be as effective in these cases. Since MRIs do not use radiation, they may be used to screen women younger than 40 and to increase the number of screenings per year for women at high risk for breast cancer.

Although it has distinct advantages over mammography, breast MRI also has potential limitations. For example, it is not always able to distinguish the difference between cancerous abnormalities, which may lead to unnecessary breast biopsies. This is often referred to as a "false positive" test result. Another disadvantage of breast MRI is that it has historically been unable to identify calcifications or tiny calcium deposits that can indicate breast cancer.

Recent research has demonstrated that using commercially available software programs to enhance breast MRI scans can reduce the number of false positive results with malignant tumors. Thus, the need for biopsies may decrease with computer-aided enhancement.

3.5 ANATOMICAL PLANES or ANATOMICAL CO-ORDINATE SYSTEM:

According to the Cartesian coordinate system, there are three axes defined in human anatomy: A longitudinal or vertical axis, a transversal or horizontal axis and a sagittal axis. Based on these axes there are three planes defined.

PLANES IN HUMAN BODY:

1.Sagittal Plane or Median Plane(Y-Z Plane)

2.Coronal or Frontal Plane(Y-X Plane)

3.Transverse plane or Horizontal Plane(X-Z Plane)

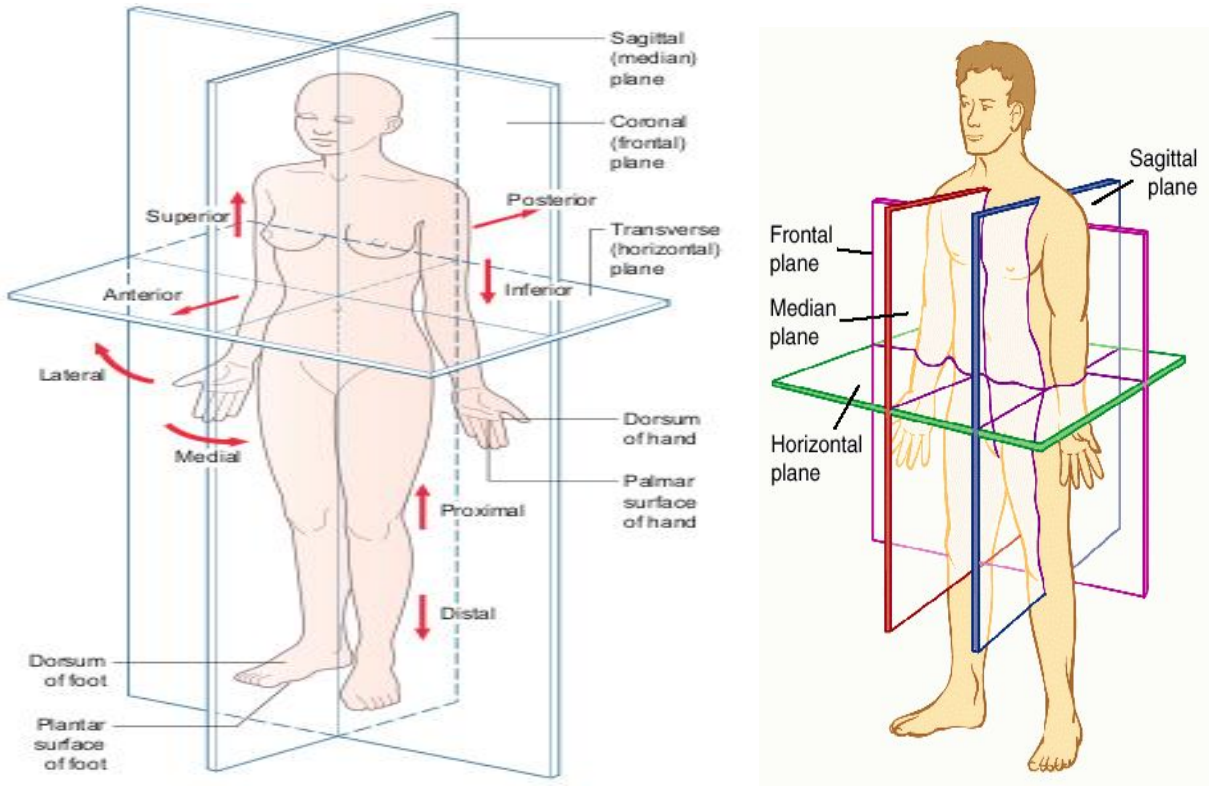

Figure 3.2: Representation of Anatomical planes[W.8]

The **transverse** plane (also called the **horizontal** plane, axial plane, or transaxial plane) is an imaginary plane that divides the body into superior and inferior parts

A **coronal** plane (also known as the **frontal** plane) is any vertical plane that divides the body into ventral and dorsal (belly and back) sections.

A **sagittal** (also known as **median or longitudinal**) plane is a vertical plane which passes from anterior to posterior, dividing the body into right and left halves.

3.6 MODELING SOFT-TISSUES FROM MRI

3.6.1 AN INTRODUCTION TO DICOM FILE FORMAT

DICOM(Digital Imaging and Communications in Medicine) is a standard for handling, storing, printing, and transmitting information in medical imaging. It includes a file format definition and a network communications protocol. The communication protocol is an application protocol that uses TCP/IP to communicate between systems. DICOM files can be exchanged between two entities that are capable of receiving image and patient data in DICOM format.

The data used in present study is MRI-Scan in DICOM (Digital Imaging and Communications in Medicine) format.

CA patient was scanned in a number of series, with a specified number of images, pixel spacing and slice thickness. There are two MRI data sets of the breasts, were made. Depending on the pixel spacing and slice thickness the image quality will vary. If the image quality is higher, the picture has more detail.Magnetic resonance imaging (MRI) produces high quality images of the human body.

A Three Dimensional mesh model can be created from a MRI image in three main steps:

Step 1: Open the MRI image.

Step 2: Image segmentation to generate object boundaries. This can be done using either the "Automatic Segmentation" or the region-based semi-automatic "Segment Object" command. Threshold-based segmentation method is normally not effective for MRI image. For small size soft tissues, the manual tracing method can be used as well. Boundaries can be edited using the boundary editor.

Step 3: Creating mesh models using the surface rendering command. The models can be used for volume calculation, rapid prototyping, simulation or treatment planning applications.

3.6.2 DIGITAL DATA PROCESSING FROM STACK OF TWO-DIMENSIONAL IMAGES:

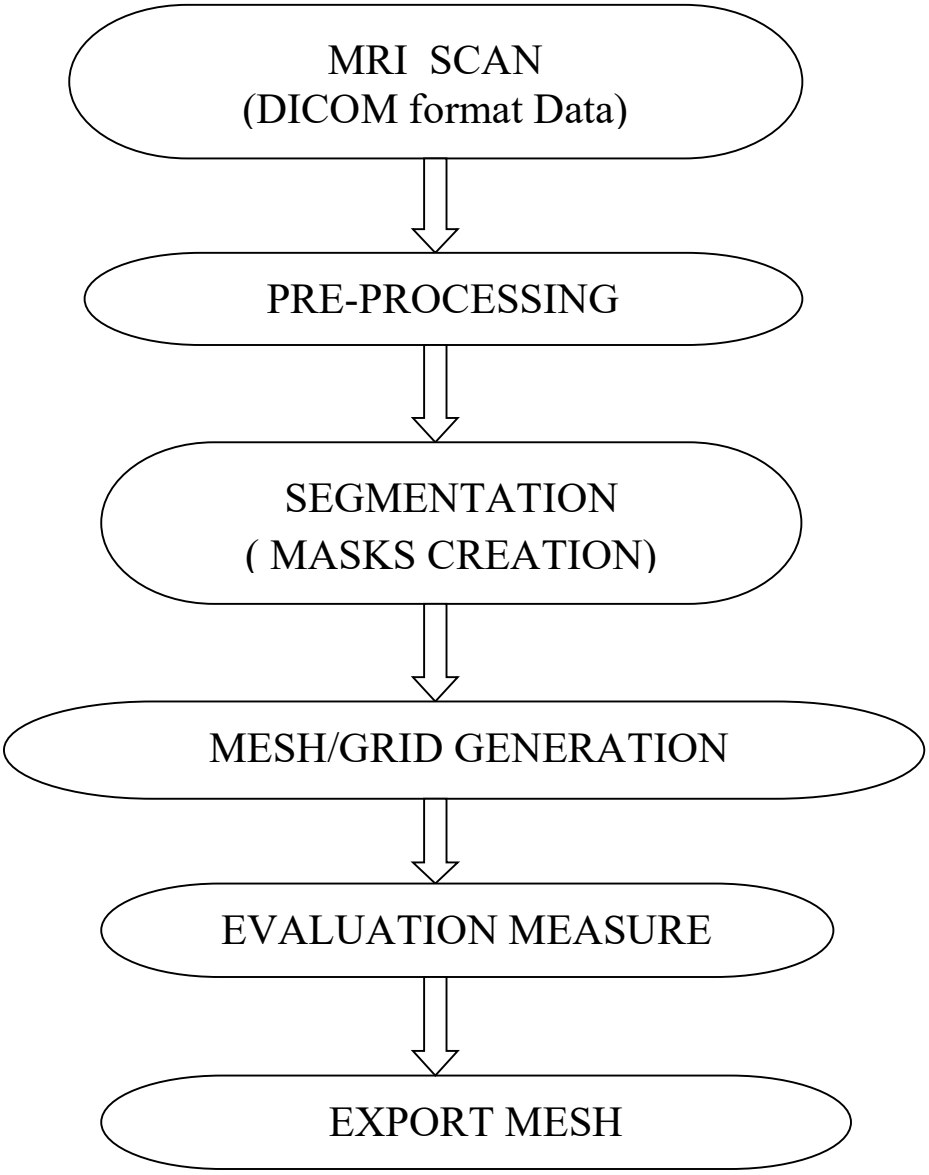

Figure 3.3: Functions of software that can process MRI data from DICOM format in MIMICS

Based on a literature review several software packages that are generally been used to process DICOM format files sets to produce FE(Finite Element) models are evaluated.

In the pre-processing a certain level of noise in the data can be removed by applying filtering, and also the data can be reduced.

The segmentation is the process where the different tissues and blood vessels in near vicinity are identified inside the slices.

The pictures are separated into different parts depending on the pixel gray value levels of the MRI scan images. Volumetric mesh is applied via 3-matic tool of MIMICS to the selected geometry and mesh is exported via COMSOL-MULTIPHYSICS17.0 thermal analysis software. To obtain the more accurate results, grid independent test is done.

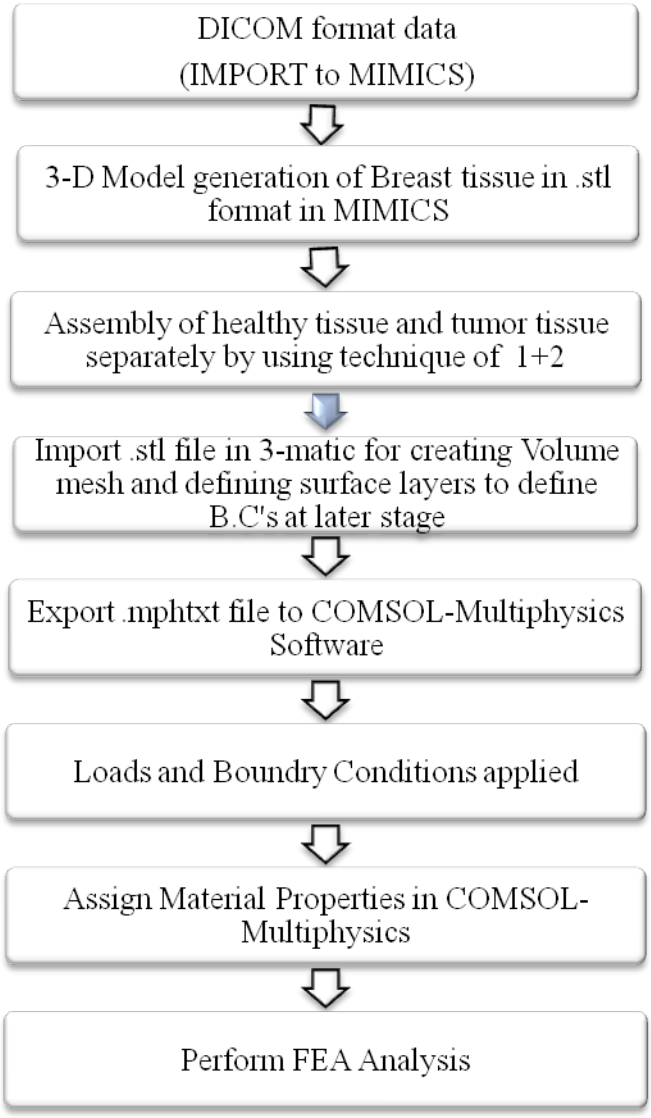

Figure 3.4 Step by step procedure to perform analysis on realistic three- dimensional model

3.6.3 MEDICAL IMAGE DATA(MRI/CT-2D) to 3D MODEL GENERATION TECHNIQUES

STEPS INCORPORATED

In MIMICS Regions Of Interest(R.O.I) are defined by using segmentation masks which can be defined and modified by several functions.

1. Thresholding: It is the first action performed to create a segmentation mask. A region of interest can be selected by defining a range of gray values (Hounsfield Units). The boundaries of that range are the lower and upper threshold value. All pixels with a gray value in that range will be highlighted in a mask.

2. Region Growing: Expands the segmentation mask to other slices and will eliminate noise and separate structures that are not connected.

3. Dynamic Region Growing: Segments an object based on the connectivity of gray values in a certain gray value range. It allows for easy segmentation of tendons and nerves in CT images, as well as providing an overall useful tool for working with MRI images.

4. Editing (Draw, Erase, Local Threshold): Manual editing functions make it possible to draw, erase or restore parts of images with a local threshold value. Editing is typically used for eliminating artifacts and to separate structures.

5. Morphology Operations: Act on the form resp. the shape of a segmentation mask(Erode, Dilate, Open and Close). All these functions remove or add pixels from the source mask and copy the results to a target mask. This tool is extremely effective when working with MRI images.

6. Boolean operations: Allows making different combinations of two segmentation masks(Subtraction, Union and Intersection). These operations are very useful for reducing the work needed to separate two joints.

7. Cavity Fill: fills the internal gaps of a selected mask and copies the result to a new mask. The filling process can be applied only in 2D.

8. Cavity Fill from Polylines: creates a segmentation mask, starting from a polyline set. This tool is very useful for filling internal cavities.

Mimics calculate 3D models based on masks. The Calculate 3D toolbox offers three predefined quality levels and the alternative to choose a custom set of parameters for shell reduction, resolution, filtering, smoothing and triangle reduction. For fast model generation the use of one

of these predefined levels is just the right way but for a specialized creation the parameters have to be fine tuned.

3.7 SOFTWARE REVIEW

MEDICAL IMAGING PROCESSING SOFTWARES

Available Image Processing Softwares

1. 3D Doctor
2. 3D Slicer
3. Osirix
4. Materialise MIMICS Innovation Suite
5. Matlab
6. Simpleware
7. Vesalius 3D

Meshing tools available

1. Materialise 3-matic
2. Comsol Multiphysics
3. Hypermesh
4. Scan-IP
5. Meshlab
6. Netfabb Studio Basic

Thermal/Design Analysis Computational tools available

1. Materialise 3-matic
2. Comsol Multiphysics-5.O
3. ABAQUS
4. ANSYS

3.7.1 AN INTRODUCTION TO MIMICS (MATERIALISE INTERACTIVE MEDICAL IMAGE CONTROL SYSTEM)

Mimics is a software for processing medical images and creating 3D models. Mimics uses 2D cross-sectional medical images such as from computed tomography (CT) and magnetic

resonance imaging (MRI) to construct 3D models, which can then be directly linked to rapid prototyping, CAD, surgical simulation and advanced engineering analysis.

IMAGE TO 3D-MODEL

A stack of images can be loaded into the software, Mimics, and this usually consists of images in the XY plane (axial images). Mimics then calculates and creates images in the XZ (coronal) and YZ (sagittal) direction. This enables a more comprehensive 3D feel of the 2D data.

The key to converting anatomical data from images to 3D models is a process called segmentation. During segmentation the user indicates the structure(s) of interest in the sliced image data. This information is then used to recreate a 3D model from the segmented structures. To describe the outer surface of the 3D model, Mimics uses the STL format, which is the common file format in RP. The STL format allows describing the most complex geometries accurately. This is necessary, since anatomical data is in general very intricate. Accurate segmentation is important in order to extract meaningful information from images.

MIMICS is an image processing software for 3D design and modeling, for medical, dental and additive manufacturing industries. Mimics is used to create 3D surface models from stacks of 2D image data(Materialise 2015). These 3D models can then be used for a variety of engineering applications.

It interfaces between scanner data (CT, MRI, Technical scanner) and Rapid Prototyping, STL file format, CAD and Finite Element analysis. It is an image-processing package with 3D visualization functions that interfaces with all common scanner formats. It also provide theinterface towards Rapid Prototyping using STL. MIMICS can be also utilized for exporting the landmarks points for another software like Anybody etc. Most common input format is DICOM, but other image formats such as: TIFF, JPEG, BMP and Raw are also supported.It enables to control and correct the segmentation of CT-scans and MRI-scans. For instance,image artifacts coming from metal implants can easily be removed. No technical knowledgeis needed for creating on screen 3D visualizations of medical objects (a cranium, pelvis, etc.).It provides several segmentation and visualization tools to process the images.

3.7.2 MESH GENERATION USING MATERIALISE 3-MATIC

MIMICS has a 3-Matic module in it.3-maticSTL offers design modification, design simplification, 3D texturing, remeshing, forward engineering, and much more, all on an STL level and other more advanced file formats. It allow seamless transition from meshes created in Mimics Innovation Suite to various FEA software's like ABAQUS, ANYSIS, HYPERMESH, COMSOL-MULTIPHYSICS etc.

Features of 3-Matic are given following-

1. Create complex non-manifold (multi-part) meshes.
2. Obtain detailed analytics of mesh and improve mesh quality.
3. Refine meshes based on geometrical characteristics.
4. Link to all major FEA and CFD Solvers.
5. Combine CAD parts to your anatomical 3D models and create multipart meshes without losing accuracy on your CAD parts.

3.7.3 LIVE INTERFACE WITHIN MATERIALISE MIMICS-17.0 AND COMSOL MULTIPHYSICS-5.O

IMPORTING 3D-MODEL FROM MIMICS TO COMSOL MULTIPHYSICS-5.O File input to Comsol from Materialise 3-matic

- **.stl**
- **.iges**
- **.step**
- **.vrml**

3.8 SOFTWARE EVALUATION

The following steps are used for evaluation of selected software packages and at the same time the compatibility of thermal analysis software COMSOL-MULTIPHYSICS to choose a software to create 3-Dimensional models.

1. Evaluation of type of license: cost and time.
2. Support manuals, learning tutorials, online support.
3. Interface interaction within program.
4. Problems and limitations.

5. Time calculations between actions taken.
6. System requirements of computer machine where the software needs to be run.

CHAPTER 4

LITERATURE REVIEW AND RESEARCH GAPS

4.1 OVERVIEW

Carrying out Literature-review is very significant in any research project as it clearly establishes the need of the work, background development and builds strong platform to carry on the research with available information and addresses the pitfalls and promises been shown by authors in their requisite work. It generates related queries regarding improvements in the study already done and allows unsolved problems to emerge and thus clearly define all boundaries regarding the development of the research project.

The author has gone through many research papers of reputed journals, relevant books, attended latest workshops and particularly the field related conferences to search the literature for deciding the final work to be performed in connection with the design and formulation of simulation for realistic breast cancer patient specific modeling. Also, the keen consideration is drawn on hyperthermic studies been performed till date to realize the real time results to set pre-treatment planning protocols and acts as a guide for surgical operations also. The significantly related ones have been discussed in this chapter.

Moreover, pre-survey of literature assists the direction of work to be performed and also at the same time keeping in preview the pros-cons, requisite constraints to restrict/explore the scope of work to surround along the important workflow parameters.

This study is a part of Interdisciplinary research where Doctors, Physicians, Engineers, Pharmacologists came on one single platform to contribute towards this noble cause CANCER.We have tried to formulate our research problem from the key aspects of *Thermal Engineering* where in we have used the image processing based computational assisted thermal analysis on “Carcinoma” as a patient specific real time study to foreseen the actual results before pretreatment and as a guide on one side to see clear results and also reducing the pains of

patients. Our keen focus is to contribute towards improving the quality standards of breast cancer patients and also to reduce loads of cancer from world.

A discrete literature review has been done to analyse the key contribution of different researchers done till date and Idea generation or simply concept building is just because of the key knowledge we gained by interaction with different researchers through their key research. The first part of literature review is Computational based where in we discuss many parameters with the variations been seen by analysts.Experimental studies done via different modalities are also been discussed.

The literature review is explained via three different sections. The first one is discrete review of computational work for hyperthermic related studies. Secondly, Summarizing of the different parameters under one roof to directly refer to the range of operating variables to be used as an input values for our simulation work. Thirdly, the tissue thermophysical properties that closely relates to the anatomical real human tissues. Computational work, Experimental-based(including in-vivo and In-vitro studies), Numerical and Theoretical studies ,Review of papers are all studied and is addressed in each of the papers been referred. The inference drawn with respect to each work is concisely presented and also to identify the research gaps with relation to progress drawn till date to realize the concept of hyperthermia, Thermal ablation, Coagulation necrosis etc

.

4.4 ELABORATIVE LITERATURE REVIEW

(COMPUTATIONAL / EXPERIMENTAL / REVIEW / NUMERICAL / THEORETICAL / ANALYTICAL)

[1] Pavel M. *et al(2009).*

Computational/ Experimental	Finite Element Method(FEM)	Physics Employed	Magnetic Nanoparticle Used	Distribution of MNP's Monodispersion/ Polydispersion
Computational	ComsolMultiphysics	Heat transfer Module	Magnetite (Fe_3O_4)	Monodispersion (Homogeneously distributed)

Objective: To compute the spatial temperature distribution within the tissues.

Work: In this paper,the author discussed about the optimum/appropriate dose (Concentration) of MNPs in tumor cells that would help to achieve therapeutic temperature of atleast 42°C.Three types of tissues namely breast tissue, liver tissue andskin tissue are used and their physiological properties are defined. The tumor isgeometrically defined as spherical shaped tumor and a healthy tissue is cubical region around the close vicinity to it.

The most accepted and studied bioheat-transfer equation i.e "Pennesbioheat equation" which combines the key contribution of blood perfusion term, heat conduction and amount of energy generated by metabolic processes is used.They performed a systematical variation of nanoparticles dosage and tumor diameter for every physical parameter namely(tissue density, tumor perfusion rate, tissue perfusion rate).By systemizing they are keen to know the interdependency of these parameters and their effects in specific relation to "Hyperthermia"therapy.Three models were investigated.

PARAMETERS	MODEL-1	MODEL-2	MODEL-3
Geometrical Configuration	Blood vessel-1 (B.V1) diameter = 0.5mm Blood vessel-2 (B.V2) diameter = 1.2mm	Blood vessel-1 (B.V1) diameter = 0.5mm Blood vessel-2 (B.V2) diameter = 1.2mm Blood vessel-3 (B.V3) diameter = 2.8mm	No Information
Type of Tissue	Skin tissue/Breast tissue	Skin tissue/Breast tissue/liver tissue	Breast Tissue
Location of blood vessels from tumor border	B.V1=7.5mm B.V2=7.5mm	B.V1=7.5mm B.V2=7.5mm B.V3=1mm to 2mm	No Information

Diameter of tumor (modeled as perfect sphere)	1 to 1.6 cms	1 to 1.6 cms	2.7mm upto 3.4mm Variable for different concentrations (6,10,13mg/cm³) and Loss Power of nanoparticles
Healthy tissue(modeled as cube)	3.5cm × 3.5cm × 3.5cm.	3.5cm × 3.5cm × 3.5cm.	1cm × 1cm × 1cm
Volume of healthy tissue	42.875cm³	42.875cm³	1cm³
Type of Distribution of n/p	Homogeneously around border	Homogeneously around border	Homogeneous
Diameter of injection region	0.9mm diameter each inside the tumor	0.9mm diameter each inside the tumor	0.9mm diameter each inside the tumor
No.ofNanoparticle Injection/ accumulation sites	6	6	6
Particles present at centre	No	No	No
Dosage of nanoparticles	3 upto 12mg/(cm³ of tumor tissue)	3 upto 12mg/(cm³ of tumor tissue)	6 upto 13mg/(cm³ of tumor tissue)
L.P values range	(0.6-1.4) × 10^9 W/m^3.	(0.6-1.4) × 10^9 W/m^3.	(3.4-6.0) × 10^9 W/m^3.

Inference drawn:

1.When the physical and physiological properties of the tumor are very different from the local tissue, the temperature distribution closely depends upon the blood vessels that are located close to tumor boundaries.

2.The presence of blood vessel near to the tumor drastically reduces the temperature achieved in the tissue in comparison when no large blood vessels are located around the tumor.

3.In specific to large breast tumors (larger than 1cm diameter),for same concentration of nanoparticles(6,10,13mg/cm³), required tumor temperatures are reached for lower loss power values that implies a decrease in field frequency and field amplitude.

4.Field frequency and amplitude has significant effect in MFH as by increasing both parameters results in increase in loss power value and the concentration of nanoparticles, the temperature suffers a sudden variations within the tissue.

Research Gaps:

One of the most challenging problems in hyperthermia is the right dose/correct dose of particles by specifying the affected region under consideration. So, far till today real time patient specific modeling is missing to give the exact measure of acceptance of hyperthermia using MNPs or any other modality. The present study assumes the healthy tissue as cubical region and affected tissue region as spherical region.But in reality neither the tissues would be rather cubical or spherical and they will be mostly of irregular shape that should be defined depending upon the simulation techniques well accepted this very day. So, the tumor exact geometry and position should be made available by using the concept of medical imaging techniques such as CT(Computed tomography), MRI(Magnetic Resonance Imaging).So, this area is been highlighted by the author too as an important Research Gap. The information regarding the local features of tumor/tissue pefusion rate, density and the type of tissue under consideration.

[2]Pavel M.,Gradinariu G. *et al(2007).*

Computational/ Experimental	**Finite Element Method(FEM)**	**Physics Employed**	**Magnetic Nanoparticle Used**	**Distribution of MNP's Monodispersion/ Polydispersion**
Computational	ComsolMultiphysics	Heat transfer Module	Magnetite (Fe_3O_4)	Monodispersion (Homogeneously distributed)

Objective: To calculate the heat dissipation from nanoparticles concentrated in tumor of various sizes.

Work: In this paper, the two nanoparticles behaviors are briefly modeled and key conclusion is drawn for internal(particle concentrations) and external guiding factors(field amplitude and frequency) for achieving the optimal temperature ranges.In alternating electromagnetic field, the heat generation inside a tissue is mainly due to the contribution achieved by nanoparticles due to the three loss processesnoteably: 1.Hysteresis (Blocked particles), 2.Relaxation (Superparamagnetic) and 3.Resonance.Since, the resonance losses occurs at higher frequencies and hence in respect of hyperthermia applications is unsuitable.

OPERATING CONDITIONS/ PARAMETERS	**TYPE OF NANOPARTICLE BEHAVIORS**	
	HYSTERETIC BEHAVIOR OR	**SUPERPARAMAGNETIC BEHAVIOR**

	FERROMAGNETIC BEHAVIOR				
	FM Regime		SPM Regime		
Field amplitude	Less than 20kA/m		6.5kA/m	13.5kA/m	20kA/m
Field frequency	Less than 600kHz		500-550kHz	160-180kHz	Less than 90kHz
Sizeof MNPs (nanoparticles)	9nm-10nm(radius) 18nm-20nm(diameter)		9nm-10nm(radius) 18nm-20nm(diameter)		
Concentration of nanoparticles	12mg/cm³	12mg/cm³	10.5mg/cm³	10.5mg/cm³	
Nanoparticles distributions	20 spherical regions	20 spherical regions	20 spherical regions	20 spherical regions	
Diameter of each spherical injection/ accumulation site	0.6mm	0.9mm	0.6mm	0.762mm	
Loss power(L.P) of each spherical region	5×10^9 W/m³	5×10^9 W/m³	1×10^8 W/m³	1×10^8 W/m³	
Optimal temperature	42-42.5°C	42-42.5°C	42-42.5°C	42-42.5°C	
Heat confined around region	2-3mm around particle	4-6mm around particle	5-6mm around particle	8-10mm around particle	

Inference drawn:

1.For maximum biocompatible values for both the nanoparticles behaviors, loss Power(L.P*fm*) in the hysteretic behavior for maximum values of amplitudes and frequencies of 20kA/m and 600kHz is lower than the loss power(L.P*spm*) for superparamagnetic model for frequencies less than 250kHz and amplitude of 6.5kA/m.

2.For denser nanoparticles distribution within the tissue, the optimum heating zones are very large when more number of particles are in very close vicinity to each other for same operating conditions of field amplitude,field frequency and concentration of particles.

Research Gaps:

The field amplitude and field frequency are most important parameters that needs to be tuned along with the loss power for each of the smaller sized nanoparticles.

[3]Pavel M.,Gradinariu G., and Stancu A.*(2008)*

Computational/ Experimental	Finite Element Method(FEM)	Physics Employed	Magnetic Nanoparticle Used	Distribution of MNP's Monodispersion/ Polydispersion
Computational	ComsolMultiphysics	Heat transfer Module	**1.**Magnetite (Fe_3O_4) **2.**Maghemite ($\gamma - Fe_2O_3$)	Monodispersion (Homogeneously distributed)

Objective: To compute heat dissipation/distribution generated by MNPs with given concentration for various types of tissues.

Work:

Experimental Study	Safe & Tolerable Limits	Loss Power
Brezovich(validated by Pankhurst) criterion of exposure	$H_o.f \le 4.85\times10^8\, Am^{-1}s^{-1}$	$L.Pspm = \pi\mu_o\chi_o f \frac{2\pi f\tau_R}{1+(2\pi f\tau_R)^2} H_o^2$ *where* , $\chi_o = \frac{\mu_o M_s^2 V_m}{k_B T}$
Hergt. weaker criterion of exposure	$H_o.f < C$ *where* , $C = 5\times10^9\, Am^{-1}s^{-1}$	$L.Pspm_{\max} = \pi\mu_o\chi_o \frac{C^2\tau_R}{\left[1+\left(\frac{C^2\tau_R^2}{H_o^2}\right)\right]}$

Geometrical details: Spherical tumor located in cubical region of volume 1cm³.

Loss power(L.P) range: $(3.4-6.3)\times10^9 W/m^3$

Three simulations were performed.

PARAMETERS	MODEL-1	MODEL-2	MODEL-3
Type of tissue	1.Liver tissue	1.Liver tissue 2.Breast tissue 3.Brain tissue 4.Skin tissue	1.Liver tissue
Distribution of MNPs	Homogeneous distribution	Less homogeneous distribution	More reduced homogeneous Distribution
Geometrical details	Spherical tumor regions surrounded by healthy tissue cubical in shape.	Existence of two blood vessels B.V1(dia.)=0.1mm B.V2(dia.)=0.1mm Diameter of tumor =2.7mm to 2.8mm	Tumor volume of 18mm³. (3mm×3mm×2mm)

			B.V1(distance from tumor reg.) =2.5mm B.V2(distance from tumor reg.) =4mm Type of particle distribution: Case-1 (Homogeneous) Case-2 (Less homogeneous)	
Particle concentrations	For Magnetite, 10mg/cm³($\phi = 3.2mm$) 3.36mg/cm³($\phi = 4.6mm$) 1.5mg/cm³($\phi = 6mm$) For Maghemite, 10mg/cm³($\phi = 3.2mm$) 3.1mg/cm³($\phi = 4.9mm$) 0.5mg/cm³($\phi = 8.9mm$) where, ϕ = tumor diameter		6 up-to 15mg/cm³	10mg/cm³ to 5mg/cm³
Field amplitude	6.5kA/m		6.5'kA/m	7.5kA/m
Field frequency	300kHz		300'kHz	250kHz
Type of Magnetic material	Magnetite	Maghemite	Magnetite	Magnetite
Diameter of nanoparticle	18nm	22nm	18'nm	18nm
Loss Power	L.Prange	L.Prange	4.15×10^9 W/m³	1.17x10^10W/m³ For magnetite concentration of 18nm in superparamagnetic regime: 1.L.P=6×10^9W/m³ →c=10mg/cm³ 2.L.P=10×10^9W/m³ →c=10mg/cm³

				3.L.P=6×10^9W/m³ →c=13mg/cm³ 4.L.P=10×10^9W/m³ →c=13mg/cm³ 5.L.P=6×10^9W/m³ →c=16mg/cm³ 6.L.P=10×10^9W/m³ →c=16mg/cm³	
Effectiveness/ special comments	No Info.	More effective at lower concentrations	No Info.	For Ferromagnetic regime: Ho=7.5kA/m f=300kHz c=15mg/cm³ temperature around tumor region 41.3°C. For optimum therapeutic temperature of 42°C from 41.3°C. Ho=14.5kA/m f=410kHz c=10mg/cm³ L.P=should be greater than 6×10^9 W/m³. For increased tumor volume, Volume=30mm³ (4mm×3mm×2.5mm) f=170kHz c=10mg/cm³.	
Number of particle distribution sites within tumor volume	6’		6	9	
Diameter of each spherical injection/ accumulation site	0.9’mm		0.9mm	0.762mm	
Tumor Volume	18’mm³		18’mm³	18mm³ (3mm ×3mm ×3mm)	30 mm³ (4mm× 3mm×

				2.5mm)
Results	Spatial temperature distribution in around tumor region shows temp. rise.	Linear increase of temperature with: 1.Concentration 2.Loss Power	For the given conc.,L.P,dia.,the temperatures achieved at tumor border,x=0.4mm,0.8 mm respectively.	

Inference drawn:

1.IMPORTANT INFERENCE: For concentrations smaller than 10mg/cm^3,the temperature depends closely upon concentration and the estimation of Loss Power(L.P) may be very difficult to obtain because of the multiple fluctuations.

2.It is been found that for maghemite particles, fluctuating heat generation patterns(too high or too low) for particle diameters larger than 23nm or less than 21nm which is big constraint to be considered for efficient MFH therapy.

3.For ferromagnetic behavior of particles, to obtain the same temperature rise the field amplitude and field frequency must be significantly increased for same concentration of nanoparticles as for superparamagnetic regime.

4.Forsuperparamagnetic regime,the generation of heat is solely depends upon the concentration of particles as opposed to external variables.

Research Gaps:

This present study wherein taking into account the internal factors or local features i.e(tumor density, type, perfusion rate) and external factors(Magnetic parameters i.e Field amplitude and field frequency.)For breast tissue wherein perfusion is very low and effective blood vessels(veins and arteries) are less compared to other organs and also chances of MTS are very less. This study can be a precursor to studies involving suitable medical imaging techniques(MRI,CT).As addressed by author the blood vessels number may also increase, tumor specific shape, location can be correctly defined by using MRI technique for soft-tissues and the 3D-model can be created by using appropriate Imaging processing software or codes specific to requirement for successful employment to clinical trials.

[4]Pavel M. *et al(2009).*

Objective: To study the optimum dose of magnetic material and to optimize the number of injection sites in order to achieve therapeutic temperature range.

Computational/ Experimental	Finite Element Method(FEM)	Physics Employed	Magnetic Nanoparticle Used	Distribution of MNP's Monodispersion/ Polydispersion
Computational	ComsolMultiphysics	Heat transfer Module	Magnetite (Fe_3O_4)	Monodispersion (Homogeneously distributed)

Work: In this paper cubical region is selected from tissue under analysis and the tumor is assumed to be perfectly spherical in shape.

Tissue region=14mm×16mm×14mm=3136mm³.

Type of tissue under consideration:1.Liver tissue

2.Breast tissue

Therapeutic loss power(L.P) range=(3.6-7.6) ×10^9W/m³.

Type of magnetite material=Magnetite

Concentration=8-12mg/(cm³ of tumor tissue)

Four different approaches are considered to address the interdependency of various parameters.These alterations are done via four noteable simulations.

PARAMETERS/ OPERATING CONDITIONS	FIRST MODEL	SECOND MODEL	THIRD MODEL	FOURTH MODEL
Brief overview	Nanoparticles located inside the spherical regions within tumor	Nanoparticles located inside the spherical regions within tumor and as well as between two metastatic regions	Variations in dimensions of one of the MTS region (tumors).i.e 2.7 to 4.2mm In particular, Range(3.8-4.2mm) Case-1 If diameter of MTS region =3.3mm Case-2 If diameter of MTS region =3.9mm Case-3 If diameter of MTS region =4.2mm	Considering case-3,for thirdmodel.Variations in the distance between two MTS regions and distance from blood vessel. Case-A If MTS1(dia)= 3.9mm Case-B If MTS2(dia)= 2.7mm
Origin/Root of Carcinoma (CANCER)	a.Colorectal carcinoma b.Cervical cancer	a.Colorectal carcinoma b.Cervical cancer	a.Colorectal carcinoma b.Cervical cancer	a.Malignant melanoma and Cervical cancer b.Colorectal

					carcinoma	
Tissues analysed	a.Metastases to Liver tissue b.Metastases to Breast tissue	a.Metastases to Liver tissue b.Metastases to Breast tissue	a.Metastases to Liver tissue b.Metastases to Breast tissue		a.Metastases to Breast tissue b.Metastases to Liver tissue	
Diameter of 1st tumor(MTS-1)	2.7mm	2.7mm	Case-1,2,3		3.9mm	
Diameter of 2nd tumor(MTS-2)	2.7mm	2.7mm	Case-1,2,3		2.7mm	
Blood vessel radius (B.V)	0.5mm	1mm	1mm		1mm	
Location of MTS-1 from B.V	4.5mm	4.5mm	4.5mm		4.5mm	
Location of MTS-2 from B.V	4.5mm	4.5mm	4.5mm		5.4mm	
Distance between two tumors(MTS)	1.3mm	1.3mm	1.3mm		Varied upto 2mm	
No. of injection/ accumulation sites	12	11	12 if MTS diameter >3.8mm	13 for case-3	12 if MTS diameter >3.8mm	
Diameter of each spherical region	0.9mm	0.9mm	0.9mm		0.9mm	
Location of spherical regions	6 within each tumor region	5 within each tumor region and 1 placed b/w two metastatic regions	6 within each tumor region and 1 placed b/w two metastatic regions		6 within each tumor region and 1 placed b/w two metastatic regions	
Loss power(L.P)	$(3.4-5.2)\times10^{9}$ W/m^3	Greater than $5\times10^{9}W/m^3$	For case-1 (4.5-5.0)×10^9 W/m³.	For case-3 (5.8-6.8)×10^9 W/m³.	For Case-A, (6.8-7.5)× 10^9 W/m³.	For Case-B, (5-5.8)× 10^9 W/m³.
Concentration of nanoparticles	8-15mg/cm³ of tumor volume.	Larger than 11mg/cm³ of tumor volume	13 mg/cm³.	(8.5-9) mg/cm³.	(10.0-10.5) mg/ cm³.	(14.0-14.5)m g/ cm³.
Results	Heating zone of atleast 1.5mm-2mm around the	Therapeutic temperature changes at a 2mm distance	Distances comparable to MTS dimensions donot considerably affect the temperatures		For very small metastases less than 2.7mm,temperatu	

	metastatic region	from the MTS for larger L.P values.	at 1.5mm-2mm around tumor border.	re difference decrease by increasing L.P value(field frequency and amplitude).
Inference drawn	1.Optimum heating zone around the tumor region is obtained by spreading the nano-particles not only inside but also in the tissue between them. 2.Higher temperature value is achieved at a minimum 1mm around tumor region when nano-particles are injected in between space also.	The temperature decreases more in the case of larger blood vessel	Temperatures for the BV on the tumor side are greater than other side. For a small shift of 1mm noticeably influence temperature field within the tissue.	Tumor densities and perfusion rate have considerable affect.

Research Gaps:

In this computational work, the nanoparticles are assumed to be monodispersed. The size polydispersity which is present in all real nanoparticles samples is still missing in this analysis.Since,the current study focused on micrometastases which is advanced cancer stage,the applicability of current approach will be possible if exact dimensions in which tumor resides is feasible before the domain researchers. So, Suitable medical imaging techniquese.g,MRI,CT should be employed and by using these models it is possible to estimate the impact of theparticle dose on the efficiency of hyperthermia therapy.Tumor density, Type of tumor, Perfusion rate, blood vessels impact that can be addressed correctly unless the geometrical information obtained

from the scans is converted into 3D Model and thermal analysis is done to obtain the required temperature elevations with feasible alterations in internal and external factors.

[5]Astefanoaei I., and Dumitro.I*et.al(2014)*

Objective:

1.To determine the temperature fields determined by heating of MNPs injected in a malignant tissue

2.To analyze the thermal influence of blood flow in vessels with different sizes on temperature fields within a tumor.

Computational/ Experimental	**Finite Element Method(FEM)**	**Physics Employed**	**Magnetic Nanoparticle Used**	**Distribution of MNP's Monodispersion/ Polydispersion**
Computational	ComsolMultiphysics	1.Heat transfer Module 2.Navier Stokes equation in laminar regime	1. $Fe_{67.7}Cr_{13}Nb_{0.3}B_{20}$ 2.Maghemite ($\gamma - Fe_2O_3$) 3.Magnetite (Fe_3O_4)	Monodispersion (Homogeneously distributed)

PARAMETERS	**EXPLANATION**
Brief Overview	**CASE-1:** No blood vessel transit the tumor. **CASE-2:** One blood vessel transits the tumor. **CASE-3:** Two blood vessels in the y-direction at distance 1mm away from each other transits the tumor at center.
Tissue under consideration	Types of Tissue:Liver tissue Type of Cancer:Primary liver cancer.
Magnetic field parameters	Field amplitude, H_o=5 kA/m Field Frequency,f=150 kHz Power density or Loss Power,L.P=5.75×10^7W/m³.
Boundary conditions	1.Dirichlet's boundary condition The temperature at the external surface of healthy tissue i.e cube is maintained to be at 37°C. 2.Newman's boundary condition Heat flux is imposed at tumor-vessel interfaces so that heat flux coming from the tumor is completely received by blood vessels. 3.Continuity's boundary condition Heat flux is imposed at the tumor-healthy region interface and tumor-injection site

	interfaces.
Geometry	Spherical shaped tumor located in a cubical region obtained from healthy tissue. Diameter of tumor=14mm Dimensions of cube=30mm×30mm×30mm=27000mm³.
Nanoparticles ($Fe_{67.7}Cr_{13}Nb_{0.3}B_{20}$)	Mass density, ρ_{MNP} =7060kg/m³. Specific heat capacity, $C_{P,MNP}$=1227 J/kg.K Thermal conductivity, k_{MNP} =528 W/m.K Specific saturation magnetization, M_s =36 emu/gm Diameter of nanoparticles =10nm. Mass concentration,c =10mg/cm³. Number of Injection /accumulation sites in tumor=16. Diameter of each spherical region=0.7mm
Assumptions	Blood is considered as Newtonian fluid in the laminar regime.
Average properties calculations	Injection of MNPs into small regions of the tumor changes their thermal properties $\rho_{mix} = \nu\rho_{MNP} + (1-\nu)\rho_{tumor},$ $C_{mix} = \nu C_{MNP} + (1-\nu)C_{tumor},$ $\frac{1}{k_{mix}} = \frac{\nu}{k_{MNP}} + \frac{1-\nu}{k_{tumor}},$ *where,* ν = is the volume concentration of the MNPs
Equations Used	To analyze heat transfer in living tissues, 1.Penne's Bioheat Equation $\rho_t C_t \frac{\partial T}{\partial t} + \nabla(-k_t \nabla T) = \rho_b \omega_b C_b (T_{art} - T) + Q_{met} + Q_{ext}$ 2.Navier Stokes Equation $\rho_b C_b \left(\frac{\partial T_b}{\partial t} + \upsilon_z \frac{\partial T_b}{\partial z} \right) = \nabla(k_b \nabla T_b) + Q_{ext}$ *where,* Second term,on the L.H.S acts as Sink Source term within the tumor to account for cooling effect of the blood vessels contrary to heat source on R.H.S. k_b = blood thermal conductivity υ_z = blood velocity

	$v_z = 2V_o(1 - r_v^2 / R_v^2)$ Blood velocities:Vo=1mm/s, 2mm/s, 3mm/s, 4mm/s

Inference drawn:

1.The cooling effect of vessels is reduced for the vessels with smaller diameter.

2.Smaller blood velocity diminishes the cooling effect and maintain therapeutic temperature in tumor.

3.The temperatures in the tumor are smaller for larger blood vessels because of the thermal heat loss caused.

4.Optimum Particle concentration is a main parameter that needs to be optimized in order to obtain therapeutic temperature range within tumor.

Research Gaps:

The hyperthermia treatment planning is necessary to find the exact tumor location, tumor geometry, tumor shape, and tumor size. The effectiveness of defining the HTP(Hyperthermia treatment planning protocol) is to study patient model is still missing. Patient specific information/preoperative procedures or any useful information before surgery is very much needed. There is a need to elaborate a patient model by segmentation of images obtained from computerized tomography or magnetic resonance imaging scans.Patient specific modeling with the aid of advanced computational tools is still not been addressed.

[6]Wu L., Cheng J.and ,Liu W.*et al. (2015)*

Objective: To analyze the temperature distributions in tumor by electromagnetically induced heating.

Computational/ Experimental	Finite Element Method(FEM)	Physics Employed	Magnetic Nanoparticle Used	Distribution of MNP's Monodispersion/ Polydispersion
Computational	ComsolMultiphysics	**1.**Heat transfer Module(bioheat transfer) **2.**AC/DC module (electromagnetic heating)	Magnetite (Fe_3O_4)	Monodispersion (Even or Homogeneously distributed)

Work: Coupling between Maxwell's equation from magnetic module with Penne's bioheat transfer equation from heat transfer module. Power density due to electromagnetic field

simulation serves as input to bioheat transfer equation and determines the heat generated by ferrofluids.

PARAMETERS	VALUES
Radius of tumor,r	5mm
Radius of concentric normal tissue,a	10mm
AC Magnetic field produced by	Two identical pairs of Helmholtz coils
Volume fraction of magnetite nanoparticles in the tumor region, ν	0.003(10mgFe/g of tumor)
Geometry details	**a.**Bilayered model of a tumor i.e central composite region of tumor tissue and magnetic nanoparticle fluid surrounded by healthy tissue. **b.**Helmholtz coil to produce electromagnetic heating effect.
Average properties calculations	$\rho_{composite} = \nu\rho_{ferrofluid} + (1-\nu)\rho_{tumor}$, $C_{composite} = \nu C_{ferrofluid} + (1-\nu)C_{tumor}$, $\frac{1}{k_{composite}} = \frac{\nu}{k_{ferrofluid}} + \frac{1-\nu}{k_{tumor}}$,
Boundary Conditions	Initial temperature is set to be To=37°C. Isothermal B.C.,the edge of normal tissues is at constant temperature of 37°C.
Alternating current in coil	5A
Field Strength/Amplitude of magnetic field,Ho	5518A/m=5.518kA/m
Field frequency ,f	300kHz
Type of Magnetic nanoparticle	Magnetite
Magnetic nano-particle diameter, d_{MNP}	18nm
Volume fraction solid, ϕ	0.071
Domain Magnetization, M_d	446kA/m
Effective Anisotropy Constant, K	1.0×10^{4} J/m³.
Attempt time, τ_o	10^{-9}s
Dynamic Viscosity, η	1.0×10^{-3}kg/(m.s)
Hydrodynamic particle volume	5.0805×10^{-22} m³
Axial component of magnetic flux density	$B = \frac{\mu_O NIr^2}{2\left[r^2+\left(\frac{d}{2}+x\right)\right]^{3/2}} + \frac{\mu_O NIr^2}{2\left[r^2+\left(\frac{d}{2}-x\right)\right]^{3/2}}$ Helmholtz coil pair, Two identical circular coil of radius,r; Equal no. of turns of wires,N; Distance b/w two coils,L.

PARAMETERS	Specific heat capacity (J/kg.K)	Thermal conductivity (W/m.K)	Density (kg/m^3)	Blood perfusion rate (1/s)
Tumor tissue	3500	0.55	1060	---------
Magnetic ferrofluid (magnetite)	4000	40	5180	---------
Composite region	3501.5	0.552	1070.4	---------
Blood in tumor	4180	0.512	1000	1.39×10^{-2}
Blood in normal tissue	4180	0.512	1000	6.67×10^{-3}
Normal tissue	2300	0.25	980	-------

Results:

Temperature distribution reaches a steady state after 200s.

Maximum temperature appears at the center of tumor region is 43.47°C.

Inference drawn:

1.Temperature decreases with increasing distance from the center at different exposure times.

2.Eddy current induced heating of minute magnetic particles is negligibly small compared with the magnetic losses.

Research Gaps:

This model takes into the account 3-D electromagnetic thermal problem by considering bilayered spherical model,but in real conditions these kinds of geometries has no existence.So, although this effort is appreciable as far as the concept of electromagnetic heating is concerned but the model must be addressed to patient specific problems.

[7]Ghosh, Gupta D., and Das S.*et al.(2013)*

Objective: To analyze theeffect of different parameters on tissue temperature rise for superparamagnetic iron oxide nanoparticles in the presence of external applied electromagnetic field.

Computational/ Experimental	Finite Element Method(FEM)	Physics Employed	Magnetic Nanoparticle Used	Distribution of MNP's Monodispersion/ Polydispersion
Computational	Comsol Multiphysics-3.4	Heat transfer Module	Magnetite (Fe_3O_4)	Monodispersion (Homogeneously distributed)

Work:

PARAMETERS	EXPLANATION
Type of Nanoparticle	Magnetite
Clinical Trial (Human/Animal)	Animal(mice)
Type of Geometry	3D model
Type of analysis (Steady state/Transient)	Transient
Geometry details	Ellipsoid(tumor bearing portion of mice) resting over cylindrical muscle tissue covered by skin tissue.
Electromagnetic Frequency	400 kHz
Field Amplitude	8.8kA/m
Exposure Duration Time	242sec
Type of Injection (Systemic(Intravenous)/ Intratumoral)	IntratumoralInjection
Nanoparticle dosage	21±9mg
Initial Temperature Given	26°C±1°C
Final Temperature Achieved	71°C±8°C
Temperature Variation (Spatial/Temporal)	Temporal
Boundary Conditions	❖ Convection heat transfer coefficient,h=10W/m²K ❖ Ambient Temperature,T=20°C ❖ At boundaries far from tumor(Normal Tissue)=Zero heat flux ❖ Temperature Equilibration occurs
Grid Independency Study	OBJECTS OF SIMULATION: ❖ To Optimize the mesh quality. ❖ Computation time taken. ❖ Mesh Element Used
Study	Transient Solution(Time Marching)
Type of Solver Used	Conjugate Gradients Linear System Solver with Algebraic Multigrid Pre-Conditioner
Method Used	Consistent Initialization of DAE System was Backward Euler
Time Step	1 Sec
Relative Tolerance	0.01
Minimum Element Quality	0.223
Mesh Element	Tetrahedral(19,942 elements)
Variation done in Current Paper	❖ Nanoparticle Concentration ❖ Depth of Tumor ❖ Size of Tumor
Parametric Variation	1.Temperature of tumor at different time duration 2.Time Duration of applying the magnetic field a.)Location of Tumor

	b.)Size of Tumor 3.Concentartion of Nanopaticles in Tumor 4.Types of Nanoparticles employed 5.Field Strength 6.Frequencies 7.Different methods of encapsulation 8.Delivery of Particles
Study/Variations	**Effect of Varying Magnetizing Field:** c=10mg/cc,r=10nm,depth=8mm,Size of tumor 4x3 1.)200kA/m 2.)250kA/m 3.)300kA/m 4.)350kA/m **Study:** a.)Temperature profile of tumor for different values of H b.)Temperature vs time c.)Maximum core temperature vs Magnetizing field
	Effect of Tumor Size: H=300kA/m,r=10nm,c=10mg/cc,16mm deep 1.)1x0.75 2.)2x1.5 3.)4x3 4.)6x4.5 **Study:** a.)Temperature profile of the tumor for different tumor sizes b.)Core Temperature vs time for different tumor sizes c.)Maximum Core temperature vs Size
	Effect of Depth of Tumor: H=300kA/m,r=10nm,c=10mg/cc 1.)At a depth of 2mm 2.)At a depth of 4mm 3.)At a depth of 6mm 4.)At a depth of 8mm **Study:** a.)Temperature profile of tumor vs different depths b.)Temperature vs time for different depths c.)Maximum Core Temperature vs depth
	Effect of Concentration of Nanoparticle: For 8mm deep tumor, H=300kA/m, r=10nm 1.)5mg/cc 2.)8mg/cc 3.)10mg/cc **Study:** a.)Temperature profile of the tumor for different concentrations b.)Temperatures vs time for different concentrations c.)Maximum Core Temperature vs concentration

Heat transfer coefficient, h	5W/m²K
Skin thickness above tumor	0.5mm
Damage Integral, Ω	$\Omega(x,y,z,t) = A\int_{t1}^{t2} \exp\left(\frac{-E}{RT}\right)dt$ ❖ 44°C<T<50°C A=4.3x10^64(s^-1) E=4,20,000(J/m) ❖ T>50°C A=9.4x10^104(s^-1) E=6,60,000(J/m) where, A=Pre-Exponential Factor E=Activation Energy for the reaction R=8.36J/mK
Loss Power, Q_{source}	$Q_{source} = Q(H, r_n, T, type\_of\_nanopartide) = \frac{c^3 N \mu_O^2 V_n^2 H^2 \sigma (r_n)^2 \pi}{M_n k_B T \tau_O \exp\left[\frac{25T_B}{T}\right]}$
Nanoparticle Density Range	5-10mg/cc(Max. Attainable=10mg/cc)
Magnetizing Field Range	200-350kA/m
Diameter of Nanoparticle	10nm per 299mm³ of tissue (10mg/cc of tissue)
Metabolic heat generation, Q_{met}	400W/m³
Heat generation	Heat generation by magnetic field is solely inside the tumor
Avogadro Constant, N	$6.022\times10^{23} mole^{-1}$
Magnetic constant/Permeability of free space, μ_O	$1.25663706\times10^{-6} mkgs^{-2}A^{-2}$
Nanoparticle volume, V_n	$V_n = \frac{4}{3}\pi r_n^3$
Radius of nanoparticle, r_n	$10nm$
Saturation magnetization of magnetite nanoparticle, σ	$62.2emu/gm$
Molecular weight of nanoparticle, M_n	$232gm/mole$
Boltzmann's constant, k_B	$1.3806503\times10^{-23} m^2 kgs^{-2} K^{-1}$
Local tissue temperature, T	T
Attempt period, τ_O	10^{-11} sec for non-interacting particles
Blocking temperature of magnetite nanoparticle, T_B	$115K$

Mixture Model:
Volume fraction, f_v or ν

$$f_v = \frac{V_{np}}{V_{np} + V_{bf}} = \frac{\left(\frac{w_{np}}{\rho_{np}}\right)}{\left(\frac{w_{np}}{\rho_{np}}\right) + V_{bf}}$$

where,

V_{np} = Volume of nanoparticles

V_{bf} = Volume of base fluid

Weight=density×Volume

$w = \rho \times \upsilon$

Volume=weight/density

$$\upsilon = \frac{w}{\rho}$$

Calculations:

Mean mass of magnetite=21mg±9

$=21\times10^{-6}$kg

$=2.1\times10^{-5}$kg

Magnetic fluid sample=50 to 100 μL

$=50\times10^{-9}$m³

$=5\times10^{-8}$m³

Density of nanoparticle=5180kg/m³

$$f_v = \frac{\left(\frac{21\times10^{-6}}{5180}\right)}{\left(\frac{21\times10^{-6}}{5180}\right) + \left(50\times10^{-9}\right)}$$

$f_v = 0.075$

Averaging of Properties:

$$\rho_{mix} = \nu\rho_{MNP} + (1-\nu)\rho_{tumor},$$

$$C_{mix} = \nu C_{MNP} + (1-\nu)C_{tumor},$$

$$\frac{1}{k_{mix}} = \frac{\nu}{k_{MNP}} + \frac{1-\nu}{k_{tumor}},$$

OR

	$\rho_{composite} = \nu\rho_{ferrofluid} + (1-\nu)\rho_{tumor},$ $C_{composite} = \nu C_{ferrofluid} + (1-\nu)C_{tumor},$ $\frac{1}{k_{composite}} = \frac{\nu}{k_{ferrofluid}} + \frac{1-\nu}{k_{tumor}},$ ν = is the volume fraction in the above equations can be considered as f_v

Inference drawn:

1.The power generation increases considerably with temperature.Heat generation by magnetic field is solely inside the tumor.That's why the heat is confined to tumor loaded region and healthy tissue region don't feel the presence of MNPs.So,local temperature has both increasing and decreasing effects.

2.Temperature increases with increasing the magnetizing field.

3.Effect of Tumor Size:

- Small Size
- Large Size

a.)Rate of heat generation in smaller space is higher as compared to large size tumor.Thus,Temperature rise is also higher for small size tumor.

b.)Surface Area to Volume Ratio is higher for smaller tumor.Therefore, Due to heat dissipation there is insufficient heating exists inside the core of tumor.This in return causes the temperature rise of neighbouring tissues due to heat diffusion.

4.As concentration of nanoparticles increases,the temperature increases.

5.With the depth,the maximum temperature decreases.The tumor near the surface is exposed to very weak natural convection.So,the heat cannot diffuse at the air side leading to higher temperatures at surface.

6.After the magnetic field is turned off,heat diffuses through the tissue.Therefore, heat diffuses to healthy tissues and ablation may occur.

7.Cooling of the surface with water after switching off the magnetizing field will help to reduce the minimal transfer of heat to healthy tissues.The optimum convection coefficient during forced cooling is $h=54W/m^2.K$

Research Gaps:

The model can be redefined for intravenous injection by taking the case for deeply penetrating tumors where intratumoral injection is not feasible.This can be only possible by taking the MRI scans(Soft Tissues) of cancerous affected organs and accordingly extend the study by seeing to the size and shape of tumor. Planning for effective hyperthermia study, simulations should guide the after effects of MNPs heating and the key cooling protocol set by the author can be an assistive tool to go for therapeutic temperature elevations.

[8]Salarian H., GarmabakiS.H.Amir, and Zakariapour M. ***et al.(2011)***

Objective: To investigate the effect of physical characteristics of nanoparticles,applied magnetic field,tissueon heat transfer phenomenon of human body in hyperthermia.

Work:

Type of study	Numerical study/Analytical
Type of nanoparticle used	FePt
Type of geometry model	Two-Dimensional geometry
Geometry Details	Core region of tumor:sphere Diameter of tumor:1cm Cooling pad surrounding the tumor core to maintain the temperature as 37°C.
Type of tissue under consideration	Eye
Averaging of tumor loaded with MNPs	$\rho_{composite} = \nu\rho_{ferrofluid} + (1-\nu)\rho_{tumor},$ $C_{composite} = \nu C_{ferrofluid} + (1-\nu)C_{tumor},$ $\frac{1}{k_{composite}} = \frac{\nu}{k_{ferrofluid}} + \frac{1-\nu}{k_{tumor}},$ $\nu = Volumefraction$
Power dissipation by MNPs	$P = \pi\mu_O\chi_O H_O^2 f \frac{2\pi f\tau_R}{1+(2\pi f\tau_R)^2}$ Where, $\chi_O = \frac{\mu_O \nu^2 M_d^2 V_M}{k_B T}$ M_d = Domain magnetization of suspended particle
Applied field, H_O	10kA/m
Applied frequency, f	300kHz

Diameter of nanoparticle, d	6nm
Volume fraction, ν	0.0006
Thermal conductivity of tissue, k	0.502W/m.K
Blood perfusion rate, w_b	$0.0064s^{-1}$
Metabolic heat generation, Q_{met}	$540W/m^3$
Specific heat of nanoparticle, C_{MNP}	670J/kg
Density of nanoparticles, ρ_{MNP}	$15200kg/m^3$
$\rho_b C_b$	$4.18\times10^6 J/m^3K$
Different variations done	**1.**To study the effect of strength of applied magnetic field(Field Amplitude) on: a.)Temperature field vs time. b.)Temperature field vs position. Ho=10kA/m,14kA/m,18kA/m **2.**To study the effect of field frequency of magnetic field on: a.)Temperature field vs time. b.)Temperature field vs position. f=300kHz,500kHz,700kHz **3.**To study the effect of nanoparticle's maximum diameter on: a.)Temperature field vs time. b.)Temperature field vs position. d=5nm,6nm,7nm **4.**To study the effect of different types of materials of magnetic nanoparticles: a.)Temperature field vs time. Magnetite, Maghemite,FeCo,FePt **5.**To study the effect of nanoparticle's volume fraction on: a.)Temperature field vs time. b.)Temperature field vs position ν = 0.0004,0.0006,0.0008

Inference drawn:

1.The strength of applied alternating current electromagnetic field has minor effect on temperature rise.

2.The volume fraction and the frequency of applied alternating current magnetic field has moderate effect on temperature rise.

3.Diameter of nanoparticles has the major effect on the temperature rise.

4.For metabolism rate, temperature dependent and temperature independent were considered. The temperature rise for temperature dependent metabolism rate is more than temperature independent metabolism rate.

5.Between all different material types,FePt is proved to be most effective material.

6.For perfusion rate,the two conditions of position dependent and position independent were considered. The temperature rise for position independent perfusion rate was more than position dependent perfusion rate.

7.Perfusion rate was more efficient than metabolism rate.

8.This study also addresses the effect of various conditions via different co-ordinate systems to account for time constants values.

a.)Cartesian Co-ordinate system

b.)Spherical Co-ordinate system

Spherical Co-ordinate system has less time constants values than cartesian.

Research Gaps:

The study must be solved in three dimensional system of coordinates. Along with the numerical schemes applied for different domains of cancerous and healthy tissues,it should also be validated by simulation tools.

[9]Wang Z., Aarya I., Gueorguieva M., Liu D., Luo H.,Manfredi L., and Wang L. *et al.(2012)*

Objective: Togenerate and analyze the Image-based 3D CAD anatomical model for FEM modeling and its application to ablate cancerous tissue via RFA(Radio Frequency Ablation).

Work: In this study breast gel phantom is prepared and a small irregular-shaped portion of fresh baby potato(maximal dimension of 25mm) was embedded inside the phantom to simulate cancerous tissue. Then, the gel breast phantom is imaged in Magnetic Resonance Imaging(MRI) scanner. The slice thickness was 2mm with zero spacing. The total acquisition time was 6min 43sec.Once the images were acquired, they were exported in DICOM format for further image processing and analysis. The DICOM compatible image slices were imported for pre-processing for applying various operations such as Gaussian filters(removing background noise), Segmentation(to identify tumor and healthy tissue) by applying different masks operations.After

threshold operation, masks were used in in a flood-fill operation during the reconstruction of the model.

PARAMETERS	EXPLANATION
Type of Modality	Radiofrequency Ablation
(FEM)Finite Element Solver	Comsol-Multiphysics
Image Processing Tool	ScanIP,Simpleware
Type of Work	Experimental/Computational ❖ Tissue mimicking breast phantom
Physics used	❖ Bio-heat transfer model ❖ Electrical heating model
Frequency employed	300-500kHz
Type of solver used	Direct linear system solver(UMFPACK) and non-symmetric matrix conditions
Blood perfusion	6.4×10^{-3}(1/s)
Type of mesh used	Coarse
Number of meshing elements	26,459
Type of probe used	RITA probe
Heat generated by metabolic heat, Q_{met}	0
Applied energy dose	2.25kJ(i.e 7.5W and 300s) 7.5kJ(i.e 25W and 300s)

Materials used in computational modeling	Thermal Conductivity (W/m.K)	Electrical Conductivity (S/m)	Density (kg/m³)	Specific heat capacity (J/kg.K)
Breast tumor	0.48	0.71	1050	3770
Breast tissue	0.499	0.28	1060	2770
Gel	0.59	0.117	1069	3676
Trocar base	0.026	10^{-5}	70	1045
Electrode	18	10^{8}	6450	840
Trocar tip	71	4×10^{6}	7900	132

Inference drawn:

The present study provides the guide pathway to develop the 3D model from scanned 2D images that are preprocessed and converted via commercial software packages i.eScanIP which was input to other commercial package i.eComsol-Multiphysics. This very study gave an approach to assist and optimize treatment protocols that improve the treatment therapeutic efficacy.

Research Gaps:

Proceeding in similar direction as the pilot study, successfully developed imaged based 3D models from real time clinical images(CANCER patients) obtained by CT or MRI to construct **patient-specific models** for planning and also simulation with a preview to optimize treatment efficacy. Patient specific image based 3D modeling could resolve the problems of heat sink effect created by blood vessels, role of healthy surrounding tissue in heat distribution, ablation etc. by permitting pre-treatment planning of the simulated thermal ablation based on preoperative images of the lesion. This research gap is very important finding for future computer assisted interventions and opens horizons towards beginning of new modalities and to improve the existing ones.

[10]LeBrun A., Manuchehrabadi N. and Attaluri A. *et al.(2013)*

Computational/ Experimental	Finite Element Method(FEM)	Physics Employed	Magnetic Nanoparticle Used	Distribution of MNP's
Computational	ComsolMultiphysics	Heat transfer Module	Magnetite (Fe_3O_4)	Heterogeneously Distribution

Objective:microCT image based simulation using MATLAB, ProE, SAS Program, Comsol-Multiphysics

Work:

Type of work	Computational
Type of analysis	Steady state
Type of tumor	PC3 Human Prostatic tumor
Type of magnetic nanoparticles	Magnetite
Diameter of nanoparticles	10nm
Type of ferrofluids	Water based
Concentration of ferrofluids	5.8% by volume
Flow rate	5µL/min
Amount of injection	0.1cm³(0.1cc contains 25.2 mg of iron)
Assumptions	SAR ∝ Nanoparticle conc. ……..(1) Nanoparticle conc. ∝ microCT pixel index number ……..(2) From (1) &(2), SAR ∝ microCT pixel index number……(3) Density elevation-→presence of MNPs--→White cloud

Type of softwares used	❖ To generate prototype of tumor geometry • MATLAB • ProE ❖ Conversion of microCT pixel index numbers into SAR values due to presence of nanoparticles in tumor • SAS program ❖ Thermal Analysis • COMSOL_MULTIPHYSICS4.3
Major Unknown addressed	Distribution of nanoparticles accumulated in tumors
Major challenges	❖ Directly importing the microCT images files into numerical simulation software packages failed due to intensive memory requirements. ❖ Very expensive to purchase. ❖ Errors of singularities during meshing in finite element simulation. ❖ Limitation of computer geometry
Pixel index numbers range for brightness of scanned and reconstructed images	0-255
Pixel index number of tumor tissue without ferrofluid injections	45-55
Pixel index number of tumor tissue with ferrofluid injections	55-255
Number of turns of coil	Two-turn coil
Field frequency	190kHz
Current	200A
Density of ferrofluid	1290kg/m³
Specific heat capacity of ferrofluid	4100J/kg.K
Cluster volume for averaging the SAR values	1.76×10^{-3} mm³(7pixel×7pixel×7pixel)
Geometry defined for simulation	Rectangular column mimics the geometric dimensions of real mouse body and a tumor shape obtained from preprocessing operations via MATLAB codes for 13-30 slices Length of rectangular column=10cm Breadth of rectangular column=3cm Height of rectangular column=1.5cm
Boundary conditions	1.Tumor surface and mouse body subjected to natural convection B.C i.e, Ambient temperature,T∞=25°C Convection coefficient,h=3.7W/m²K 2.B.C on mouse bottom surface=37°C

Type of meshing elements	Tetrahedral elements
Total number of tetrahedral elements	146062
Type of meshing	Finer
Growth factor	1.1
Grid Independency test	❖ Done 1.Changing mesh to be extremely fine,there is an increase in computational effort of the machine to calculate the requisite temperature elevations for the domain. 2.Total number of elements=644035 3.Difference in temperatures=less than 0.1°C.
Average pixel number for 5.8% concentration of nanoparticles	123
SAR(W/m³) $= \frac{9.8 \times 10^5 (pixel\ index\ number - 55)}{(123 - 55)}$	SAR Range=1.5×10^4 W/m³ to 2.9×10^6 W/m³ SAR=zero(for pixel index number<55) Average SAR=$9.8\times10^5 W/m^3$ (before ferrofluid injection into tumor).
Total energy deposition	0.62W,0.33W,0.39W
Number of slices used	13
Results/Inference drawn	Maximum temperature=51°C-55°C Minimal temperature= interface b/w tumor and mouse body(41°C-45°C) 16°C-20°C temp. rise from baseline temperature of 35°C.

Research Gaps:

1.The temperature elevation measured in this current study are steady-state variations.In concern of Hyperthermia,the model must be addressed for temperature transient studies during magnetic field heating.

2.Since, the composition of ferrofluid is different from the actual tumor tissue(80% tissue is water) and in this very study a linear relationship between SAR value and microCT pixel index number is assumed.It should be addressed to real tumor.

3.The model doesnot takes into account the local vasculature which might be damaged during the heating.

4.This present study is an attempt to computationally develop algorithms to ensure smooth transfer of data obtained from several sets of microCT images to advanced simulation tools such as comsolmultiphysics.This study can be more effective if some real time data of cancer patients

is obtained and also the real tumor tissues should be made available for experimentation to compare the results with computational transient/time dependent studies.

5.The present study can also be coupled with electromagnetic heating module of comsol and then it can be even more reliable.

[11]Cepeda J.,Birla S., and Subbiah J. ***et al.(2013)***

Objective: To reconstruct complex three dimensional geometries of heterogeneous materials from two dimensional cross-sectional images and defining non-uniform material properties in comsol.

Work: In this study, author discussed step wise procedure to construct geometries from the information available via two dimensional cross-sectional images. There may be different techniques that can extract the information from two dimensional image sets and convert that into three dimensional model. This can be made feasible by writing your own codes specific to study. In this paper key emphasis is laid on the CT(Computed Tomography) scan and generation of geometry via MATLAB and MATERIALISE-MIMICS version 16.0. For the thermal analysis,COMSOL-MULTIPHYSICS is used as a computational tool which offers multiphysics interaction between different physics incorporation. Since, MIMICS and COMSOL are compatible and inbuilt interface allows to import multipart assembling of parts as single unit and can be exported to comsol as .mphtxt file. Moreover, to do the closely related thermal analysis,there are several ways to define materials. Interpolation functions are one of them or one can extract the model from the mesh file and then gave the properties to individual parts/subparts of geometry. So, in nutshell, briefly the sharing interface is defined which can be a precursor to the hyperthermia modeling of real time breast tumors in which we want to simulate the results in therapeutic range of 42°C-46°C.

Surface layers are defined on specific parts to define boundary conditions via Materialise 3-matic version 8.0.

Type of elements:

- Tetrahedral elements(4-nodes)
- Triangular elements(3-nodes)

Modules/Physics used in Comsol:

- Heat transfer in solids

- Transport of diluted species

Errors addressed:

1.Incompatibilities between different CAD file formats and simulation softwares.

2.Nodes on interfaces between neigbouring subparts may be displaced or not fully connected creates voids or overlapped regions.

3. Inconsistencies such as Face cannot be parameterized.

4.Internal error in geometry decomposition.

Defining material properties(INTERPOLATION Functions of Comsol):

To define specific heat(C_P), thermal conductivity(k), moisture diffusivity(D_m), and density(ρ) as a function of mesh co-ordinates, Interpolation functions are created.Then, material properties corresponding to different sections can be easily defined without assembling or defining individual sub-parts in geometry.

Inference drawn:

This study is an assistive tool that addressed the challenges of computational world of simulation and the specifically in concern of 3D-Imaging.

Research Gaps:

This study can be extended for soft tissues from the information obtained from MRI scans to direct the study to patient specific models.

[12]Li.Z, Kawashita M., and Araki N. ***et al.(2011)***

Objective: To find the optimum particle size which has high heating efficiency/ high heat generation ability under alternating magnetic field.

Work:In this study agar phantom is used.

Type of work	Experimental
Type of study	In-vitro
Type of particles	Magnetite
Size of particles	8nm to 103nm
Type of methods used for synthesis	❖ Chemical co-precipitation ❖ Oxidation precipitation method
Applied frequency	100kHz
Applied field	9.6kA/m to 23.9kA/m
Concentration of MNPs	58mgFe/ml
Measurements of temperature rise in phantoms	Fluor optic thermometer
Measurements of magnetic properties of sample	Vibrating sample magnetometer(VSM)

Measurements of crystalline phase of samples	Powder X-ray Diffractometer

PARAMETERS	SAMPLES				
	A	B	C	D	E
Saturation magnetization, M_s (Am^2/kg)	67.3	76.5	76.7	89.2	79.3
Coercive force, H_C (kA/m)	0.7	8.4	11.1	15.1	13.9
Heat generation, P(W/g)	0.33	16.5	8.1	6.6	4.9
Lattice constants calculated from XRD patterns	0.8393nm	0.8375nm	0.8371nm	0.8398nm	0.8388nm
Synthesis	Chemical co-precipitation method	Oxidation precipitation method	Oxidation precipitation method	Oxidation precipitation method	Oxidation precipitation method
Shape of particles as measured by TEM(Transmission Electron Microscope)	Nearly spherical particles	Nearly spherical particles	Nearly spherical particles	Square shaped with little of spherical	Square shaped with little of spherical
Particle size as estimated by TEM	8nm	24nm	36nm	65nm	103nm
Heat generation behavior	Super-paramagnetic	Ferro-magnetic	Ferro-magnetic	Ferro-magnetic	Ferro-magnetic
Single domain/ Multi domain	No Coercivity, No Remanence	Single domain	Single domain	Single domain	Multi Domain
Temperature increase, ΔT under given conditions:1.Field amplitude of 9.6kA/m 2.Field frequency of 100kHz 3.Time= 30sec 4.Particle size=8nm	9.3°C Reason: Relaxation loss	2°C Reason:	1°C Reason: Heat generation unavailable due to hysteresis loss	1°C Reason: Heat generation unavailable due to hysteresis loss	1°C Reason: Heat generation unavailable due to hysteresis loss
Temperature increase, ΔT under given conditions: 1.Field amplitude of 23.9kA/m	25°C	55°C	B>C>D>E	B>C>D>E	B>C>D>E

2.Field frequency of 100kHz 3.Time= 30sec 4.Particle size=24nm					

Saturation Magnetization,

$M_S = \gamma - Fe_2O_3 = 56 Am^2 / kg$

$M_S = Fe_3O_4 = 92 Am^2 / kg$

Lattice Constants,

$\gamma - Fe_2O_3$=0.8345nm

Fe_3O_4=0.8396nm

Inference drawn:

1.H_C ,Coercive force increase as particle size increases.

2.The heat generation is not only depends upon particle size but also highly dependent upon on magnetic field intensity.

3.The MNPs of 24nm shows excellent heating characteristics because of combined effect of loss mechanisms of relaxation and hyteresis.

Research Gaps:

These kind of experiments must be extended to real tissue samples and by taking into account the nature of SPION's particles.

[13]Arum Y.,and Song Y. ***et al.(2011)***

Objective: To simulate the heat dissipation within the tissue:

- For typical configurations of tumor position
- Particle distributions within tumor

Computational/ Experimental/ Numerical/ Analytical	**Finite Element Solver(FEM)**	**Physics Employed**	**Magnetic Nanoparticle Used**	**Distribution of MNP's Monodispersion/ Polydispersion**
1.Computational 2.Experimental	Comsol-Multiphysics3.5	Heat transfer Module	Magnetite (Fe_3O_4 - APTMS)	Monodispersion (Homogeneously distributed)

Work:

Concentration (mg / g_{tissue})	$Fe_3O_4 - APTMS$ **(MNP)diameter**	**Loss power density,**	**Heat dose or SAR**	**Temperature(**°C) Experimental (Computational)

	region (mm)	P(W/m^3)	(W/g_{tissue})	Without Agarose gel	With Agarose gel
10	8.2	2.07×10^6	14.9	38.4(38.0)	34.5(34.0)
12	10.0	4.99×10^6	15.9	42.6(42.8)	38.6(38.1)
15	11.0	6.26×10^6	19.9	55.1(55.3)	49.1(48.8)
17	12.6	8.38×10^6	25.0	68.1(68.2)	61.4(61.0)

PARAMETERS	DISCUSSION	
Type of study	In-vitro study(in dish)	
Computational platforms used in current study	❖ MATLAB procedure to estimate effective power density ❖ Comsol-Multiphysicsto analyze temperatures variations	
Problem description	Transient conduction problem with no convection. For present analysis, temperatures are dependent on time and there is no fluid flow. $\rho C_P \frac{\partial T}{\partial t} - \nabla(k\nabla T) = Q$	
Diameter of tumor cell	5mm	
Heat dose for 5mm tumor	19.9W/g_{tissue}	
Effective temperature requirements for 5mm tumor	50°C for 10minutes	
Boundary conditions	Initial temperature of 20°C except on bottom surface.	
Geometry description	Modeled as sphere with 0.5mm thick wall	
Magnetic heating experiment	Coil used=	3-turn coil
	Diameter of coil=	$45mm$
	Induction heating system used to power coil=	$7.5kW$
	Amplitude of magnetic field=	$130Oe \approx 10.345kA/m$
	Frequency=	$154kHz$
Measurement of SAR/heating power of particles	❖ $SAR[W/g_{Fe_3O_4\_APTMS}] = \frac{C_{gel}}{x}\frac{dT}{dt}$ where, ✓ C_{gel} = specific heat of water=4.18J/g°C ✓ $\frac{dT(°C)}{dt(\sec)}$ = is the initial 30 sec slope of temperaturevs time curve. ✓ x is the weight fraction of magnetic	

	elements in gel. $x = \frac{m(sampleFe_3O_{4\_}APTMS)}{m(H_2O)+m(agarose)}$ where, m is the masses of MNP, water, and agarose
Loss power, L.P or P	$L.P = \pi\mu_O\chi_O H_O^2 f \frac{2\pi f\tau_R}{1+(2\pi f\tau_R)^2}$ where, $\chi_O = \frac{\mu_O M_S^2 V}{k_B T}$ $\tau_R \approx \tau_N = \frac{\sqrt{\pi}}{2}\tau_O \frac{\exp\left(\frac{KV}{k_B T}\right)}{\sqrt{\frac{KV}{k_B T}}}$ τ_B is neglected because ~10^3 times larger than néel relaxation i.e τ_N. V = particle volume M_S = saturation magnetization k_B = boltzmann's constant
Analysis time	1200sec
Heat Source	Heat source is addressed on MNP's region
Type of meshing elements	Tetrahedral
Type of solver used	UMFPACK direct solver automatically selected by COMSOL.
Saturation Magnetization of $Fe_3O_{4\_}APTMS$ MNP's	$38.4 emu/g \approx 38.4 Am^2/kg$
Saturation Magnetization of $Fe_3O_{4\_}oleic\_acid$	$57 emu/g$
Key finding	Remanence,(M_r)and Coercivity,(H_C) were close to zero

Inference drawn:

1.The increase of temperatures is proportional quantity of particles.

2.Each concentration of MNPs was distributed in one spherical region whose diameter size depends upon amount of concentration.

3.Forsuperparamagnetic behavior, the concentration of particles is much more significant in determining the amount of heat generation as opposed to parameters of field amplitude and field frequency.

4.The relationship to concentration indicates that at higher concentrations the cells died more quickly rather at lower concentrations.

Research Gaps:

Since, this a phantom agarosegel(transparent gel) based study and it is able to co-relate the experimental values with computational work but still it has limitations. The effect of blood flow, metabolic heat generation term are missing which must be addressed in order to co-relate the outcomes of the research work to patient specific studies. The anatomy of local vasculature can be obtained from CT/MRI scans and with the help of advanced commercial setups the two dimensional information can be converted into three dimensional more detailed information. This model can be analyzed with most accepted pennesbioheat transfer equation. Many parameters which are been addressed can be an input parameter to other studies to have more refined, concise and reliable results.

[14]Javidi M., Heydari M., Karimi A. *et al.(2014)*

Objective: To evaluate the effects of injection velocity and different gel concentrations.

Work:

PARAMETERS	EXPLANATION
Type of work	❖ Experimental ❖ Computational ❖ Numerical methods
FEM Solver	Comsol-Multiphysics
Geometry details	Axisymmetric geometry
Type of particle	Magnetite
Experimental Parameters	Volume of magnetite fluid =0.3cm³ with 7% concentration poured in 6.7cm³ of 1% agar gel solution
	Field frequency, $f = 164kHz$
	Field amplitude, $H_O = 1.2kA/m$
	Magnetocrystalline anisotropy, $K = 9kJ/m^3$
	Saturation Magnetization, $M_S = 300gauss$
	Nanoparticles diameter, $D_{np} = 8nm$
	Nanoparticles heat capacity, $C_{np} = 670J/kg.K$
	Axial finite cylinder, $D_i = 1.4cm$ and $h = 4.5cm$ Container thickness, $t = 1nm$ $R_i = \frac{D_i}{2}$ and $R_O = \frac{D_i}{2} + t$

Computational Parameters	$\rho_{mix} = \phi\rho_{MNP} + (1-\phi)\rho_{gel}$, $C_{mix} = \phi C_{MNP} + (1-\phi)C_{gel}$, ϕ $\frac{1}{k_{mix}} = \frac{\phi}{k_{MNP}} + \frac{1-\phi}{k_{gel}}$, where, ϕ is the volume fraction
	Volume fraction, $\phi = 0.003$
	Ambient air temperature, $T_{ambient}$ or $T_{air} = 20.15°C$
	Natural convection coefficient, $h_{air} = 10W/m^2.K$
	Initial temperature, $T_i = 20.15°C$
	Loss Power, $L.P = 0.11\times10^5 W/m^3$
	Homogeneous medium of nanoparticles and agarose gel
	Mixture heat capacity, $C_{mix} = 3890.31J/kg.K$
	Mixture heat conductivity, $k_{mix} = 0.566W/m.K$
	Mixture density, $\rho_{mix} = 1011.85kg/m^3$
	Amount of magnetite fluid= $0.3cm^3$
	Magnetic fluid inside the tumor region.
	Density of gel, $\rho_{gel} = 1000kg/m^3$
Numerical Methods Parameters	Radius of cylinder, $r = 0.0212m$
	Height of cylinder, $h = 0.05m$
	Depth of injection, $b = 0.0125m$
	Type of particle=magnetite
	Diameter of nanoparticle, $d = 10nm$
	Density of nanoparticle, $\rho = 5240kg/m^3$
	Specific heat capacity, $C_P = 670J/kg.K$
	Ligand layer thickness, $\delta = 1nm$
	Ferrofluid solution=0.3cm³
	Field amplitude, $H_O = 3kA/m$
	Field frequency, $f = 300kHz$
	Dynamic viscosity, $\eta = 0.001Pa.s$
	Average relaxation time, $\tau_O = 10^{-9}$ sec
	Anisotropy constant, $K = 9\times10^3 J/m^3$
	Domain magnetization, $M_d = 4.46\times10^5 A/m$

Inference drawn: Temperature variations along the center line and along the radial direction are studied for:

- For four gel concentrations of 0.5%,1%,2% and 4%

- For four injection velocities of 4μL/min, 10μL/min, 20μL/min, 40μL/min.

1.By increasing the injection flow rate at determined concentrations, mean temperature drops.

2.With increasing the concentration there is no regular pattern. From 0.5% to 2% concentration mean temperature increases and from 2% to 4% there is decrement.

3.By increasing the injection rate maximum temperature drops from 41.3°C to 38.37°C.

Research Gaps:

The study though relates three types of evaluation techniques i.e Experimental, Computational and Numerical Methods but since the study is based upon agar gel and nanoparticle mixture, it must be done for real tissues.The effect of metabolism rate and local vasculature is missing.

[15]Taloub S., Hobar F., and Astefanoaei I. *et al.(2016)*

Computational/ Experimental	Finite Element Method(FEM)	Physics Employed	Magnetic Nanoparticle/ Magnetic core	Type of Approach Used
Computational	ComsolMultiphysics	Heat transfer Module	$MnFe_2O_4$	Particle level approach i.e Single nanoparticle

Objective: To analyze the thermal response of the living tissue when a nanoparticle used as heating source has

- Different shapes(sphere, cube, and rod)
- Complex core-shell structure
- Different surface coating patterns

Work:

In this computational work, the comparative study involves behavior of heat generation with different shapes and having same volume i.e $V_{sphere} = V_{cube} = V_{rod}$ is analyzed for single nanoparticle encased in spherical shaped tumor tissue. Also the thermal response of different coating materials and shell thickness is well discussed.

PARAMETERS	EXPLANATION
Number of nanoparticles	One
Shape of nanoparticle	❖ Spherical in shape(radius, r_{np} 20nm) ❖ Nanocube shape(side length, $L_c = 32nm$) ❖ Nanorod as cylinder(length, $L_{cyl} = 73nm$ and radius, $R_{cyl} = 11nm$) ❖ Hemispherical caps, $R_{cap} = 11nm$

Geometry details	Tissue is of spherical domain and the nanoparticles of different shapes are put one by one inside the tissue domain.
Specialty of magnetic core or nanoparticle used in current simulation	High Magnetization values and single magnetic domain of $MnFe_2O_4$
Volumetric power density, Q	$10^{16} W/m^3$
Type of meshing elements	Free tetrahedral elements
Number of meshing elements	62070 domain elements
Equation used	Fourier heat transport equation $\rho C_P \frac{\partial T}{\partial t} + \nabla(-k\nabla T) = Q$
Materials of nanoshells	❖ Au shell ❖ PEG polymer shell
Thickness of nanoshell	5nm,10nm,20nm,30nm and 40nm
Coating	❖ Spherical shell surface coating, radius= 30 nm ❖ Ellipsoidal surface coating • Ellipsoid[1] shell (Dimensions=25-25-43.2nm) • Ellipsoid[2] shell (Dimensions=22-25-49nm)
Radius of spherical domain of tissue under consideration	0.5μm
Boundary conditions	**B.C-1:**Condition of the continuity of the thermal flux between domains. The thermal flux from the particle is completely received by the tumor cell. **B.C-2:**Temperature at outer surface. The tem perature on outer surface of tissue is maintained at body core temperature of To= 37°C. **B.C-3:**Initial temperature, $T_i = 37^{\circ}C$
Radius of gold nanoparticles	4nm
Number of gold nanoparticles making incomplete shell	10,40,80
Key finding	The $Au - MnFe_2O_4$ Nanoparticles combines the effect of magnetically active $MnFe_2O_4$ and optically active Au within one nanostructure which is a promising nanoparticle platform for multimodality therapeutics and imaging.

Inference drawn:

1.Thethermal field distribution achieved in therapeutic range is larger for rod shape nanoparticles than other two shapes of sphere and cube.

2.The temperature achieved by same volume of magnetic materials is maximum for spherical particle comparing with cubic or rod shaped nanoparticles.

3.The temperature decreases with the increase of the shell thickness for gold shell and increases with the increase of the shell thickness for the polymer shell.

4.Gold shell is having higher values of thermal conductivity transfers the heat generated by magnetic core more rapidly to external medium and for polymer coating, the heat generation was confined to the region inside the particle and ensuring temperature rise patterns up till reach to thermal equilibrium.

5.The maximum temperature rise on the nanoparticle surface, $T_{\max} = 46.8°C$ for bared(uncovered) particle while there is a continuous decrease of temperature related to volume/coverage ratio with minimal temperature for complete shell, $T_{\min} = 43.9°C$.

Research Gaps:

In this computational work, author tries to simulate for nanometer(nm) range simulations which till date is absent in most of the simulations. The nanometer range work done till date is by other techniques such as Lattice-Boltzmann method or multi-scale approach. Since, for the studies discussed in most of the bioheat transfer simulations the concept of Mixture is applied or simply say averaging of properties is done to evaluate for the loss power calculations which will be an input to penne's equation. In this work, penne's equation is overlooked by Fourier equation and more concern/ focus is emphasized on single particle of size 40nm diameter. For seeing to the potential of nanoparticles, the present study moves around delivery of drug from single molecule. In no case single nanoparticle will assist hyperthermia in different sized tumors. This studycan be extendedto different kind of magnetic materials and different type of shells along with study extension from one specific nanoparticle to number of nanoparticles.

[16]Miaskowski A. and Sawicki B.*(2013)*

Objective:

To investigate the numerical methodology with the experimental work on anatomically correct female breast cancer model.

Computational/ Experimental/ Numerical/ Analytical	Type of Solver	Magnetic Nano-particle Used	Physics used in Numerical model	Distribution of MNP's Monodispersion/ Polydispersion

1.Experimental 2.Numerical	Self developed solver based on finite element method(C++) in the form suitable for libraryFEniCS	Magnetite (Fe_3O_4)	1.magnetic field simulation 2.Heat transfer simulation	Monodispersion (Homogeneously distributed)

Work:

In this work,Female breast corresponding to class-1 which is called mostly fatty where breast fat tissue constitutes 97.3% of breast is considered.

PARAMETERS	DISCUSSION
Type of tissue	Breast tissue
Number of models	Two models ❖ Water based model ❖ Human tissue model
Type of magnetic material	Magnetite
Tissue under consideration	Female mammary gland
Type of coating	Dextran coated
Equation used	Pennesbioheat equation
Type of solver	Self developed solver based on FEM
Type of numerical scheme	Backward Euler scheme
Effects considered	1.Metabolic and ohmic heat 2.Blood perfusion 3.Convection skin cooling
Geometry details	❖ Simplified three-layer (layer of Skin, fat, tumor) breast phantom. ❖ Phantom dimensions:17cm×12cm×4.5cm. ❖ Volume of tumor layer:1.6cm³. ❖ Initial temperature of phantom:8.5°C ❖ Heating time:30min.
Convection coefficient in case of water based model, h	$h = 20W/m^2$
Convection coefficient in case of tissue equivalent model, h	$h = 9.5W/m^2$
Number of turns of coil	5
Operating frequency	$150kHz$
Current	$400A$
Loss power, L.P	$L.P_{spm} = \pi\mu_O\chi_O H_O^2 f \frac{2\pi f\tau_R}{1+(2\pi f\tau_R)^2}$ ----------(1) where, $\chi_O = \frac{\mu_O M_S^2 V_M}{k_B T}$ ----------(2) Eqn(1) is valid for magnetic nanoparticles with a strong

	anisotropy, $\sigma_a >> 1$ $\sigma_a = \frac{KV_M}{k_B T}$ In this case, $\sigma_a \approx 21.2$
Boundary condition	1.Natural Neumann B.C 2.Robin's B.C
Ferrofluid volume fraction, θ	$\theta = n\frac{V_M}{V}$ where, V_M = Magnetic volume of one magnetite particle V = Tumor volume n = Number of magnetic nanoparticles Water based model, $\theta = 6.8\times10^{-6}$ Human tissue model, $\theta = 3.6\times10^{-5}$
Model of mixture (magnetic fluid + tumor tissue) i.e Cancerous subregion is treated as homogeneous composite.	❖ Effective density, ρ_{eff} : $\rho_{eff} = (1-\theta)\rho_{tumor} + \theta\rho_{MF}$ ❖ Effective specific heat, C_{eff} : $C_{eff} = (1-\theta)C_{tumor} + \theta C_{MF}$ ❖ Effective thermal conductivity, k_{eff} : $\frac{1}{k_{eff}} = \frac{(1-\theta)}{k_{tumor}} + \frac{\theta}{k_{MF}}$ ❖ Effective electrical conductivity, σ_{eff} : $\frac{1}{\sigma_{eff}} = \frac{(1-\theta)}{\sigma_{tumor}} + \frac{\theta}{\sigma_{MF}}$ where, subscript MF indicates magnetic fluid.

Physical properties of Magnetite	**Values**
Saturation magnetization, M_S	$446kA/m$
Magnetocrystalline anisotropy, K	$41kJ/m^3$
Radius of nanoparticle, r_{np}	$9.5nm$
Specific heat capacity, C_P	$670J/kg.K$
Density, ρ	$5180kg/m^3$
Electrical conductivity, σ	$25\times10^3 S/m$
Thermal conductivity, k	$9.7W/m.K$
Boltzmann's constant, k_B	$1.381\times10^{-23} J/K$

Average relaxation time, τ_O	10^{-9} sec
Effective relaxation time, τ_R	10^{-5} sec
Viscosity of medium, η	$0.001 Pa.s$
Ligand layer thickness or surfactant layer thickness, δ	$2nm$
Density of ferrofluid	$582 kg/m^3$
Weight fractions of ferrofluid	$42 kg/m^3$

Inference drawn:

1. Model without blood perfusion heats up much faster and after 20minutes reaches the temperature of nearly 70°C but the circulating blood will cool down the tumor to 44°C.

2.Relative location of injected magnetic fluid is important to determine the final temperature of tumor.

3.Higher temperature is observed when tumor is shifted to the side rather than located at the center of the coil.

4.Size of tumor is important not only because of magnetic field distribution but also due to heat exchange caused with surrounding tissue.

5.The concentration of injected magnetic fluid has to be the function of relative position and diameter of a tumor, to obtain the therapeutic temperature.

Research Gaps:

Since, the present study is a phantom based study which doesn't takes into account the effect of metabolic heat generation in living tissues and also the effect of blood perfusion. The study can be extended for more realistic coils where one can analyze the magnetic field distribution to be more uniform. Also, the breast anatomical model needs to be redefined with more realistic data extracted from large sets of DICOM images. Computational algorithms can assist such studies.

[17]Maenosono S. and Saita S. ***(2006)***

Objective:

1.To calculate the heat generation and heat transfer in the tissue when magnetic nanoparticle(MNP)-loaded tumor is placed in an external magnetic field.

2.To estimate the performances of magnetite, maghemite, FeCo, $L1_0$-phase FePt, fcc-FePt magnetic nanoparticles.

Computational/ Experimental/ Analytical/ Numerical	Magnetic Nanoparticle Used	Distribution of MNP's Monodispersion/ Polydispersion

Analytical	Comparative study 1.Magnetite(Fe_3O_4) 2.Maghemite($\gamma - Fe_2O_3$) 3.Permendur or Iron- -Cobalt($FeCo$) 4. $L1_0$ -phase $FePt$ 5. *fcc* **-phase Iron-Platinum(** $FePt$**)**	Monodispersion (Homogeneously distributed)

Work:

PARAMETERS	DISCUSSION
Geometrical details	Spherical tumor Diameter of tumor=1cm
Energy dissipation, $L.P$	❖ L.P=3.97×10^5W/m³(fcc-FePt) ❖ L.P=1.95×10^5W/m³(Magnetite)
Optimum temperature requirements	42.5°C
Type of study	Steady state
Typical size range of standard ferrofluids, D_{np}	8nm-10nm
Time of evaluation	600sec
Interface distance between tumor and normal tissue	$x = 5mm$
Amplitude of applied magnetic field, H_O	50mT
Frequency of applied magnetic field, f	300kHz
Volume fraction, ϕ	2×10^{-5}
Average relaxation time, τ_O	10^{-9}sec
Magnetocrystalline anisotropy, K	$K = \frac{25kT_B}{V_M}$ where, T_B = Blocking temperature For fcc-phase FePt particles T_B = 20K to 30K $K \cong 2.06\times10^5 J/m^3$
Carrier liquid	Pure water
Surface ligand layer thickness, δ	1nm
Operative size for different MNPs,D_{max}	❖ *fcc* -phase $FePt$=9nm ❖ $L1_0$ -phase $FePt$=9nm ❖ Magnetite=19nm ❖ Maghemite=23.5nm ❖ FeCo=34nm
Effectiveness of $FePt$ than other MNP's	1.High curie temperature 2.High saturation magnetization 3.High chemical stability

Thermophysical properties	Values
Thermal conductivity of tissue, k_t	0.502W/m.K
Density of blood, ρ_b	1000kg/m³
Specific heat of blood, C_b	4180J/kg.K
Blood perfusion rate, ω_b	6.4×10^{-3}[(ml/s)/ml]= 6.4×10^{-3} s^{-1}
Temperature of arterial blood, $T_a or T_b$	37°C=310K
Metabolic heat generation, Q_{met}	540W/m³

Inference drawn:

1. Dependence of heating rates on amplitude of applied magnetic field:

For operating frequency of $f = 300kHz$,

Field amplitude, H_O=25mT, 50mT, 75mT.

Heating rates increases with increasing H_O.

2. Dependence of heating rates on frequency of applied magnetic field:

For field amplitude of $H_O = 50mT$,

Field frequency,f=100kHz,300kHz,500kHz

Heating rates increases with increases f.

3. *fcc* -phase $FePt$ and $L1_0$ -phase $FePt$ MNPs yields largest heating rates in the size range of D<20nm.

4.At low frequency range(f <500kHz),the magnetic heating rate of *fcc* -phase $FePt$ MNPs are larger than those of magnetite MNPs and also for frequency range (f >500kHz)the MHR of magnetite is more than fcc-phase FePt.

5.The fcc-FePt MNPs are more superior than magnetite when H_o is high and f is low and also specific surface area of FePt increases when the size of MNPs decreases, thus specificity of tumor increases.Hence, higher volume fraction can accommodate in the tumor tissue than magnetite particles.

6.Increasing the medium viscosity, $\eta$from the viscosity of water is considered for loss power for both the particles. In case of magnetite nanoparticle, loss power is independent of viscosity because néel relaxation dominates. For Iron platinum loss power becomes independent of $\eta$when viscosity increase ten times the viscosity of water.

Research Gaps:

The polydispersity of MNPs is not considered.Since, magnetic anisotropy vary considerably due to shape contributions of MNPs, the shape effect is also not considered. Also, the biocompatibility and toxicity of FePt MNPs can be studied for making them as potential candidates for magnetic hyperthermia.

[18]Henrich F., Rahn H. and Odenbach S.*(2015)*

Objective:

1. To study temperature profiles and to understand the heat transfer processbetween the tissue which is enriched with MNPs and tissue with no or little enrichment.

2.To study the influence of surface-to-volume ratio.

Computational/ Experimental/ Analytical/ Numerical/ Review	Finite Element Method(FEM)	Physics Employed	Magnetic Nanoparticle Used	Distribution of MNP's Monodispersion/ Polydispersion
1.Experimental 2.Computational	ComsolMultiphysics	Heat transfer Module	Magnetite (Fe_3O_4)	Monodispersion (Homogeneously distributed)

Work:

The present work isa phantom based studymade of polyurethane(PUR) comprises of heat transfer properties properties close to biological tissue. In this study four cylindrical phantoms A,B,C,D(D1,D2)

PARAMETERS	DESCRIPTION
Diameter of cylinder	18mm
Diameter of two ferrofluid enriched spheres	10mm
Thermal conductivity of tumor, k_{tumor}	0.641W/m.K
Thermal conductivity of Polyurethane(PUR), k_{PUR}	0.64W/m.K
Diameter of nanoparticles, D_{np}	10nm
Concentration of nanoparticles,c	7.2mg/ml

Alternating magnetic field generated by using inductive coil:	❖ No. of windings=22 ❖ Inner diameter of coil=27mm ❖ Frequency, $f = 284 \pm 0.1$kHz ❖ Magnetic field strength/Field amplitude=4.4kA/m -8.7kA/m ❖ Atkinson's condition= $H_O \times f = 5 \times 10^9 \, A/m.s$

Geometrical details	❖ Cylindrical tissue made of PUR(Polyurethane material) ❖ Spherical region enriched with ferrofluids.			
PARAMETERS	Phantom A	Phantom B	Phantom C	Phantom D
Height of cylinder	40mm	40mm	40mm	40mm
Diameter of cylinder	18mm	18mm	18mm	18mm
No. of spherical regions	1	1	1	2
Diameter of spherical ferrofluid enriched region	5mm	10mm	15mm	D1=10mm D2=10mm
Distance between center of sphere to top face of cylinder	20mm	20mm	20mm	12.5mm
Distance between center of sphere to bottom face of cylinder	20mm	20mm	20mm	12.5mm
Center distance between two spheres	N.A	N.A	N.A	15mm
Diameter of outer cylinder carrying water	20mm	20mm	20mm	20mm

SIMULATION PARAMETERS:

Phantoms	Concentration of magnetite $(\frac{mg_{magnetite}}{ml_{PUR}})$	Number of spherical regions enriched with MNPs or ferrofluids with PUR	Diameter [mm]	Surface to volume ratio
A	12.38±0.6	One	5	0.6
B	10.65±0.6	One	10	0.3
C	12.38±0.6	One	15	0.2

D1	9.36±0.6	Two	10	----
D2	11.35±0.6	Two	10	----

THERMOPHYSICAL PROPERTIES	MATERIAL		
	SPHERE	CYLINDER	WATER
Heat Conductivity, k $(W/m.K)$	0.65	0.65	0.626
Heat Capacity, C_P $(J/kg.K)$	1400	1400	4186
Density, ρ (kg/m^3)	1546	1546	993.3

Magnetic Field Strength/ Field Amplitude [kA/m]	Specific Absorption Rate(S.A.R) or Heating Capacity $[W/m^3]$
4.4	1.5×10^4
5.3	2.0×10^4
6.2	2.5×10^4
7.0	3.0×10^4
7.9	3.5×10^4
8.7	4.0×10^4

Inference drawn:

1.The hottest region is at the center of the ferrofluid enriched area and temperature decreases towards surface of phantom.

2.The temperature difference in phantom C increases significantly 0.95K than phantom B(0.55K) and phantom A(0.15K).This is due to surface-to-volume ratio is lower in phantom C than in phantom B and A.

Research Gaps:

The present work is based upon the comparatively simple geometry and easy behavior. The model can be extended towards more realistic conditions and processes in biological tissues. The possible impact on the theoretical use of magnetic heating treatment(MHT) in reduction of negative influence on the patient's discomfort can only be realized if true model geometries can be obtained with respect to hyperthermia studies. Patient specific models can be explained since all the simulation parameters which are defined in given paper can support the studies for future computational work.

[19]Lin C. and Liu K.*(2009)*

Computational/ Experimental/ Analytical/ Numerical	Magnetic Nanoparticle Used	Type of Analysis Steady state/ Transient	Distribution of MNP's Monodispersion/ Polydispersion
1.Numerical 2.Analytical	1.IronPlatinum(FePt) 2.Magnetite(Fe_3O_4)	1.Transient state 2.Steady state	Monodispersion (Homogeneously distributed)

Objective: To estimate the temperature rise in biological tissues for FePt MNPs and analyze the temperature distributions with numerical scheme and analytical validation.

Work:

In this work, a numerical scheme is developed for solving the transient bio-heat equation in spherical co-ordinates to account for comparative results for the two nanoparticles.The plots are analyzed for radial distance for steady state analysis and at center of tumor for transient analysis.

Geometrical description and field parameters	
Geometrical description	Bi-layered spherical tissue
Radius of tumor, R	5mm
Radius of healthy tissue, a	15mm
Amplitude of magnetic field, H_O	50mT=39.885kA/m
Frequency of magnetic field, f	300kHz
Volume averaging of tumor: The region $0 \le r \le R$, considered as a composite of tumor and magnetic particles.	Effective density: $\rho_1 = \psi\rho_M + (1-\psi)\rho_T$ Effective specific heat: $C_1 = \psi C_M + (1-\psi)C_T$ where, ψ = volume fraction of magnetic particles $Subscripts = M, T$ denotes magnetic particles and tumor tissue respectively.

PARAMETERS	DESCRIPTION	
	Iron Platinum (FePt)	**Magnetite (Fe_3O_4)**
Diameter of magnetic nanoparticle, D_{MNP}	9nm	19nm
Loss Power, $L.P$	3.97×10^5W/m³	1.95×10^5W/m³
Density of MNP, ρ_{MNP}	15200kg/m³	5180kg/m³
Specific heat capacity of MNP, C_{MNP}	327J/kg.K	670J/kg.K
Volume fraction, ψ	2×10^{-5}	2×10^{-5}
Time(Transient state analysis)	1200sec	1200sec
Time(Steady state analysis)	600sec	600sec

Density of blood, ρ_b	1000kg/m³	1000kg/m³
Specific heat capacity of blood, C_b	4180J/kg.K	4180J/kg.K
Blood perfusion rate, ω_b	6.4×10^3[(ml/s)/ml]= 6.4×10^{-3} s^{-1}	6.4×10^3[(ml/s)/ml]= 6.4×10^{-3} s^{-1}
Metabolic heat, Q_{met}	540W/m³	540W/m³
Thermal conductivity, k	0.502W/m.K	0.502W/m.K
$\rho_2 C_2$	1060×3600J/m³K	1060×3600J/m³K

Inference drawn:

At time reaches 300seconds for transient analysis, the temperature at the center of tumor has reached to steady state while the same results for radial distance have been achieved for time of 600seconds. This fact is account for the reason of heat loss rate through the blood perfusion should be equal to heat generation rate of heat source and metabolism for the Neuman boundary condition.

Research Gaps:

The present work compares the temperature elevations of two different particles i.e magnetite and iron-platinum. The geometry considered is an ideal geometry of considering the region of tumor symmetrically lies inside the another region of similar or dissimilar shape. The work can be extended for different amplitudes of magnetic field and frequencies by taking into account the safe exposure limit.

[20]Rosensweig R.*(2002)*

Computational/ Experimental/ Numerical/ Analytical/ Review	Magnetic Nanoparticle Used	Domain of particle (Single domain/ Multi-domain)	Distribution of MNP's Monodispersion/ Polydispersion
1.Experimental 2.Analytical	Magnetite (Fe_3O_4)	Single domain	1.Monodispersion (Homogeneously distributed) 2.Polydispersion

Objective:

To formulate and compute the heating rates in samples subjected to an alternating magnetic field.

Work:

In this paper, the author develops the heat dissipation relationships based on rotational relaxation of single domain magnetic particles dispersed in medium. The important relationships are derived and well defined for monodispersion and polydispersion particle distribution.

Type of carrier fluid	Tetradecane
Properties of carrier fluid	Specific heat capacity=2080J/kg.K

	Mass density=765kg/m³
	Viscosity=0.00235kg/m.s
	Surfactant layer thickness=2nm
Volume fraction , ϕ	0.071
Radius of nanoparticle, R	7nm
Frequency, f	300kHz(monodispersion) 900kHz(polydispersion)
Magnetic induction, $B_O = \mu_O H_O$	0.06T

PHYSICAL PROPERTIES	MAGNETIC SOLIDS			
	Magnetite	Maghemite	Cobalt ferrite	Barium ferrite
Domain magnetization of suspended particle,M_d(kA/m)	446	414	425	380
Anisotropy constant,K(kJ/m³)	23-41	4.6	180-200	300-330
Specific heat capacity,c(J/kgK)	670	~746	700	~650
Density, ρ(kg/m³)	5180	4600	4907	5280

Inference drawn:

1.The highest heating rates are observed for magnetite and maghemite, however the size range is quiet larger than stable ferrofluids.

2.For particle size of 8nm-10nm, the barium ferrite and cobalt ferrite yield the maximum heating rates.

3.Theanisotropy constant and domain magnetization are the two important factors that contributes more towards performance characteristics of resultant ferrofluids.

Research Gaps:

Though the work done under this article is itself an achievement and a milestone but with respect to applicability to hyperthermia studies the work can be extended for mediums of different viscosities or for surface coatings and also by taking into account the biocompatibility requirements. Although the Loss Power(L.P) calculations which are been defined in this research article is considered as a base for all the computational heat input into various commercial packages.

[21]Purushotham S. and Ramanujan R.*(2010)*

Objective:

To study the effect of particle properties such as magnetic particle size, anisotropy constant, hydrodynamic diameter, and alternating magnetic field parameters on heat generation in magnetic nanoparticles.

Computational/ Experimental/ Analytical/ Numerical/ Review	**Magnetic Nanoparticle Used**	**Shape of particle**	**Distribution of MNP's Monodispersion/ Polydispersion**
Analytical	1.Magnetite (Fe_3O_4) 2.Maghemite ($\gamma - Fe_2O_3$)	Spherical in shape	Monodispersion (Homogeneously distributed)

Work:

In this work, the author considers the uniform distribution of magnetic nanoparticlesclusters inside the tumor domain. The tumor is assumed to be heated by large number of point sources as analyzed on microscopic scale.

PARAMETERS	**DESCRIPTION**
Experimental quantification of Specific absorption rate(S.A.R)	$S.A.R = C\left(\frac{\Delta T}{\Delta t}\right)\frac{mass_{ferrofluid}}{mass_{nanoparticles}}$, where, C is the mass weighted heat capacity of the ferrofluid $\Delta T/\Delta t$ is the slope of initial section of temperature versus time curve.
Volumetric power dissipation, L.P	$L.P = \pi\mu_O\chi_O H_O^2 f\frac{2\pi f\tau_R}{1+(2\pi f\tau_R)^2}$
Specific heat capacity of tumor tissue, $C_t\,(J/kg.K)$	3500
Density of tumor tissue, $\rho_t\,(kg/m^3)$	1.04×10^3
Thermal; conductivity of tumor tissue, $k_t\,(W/m.K)$	0.57
Normal tissue temperature(°C)	37
Exposure time(sec)	1800
Tumor diameter(cm)	1-4
AMF field strength(kA/m)	1-20
AMF frequency(kHz)	375

PARAMETERS	NANOPARTICLE TYPES	
	MAGNETITE (Fe_3O_4)	MAGHEMITE ($\gamma - Fe_2O_3$)

Temperature,T(K)	310	310
Viscosity of carrier fluid, η(Ns/m^2)	6.92×10^{-4}	6.92×10^{-4}
Anisotropy constant,K(kJ/m$^{3)}$	23,32,41	4.6
Domain magnetization,M_d(kA/m)	446	414
Mass fraction of MNP in ferrofluid	3.86×10^{-4}	1.93×10^{-4}
MNP concentration in ferrofluid(mg/ml)	10	10
AMF frequency,f(kHz)	50-800	50-800
AMF field strength/amplitude,H_o(kA/m)	4-20	4-20

Variations incorporated:

1.Relaxation time vs MNP diameter for both the particles.

2.Variation between SAR(W/g) vs MNP diameter(nm) at different frequency range(50,100,200,375,800kHz) for both the particles for field strength of H_o=4kA/m.

3.Variation between SAR(W/g) vs MNP diameter(nm) at different field strength range (4,8,10,16,20kA/m) for both the particles for frequency of f=375kHz.

4.Variation between SAR(W/g) vs MNP diameter(nm) at different anisotropy constants(K=23,41kJ/m) at different frequency range(50,100,200,375,800kHz) for field strength H_o=16kA/m for magnetite nanoparticle.

5.Variation between SAR(W/g) vs MNP hydrodynamic diameter(nm) at frequency f=375kHz,field strength H_o=4kA/m for different MNP diameter(nm) range of(10,11,12,13,14,15nm).

6.Variation between Field strength(kA/m) vs MNP conc^n(g/ml) at frequency of 375kHz for complete thermal coverage of tumor for both the particles.

Inference drawn:

1.Hyperthermia in a tumor strongly depends upon AMF strength and the mass of magnetic nanoparticles distributed in the tumor.

2.In the superparamagnetic range regime,

a.)at low AMF frequencies($f\tau << 1$),power output increases as the square of the frequency.

b.)When ($f\tau >> 1$) power loss is insensitive to frequency.

c.)When($f\tau = 1$)maximum output occurs.

3.For AMF frequency(f=375kHz), bare nanoparticles considerationoptimum particle size showing maximum powerFe_3O_4(12-18nm) and $\gamma - Fe_2O_3$ (23-24nm).

4.Increase in MNP concentration results in decreased field strength requirements.

Magnetite for H_o=19.5kA/m,Conc^n=~0.12g/ml and for Conc^n=~1.13g/ml,H_o decreases to 4kA/m.

5.As tumor size increases, the hyperthermia can be maintained by increasing either the MNP mass(nanoparticle concentration in the tumor) or the applied AMF field strength. The 0.5g magnetite MNP fully heats up the 1.5cm tumor for H_o=11kA/m andwhen MNP mass increases to 1g the H_o decreases to 7kA/m.

6.MNP concentration in the tumor for hyperthermia coverage is in the range of 0.06-1.7g/ml(maghemite) and 0.12-2.2g/ml(magnetite).

Research Gaps:

The research analysis done in present case doesn't incorporate polydispersity,interparticle interactions, viscosity changes with temperature and the effect of viscous and hysteresis losses.Also, the tumor is assumed to be spherical for the sake of ease but in realistic conditions the tumors are of irregular shape. The study incorporates the effect of two biocompatible nanoparticles behavior in presence of magnetic field and the results may assist the computational modeling for advanced bioheat models.

[22]Xu R., Zhang Y., and Ma M. ***et al.(2007)***

Objective:

To simulate the thermal distribution in maghemite-gelled composite model and to establish a model which can realize inhomogeneous heat generation induced by external magnetic field.

Work:

PARAMETERS	DESCRIPTION
Geometrical details	Cylindrical phantom containing maghemite particles
Type of cancer	Hepatocellular carcinoma
Type of study	Experimental, Numerical
Diameter of particles	20nm
Type of heat generation	Inhomogeneous heat generation
Transient/steady state	Transient heat transfer problem
Frequency	80kHz
Field strength	0-10kA/m
Assumptions made	Non-interacting particles
Specific absorption rate(S.A.R)	❖ When r=0.7cm,distance,z=1cm, S.A.R=6.2×10^3W/kg of NP or 8.9×10^3 W/kg of Fe ❖ When r=0.7cm,distance,z=2cm, S.A.R=4.9×10^3W/kg of NP or 7.0×10^3 W/kg of Fe ❖ When r=0.7cm,distance,z=3cm,

	S.A.R=4.0×10^3 W/kg of NP or 5.7×10^3 W/kg of Fe
Time required to reach a steady state	2400 sec

Inference drawn:

1.The temperature induced by nanoparticles inside tumors under alternating current magnetic field is dose dependent.

2.Inhomogeneous heating is caused by two factors i.e Inhomogeneous physical parameters of magnetic field and heterogeneous particle distributions.The results variation is significant as compared to assumptions of homogeneous distribution. So, accurate results can be obtained by considering above two factors.

Research Gaps:

The accurate inhomogeneous model in future could possibly be applied in hyperthermia treatment planning and helps to better optimize the surgical procedures.

[23]Balusu K., Suganthi S., and Ramakrishan S.*(2016)*

Computational/ Experimental	Finite Element Method(FEM)	Physics Employed	Type of Analysis Steady-State/ Transient	Type of Modeling
Computational	ComsolMultiphysics	Heat transfer Module	Steady state	Two-dimensional

Objective:

To simulate skin temperature profile of breasts in the presence of cysts and early diagnose of the breast cancer using infrared imaging.

Work:

PARAMETERS	DESCRIPTION
Equation used	Pennes-bioheat equation
Type of meshing elements	Triangular elements
No. of meshing elements	3000
Geometry details	❖ Breast as Axisymmetric (semicircle) ❖ Radius of semicircle=9cm ❖ Radius of cyst=3cm ❖ Depth of cyst (from top surface to center of cyst)=4.5cm(Between 3cm to 5.5cm)
Boundary conditions	❖ Surface joining the organ to body i.e Body core temperature, T_b = 37°C

	❖ $T_{ambient}$or T_e=25°C i.e 298K ❖ Heat transfer coefficient, h=20W/m².K
Arterial blood temperature, T_a	37.15°C=310.15K
Density of blood, ρ_b	920kg/m³
Specific heat of blood, C_b	3000J/kg.K

Thermophysical Properties	**Type of Tissue**	
	Normal breast tissue	**Cyst**
Thermal conductivity, k_t $(W/m.K)$	0.42	0.56
Blood perfusion rate, ω_b $(ml/s/ml) \approx 1/s$	0.00018	0
Metabolic heat generation, Q_{met} (W/m^3)	450	0

Inference drawn:

1.The surface temperature is having negligible effect if the cysts are located at depths greater than 5cm and of sizes less than 0.5cm.

2.Cyst having the maximum radius when placed closed to skin surface, the temperature decline is very large.

3.There is considerable decrease in surface temperature in presence of cysts because of absence of metabolic activity.

Research Gaps:

We come to the conclusion that the present analysis is helpful in the design of thermal image camera and also the correlation drawn with respect to infrared images in the automated diagnosis of breast cancer that initially call upon as cysts that can be benign or malignant.To graphically maps the temperature distribution of skin and measures the naturally emitted radiations to display as color code image that indicates the presence of abnormal tissue via thermography. There is need for an effective screening tool that is non invasive, non-contact, painless and radiation free such as medical thermography. This study will proved to be an additional assistance before the patient go for actual screening via computed tomography or magnetic resonance imaging and reduce the discomfort caused to patients via mammography(2D-procedure).

[24]Tabatabaei S. and Martel S.*(2013)*

Computational/ Experimental/ Analytical/ Numerical/ Review	Type of particle (Super-paramagnetic/ Ferromagnetic)	Magnetic Nanoparticle Used	Distribution of MNP's Monodispersion/ Polydispersion
Experimental	Superparamagnetic Iron oxide nanoparticles (SPIONs)	Magnetite (Fe_3O_4)	Monodispersion (Homogeneously/ Uniformly distributed)

Objective: To measure the temperature variations with time for three concentrations of 10,25,50mg Fe/ml magnetic fluid nanoparticles.

Work:

PARAMETERS	DESCRIPTION
Type of coating	Dextran coated
Concentration of MNPs	❖ 10mg Fe/ml ❖ 25 mg Fe/ml ❖ 50 mg Fe/ml
Time	750sec
Mean size diameter of MNP, D_{np}	7nm
Hydrodynamic mean diameter, D_H	58.77nm
Number of turns of coil	8 turns copper tube
Diameter of coil	15mm
Power of induction machine	1.5kW
Frequency of coil,f	150kHz
Magnetic field	80kA/m
Experimental S.A.R	1.156W/g_{Fe}
Theoretical S.A.R	1.295W/g_{Fe}

Inference drawn:

As the concentration of MNP increases, the higher rise in temperature is observed.

Research Gaps:

There are certain biocompatibility uncertainties to MNP and also the constraint of space in micro-carriers that extends the limitations to concentration of MNPs. Such kind of experiments can be extended for particular temperature requirements by doing variations in concentrations of MNPs.

[25]Gas P.*(2010)*

Objective: To analyze the transient temperature distributions within tumor region.

Work:

PARAMETERS	DESCRIPTION
Type of modality used	Radiofrequency induced hyperthermia
Model considerations	Two-dimensional

Type of analysis	Steady state analysis	
Equations used	❖ Penne's bio-heat equation ❖ Maxwell's equation	
Geometry details	❖ Human body as an ellipse Major diameter of human body,a=40cm Minor diameter of human body,b=24cm ❖ Spherical tumor Diameter of tumor=5cm ❖ Exciting coil as an ellipse in which human body is placed. Major diameter of exciting coil, A=100cm Minor diameter of exciting coil, B=80cm Current flowing in exciting coil, I_m=16A Frequency,f=100MHz	
Assumption in Penne's model	The heat exchange with the blood takes place only through the capillary perfusion neglecting heat transfer derived from larger blood vessels.	
Heat transfer coefficient, h	$10 W/m^2.K$	
Temperature of ambient air, T_{air}	20.15°C=293.15K	
Homogeneous/Heterogeneous media	Homogeneous media of tumor and human body	
Time to reach steady state, t	6000seconds	
Thermophysical properties of blood	Density of blood, ρ_b	$1020 kg/m^3$
	Specific heat of blood, C_b	$3640 J/kg.K$
	Temperature of arterial blood, $T_{arterial}$or T_b	$37°C \approx 310.15K$
	Blood perfusion rate, ω_b	1.In human body (healthy tissue) =0.0059(1/s) 2.In tumor =0.0004(1/s)

PARAMETERS	TISSUE	
	Human Body	**Tumor**
Density, ρ $[kg/m^3]$	1050	1050
Specific heat, C $[J/(kg.K)]$	3700	3700
Metabolic heat, Q_{met} $[W/m^3]$	300	480
Thermal conductivity, k $[W/(m.K)]$	0.22	0.56
Electrical conductivity, σ $[S/m]$	0.053	0.64
Permittivity, ε_R [Dimensionless]	29.6	160

Inference drawn:

The greatest value of the temperature is inside the tumor but there are possible local maxima of temperature near the surface of the body. The temperature is achieved to 44°C from body core temperature of 37°C.In order to avoid the surface burns, the human body would be surrounded with cold water bolus.

Research Gaps:

The trend of double peaks for tumor with depression in the center of tumor that was discussed in this study for 2-D geometry can be analyzed for 3D model. This trend is very useful in case of analyzing the realistic cases of cancer patients in presence of alternating electromagnetic fields, although the type of modality may vary from the present case of RF-induced hyperthermia and can be extended for SPION's-induced hyperthermia. The computational tool used as finite element solver was missing/not discussed in this current study.

[26]Manjunath N., Sanchu S. *et al.(2014)*

Objective: To analyze the heat transfer occurring in RFA procedure of liver/hepatic tumor.

Work:

PARAMETERS	DESCRIPTION
Type of modality used	RF-Ablation
Type of tumor	Hepatic tumor
Type of tissue	Liver tissue
Type of meshing elements	Tetrahedral elements
Equations employed in current study	1.Penne's bio-heat equation 2.Maxwell's equations
Type of analysis	Three dimensional
Geometrical details	❖ Solid cylindrical tumor tissue without any blood vessels ❖ Cool-tip region consists of two parts: 1.Conducting region 2.insulating region
Physics used	❖ AC/DC module Electric current interface ❖ Heat transfer module Bio-heat transfer interface
Initial & Boundary conditions	1.Electrical insulation at outer boundaries of tissue cylinder=0V(on cylinder walls). 2.Applied initial voltage=22V 3.Continuity boundary condition: No contact resistance between internal organs of body 4.Body core temperature and blood temperature,T_b=37°C.

Damage model	Arrhenius damage model based on first order kinetics. $\frac{d\Omega}{dt} = \frac{1}{\tau} = Ae^{-E/RT}$ Ω = Threshold of damage τ = Time required to accumulate irreversible damage E_a = Activation energy(kJ/mol)=667kJ/mol. A = Frequency factor(s^{-1})=$1.98\times10^{56}s^{-1}$. R = Universal gas constant,(8.315J/mol.K) T = Absolute temperature

Inference drawn:

1.Temperature variation has attained a steady state after 8minutes.

2.Maximum temperature rise is found at the electrode tip.

Research Gaps:

Since, the RFA assisted procedures are used in tumors in size greater than 3cm.Therefore, to address the tumors of size less than 3cm, Magnetic nanoparticle induced hyperthermia is a modality that can be used in conjunction with radiation or chemotherapy. Also, these nanoheaters under the influence of external alternating electromagneticfield release heat that is self-sufficient to do apoptosis in those regions where the RFA assistive antennas or rods cannot reach. Also, the effect of blood vessels is not considered which is there for realistic case. The model would be more effective if the actual size(small or large), shape(irregular) and location of tumor(depth from surface) is known. By obtaining the defined pre-cursors from the computed tomography scans or magnetic resonance imaging scans, the three dimensional model generation from the large sets of two dimensional images is made possible by advanced computational tools. It consists of writing your own codes in programming languages like MATLAB to extract the requisite information of concern from images and convert into three-dimensional model for pre-operative surgical planning or resection from body or to apply such modalities that will induce apoptosis. So, biomedical imaging assisted with the nanoparticles localization to the affected minute tumor areas can solve the purpose.Geometry considered was simple which is itself a gap that needs to be updated for realistic body.

[27]Cervadoro A., Giverso C., and Pande R. *et al.(2013)*

Computational/ Experimental/ Analytical/ Numerical/ Review	Finite Element Method(FEM)	Physics Employed	Magnetic Nanoparticle Used	Distribution of MNP's Monodispersion/ Polydispersion
1.Experimental 2.Computational	Comsol Multiphysics-3.5a	Heat transfer Module	Magnetite (Fe_3O_4) (SPIONs)	Monodispersion (Homogeneously/ Uniformly distributed)

Objective: To study the hyperthermic performance of superparamagnetic iron oxide nanoparticles(SPIONs) with core diameter of 5nm,7nm,14nm in terms of absolute temperature increase and S.A.R.

Work:

The present research work incorporates the effect of frequency variations(High frequency field~30MHz and Low frequency field~<1MHz)

PARAMETERS	DISCUSSION
Type of solver	UMFPACK linear system solver
Geometrical Configuration	2D square domain of 10mm side inside which tumor is assumed irregular
Type of meshing elements	Triangular
Number of meshing elements	3816 elements
AMF conditions	Frequency, f = 100kHz to 30MHz Field strength, H= 4 to 10kA/m Concentration,C_{MNP}=0.02-3.5mg/mL
Experimental S.A.R	$S.A.R_f = \left.\frac{\Delta T}{\Delta t}\right\|_{t=0} C_f \approx$ [W/kg of colloidal suspension] $S.A.R_{MNP} = \left.\frac{\Delta T}{\Delta t}\right\|_{t=0} \frac{C_f}{m_{MNP}} \approx$ [W/kg of Fe] Mass fraction, $m_{MNP} = \frac{M_{MNP}}{\rho_f V_f}$ where, C_f= heat capacity of ferrofluid SAR_{MNP} = Specific absorption rate of the sole magnetic nanoparticles $S.A.R_f$= Specific absorption rate of ferrofluid.
Mixture theory	For volume fraction, ϕ_{MNP} Outer healthy tissue, Ω_1 Central region with tumor tissue where magnetic nanoparticles are

	uniformly distributed, Ω_2 Effective density, ρ_2 Effective specific heat, C_2 Effective thermal conductivity, k_2 $\rho_2 = \rho_1(1-\phi_{MNP}) + \rho_{MNP}\phi_{MNP}$, $C_2 = C_1(1-\phi_{MNP}) + C_{MNP}\phi_{MNP}$, $k_2 = k_1(1-\phi_{MNP}) + k_{MNP}\phi_{MNP}$.
Key equation	$C_{MNP} \times SAR_{MNP}^{a} \geq b$ where, *for T=42°C*, a=1.0616, b=2.2714×10^{6}W/m^3 *for T=50°C*, a=1.0737, b=7.1565×10^{6}W/m^3 Three characteristic operating regimes are identified as: 1.$T_{equivalent}$<*42°C*(INSUFFICIENT HEATING) 2.*42°C*≤$T_{equivalent}$<*50°C*(HYPERTHERMIA) 3. $T_{equivalent}$≥*50°C*(THERMAL TISSUE ABLATION)
Low frequency field (SPIONs) Consideration	❖ Diameter of particle=5nm,7nm,14nm ❖ Saturation magnetization =65emu/gm, 10emu/gm, 82emu/gm respectively ❖ Characteristic frequencies =200kHz,500kHz,1000kHz ❖ Field amplitude=10kA/m ❖ Nanoparticle concentration=50 and 200mg/mL ❖ Volume fraction, ϕ_{MNP}=4.3×10^{-6} ❖ Heat exchange coefficient, h_v=1.65×10^{-3}W/(mm^2.K) ❖ SAR_{MNP} =6400W/kg for 200kHz and 10kA/m SAR_{MNP} =16,800W/kg for500kHz and 10kA/m ❖ Steady state conditions are reached within almost 200seconds(~3minutes) ❖ At highest concentration of 200mg/ml 47°C is met.

Inference drawn:

1.At high frequency ~30MHz, non-specific heating dominates while for low frequency <1MHz, non-specific heating is negligible and the relaxation of SPION within AMF is sole energy source.

2.At$SAR_{MNP}$is independent of C_{MNP}but SAR_{MNP} varies as linear relationship for f and H^2.

3.SAR_{MNP} increases as crystalline energy decreases and SAR_{MNP} increases as magnetization saturation increases.

Research Gaps:

This study presents a rationally design hyperthermic treatment to identify proper route of administration depending upon bio-distribution and magnetic properties of nanoparticles. This

study extends its depth to address that hyperthermia and thermal ablation can be achieved forsystemic injection of magnetic nanoparticles. The parameters of SAR can be used in future computational studies to analyze the damage integral for realistic human studies.

[28]Hilger I., Andrä W., and Hergt R.*et al.(2001)*

Computational/ Experimental/ Analytical/ Numerical/ Review	**Type of tissue**	**Type of study**	**Magnetic Nanoparticle Used**	**Distribution of MNP's Monodispersion/ Polydispersion**
Experimental	Human breast tissue	1.In-vitro 2.In-vivo	Magnetite (Fe_3O_4) (SPIONs)	Monodispersion (Homogeneously/ Uniformly distributed)

Objective:

To identify relevant parameters for exposure of breast tissue in alternating magnetic field.

Work:

Two types of studies are broadly discussed as In-vitro and In-vivo studies.

PARAMETERS	DISCUSSION
Experimental set up details	Breast tissue sample(B) containing iron oxide(magnetite-I) is placed at the center of magnetic field applicator 9cm diameter coil(C).
Calorimetric measurements/SAR evaluation	$S.A.R = \frac{\Delta Q}{\Delta t}.\frac{1}{m_f}$, where, ΔQ = Energy converted into heat per time(Δt) m_f = Magnetite mass $\Delta T = \frac{0.26°C}{\left(kA/m\right)^3}.H_o^3$ where, H_o=Magnetic field amplitude
Magnetic field amplitude	1.2-6.5kA/m(~6.5kA/m)
Magnetite mass	7-112mg(~21mg±9)
Frequency	400kHz
Time exposure	242seconds
Tumor volume	299mm³±158

	V= $\frac{\pi}{6}$ × Product of three principal diameters
Room temperature	21°C±2
In-Vitro Experiments	28 isolated breast tissue specimens(60-80gm) having diameter=70mm.Injecting the tissue specimens with different masses(7-112mg) of magnetite sample(*).Volume of breast tissue occupied by magnetite(0.050-0.6mm³).50-100μL of magnetic fluid sample(*) was injected intratumorally.
In-Vivo Experiments	Temperature elevation vs amount of magnetite is analyzed. $\Delta T = 2.31M$, where, ΔT = Temperature elevation M = Mass of magnetite
Important consideration	❖ Breast tissue is composed mainly of Fat which has lower thermal conductivity. ❖ Breast tumors seems to be favourable for magnetic heating because breast is poorly vascularized as compared to spleen and kidney. ❖ Blood flow within tumor region is important since heat exchange results in lower temperature range. ❖ Stauffer and Atkinson considered diameter of exposed tissue as 30cm for a product of frequency and amplitude below 4.85×10^8A/m. ❖ Brezovich considered deposited power is proportional to square of diameter. ❖ For a frequency of 400kHz, estimated diameter of field exposed breast tissue as 15cm, field amplitude to be adjusted below 4.85kA/m.

Rate of energy per magnetite mass for a magnetite mass under AMF conditions of frequency 300kHz and field amplitude of 14kA/m

SAR (W/g)	Total Particle Diameter (nm)	Particle Shape
3	50×1500	Needle
8	250	Polyhedra
13	250	Polyhedra
80	280	Spherical
144	220	Spherical
211*	10*	Spherical*

Inference drawn:

1.Tumors could be treated by using lower temperature(48°C-50°C) for long exposure times of 30minutes to 60 minutes or short duration times within 4minutes at thermoablasive temperature range of 55°C.

2.Tumor shrinkage is attributed to effective magnetic heating.

Research Gaps:

Accurate localization of tumor margins at imagingis an important limitation been addressed although the solution to this could be circumvented by heating additional small fringe of normal tissue around the tumor. Also, the present study incorporates the variation of temperatures with field amplitude only and the effects of frequency based variations in tissue penetrations is missing. The inhomogeneity of the field amplitude across the animal body region of interest is considered negligible. The results of this study is a precursor to computational frame of studies to analyze the realistic tissue damage.

[29]Hilger I., Hergt R. and Kaiser W.*(2005)*

Computational/ Experimental/ Analytical/ Numerical/ Review	**Type of particle (Super-paramagnetic/ Ferromagnetic)**	**Magnetic Nanoparticle Used**	**Type of Tissue**
Review	Superparamagnetic Iron oxide nanoparticles (SPIONs)	1.Magnetite (Fe_3O_4) 2.Maghemite ($\gamma\_Fe_2O_3$)	Breast tissue

Objective:

1. To study the likely effects of maximum core temperature achieved with respect to magnetic field parameters(Field amplitude and frequency), concentration and its particle distribution for breast tumors for in-situ and multi-focal tumors.

2. To realize the hyperthermia(42°C for 60 minutes) and thermoablation(51°C-55°C).

Work:

This review paper deals with the key contribution done with respect to breast tumor. In this two different approaches in relation to magnetic heating i.e hyperthermia and thermoablation for particularly with respect to breast cancer is discussed. When the magnetic nanoparticle loaded tumor is exposed to alternating magnetic field two different situations that can occur are discussed broadly in shadow of review work findings.

1.Treatment of in-situ breast tumors:

Tumors which remains at the site of origin when they are still small and confined. This is the case when cancer cells remains within the borders of duct or lobule and have not grown into surrounding tissues.

2.Treatment of multi-focal breast tumors:

In-vitro experiments were performed for demonstrating the capabilities under this aforementioned approach. Intravasal accumulation of the magnetic material is proposed.

Inference drawn:

1.Minimal invasive treatment of in-situ breast cancers could be implemented in clinical practice in near future.

2.The treatment of multi-focal ones is determined by a higher complexity of interacting parameters. Accumulation of magnetic material through vessel system is still requires further studies to implement it on able to perform experiments practices.

3.In order to keep the particle dose minimal, high value of specific heating power(S.H.P) is necessary. But also the parameters(field amplitude and frequency) should be increased upto certain limit only because beyond that there are chances of occurrence of inductive heating to healthy tissues and do the undesired damage.

Research Gaps:

This is a peer reviewed study based on experimental results. The results obtained from the sets of experimental readings obtained on animal experiments or in-vitro studies or specifically in-vivo studies is a precursor to operate the patients based on experimental conditions is still needs to be verified for the computational based studies.

[30]Hilger I., Hergt R. and Kaiser W.*(2005)*

Computational/ Experimental/ Analytical/ Numerical/ Review	**Type of particle (Super-paramagnetic/ Ferromagnetic)**	**Magnetic Nanoparticle Used**	**Type of Tissue**
Review	Superparamagnetic Iron oxide nanoparticles (SPIONs)	1.Magnetite (Fe_3O_4) 2.Maghemite ($\gamma\_Fe_2O_3$)	Breast tissue

Objective:

1. To study biophysical basis of magnetically-induced heating
2. To study magnetic and structural properties of magnetic nanoparticles and the relationships found in model tissues.
3. To analyze the results of In-vivo experiments in tumor bearing animals

Work:

The presented work under this research article is a review done with respect to the hyperthermic studies and special concentration is given to breast conserving therapies. In considering the biophysical aspects of magnetic heating modality, Hyperthermia, Thermoablation, Tissue-coagulation is required under specific sets of conditions. The problem of reliable detection of tumor border(security rim of 1cm around border), dependence of the required heating power on the tumor radius and Brezovich and Atkinson criterion of safe exposure is discussed.

By keeping in consideration the demands of biocompatible aspects, preparation of nanoparticles samples are defined. Certain important parameters such as large saturation magnetization, single domain particles, shape aspects, hydrodynamic properties, particle size distribution, SLP, reduction in nanoparticle dosage by optimizing the particle properties are explained. Tumor-Angiogenesis of creating own network of vessels is discussed.

In this aspect of conducting In-vivo feasibility experiments in animal models, the rectal and intratumoral temperatures are measured after exposure to alternating magnetic field conditions. As far as tumor morphology is concerned, the magnetic material dispersion to achieve the temperature ranges well above 55°C for short exposure period is proposed. The results shows very keen success for near collapse of tumors after such heat treatments.

Inference drawn:

The review paper can be considered as breast conserving therapy and it can be inferred from the discussion that magnetic nanoparticles has a promising potential to assist the future techniques of curing the incurable cancers.

Research Gaps:

The present work considers various aspects of biocompatibility, magnetic parameters discussion in purview of previous conducted experiments to support the hyperthermic damages to unwanted tumor cells. The present studies can be a precursor to computer simulations for careful selection of important parameters to address the results of experimentation on realistic human trials practices. There can be many more materials that can be worked out by quantifying different aspects as discussed to successfully employ the treatment procedures.

[31]Roca A., Morales M., and Grady K. *et al.(2006)*

Computational/ Experimental/ Analytical/ Numerical/ Review	Magnetic Nanoparticle Used	Shape of particle	Important Consideration	Monodispersion/ Polydispersion

Experimental	1.Magnetite (Fe_3O_4)	1.Spherical 2.Cubical	Non-interacting particles	Monodispersed iron oxide MNPs

Objective:

To analyze the effect of different parametersi.e(Particle size, Particle shape, Particle distribution, Crystallinity, Colloidal properties, Surface coating,Magnetic properties(such as Susceptibility, Magnetic anisotropy) synthesized by high temperature thermal decomposition.

Work:

Synthesis of nanoparticles, magnetic measurements were made by VSM(Vibrating Sample Measurement).Magnetization curves were measured at room temperature and 5K in a maximum magnetic field of 5T.Parameters such as Coercive field,H_c and initial susceptibility, χ_i were obtained. Saturation magnetization was obtained by extrapolation.

PARAMETERS	SAMPLES		
	MAG1	MAG2	MAG3
Reflux	Reflux in Octyl ether	Reflux in Phenyl ether	More reflux in Octyl ether
Mean particle size,D_{TEM}(nm)	11.0±1.4	6.9±1.2	5.7±1.1
D_{XRD}(nm)	13.6±1.4	6.7±1.5	5.8±1.3
Magnetic particle size,D_{MAG}(nm)	8.2s±0.9	6.3±0.9	5.1±0.7
Particle shape	Mixture of diamond,cubic, triangular~Cubic	Spherical	Spherical
m_S^{RT} (emu/gm)	72±2	71±2	65±3
m_S^{5K} (emu/gm)	80±2	84±3	81±2
χ_i^{RT} (emu/(gm.T)	1000±30	450±10	260±10
H_C^{5K} (Oe)	300±10	250±10	175±10
$T_{\max}^{ZFC-FC}$ (K)	>290	45±5	20±5
Magnetic anisotropy constant, K_{eff} (ergs/cm³)	4.1×10^5	-------	3.0×10^5

Mathematical relations: Chantrell's equation for non-interacting particles	$D_{Mag} = \left[\frac{18 k_B T}{\pi M_S} \sqrt{\frac{\chi_i}{3 m_S} \frac{1}{H_O}} \right]^{1/3}$, $\sigma = \frac{1}{3} \left[\ln \left(\frac{3\chi_i / m_S}{1/H_O} \right) \right]^{1/2}$, $K_{eff} = \frac{25 k_B T_B}{V_{crit}}$, where, M_S = Saturation magnetization of the bulk phase m_S = Saturation magnetization of the nanoparticles χ_i = Initial susceptibility calculated at low fields, in the region where variation of M and H is linear $1/H_O$ = is obtained by extrapolating a tangent to a plot of M vs $1/H$ at high fields in the region where relationship between M and $1/H$ is a straight line to the $1/H$ axis at M=0

Inference drawn:

1.With the decrease in particle size(diameter), a slight decrease in m_s was observed at room temperature due to increase in surface area/volume ratio results in spin canting effects at the surface.

2. Particles obtained by this method are very uniform in size, highly crystalline and their shape changes from spherical to cubic when the particle size increases.

Research Gaps/Future directions:

The work presented in this paper is a precursor to the the particle synthesis studies by different methods but also the key parameters addressed can be used to input certain parameters in computational studies(FEM simulations).

[32]Pradhan P., Giri J., Samanta G. and Bahadur D. *et al.(2006)*

Computational/ Experimental/ Numerical/ Analytical/	Magnetic Nanoparticle Used	Type of coating	Type of study

Review			
Experimental	1.Magnetite (Fe_3O_4) 2. $MnFe_2O_4$ 3. $CoFe_2O_4$	Lauric acid	1.In-vitrocytocompatability study 2.In-vivo biocompatibility study on animal model(female mice) 3.Statistical analysis(ANOVA)

Objective: To investigate the heating ability of magnetic fluids which is measured by SAR on physical(particle size, shape, distribution) and magnetic properties of particle.

Work:

This study has key focus on synthesis of magnetic nanoparticles in lauric acid coating for different ferrites of Co-Fe_2O_4 and Mn-Fe_2O_4 and Fe_3O_4 based magnetic fluids.SAR evaluation is done.

PARAMETERS	MAGNETIC FLUID SAMPLES		
	Fe_3O_4	$MnFe_2O_4$	$CoFe_2O_4$
Particle shape	Spherical	Spherical	Spherical
Anisotropy constant,K (ergs/cm^3)	1.4×10^5	3.3×10^4	1.8×10^6
Ferrite concentration, C (mg/mL)	27.12	32.20	27.74
Lauric acid per gram of ferrite	0.100	0.115	0.110
Average physical diameter by TEM(nm)	9-10	10-11	9-10
Hydrodynamic diameter by PCS(nm)	100	70	90
Magnetization at 18kOe(emu/gm)	64.54	58.18	59.56
Magnetocrystalline anisotropy constant,K_1(joule/m^3)	1.4×10^4	3.3×10^3	1.8×10^5
Superparamagnetic critical size,D_P(nm)	25	50	14
Optimum particle size at 300kHz,D_1(nm)	15	24	7
Average particle size,D_{exp}(nm) range (9-11nm)	10	10	10
Lower field specific magnetization at 200Oe, m(emu/gm)	19.92	18.58	6.56
Specific absorption rate, SAR(W/$g_{ferrite}$)	120	97	37
SAR(W/g_{metal})=1.40×SAR(W/$g_{ferrite}$)	168	135.8	51.8
$\omega\tau_N$ for $\omega=1.88\times10^6\,s^{-1}$ i.e 300kHz, average particle size(D_{exp}=10nm), Amplitude(H_O=15kA/m)	0.0197	0.00327	1.33×10^7
Temperature range for time=200sec	45°C-46°C	33°C -35°C	25°C-26°C

PARAMETERS	DISCUSSION
Field amplitude,H_O	15kA/m

Field frequency,*f*	300kHz
Maximum S.A.R condition or maximum power loss condition	$\omega\tau_N = 1$
Experimental calculations for *S.A.R*	$S.A.R = C\frac{\Delta T}{\Delta t}\frac{1}{m_{Fe}}$, where, C is the specific heat of sample and sample holder. $\Delta T/\Delta t$ is the slope of time-dependent temperature curve. m_{Fe} is the mass of ferrite in grams.
Brownian relaxation time, τ_B	$\tau_B = \frac{4\pi\eta r^3}{k_B T}$, where, η is the viscosity of carrier fluid r is the hydrodynamic radius of particles.
Néel relaxation time, τ_N	$\tau_N = \tau_O \exp\frac{KV_n}{k_B T}$, where, τ_O is the time constant=10^{-9}sec. K is the anisotropy constant
Power loss, P	$P = \frac{(mH_O\omega\tau)^2}{\left[2\pi k_B T\rho V_n(1+\omega^2\tau^2)\right]}$, where, m is the particle magnetic moment, H_O is the field amplitude ω is the angular frequency ρ is the density of ferrite V_n is the nanoparticle volume k_B is the boltzmann's constant
Threshold concentration for lauric acid coated	0.1 mg/mL
Threshold concentration for dextran coated	1-2mg/mL

Inference drawn:

1.Cobalt ferrite is having lower heating ability as compared to magnetite and manganese ferrite particles.

2.SAR of magnetite and manganese ferrite are comparable but SAR values can be further increased by increasing the particle size to optimum particle size.

3.Magnetite and manganese ferrite both the particles are suitable for hyperthermic applications but Cobalt ferrite is not suitable for this purpose.

Research Gaps/Future directions:

The work illustrated under this research article where at one end addresses the biocompatibility issues, and also on the other way compared the three ferrites effectiveness by analyzing lauric acid based coatings than dextran coating.Such results presented in this work needs to be computationally examined and such quantization of parameters can be an input to resolve the fundamentals of hyperthermic studies with the aid of computational work.

[33]Ghosh S., Das T., and Chakraborty S. *et al.(2011)*

Objective: To investigate the effects of different tunable parameters i.e magnetizing field strength, nanoparticle size, diffusion coefficients, porous media parameters and different oligonucleotide sequences on temperature rise and site-specific drug release.

Computational/ Experimental/ Numerical/ Analytical/ Review	Finite Element Method(FEM)	Physics Employed	Magnetic Nanoparticle Used	Assumption Made
Computational	ComsolMultiphysics	1.Transient biological heat transfer Module 2.Statistical mechanics 3.Thermo-fluidic module	Magnetite (Fe_3O_4)	Porous media model of carcinoma

Work:

In this paper, A fundamental mathematical model for superparamagnetic nanoparticle assisted drug delivery under external low frequency magnetizing field applicable for DNA mediated therapy is been proposed.

PARAMETERS	DESCRIPTION
Equations used	1.Transient 3-D Penne's bioheat equation 2.Transient 3-Ddiffusion equation 3.Equation of loss power generated by nanoparticle in electromagnetic field which is

	heat input parameter to pennes equation.
Special considerations	1.Brownian relaxation time is considered infinite for large oligo-nucleotide-drug-assembly. 2.Power generated per unit volume i.e loss power is frequency independent. 3.Porous media model of the tumor is assumed.
Geometrical details	❖ 3D tumor model ❖ Tumor as sphere resting over cylindrical muscle covered by skin. ❖ Diameter of spherical shaped tumor=8mm ❖ Tumor modeled as situated deep inside healthy tissue
Number of meshing elements and meshing points	157 elements and 330 mesh points
Type of solver	Conjugate gradients linear system solver with algebraic multigridpreconditioner.
Frequency	400kHz
Amplitude	8.8kA/m
Time	242sec
Type of injection	Intratumoral
Distribution of particles	Homogeneous
Concentration of particles in tumor	21mg±9 of magnetite sample of diameter 10nm per 299mm^3(70mg/cm^3)
Maximum achievable temperature in tumor	71±8°C
Diameter of nanoparticle	10nm

Inference drawn:

Regarding hydraulic permeability that small structural change in tissue can lead to large variations in hydraulic parameters.

Research Gaps:

The present work is an attempt to computationally predict a multiphysics phenomenon for drug delivery applications to tumor specific applications and analyze the combined effect of diffusion and heat transfer.The problem is summarized as thermofluidic problem which is an assistance to provide the key parameters the author mentioned to this work in his next paper. The present study can be extended for double layer effects, osmosis, hydration forces and steric effects on the diffusion parameters. The model can also be extended by considering poroelastic model.

Sr.No.	Author &Year	Experimental /Computational /Analytical/	Work	Key Findings and Observations

		Numerical/ Review		
[34]	**Gedik et al. [2012]**	Computational	Two different flow models with (non-newtonian flow) and without (newtonian flow) magnetic field are considered in valve-mode under applied external magnetic field,having step-size of 0.5T and variation between 0 and 1.5T. Distance in x-direction 0-0.3m and in y-direction 0.005m.	**1.**Variation of velocity and pressure profiles for different range of magnetic field. **With increase in magnetic field velocity decreases** as 25.4%,63.4% and 80.6% at Bo=0.5,1,1.5T. **2**.**Pressure drop** from 350Pa to 120Pa.
[35]	**Pankhurst Q.et al.[2003]**	Review	Physical principles of magnetic nanoparticles stating their biomedical applications are extensively reviewed.Physics of heat generation in the presence of magnetic field is explained in concern of hyperthermia, Targeted drug delivery, Contrast enhancement agents for imaging applications.	**1.**M-H curves stating FM and SPMbehaviour **2.**Concept of magnetic separation. **3.**Drug delivery **4.**Hyperthermia **5.**Heating mechanism **6**.MRI contrast enhancements **7.**Safe Exposure condition
[36]	**Chang C.et al.[2010]**	Computational/Experimental	Simulation of magnetic fluid in 2-D Square under different positions and intensities of magnetic sourceand to study effect of particle size and mass fractions on fluid behaviour(velocity and flow pattern). Three particle sizes of 18nm,45nm, 110nm are considered for three positions.	**1.**Variation in distance from magnetic source in x-direction lead to symmetry of flow pattern and in y-direction as it is closer have more influence area with intensified flow. **2**.Largest particle(110nm) has highest flow velocity and highest temp. **3**.With three different mass fractions of 10wt%,20wt%,30wt%,the 30w% magnetic particles have highest flow velocity and largest influence area. **4.**Viscosity of 18nm particle is more than 45nm and 110 nm particles. **5.**For particle size of 45nm

				and for different mass fractions of 10wt%,20wt%,30wt%,at mass fraction of 30wt% have least viscosity. **6**.Particles with smaller size have better ability to dissipate heat and larger mass fractions provide stronger driving force
[37]	**Aminfar H.et al.[2012]**	Computational/numerical	Behavior of 2-D tube with an elastic segment containing ferro-fluid(blood & 3%) in presence of non-uniform magnetic field.To determine the position of elastic segment and flow characteristics.One part of tube is rigid.Length of the tube is 14cm.The tube is horizontal.Magnetic field is only applied in elastic part and not in the rigid part.Effect on Wall Shape, Pressure distribution,Vorticity distribution along with magnetic field for elastic membrane.The results were checked for two values of Reynold no. of 50 and 100. Placing a thin wire carrying electric current vertically to x-y plane.	**1.**For the Laminar flow having Re=500,The grid consists of 35 nodes in y-direction,350 nodes in x-direction and 150 nodes for elastic segment.It shows that changing grid numbers doesn't Change Vorticity profile except for intial iteration. **2**.Applying positive gradient magnetic field makes the tube narrower but the negative one and magnetic field of electric wire opens the tube up. **3.**The position of elastic wall doesn't change when the nano-fluid add to the blood with respect to pure blood but on applying magnetic fieldsignificant displacement occur.Re=50 **4.**For negative gradient the minimum cross-section area of tube moves downwards. **5.**Low Pressure for positive-gradient makes the tube narrower and high pressure for neagtive gradient makes the tube opens up.For Positive gradient zero pressure drop is there. **6.**None of the curve have negative value of vorticitystating no back flow. **7.**More the slope of Magnetic field more narrower the tube.

				8.Opening of channel due to pressure increment produced either by placing a wire carrying electric current or by applying negative gradient.
[38]	**Habibi Reza M et al.[2011]**	Computational/ Mathematical	To investigate the effect of non-uniform magnetic field on bio-fluid(blood) with magnetic nanoparticles.Effect of particles, mass fraction on flow field and volume concentration.Width and length of vessel are considered as 0.001m and 0.02m,for laminar 2-D flow,External permanent magnet of 4mm diameter is placed in center of vessel a=L/2.Blood is taken as non-newtonian model	**1.**When velocity decreases near magnetic source,the pressure increases due to restriction.with increase in blood velocity particles injection and aggregation near the magnet donot change the pressure. **2.**Increasing injection velocity changes the flow field before the magnetic source and increases the shear stress on upper wall. **3.**Decreasing the distance between permanent magnet and upper wall(2mm) donot severely increase the absorption of the particles. **4.**Decreasing average velocity from(0.028m/s to 0.0028m/s) magnetic nanoparticles remain in blood flow for longer period of time.
[39]	**Ashtiani M.et al.[2013]**	Theoretical/ Review	MR Fluid belongs to class of Smart Materials whose viscosity increases considerably in presence of magnetic field. Dispersing magnetizable particles into carrier fluid with stabilizer additives. Ability to change from liquid to semi-solid state should be enhanced.	**1.**Reducing sedimentation of magnetizable particles due to gravity **2.**To obtain great yield stress **3.**Carbonyl iron micro-particles are most promising particles to achieve high magnetization, low cost, low coercivity. **4.**Coating the particle to reduce particle to particle interaction and particle density. Carbonyl iron particles are used along with polymeric material. **5.**Using a combination of

				both nanoparticles and microparticles to enhance the yield stress.
[40]	**Kenjeres S.[2007]**	Computational	The model is validated for different test cases ranging from a simple cylindrical geometry to real-life right-coronary arteries in humans. The time-dependency of the wall-shear-stress for different stenosis growth rates and the effects of the imposed strong non-uniform magnetic fields on the blood flow pattern are presented and analysed.	It is concluded that an imposed non-uniform magnetic field can create significant changes in the secondary flow patterns, thus making it possible to use this technique for optimisations of targeted drug delivery.

4.5 RESEARCH GAPS

One of the most challenging problems in hyperthermia is the right dose of particles by specifying the affected region under consideration. So, far till today real time patient specific modeling is missing to give the exact measure of acceptance of hyperthermia using MNPs or any other modality. The possible impact on the theoretical use of magnetic heating treatment(MHT) in reduction of negative influence on the patient's discomfort can only be realized if true model geometries can be obtained with respect to hyperthermia studies. Focus should be to approach towards *model* to *clinic.*

In general, most of the computational based studies assumes the healthy tissue as cubical region, cylindrical region, spherical region and affected tissue region as sphere or ellipsoid. But in reality neither the tissues would be cubical or spherical and but mostly composed of irregular shape that should be defined properly depending upon the simulation software techniques well accepted this very day.

So, the tumor exact geometry and position should be made available by using the concept of medical imaging techniques such as CT(Computed tomography), MRI(Magnetic Resonance Imaging).So, this area is been highlighted by the author too as *an important Research Gap*. Successfully developed imaged based 3D models from real time clinical images(CANCER patients) obtained by CT or MRI to construct **patient-specific models** for planning and also

simulations with a preview to optimize treatment efficacy. Such patient models can be developed by segmentation of images and applying some imaging operations. Patient specific image based 3D modeling could resolve the problems of heat sink effect created by blood vessels, role of healthy surrounding tissue in heat distribution, ablation etc. by permitting pre-treatment planning of the simulated thermal ablation based on preoperative images of the lesion. This research gap is very important finding for *future computer assisted interventions* and opens horizons towards beginning of new modalities and to improve the existing ones.

The information regarding the local features of Tumor/Tissue pefusion rate, and the type of Tissue, Tumor density, Type of tumor, blood vessels impact that can be addressed correctly unless the geometrical information obtained from the scans is converted into 3D Model and thermal analysis is done to obtain the required temperature elevations with feasible alterations in internal and external factors.

The present work is an attempt to computationally predict a multiphysics phenomenon for applications tumor specific applications and analyze the combined effect of magnetic field heating and Bio-heat transfer phenomenon. The problem is summarized as thermal analysis problem which is an assistance to provide the key parameters. For *breast tissue* wherein perfusion is very low and effective blood vessels(veins and arteries) are less compared to other organs and also chances of MTS are very less. 3D-model generation can be feasible by using appropriate Imaging processing software or codes specific to requirement for successful employment to clinical trials.

There is foremost need that experimental results needs to be examined and such quantization of parameters can be an input to resolve the fundamentals of hyperthermic studies with the aid of computational work. The field amplitude and field frequency are most important parameters that needs to be tuned along with the loss power for each of the smaller sized nanoparticles. The work that states on these magnetic parameters is still not well addressed in computational studies been examined.

In most of computational work, the nanoparticles are assumed to be monodispersed. The size polydispersity which is present in all real nanoparticles samples is still missing in most of analysis been performed in similar studies. and by using these models it is possible to estimate the impact of the particle dose on the efficiency of hyperthermia therapy.

The cooling protocol is defined by only one author as found by literature survey. This is also an interesting gap finding because such studies can be an assistive tool to go for therapeutic temperature elevations.

The model that takes into the account 3-D electromagnetic thermal aspects of hyperthermia domain is missing. So, We tried to address the concept of electromagnetic heating and define the problem addressal to patient specific problems and analyzed with most accepted pennes bioheat transfer equation. Since, for the studies discussed in most of the bioheat transfer simulations the concept of Mixture is applied or simply say averaging of properties is done to evaluate for the loss power calculations which will be an input to penne's equation.In no case single nanoparticle will assist hyperthermia in different sized tumors. This study can be extended to different kind of magnetic materials with study extension from to number of nanoparticles accumulated in tumor region to produce more uniform heating by assuming important considerations of homogeneous distribution for nanoparticles by the concept of averaging because nano-scale simulations with large number of particles are difficult to address by computational softwares because of their inability to perform simulations due to large number of domain elements and more computational time requirements and selection during heat loading.

The model can be extended towards more realistic conditions and processes in biological tissues. Also, the work can be extended for different amplitudes of magnetic field and frequencies by taking into account the safe exposure limit. Patient specific information/preoperative procedures can assist the surgeries been performed or to completely eliminate current practices with MNP induced mono-therapy.

CHAPTER 5

PROPOSED WORK AND METHODOLOGY

5.1 OVERVIEW

This chapter contains four distinct discussions namely Research gaps, Proposed work, Schematic flow chart representation, and Research design. The research gaps which are been presented in chapter-5, contains individual literature review helps to build broader perspective of important research gap findings. Based upon the research gaps, computational problem is formulated and work is proposed. A very important component of research problem is "Research methodology" which quantifies all individual components presented in a step-by-step schematic representation. The Research design discretizes the important input design variables as independent and dependent variables that bridge the important relationship between them.

5.2 PROPOSED WORK

1. To convert the DICOM format data(images)
2. In order to understand the physics of heat generation, heat dissipation, a computational model will be developed using a commercial design and analysis softwares using:
   - ❖ Materialise MIMICS 17.0
   - ❖ Materialise 3-matic 8.0
   - ❖ COMSOL-MULTIPHYSICS 5.O
   - ❖ MATLAB
3. The effect of magnetic field on the Magnetic nanoparticles(MNPs) will be studied with respect to transient temperature variations in and around the tumor.
4. The effect of different composition of nanoparticle within the ferrofluid will be studied on temperature variations.
5. The effect of variable blood perfusion for breast tissue will be studied.

6. The effect of alternating magnetic field parameters i.e field amplitude and frequency on temperature elevation profiles.
7. The effect of variable heat transfer convection coefficient on temperature achievement inside the domain of concern.
8. To study the plots of necrosis or effective damage integrals for breast tissues.
9. To study the effect of depth of tumor tissue from the base of application of heat.
10. Verification & Validation: Verifying the results and validate the work with respect to benchmark result paper and experimental studies(literature).

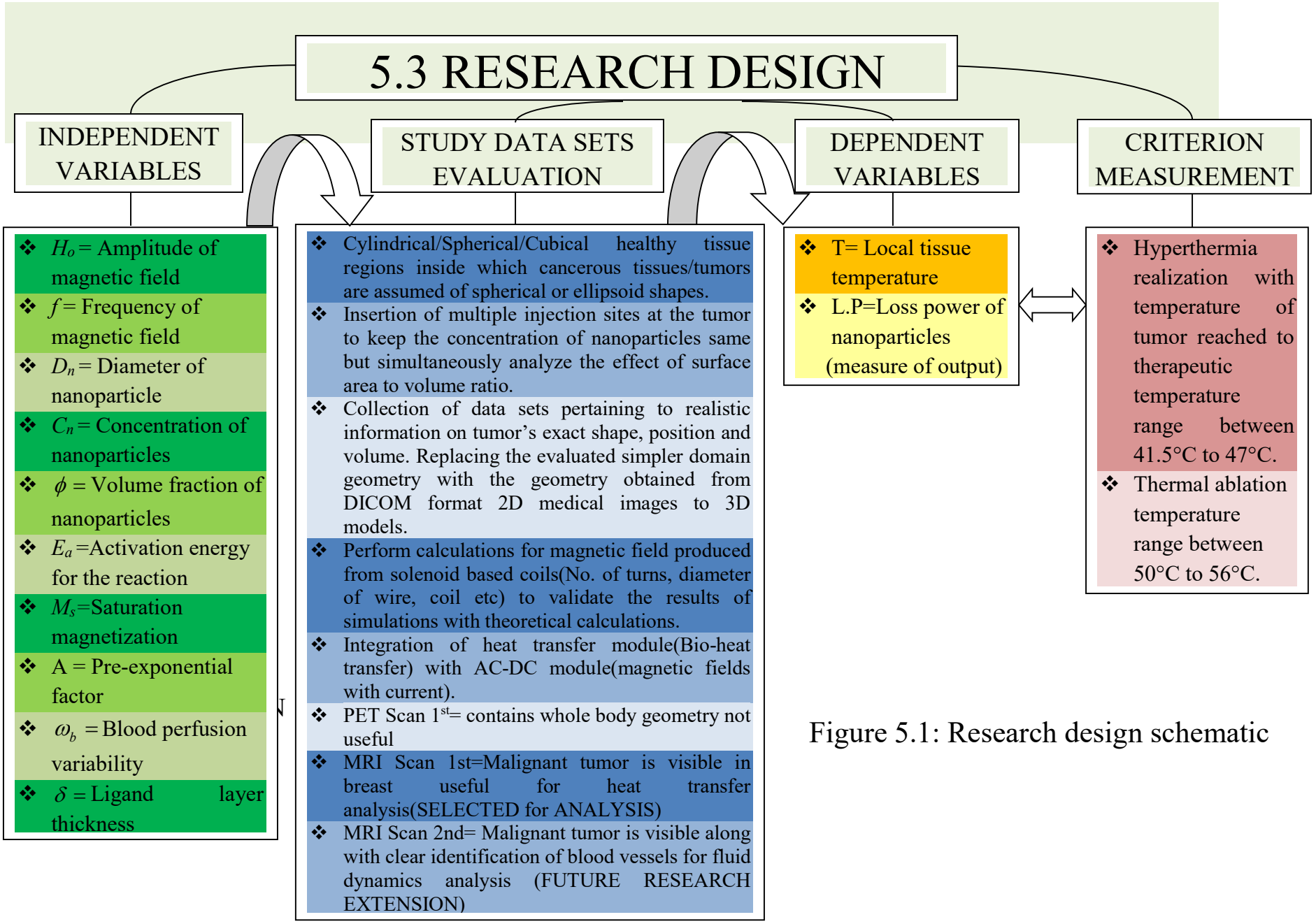

Figure 5.1: Research design schematic

5.4 FLOW CHART REPRESENTATION OF PROPOSED COMPUTATIONAL WORK:

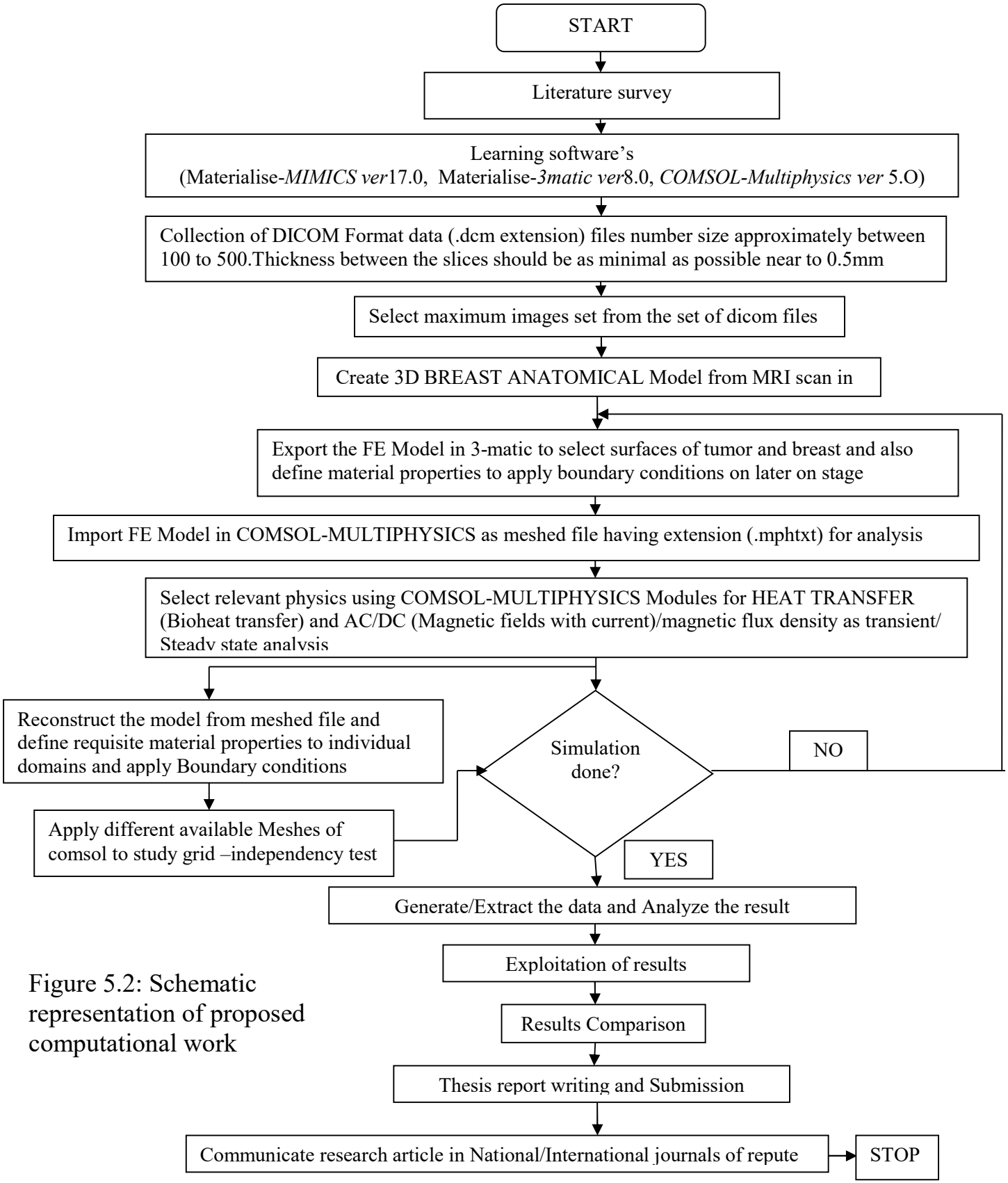

Figure 5.2: Schematic representation of proposed computational work

CHAPTER 6

COMPUTATIONAL MODEL DESCRIPTION

6.1 OVERVIEW

MFH is a complicated multiphysics problem which is covered by two partially independent solutions: one solution that accounts for magnetic field equation and the other considers heat transfer equation. As reported in computational literature review, we found that till now no coupling interface is defined between the two studies and are individually considered. In the context of estimating the problem from view point of hyperthermic studies, initially we consider the bioheat transfer problem and employ heat parameter as value calculated by matlab problem which validates our considered value with literature. Similarly, further extension of the study leads us to also estimate the heat inputs via defining important coupling between bioheat transfer module and magnetic field with currents with transient analysis. This again satisfies the requirements and validates and agrees upon the estimates done by researchers in clinical trials or experimentally conducted phantom based studies or animal experiments. The calculated temperature profiles of healthy tissue and the diseased cancerous tissue validates the proposal of concept of hyperthermia as an adjuvant to other modalities of chemotherapy and radiotherapy, or also further heating extends the temperatures to thermal ablation or coagulation necrosis.

In this current study, a complete mathematical model of MFH is proposed and analyzed to simulate heat generation and transfer during magnetic hyperthermia. The problem is formulated by considering simpler geometries(cylindrical domains of healthier tissues) as mostly studied by researchers in their computational studies as reported in literature reviewwith cancerous tissue(ellipsoid) been placed inside the domain walls. The estimation of temperature distribution in tumor regions and surrounding normal tissues, both electromagnetic and thermal problems are solved using the finite element analysis(FEA) method in COMSOL-MULTIPHYSICS5.O. PD(Power density) or S.L.P(Specific Loss Power) or S.A.R(Specific

Absorption Rate) is derived from electromagnetic field simulation performed in MATLAB and is computed as the input of Penne's Bio-heat Equation(P.B.H.E).After the successful results, we modeled it on realistic breast tissue model which is itself a novel approach and till now no work has been done in this direction except the directional approach that we have proposed in relation to reported computational studies been done till date. We have formulated the problem by taking into consideration the important aspects of Image processing and made the model from large sets of 2D images obtained from PGIMER, Chandigarh.

The study involves advanced computational machines with RAM requirements of 64GegaBytes(GB) and still the time required by Comsol to calculate the results for temperature profiles is almost 18hours to 24hours due to large number of meshing elements. Time taken by solver is huge.

Maxwell's equations in magnetic problems are computed according to appropriate boundary, whereas Penne's bioheat equation in thermal problems is calculated by considering blood perfusion. In present work, both electromagnetic and thermal problems are solved by FEA. The concept of averaging of properties is also been incorporated.To increase the efficiency in the healing treatment by hyperthermia, a precise control of local temperature determined by a heat source within the living tissue is required.

COMSOL is a general purpose software to compute electromagnetic fields interaction with tissue matter.In the current work, the problem is defined as multiphysics problem by incorporating the two types of coupling i.e Uncoupled, One-way coupled. Uncoupled analysis involves calculation of temperature distribution by pennes bio-heat equation. One-way coupling which is absent in other computational softwares like ANSYS is provided in Comsol-multiphysics. In comsol –multiphysics model, Heat Transfer Analysis typically involves

1. Geometry creation
2. Materials selection to number of domains
3. Type of Physics incorporated
4. Mesh generation
5. Type of study to calculate temperature distributions

a.)For steady state

b.)For transient state

6.2 GOVERNING EQUATION

PENNES BIO-HEAT EQUATION

$$\rho_t c_t \frac{\partial T_t}{\partial t} + \nabla.(-k_t \nabla T_t) = Q_{blood} + Q_{metabolic} + Q_{source} \quad (6.1)$$

$$Q_{blood} = \rho_b \omega_b c_b (T_b - T_t) \quad (6.2)$$

$$\rho_t c_t \frac{\partial T_t}{\partial t} + \nabla.(-k_t \nabla T_t) = \rho_b \omega_b c_b (T_b - T_t) + Q_{metabolic} + Q_{source} \quad (6.3)$$

where,

ρ_t =Density of tissue

c_t =Specific heat capacity of tissue

T_t =Temperature variations of tissue with time t

t =Exposure time duration

k_t =Thermal conductivity of tissue

Q_{blood} =Contribution of blood perfusion rate

ρ_b =Density of blood

ω_b =Blood perfusion rate

c_b =Specific heat capacity of blood

T_b =Arterial blood temperature

$Q_{metabolic}$ =Amount of energy generated by metabolic processes or volumetric rate of metabolic heat generation

Q_{source} =Heat generation by loss power or Power generated per unit volume of nanoparticle or distributed volumetric heat generation due to spatial heating

6.3 INITIAL & BOUNDARY CONDITIONS

Boundary conditions are used to account for convective or sweating heat loss at patients surface. Initial conditions are defined by keep in preview.

BOUNDARY CONDITIONS

- DIRICHLET's B.C- Constant Temperature Condition(B.C of Ist Kind)

  (External surface of geometry to be at core temp.of 37°C)

Value of variable is provided along the boundary

- NEUMANN's B.C-Tumor-Vessel Interface(B.C of IInd Kind)

  (Heat flux coming from the tumor is completely received by B.V)

  The normal gradient of the variable is provided along the boundary
- CONTINUITY B.C

  (Heat flux is imposed at the tumor-healthy region interface and

  tumor injection site interface too)
- ROBIN's B.C(Impedance B.C or Convective B.C)or(B.C of IIIrd Kind)

  Linear combination of first two B.C's

  Ambient Conditions of Convection coefficient of 5W/m^{2}K and Ambient temperature of 26°C
- MIXED B.C

  The condition is like a Dirichlet along a portion at the boundary, like Neumann along another portion

6.4 TYPE OF SOLVERS

There are different solvers available by the Comsol-Multiphysics to compute the results of geometrical domain under study by specific nodes. There are several features available under mesh settings to see for more accurate results by upgrading the mesh from coarser to very fine. The mesh refinement results in the very small grid size which further increase accuracy in results obtained at the cost of increased computation time.

Self-selection feature of Comsol based upon the selected physics results in defining the solvers that are well suited to show the coupling between different interfaces and also between the different software's that are been employed in computational studies to design and propose new methodologies.Solvers are summarized as follows:

1. Direct PARDISO Solver
2. FGMRES Iterative Solver
3. UMFPACK Solver
4. GMRES Solver

Explanatory notes:

Comsol has Direct PARDISO Solver which is a highly efficient solver for symmetrical and non-symmetrical systems. It often uses less memory.

FGMRES Iterative Solver is a solver for non-symmetrical problems specifically, it can handle more general preconditioner but also uses more memory than GMRES.

In the current analysis, MUMPS and PARDISO solvers compute the temperature results for transient study.

6.5 MODEL-1:BIOHEAT TRANSFER ANALYSIS OF ANIMAL MODEL(RAT)

6.5.1GEOMETRY DETAILS

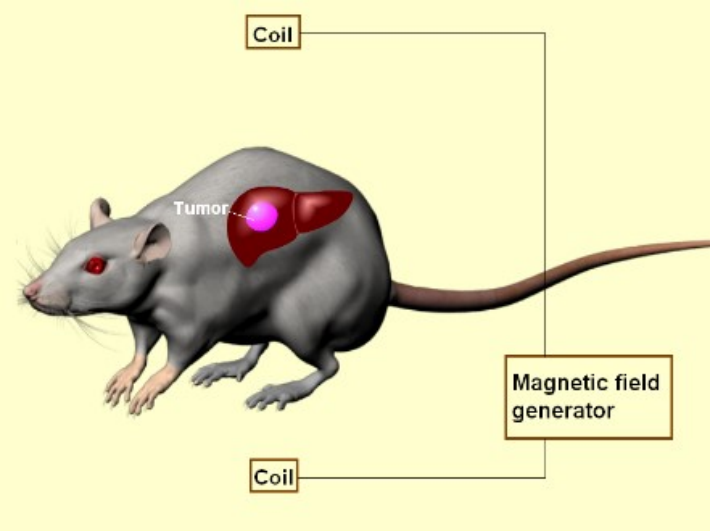

Figure6.1**:**Tumor bearing mouse placed in the magnetizing field

Table 6.1: Properties of blood

Name	**Value**	**Description**
rho_b	1000.0 kg/m³	Density, blood
c_b	4200.0 J/(kg·K)	Heat capacity, blood
omega_b	0.0064000 1/s	Blood perfusion rate
T_b	310.15 K	Arterial blood temperature
T0	310.15 K	Initial and boundary temperature
h_h	5.0000 W/(m²·K)	Heat transfer coefficient

Name	Value	Description
T_B	115.00 K	Blocking temperature of magnetite nanoparticle
T_ambient	293.15 K	Ambient temperature

Table 6.2: Geometry Statistics

Property	Value
Space dimension	3
Number of domains	136
Number of boundaries	1035
Number of edges	1542
Number of vertices	770

Table 6.3: Healthy tissue(muscle tissue properties)

Name	Value	Unit
Thermal conductivity	73.5	W/(m*K)
Density	5175	kg/m^3
Heat capacity at constant pressure	143500	J/(kg*K)
Frequency factor	0	1/s
Activation energy	0	J/mol

Table 6.4: Tumor properties

Name	Value	Unit
Thermal conductivity	0.5	W/(m*K)
Density	1050	kg/m^3

Name	Value	Unit
Heat capacity at constant pressure	3700	J/(kg*K)
Frequency factor	4.3*10^64	1/s
Activation energy	420000	J/mol

Table 6.5: Skin tissue properties

Name	Value	Unit
Heat capacity at constant pressure	3391[J/(kg*K)]	J/(kg*K)
Density	1109[kg/m^3]	kg/m^3
Thermal conductivity	0.37[W/(m*K)]	W/(m*K)
Frequency factor	4.575e72	1/s
Activation energy	4.71e5	J/mol

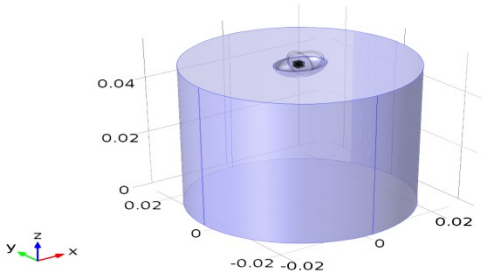

Figure 6.2: Representation of complete domain

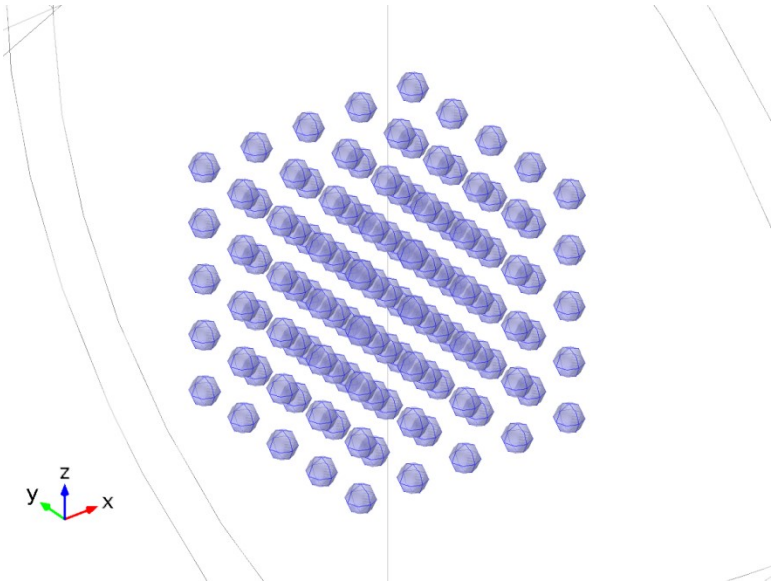

Figure 6.3: Representation of domain of particles

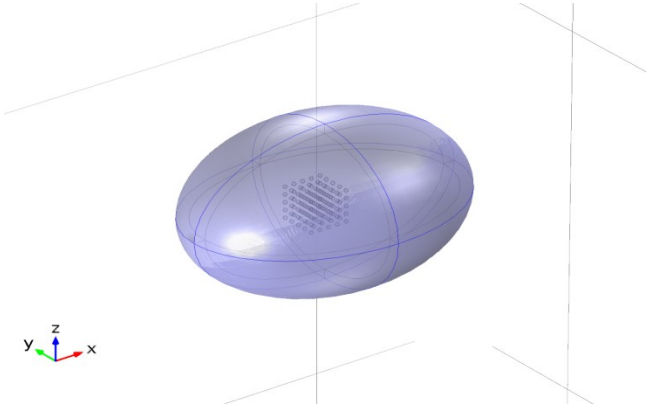

Figure 6.4: Elliptical tumor enriched with nanoparticles

6.5.2 MESH STATISTICS

Table 6.6: Mesh properties

Property	Value
Minimum element quality	2.797E-5
Average element quality	0.6527

Property	Value
Tetrahedral elements	27911
Triangular elements	4164
Edge elements	1796
Vertex elements	770

Table 6.7:Mesh Size properties

Name	Value
Maximum element size	0.0054
Minimum element size	9.72E-4
Curvature factor	0.6
Resolution of narrow regions	0.5
Maximum element growth rate	1.5

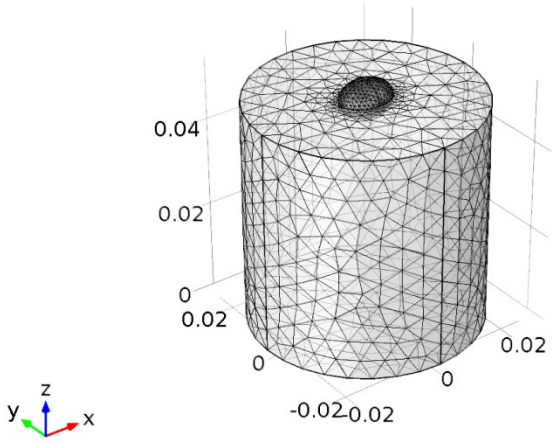

Figure 6.5:Representation of mesh on animal(muscle tissue) model.

6.5.3 BOUNDARY CONDITIONS

Initial B.C imposed on tissue is temperature of arterial blood(T_b).

Heat source is via electromagnetic heating which produces the desired heating effect.

Initial and boundary temperature is 37°C.

Temperature of surrounding is 26°C

Convective heat transfer coefficient, h=5W/m^2K

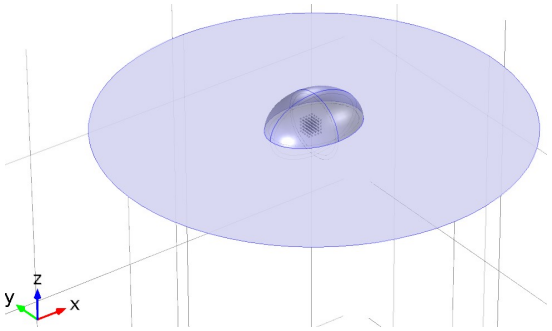

Figure 6.6:Boundary condition of convective heat flux

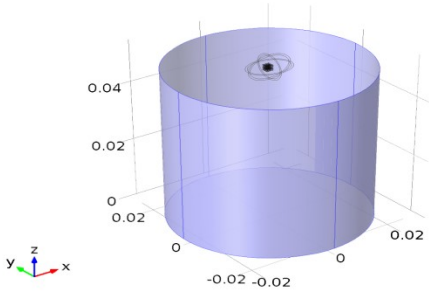

Figure 6.7: Boundary electromagnetic heat source

6.5.4 GRID INDEPENDENCY TEST

Fine mesh is used to compute the results and the small variation is found in results to normal.

6.6 MODEL-2: BIOHEAT TRANSFER AND MAGNETIC FIELD COUPLING ANALYSIS OF ANIMAL MODEL(RAT)

6.6.1 GEOMETRY DETAILS

Table 6.8: Representation of blood properties

Name	Value	Description
rho_b	1000.0 kg/m³	Density, blood
c_b	4180.0 J/(kg·K)	Heat capacity, blood
omega_b	0.0064000 1/s	Blood perfusion rate
T_b	37[degC]	Arterial blood temperature
T0	37[degC]	Initial and boundary temperature
T_ambient	26[degC]	Ambient Temperature

Table6.9: Geometry statistics of animal model

Property	Value
Space dimension	3
Number of domains	4
Number of boundaries	37
Number of edges	68
Number of vertices	38

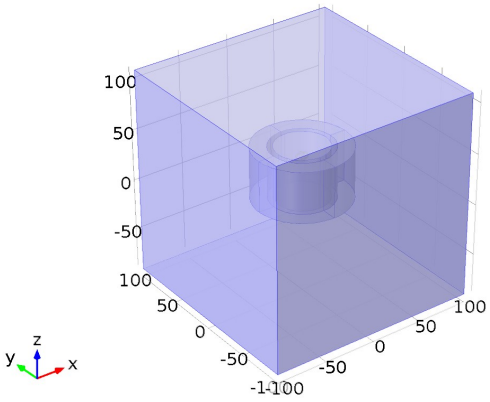

Figure6.8: Block representing air domain(Dimensions of block 200mm, 200mm, 200mm)

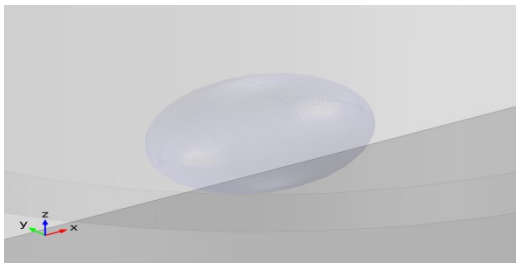

Figure 6.9: Tumor domain(cancerous tissue)

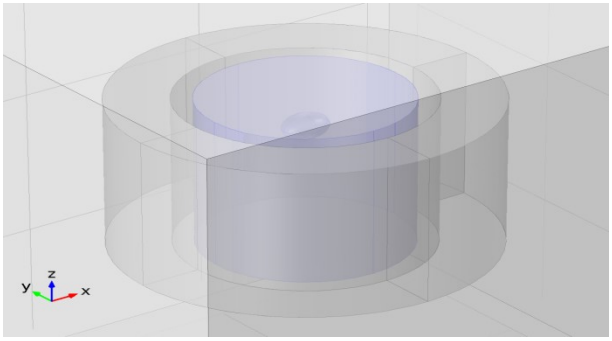

Figure 6.10 Muscle tissue(Rat model)

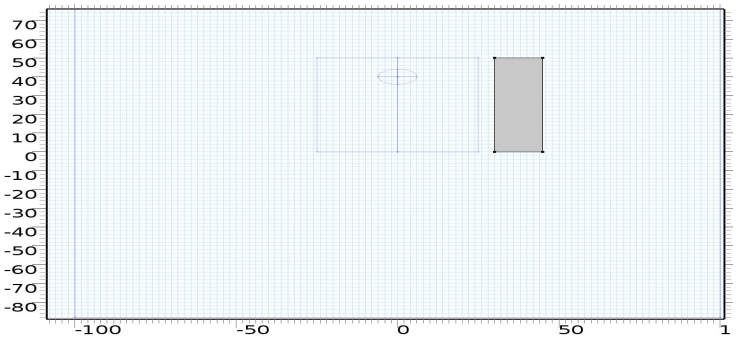

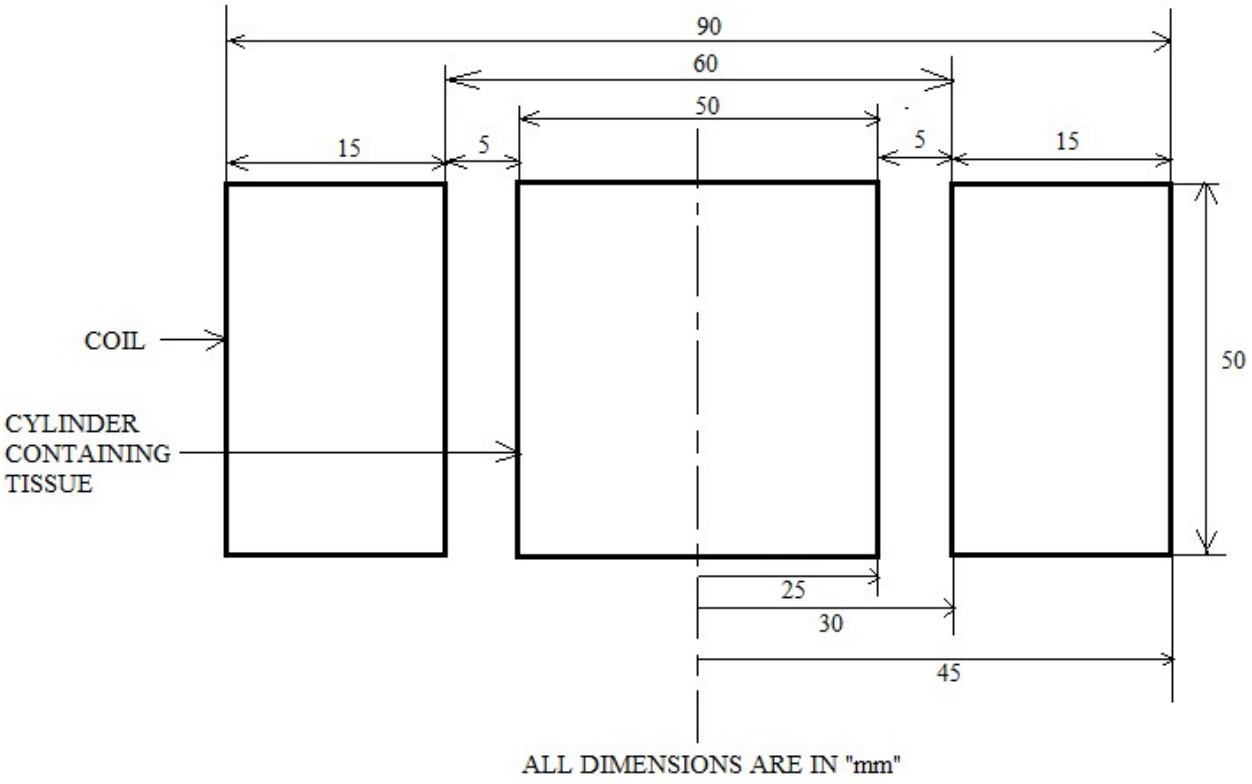

Figure 6.11: Representation of model geometry

6.6.2 MATERIAL PROPERTIES

Table 6.10 :Materialproperties of Air

Name	Value	Unit
Relative permeability	1	1
Relative permittivity	1	1
Electrical conductivity	10[S/m]	S/m
Heat capacity at constant pressure	Cp(T[1/K])[J/(kg*K)]	J/(kg*K)
Density	rho(pA[1/Pa],T[1/K])[kg/m^3]	kg/m^3
Thermal conductivity	k(T[1/K])[W/(m*K)]	W/(m*K)
Frequency factor	0	1/s
Activation energy	0	J/mol

Table 6.11:Material properties of tumor

Name	Value	Unit
Relative permittivity	74	1
Electrical conductivity	0.89	S/m
Density	1047	kg/m^3
Thermal conductivity	0.55	W/(m*K)
Heat capacity at constant pressure	3560	J/(kg*K)
Relative permeability	1	1

Table 6.12: Material properties muscle tissue

Name	Value	Unit
Heat capacity at constant pressure	3421[J/(kg*K)]	J/(kg*K)
Density	1090[kg/m^3]	kg/m^3
Thermal conductivity	0.49[W/(m*K)]	W/(m*K)
Electrical conductivity	0.72	S/m
Relative permittivity	62.8	1
Relative permeability	1	1
Frequency factor	0	1/s
Activation energy	0	J/mol

6.6.3 ELECTROMAGNETIC COUPLING

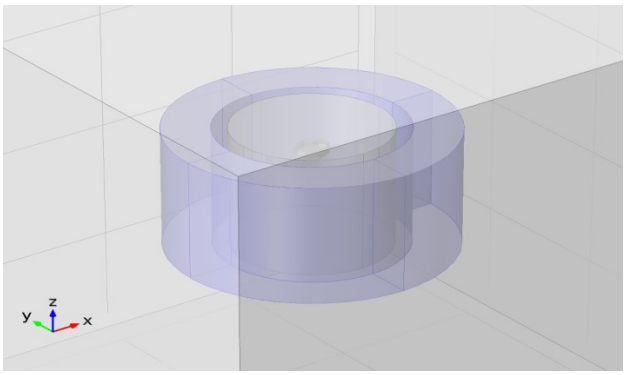

Figure 6.12: Domain which produces the electromagnetic heating effects

6.6.4 GOVERNING EQUATION

Current calculations

$$B = \nabla \times A \quad (6.4)$$

Ampere's law

$$\nabla \times \left(\mu_o^{-1} \mu_r^{-1} B\right) - \sigma v \times B = J_e \quad (6.5)$$

Multi-turn coil

$$J_e = \frac{N I_{coil}}{A} e_{coil} \quad (6.6)$$

where,

J_e =Current density

B=Magnetic flux density

μ_o = Absolute permeability of free space

μ_r = Relative permeability

I_{coil}= Current in coil

N= Number of turns

Table 6.13: Properties of coil

Description	Value
Coil type	Numeric
Coil excitation	Current
Constitutive relation	Relative permeability
Relative permeability	1
Coil name	1
Number of turns	1126
Coil conductivity	$6x10^7$[S/m]
Coil wire cross-section area	American wire gauge (Brown & Sharpe)
American wire gauge (Brown & Sharpe)	20
Coil current	10[A]

Table 6.14:Properties of blood

Name	Value	Description
ρ_b	1000.0 kg/m³	Density, blood
Cb	4180.0 J/(kg·K)	Heat capacity, blood
ω_b	0.0064000 1/s	Blood perfusion rate
Tb	37[degC]	Arterial blood temperature
To	37[degC]	Initial and boundary temperature
T_ambient	26[degC]	Ambient Temperature

6.6.5 MESH STATISTICS

Table 6.15: Representation of different meshing elements for coupled geometry

Property	**Value**
Minimum element quality	0.06341
Average element quality	0.7356
Tetrahedral elements	21522
Triangular elements	2678
Edge elements	335
Vertex elements	38
Maximum element size	20
Minimum element size	3.6
Curvature factor	0.6
Resolution of narrow regions	0.5
Maximum element growth rate	1.5

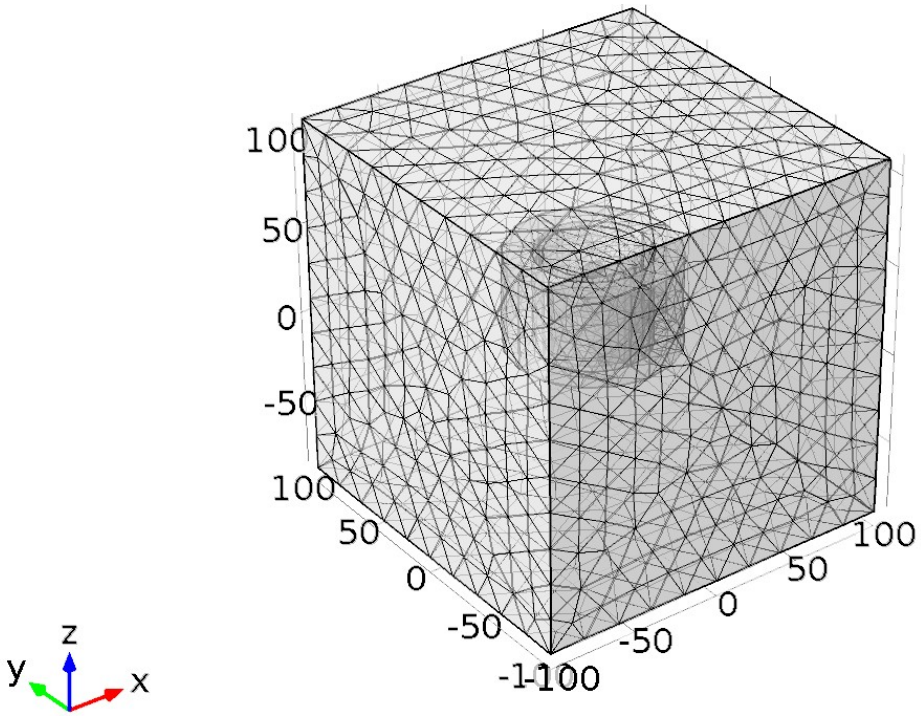

Figure 6.13: Representation of mesh for animal model

Frequency Range to which calculations are performed are range of (1,10,400), (1,10,500), (1,10,600)

Type of solver used are BICGStab and PARDISO(Direct solver), Linear solver(Iterative).

6.6.6 BOUNDARY CONDITIONS

Initial B.C imposed on tissue is temperature of arterial blood(T_b).

Heat source is via electromagnetic heating which produces the desired heating effect.

Initial and boundary temperature is 37°C.

Temperature of surrounding is 26°C

6.6.7 GRID INDEPENDENCY TEST

Grid Independency test is performed with extremely coarse, extra coarser, coarser, coarse, normal, fine, finer. The results with fine mesh and finer mesh are in relation and close

6.7BREAST MODEL

6.7.1GEOMETRY DETAILS

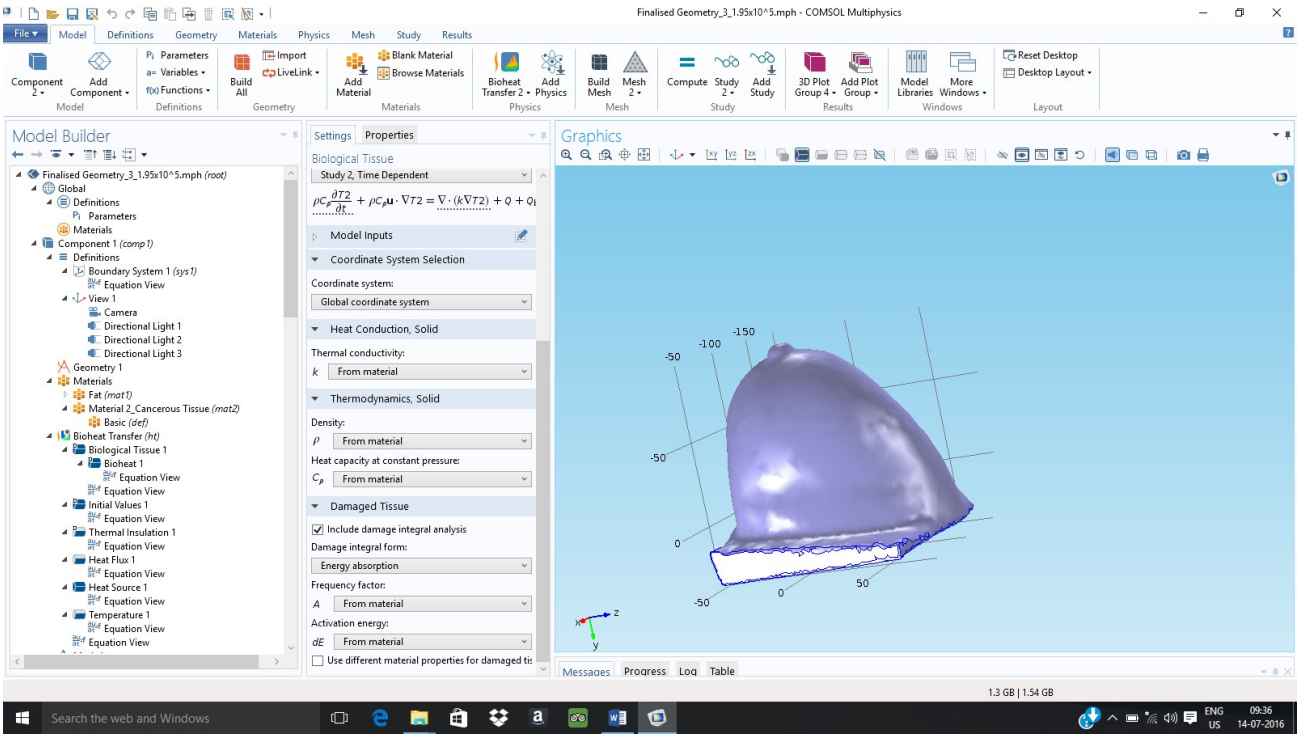

Figure6.14 : Breast model outer domain.

It consists of two domains. Outer domain is fat tissue(breast composed mainly of fat). The inner cancerous tissue(inner domain) is breast tumor is defined in three co-ordinate planes to calculate effective volume of tumor.

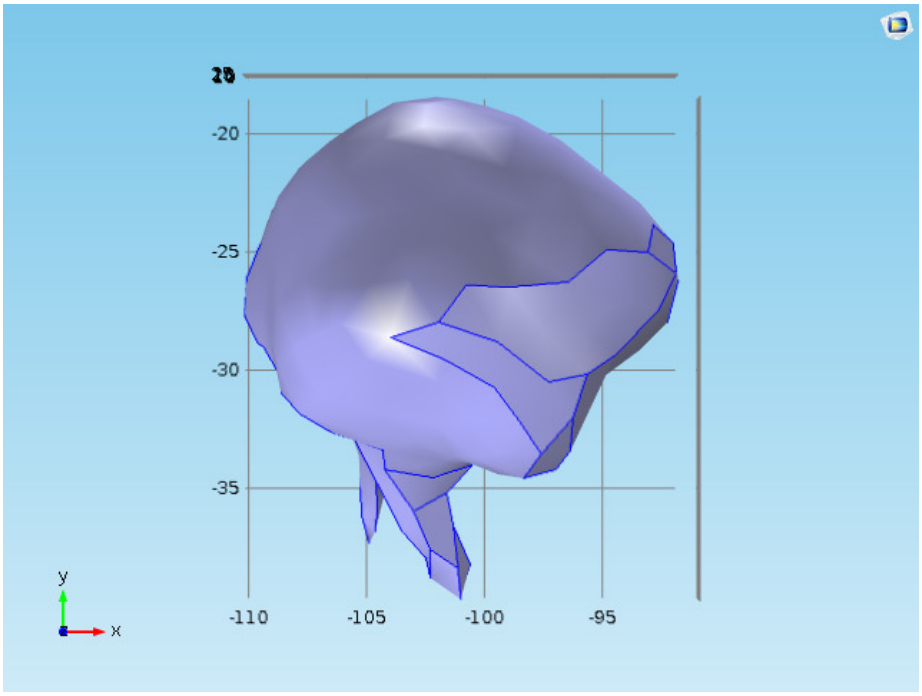

Figure 6.15 Tumor in X-Y co-ordinates

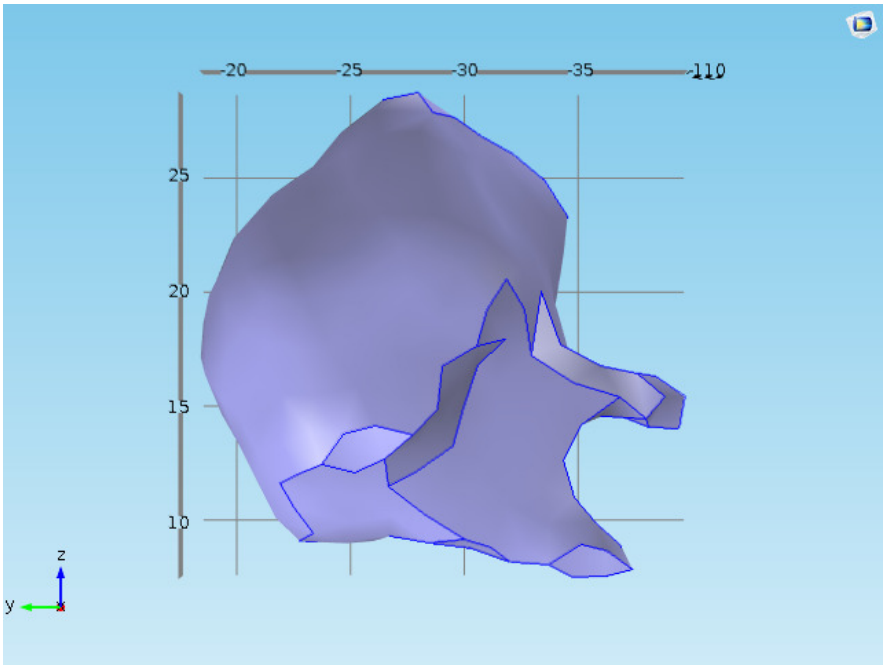

Figure 6.16 Tumor in Y-Z co-ordinates

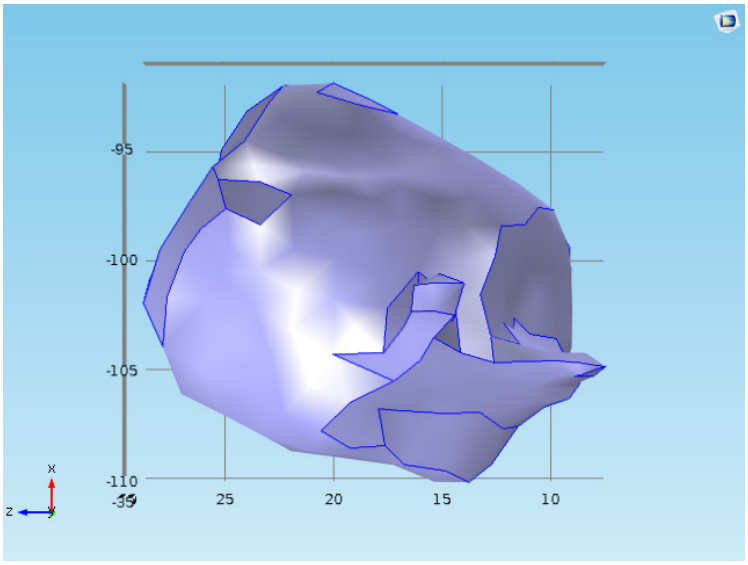

Figure 6.17 Tumor in Z-X co-ordinates

Volume of whole breast model is 1106000mm3.

Surface area of the model is 64200mm2.

Total number of domains are two contains 120 boundaries and 433 edges.

Volume of tumor as defined by comsol is 2447mm3.

Surface area is 1013mm2.

The tumor is assumed spherical by calculating tumor major axis as 17mm and tumor minor axis is 15mm. The diameter of tumor is 17mm(radius 8.5mm) and for this volume comes out to be 2572mm3.

Physics Interface used is Bioheat transfer

Type of Analysis is Transient

Solver used is PARDISO

Type of physics controlled mesh used is Finer

Table 6.16: Parameters for Blood

PARAMETER	**SYMBOL**	**VALUE**
Density of blood	ρ_b	1000.0 kg/m³
Heat capacity of blood	C_b	4180.0 J/(kg·K)
Blood perfusion rate	ω_b	0.0064000 1/s

Arterial blood temperature	T_b	37°C
Initial and boundary temperature	T_o	37°C
Ambient temperature	T_b	26°C
Frequency factor	A	9.4*10^104
Activation energy	E_a	660000
Convective heat coefficient	h	5W/m^{2}K

6.7.2 MESH STATISTICS

Table 6.17:Mesh specific parameters of breast tissue

PROPERTY	VALUE
Minimum element quality	0.03856
Average element quality	0.7117
Tetrahedral elements	264753
Pyramid elements	0
Prism elements	0
Hexahedral elements	0
Triangular elements	35352
Quadrilateral elements	0
Edge elements	2222
Vertex elements	329
Minimum element quality	0.008931
Average element quality	0.4092
Tetrahedral elements	44056
Triangular elements	19480
Edge elements	1023

PROPERTY	VALUE
Vertex elements	329
Maximum element size	0.00854
Minimum element size	6.21E-4
Curvature factor	0.4
Resolution of narrow regions	0.7
Maximum element growth rate	1.4
Predefined size	Finer
Relative tolerance	0.01
Time	30min.

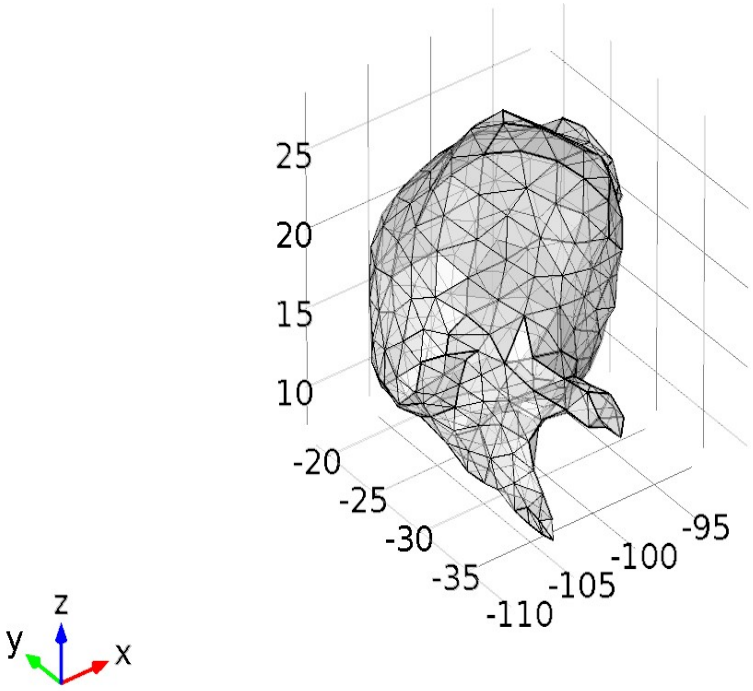

Figure 6.18: Mesh on tumor (finer mesh)

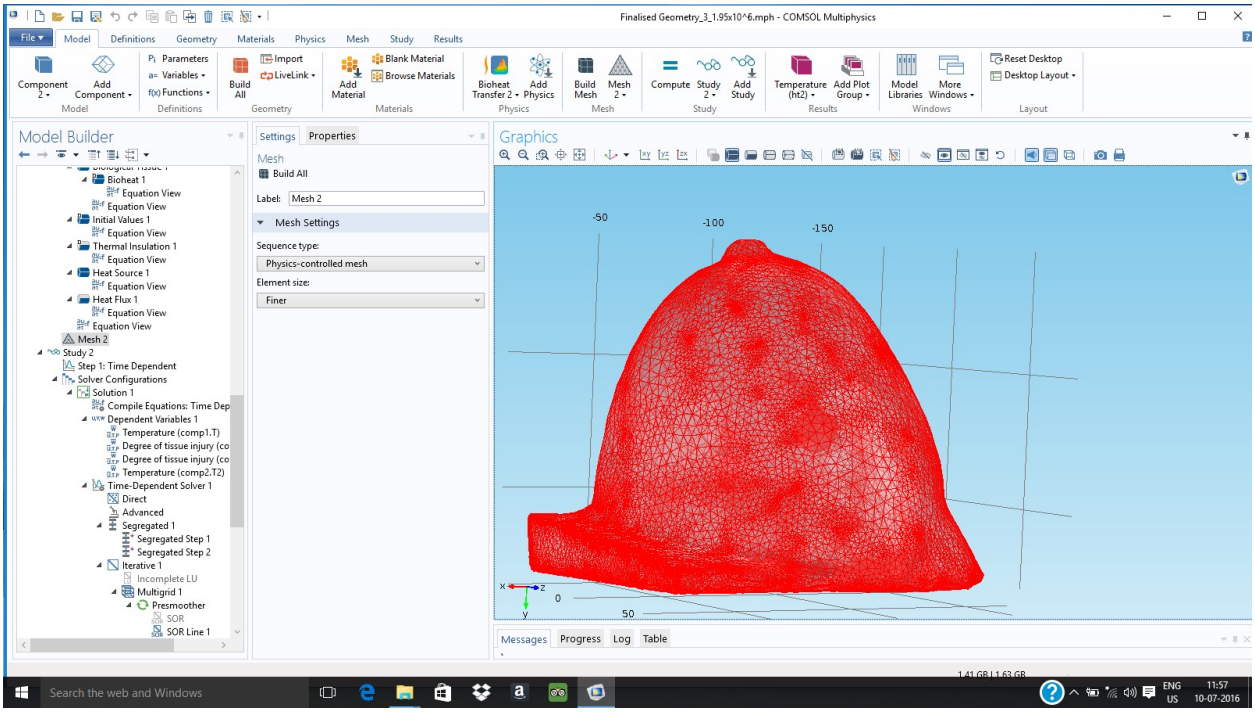
Finalised Geometry_3_1.95x10^6.mph - COMSOL Multiphysics
Model Builder
Settings
Properties
Mesh
Build All
Label: Mesh 2
Mesh Settings
Sequence type:
Physics-controlled mesh
Element size:
Finer
Graphics
Messages
Progress
Log
Table

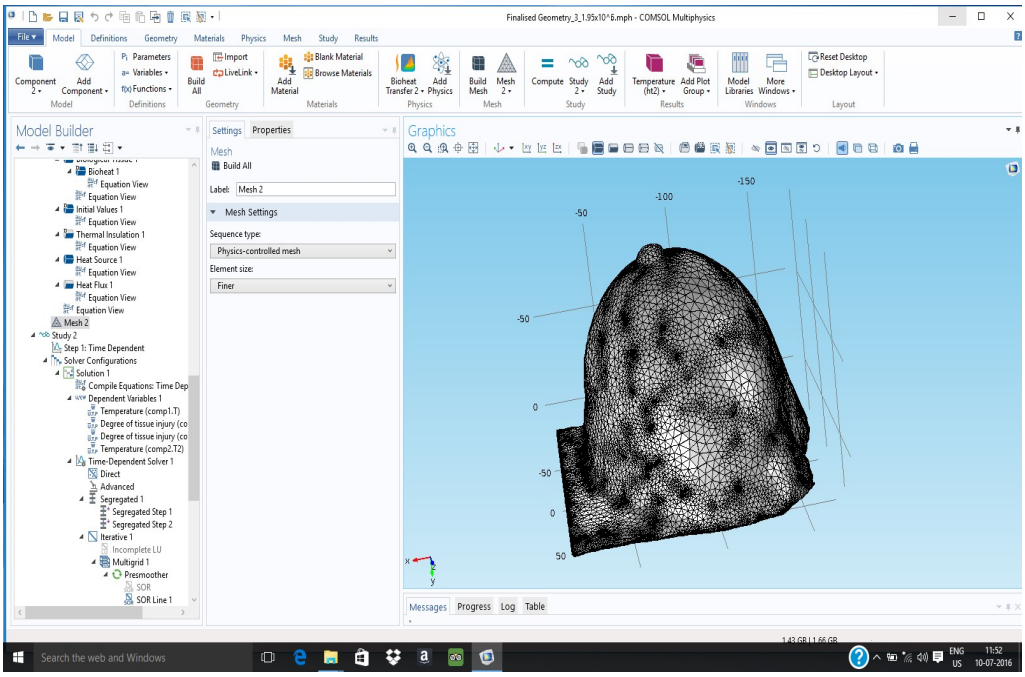
Finalised Geometry_3_1.95x10^6.mph - COMSOL Multiphysics
Model Builder
Settings
Properties
Mesh
Build All
Label: Mesh 2
Mesh Settings
Sequence type:
Physics-controlled mesh
Element size:
Finer
Graphics
Messages
Progress
Log
Table

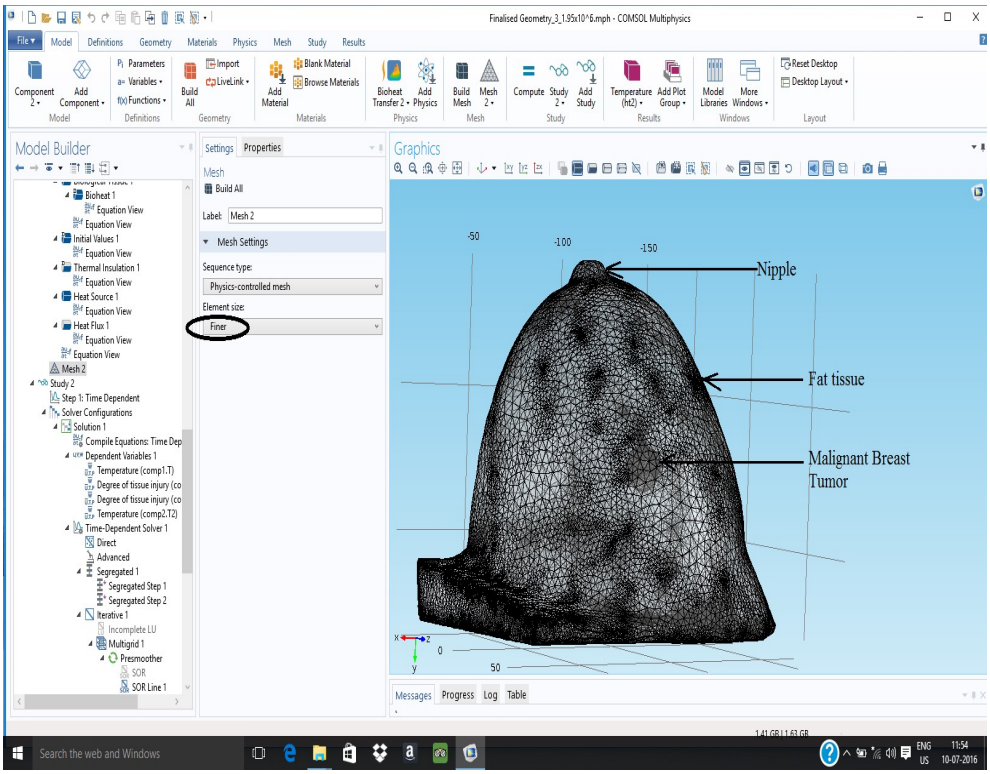

Figure 6.19 : Representation of finer mesh

Table 6.18: Materialproperties for Fat tissue

Heat capacity at constant pressure	2348 [J/kg.K]
Density	911[kg/m^3]
Thermal conductivity	0.21[W/m.K]
Frequency factor	4.436×10^{16}[1/s]
Activation energy	1.3×10^{5}[J/mol]

Table 6.19: Material properties for Cancerous tissue

Heat capacity at constant pressure	3700[J/kg.K]
Density	1050[kg/m^3]
Thermal conductivity	0.5 [W/m.K]
Frequency factor	9.4×10^{104}[1/s]
Activation energy	660000[J/mol]

6.7.3 BOUNDARY CONDITIONS

Initial B.C imposed on breast tissue is temperature of arterial blood(T_b).

Condition of convective heat flux is imposed, $q_o=h(T_{ext}-T_2)$

Where, $T_{ext}= T_{ambient}$

Initial and boundary temperature is 37°C.

6.7.4 GRID INDEPENDENCY TEST

Grid Independency test is performed with extremely coarse, extra coarser, coarser, coarse, normal, fine, finer. Extra fine and Extremely fine meshes are also processed but very long time is taken by the comsol to calculate the solution.(Times is approximate 24-26 hours). Results are come in agreement with 0.2% errors in results with fine to finer. So, results are considered reliable.

CHAPTER 7

RESULTS AND DISCUSSIONS

7.1 OVERVIEW

This chapter deals with the important results obtained as per model specifications and the validation of current work with the literature. The trends obtained with bio-heat transfer analysis, magnetic fields with current interface are obtained with comsol-multiphysics as computational tool to generate plots. First of all MATLAB code is verified with analytical results and literature work performed to calculate the values for tuneable parameter SAR. Then the analytical calculations are performed to calculate number of turns for given values of magnetic flux density. Simulation for magnetic field generationverifies the value of magnetic field for given number of turns. Then nanoparticles enriched tumor(animal model) is studied and higher range of values of SAR are used to obtain temperature plots. Then coupling between bio-heat transfer module and magnetic fields with current interface is performed to obtain the temperature variations for muscle tissue. The simulations are performed on breast tumor to account for maximum temperature ranges for different heat inputs. Then the results obtained are verified with literature.

7.2 MATLAB PROGRAM AND ANALYTICAL CALCULATIONS

7.2.1.PLOTTING FOR SPECIFIC ABSORPTION RATE(S.A.R or S.L.Pspm) vs DIAMETER OF MAGNETIC NANOPARTICLES

Magnetite nanoparticle is an extensively studied particle as reported in literature review and verified by clinical trials on animals and humans. The heat dissipation/absorption characteristics in the presence of alternating magnetic field is governed by relaxation mechanisms i.e. Brownian relaxation and Néel relaxation. The magnetic nanoparticles excites in the presence of magnetic field to release heat energy and is quantized in terms of important heat input parameter S.A.R. Specific Absorption Rate(SAR) or Specific Loss Power(SLP) is a tunable parameter that

accounts for the heat generation by magnetite nanoparticles. As per literature review, magnetite nanoparticles shows superparamagnetic behavior, when their size is less than 20nm. At these small values, these SPION's have single domain and they release energy untill the application of magnetic field and the heat generation due to hysteresis or multidomain behavior or brownian relaxation is absent.

In the present work, in order to select the effective size of nanoparticle that generates maximum heat in presence of magnetic field exposure, two types of variations are performed.

1. Variation of S.A.R with diameter of nanoparticle
2. Variation of S.A.R with frequency is performed.

A program or algorithm is written in MATLAB to select the operating range of S.A.R heat input parameter. Figure 8.1states that the effective diameter of magnetite nanoparticle is 19nm and at this value the nanoparticle is essentially of single domain and multi-domain walls are absent. Effective value of S.A.R value is 1.91×10^{5}W/m^3 which is the maximum peak value as read from figure 8.1. The parameters which are given as input are volume fraction; ϕ=2.3x10^{-5}W/m^3, anisotropy constant; $K = 23\text{x}10^{3}$J/m^3, viscosity of medium; $\eta = 1\times10^{-3}$Ns/m^2, domain magnetization;M_d= 446x10^{3}A/m, magnetic field strength;H_o=39x10^{3}A/m, operating frequency ;f=300kHz, Ligand layer thickness; δ =1×10^{-9}m, Attempt Period or average relaxation time; $\tau_O = 10^{-9}$sec.The magnetite particle is giving maximum S.A.R value for operating frequency of 300kHz.

To validate the effective diameter of magnetite particle, now for diameter of 19nm, the frequency lead variations are performed via written algorithm to analyze the maximum S.A.R value for different sets of frequencies. Fig.8.2 illustrates, the optimum frequency range is between 250kHz to 350kHz and the frequency is again in permissible limits. So, the two variations are satisfying the selection of magnetite as an appropriate bio-compatible material for hyperthermia studies. The increase or decrease of S.A.R value associates with concentration of nanoparticles that are desirable depending upon size of tumor to do effective damage to tumor tissue. The value of S.A.R calculated is close to 1.95×10^{5}W/m^3.

Editor - H:\documents_manpreet\Magnetic Fluid Hyperthermia\MATLAB_Programs_ManpreetSingh\Plot_graph_LP_vs_MNPdia.m

File Edit Text Go Cell Tools Debug Desktop Window Help

```
clc;
clear all;
%LPspm = 1.95*10^5;%W/m^3

Pie = 3.14;%Pie is a Constant
Mu_not = 4*Pie*10^-7;%Permeability of Free Space
H_not = 39*10^3;%AMF Field Strength
f = 300*10^3;%Frequency
d = 1*10^-9;%Ligand Layer Thickness

K = 23*10^3;%K=Anisotropy Constant for Magnetite
Phi = 2.3*10^-5;%Phi is the Volume Fraction
Md = 446*10^3;%Domain Magnetisation of suspended particle
Ms = Phi*Md;%Saturation_Magnetisation of Ferrofluid
kB = 1.38*10^-23;%Boltzmann Constant
T = 300; %Absolute Temperature
TOU_not = 10^-9;%Average Relaxation time
ITTA = 1*10^-3;%Viscosity of the medium

for i=1:60
D = i*10^-9;%Diameter of Magnetic Nano-particle
Vh = (Pie*(D+(2*d))^3)/6;%Hydraulic Volume of the Magnetic Nano-particle
Vm = (Pie*(D)^3)/6;%Volume of Magnetic Nano-Particles
TOU_n = ((0.886*TOU_not*exp((K*Vm)/(kB*T)))/((K*Vm)/(kB*T)));%TOU_n is the Neel Relaxation time
TOU_b = ((3*ITTA*Vh)/(kB*T));%TOU_b is the brownian Relaxation time
TOU_r = ((TOU_n*TOU_b)/(TOU_n+TOU_b));%TOU_r is the Effective Relaxation time
FACTOR = 2*Pie*f*TOU_r;
Jai_I = ((Mu_not*Phi*(Md^2)*Vm)/(3*kB*T));
zeta = ((Mu_not*Md*H_not*Vm)/(kB*T));
fraction = (1/zeta);

Jai_not = ((Jai_I*3*(coth(zeta)-fraction))/(zeta)) ;%Chord Susceptibility corresponding to Langevin function
```

Figure 1

File Edit View Insert Tools Desktop Window Help

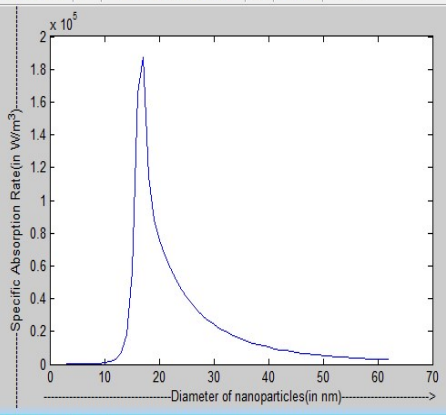

script Ln 12 Col 10 OVR

4:52 PM 7/12/2016

Editor - H:\documents_manpreet\Magnetic Fluid Hyperthermia\MATLAB_Programs_ManpreetSingh\Plot_graph_LP_vs_MNPdia.m

File Edit Text Go Cell Tools Debug Desktop Window Help

```
ITTA = 1*10^-3;%Viscosity of the medium

for i=1:60
D = i*10^-9;%Diameter of Magnetic Nano-particle
Vh = (Pie*(D+(2*d))^3)/6;%Hydraulic Volume of the Magnetic Nano-particle
Vm = (Pie*(D)^3)/6;%Volume of Magnetic Nano-Particles
TOU_n = ((0.886*TOU_not*exp((K*Vm)/(kB*T)))/((K*Vm)/(kB*T)));%TOU_n is the Neel Relaxation time
TOU_b = ((3*ITTA*Vh)/(kB*T));%TOU_b is the brownian Relaxation time
TOU_r = ((TOU_n*TOU_b)/(TOU_n+TOU_b));%TOU_r is the Effective Relaxation time
FACTOR = 2*Pie*f*TOU_r;
Jai_I = ((Mu_not*Phi*(Md^2)*Vm)/(3*kB*T));
zeta = ((Mu_not*Md*H_not*Vm)/(kB*T));
fraction = (1/zeta);

Jai_not = ((Jai_I*3*(coth(zeta)-fraction))/(zeta)) ;%Chord Susceptibility corresponding to Langevin function

LPspm = ((Mu_not*Pie*Jai_not*f*(H_not^2)*FACTOR)/(1+(FACTOR^2)));
Z(i)=LPspm;
end;
Z=Z';
 for j=1:60
      k=j+2;
      x(j)=k;
  end
x=x';
plot (x,Z);
```

script Ln 12 Col 10 OVR

4:56 PM 7/12/2016

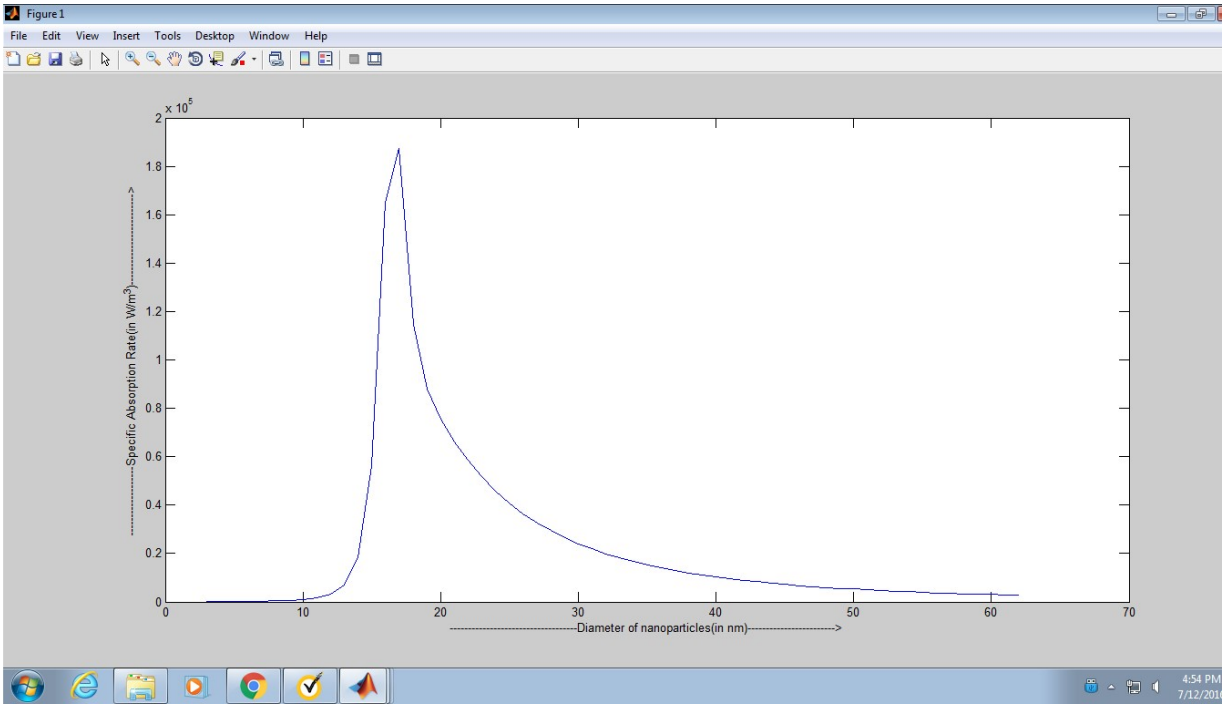

Figure 7.1: Variation of Specific Absorption Rate(W/m^3) with diameter of nanoparticles(nm) for magnetite nanoparticle.

7.2.2.PLOTTING FOR SPECIFIC ABSORPTION RATE (S.A.R or S.L.Pspm) vs FREQUENCY

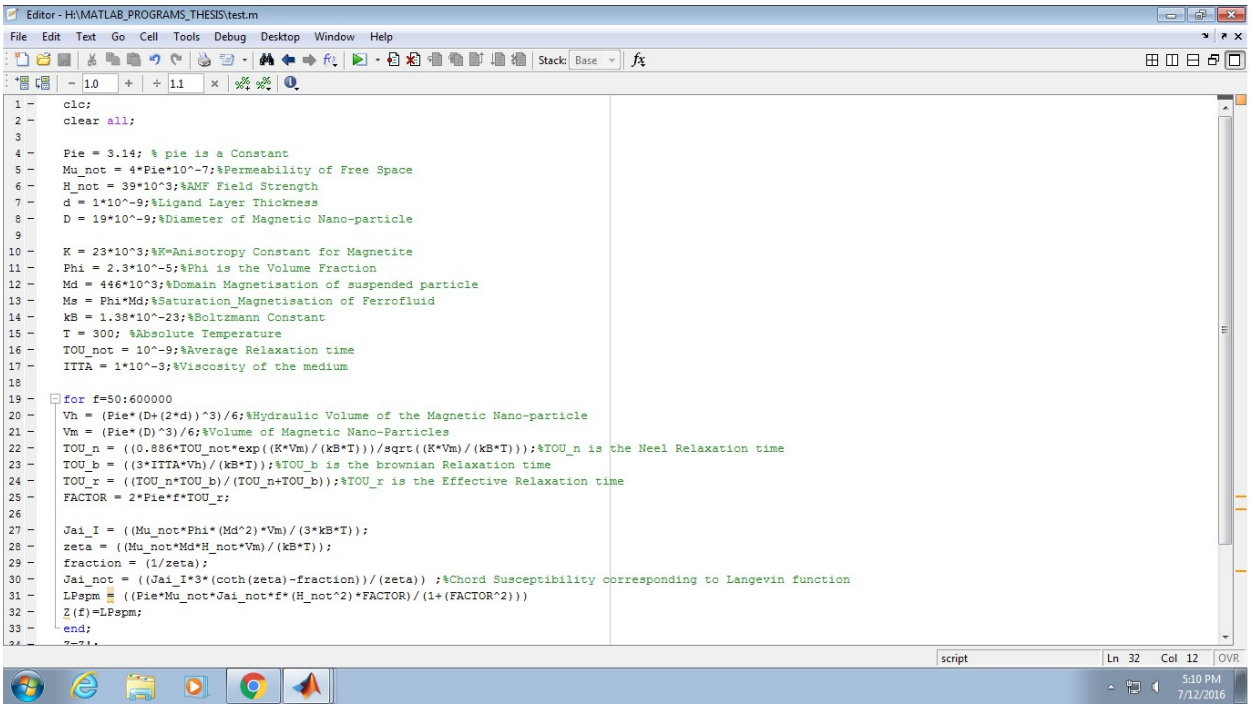

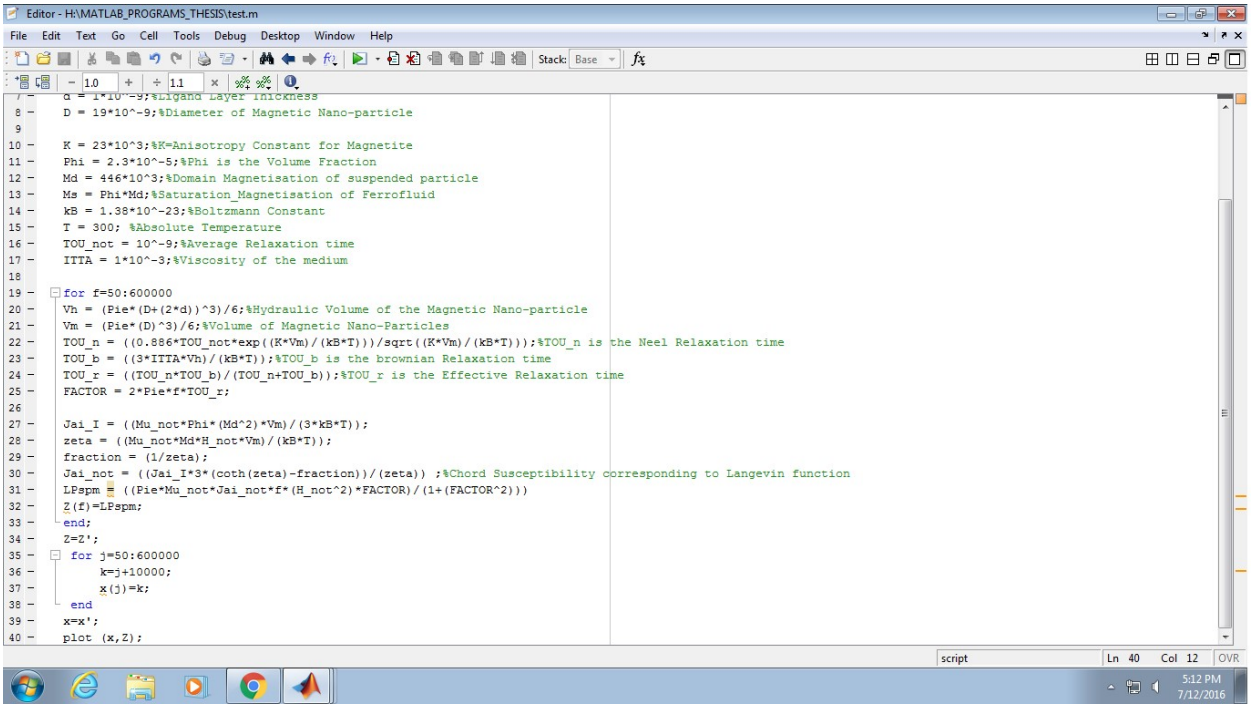

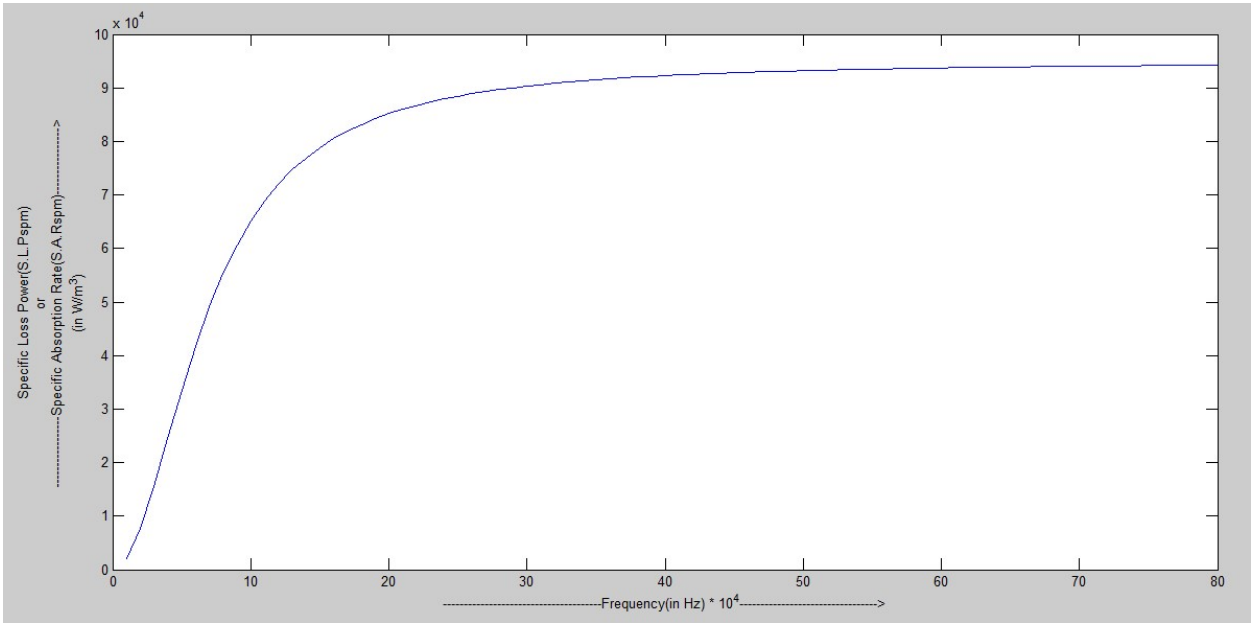

Figure 7.2: Variation of Specific Absorption Rate(W/m^3) with frequency(Hz) for magnetite nanoparticle.

7.2.3 ANALYTICAL CALCULATIONS FOR S.A.R

The S.A.R value is an important heat input parameter to Penne's bioheat equation(P.B.H.E). This is a tunable parameter. The prior analytical calculations for given inputs considered by various researchers via their numerical studies, theoretical calculations or experimental values are

considered in this study verifies with MATLAB written algorithm. The results validation is performed with literature.

Table 7.1: Illustration of numerical values obtained by theoretical calculations to calculate S.A.R

PARAMETERS/INPUT VALUES	PARTICULARS
Formula used	$L.P = \pi\mu_o \chi_o H_o^2 f \frac{2\pi f\tau_R}{1+(2\pi f\tau_R)^2}$
Volume fraction, ϕ	2.3×10^{-5}
Attempt period or average relaxation time, τ_o	10^{-9}sec
Induction of magnetic field, B_o	50mT
Frequency, f	300kHz
Ligand layer thickness, δ	1nm
Anisotropy constant, K	23,32,42kJ/m^3
Amplitude of magnetic field, H_o	39kA/m
Effective relaxation time, τ_R	0.000000637
Néel relaxation time, τ_N	0.000000779
Brownian relaxation time, τ_B	0.000003513
Factor used in Néel relaxation time, $\Gamma = \frac{KV_m}{k_B T}$	7.807313048
Factor used in Néel relaxation time, $\frac{\exp\Gamma}{\sqrt{\Gamma}}$	879.8774318
Factor used in L.P, $2\pi f\tau_R$	1.202143431
Factor used in L.P, $\frac{2\pi f\tau_R}{1+(2\pi f\tau_R)^2}$	0.491644278
Initial susceptibility, χ_i	0.001445597
Langevin equation factor, ξ	18.96131328
Chord susceptibility, χ_o	0.000216655
Factor in L.P, $\pi\mu_o H_o^2 f$	1801400195
Factor in L.P, $(\pi\mu_o H_o^2 f)\times\chi_o$	390283.2914
Calculated L.P	1.91880547×10^5

The value of S.A.R by numerical calculations is 1.91880547×10^5W/m^3≈1.92×10^5W/m^3. The S.A.R value comes in close similarity to the results of Chin-Tse Lin et al.,2009[19] and Maenosono and Saita,2006[17] value of $1.95\text{x}10^5$W/m^3, and also the Lahonian et al.,2011[120].The results are illustrated in Table 7.1 and in Fig.7.1.The matlab program is

developed also validates the results with literature and the similar peaks are obtained for 19nm range nanoparticles.

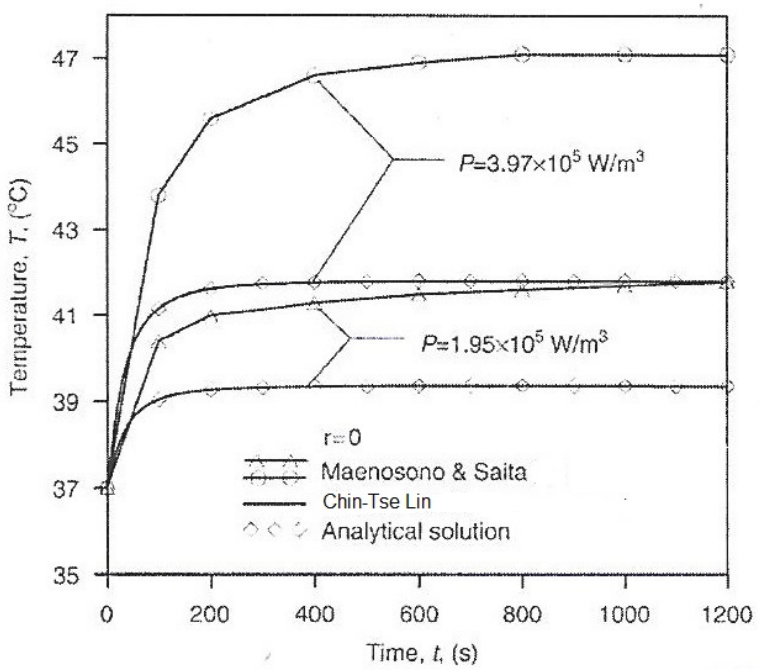

Figure 7.3: Results Plots of Chin-Tse Lin et al.,2009[19] for S.A.R.

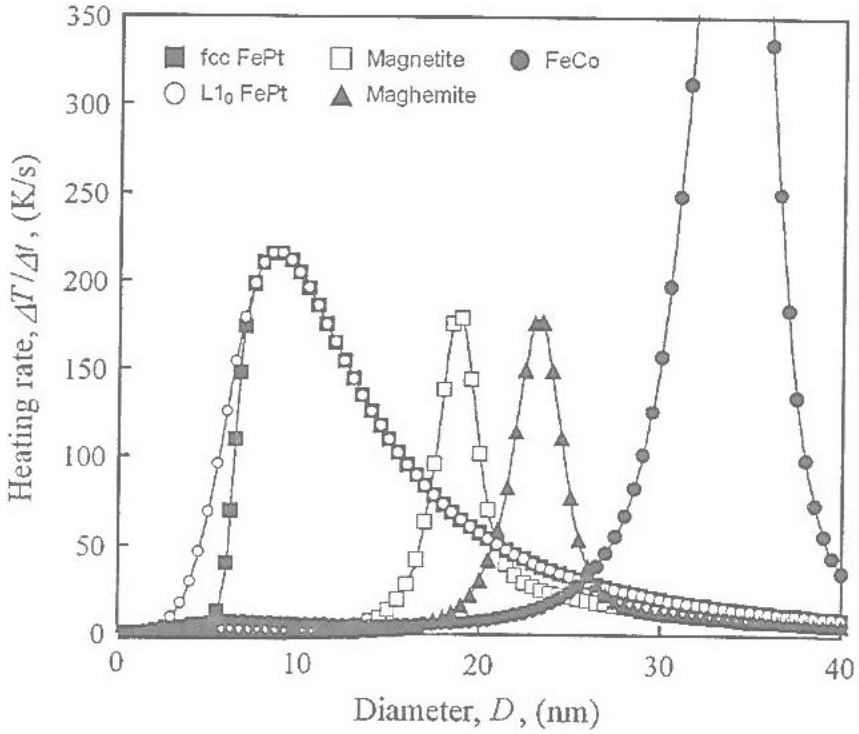

Figure 7.4: Results Plots of Maenosono & Saita,2006[19] for different magnetic nanoparticles.Peaks are obtained for magnetite particles at 19nm size.

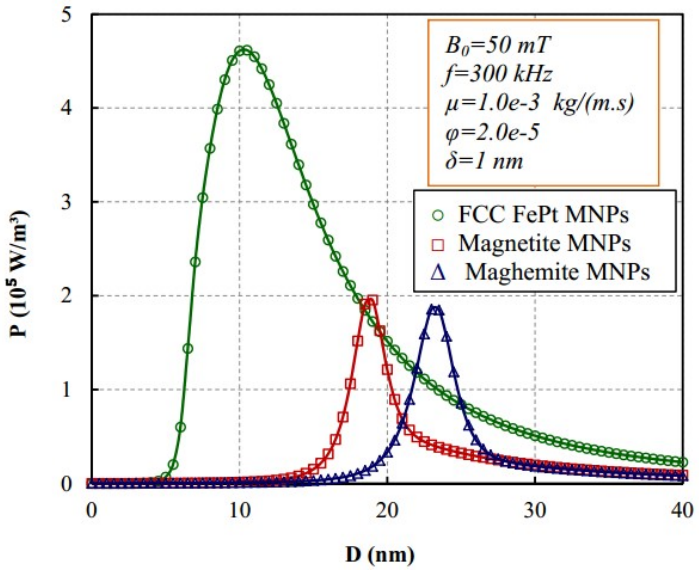

Figure 7.5: Result plot of Lahonian et al.,2011[120] for power dissipation of magnetic nanoparticles as a function of diameter of nanoparticle. Peak obtained for magnetite particles is at 19nm size representing value of $1.95\times10^5 W/m^3$.

Figure 7.3; 7.4; 7.5 validates the curve of figure 7.1 and also the numerical values are well in acceptance with the above results. Thus, it can be concluded that Specific absorption rate is a tunable parameter and the further increase in heat inputs depends upon the tumor tissue size and number of particles that can accumulate in tumor solely depends upon the heat increase.

7.3 BIOHEAT TRANSFER ANALYSIS ON ANIMAL MODEL(RAT) WITH MULTIPLE INJECTIONS OF MAGNETIC NANOPARTICLE ENRICHED REGIONS

The computational model is developed in COMSOL-MULTIPHYSICS 5.O. The model is simple as considered by researchers in most of the computational studies. The model consists of three domains, cylindrical healthy tissue, Ellipsoid tumor tissue, and multiple injection sites of nanoparticles of micrometer range. Figure 8.4 illustrates, the maximum temperature achieved by particles in the center of tumor as 84.3°C achieved in 30s. At these higher range of temperatures, coagulation necrosis is caused to occur. Figure 7.6 illustrates the multiple injection of magnetite nanoparticles, monodispersed and uniformly distributed over the central core region of ellipsoid (tumor domain).

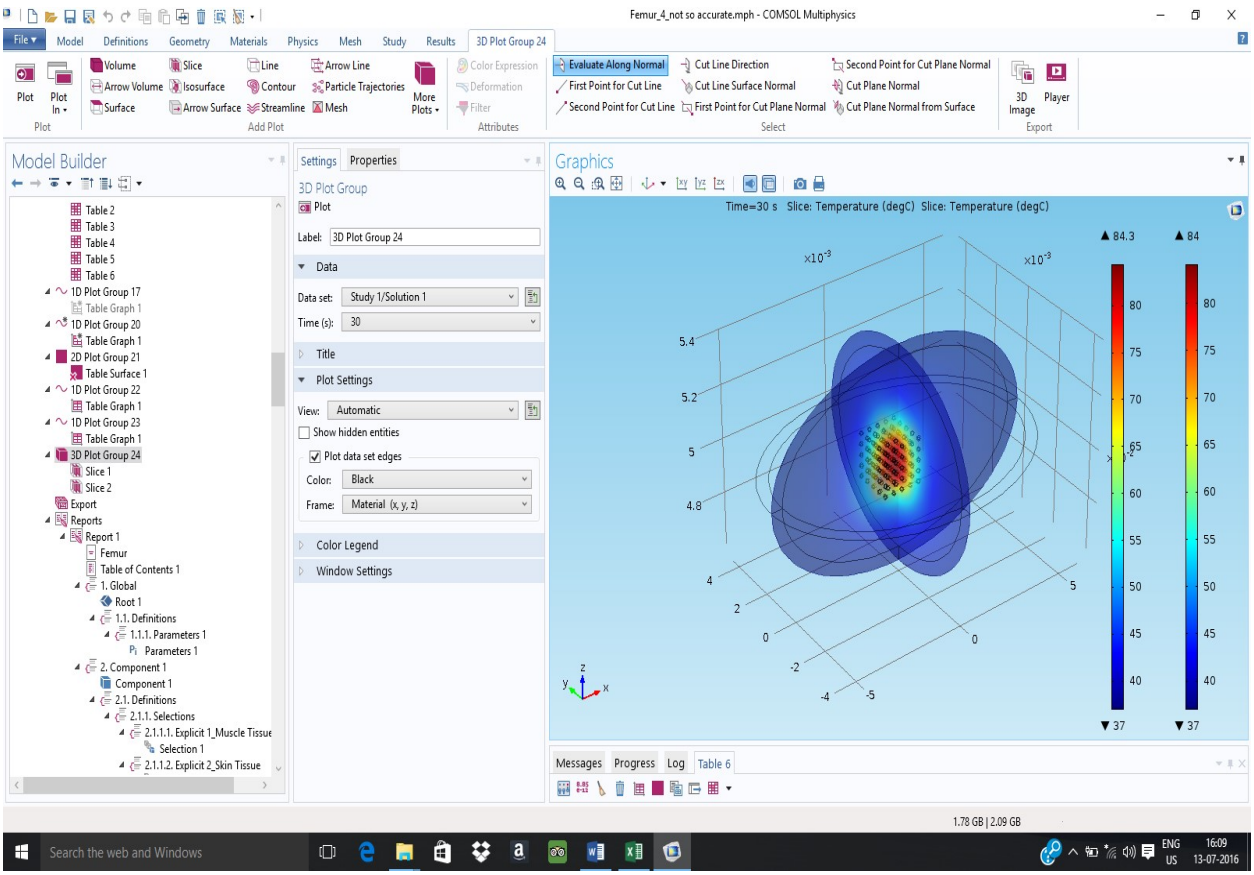

Figure 7.6: Representation of temperature distribution in central core region of elliptical tumor of rat(animal model) with higher range of S.A.R($1.95x10^5 W/m^3$)

Two slice plot is generated in Figure 7.6; which illustrates the maximum temperature range obtained in tumor is 84.3°C in 30seconds. The reasons for the sudden high temperatures are due to high input(SAR) value to tumor. The model geometry is similar to the work of Ghosh et al.,2013[7]. The equation defined to account for SAR values is found lack of appropriate units of SAR in W/m^3 or W/g. The sole purpose to perform this calculation is to quantify the value of heat input parameter.

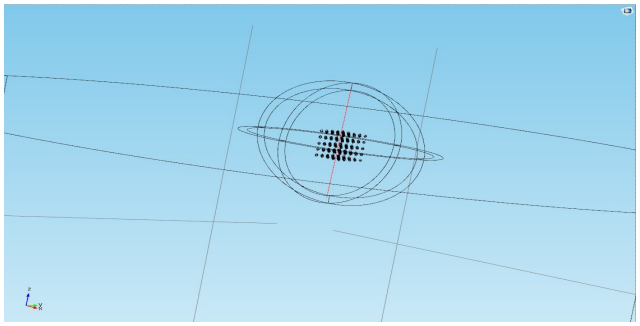

Figure 7.7: Centre line (vertical direction) passing through the tumor; particles(multi-site injection) are uniformly distributed in the central core region of tumor

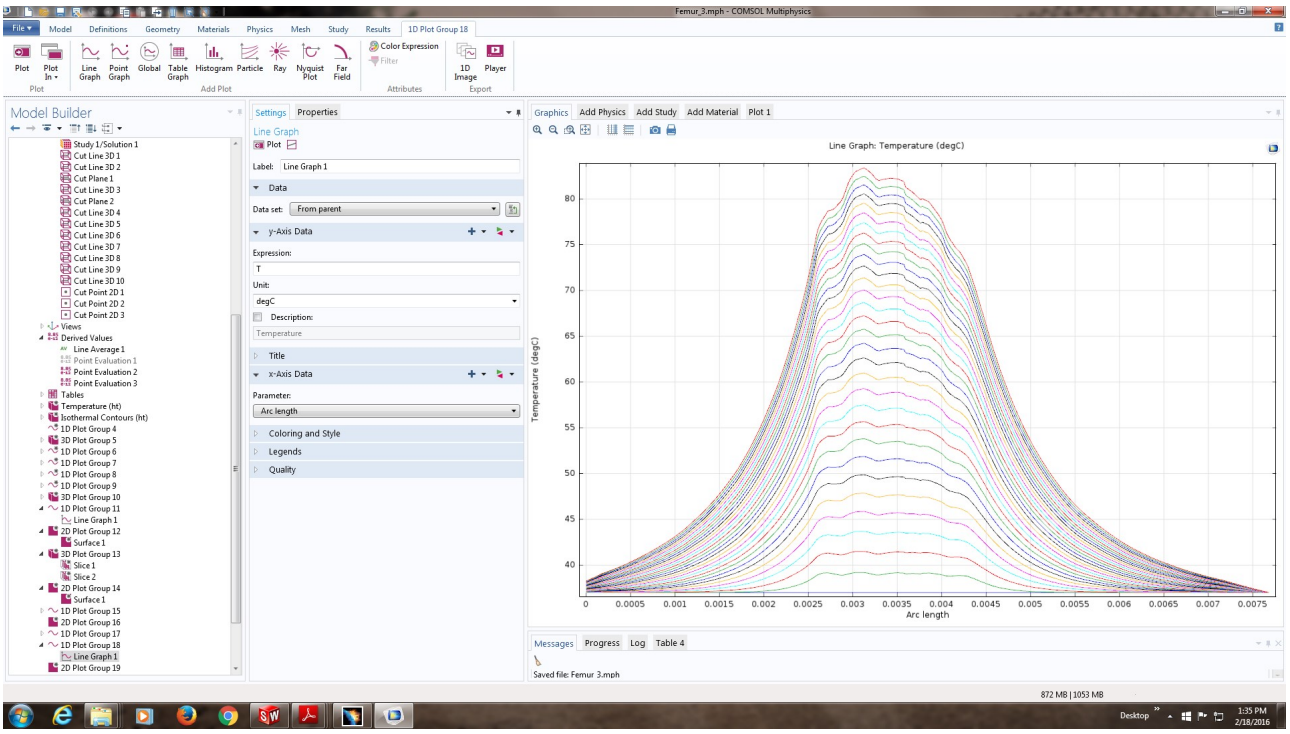

Figure 7.8: Representation of temperature rise along the center line passing through tumor only.

Figure 7.7;7.8 illustrates the plot of center line passing through center of tumor in vertical direction. The plots are uniform and forms a distorted bell shaped pattern.

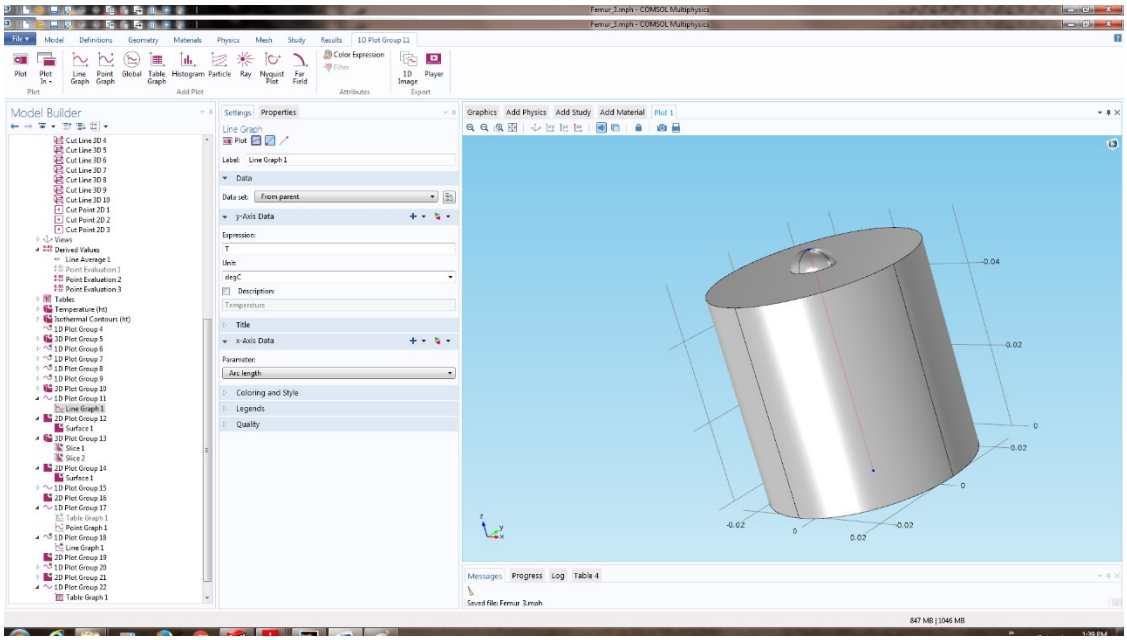

Figure 7.9: Spatial temporal rise along the center line passing through whole body by 1D plot group representation.

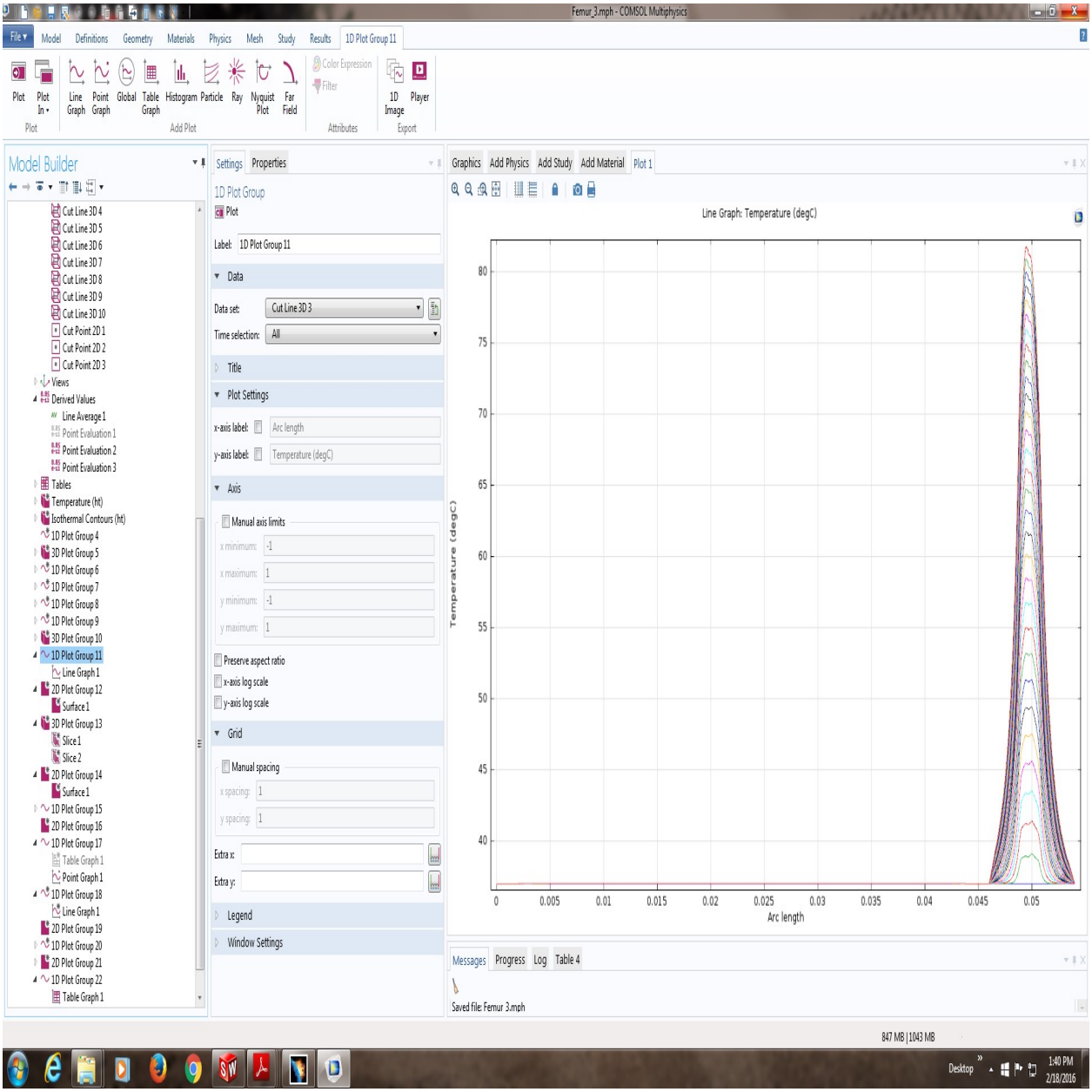

Figure 7.10: Temperature rise along the centre line (vertical direction) passing through the whole body

Figure 7.9;7.10 shows the maximum temperatures along the nanoparticles enriched injection sites for vertical line passing from healthy tissue to tumor.Bell shaped curved is obtained along the spatial co-ordinates and the peak is constrained to tumor part only. Spatial-temporal temperature achievement in muscle tissue is obtained.

Figure 7.11 represents the two slice plot for maximum temperature achieved in tumor.

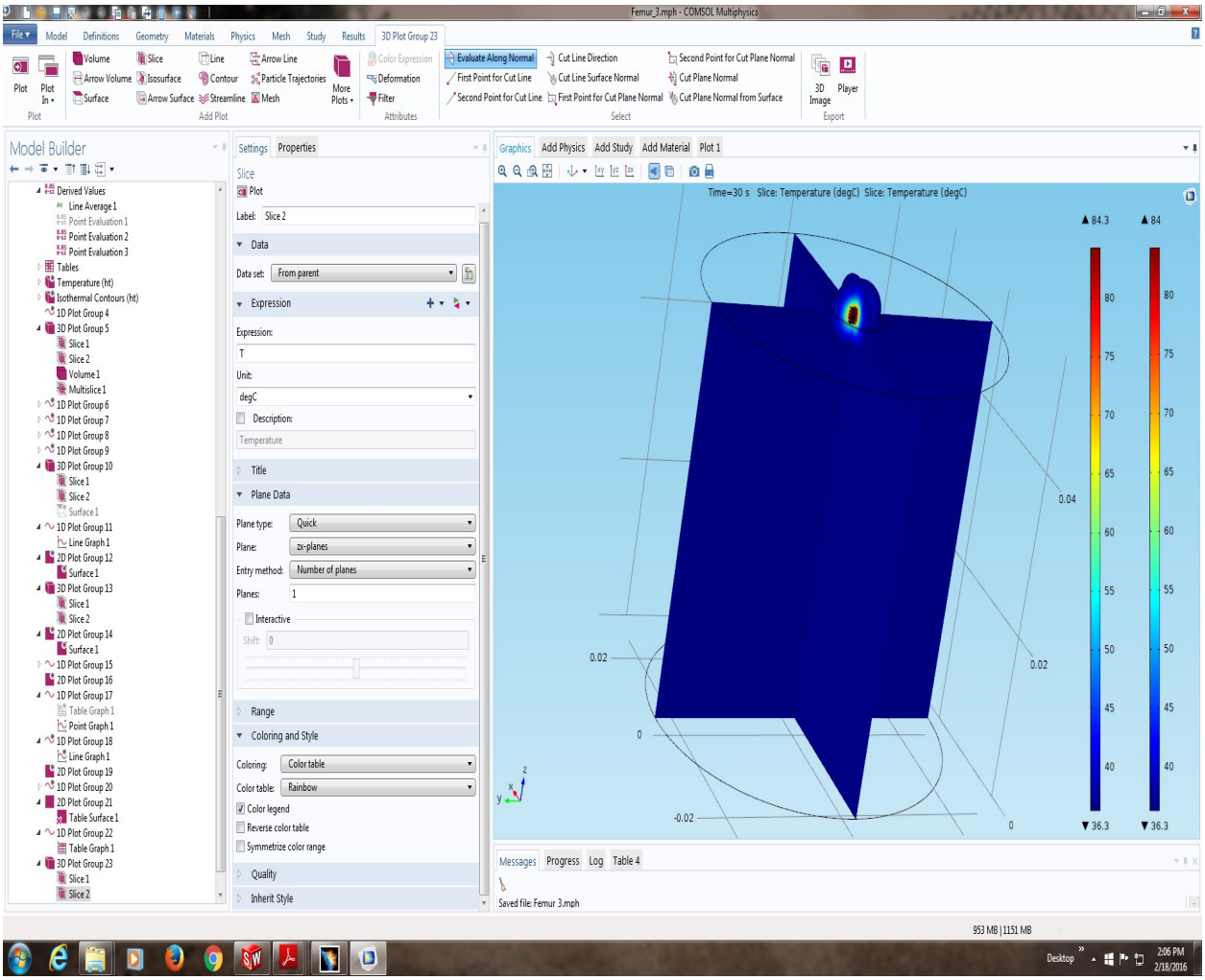

Figure 7.11:Representation of temperature by two slice plot of whole body of an animal (rat) model.

In Figure 7.12; 7.13, the point is marked at center of tumor and transient temperature profile is obtained which shows linear rise in temperature with time.

In figure 7.14; the volumetric temperatures are obtained for particles enriched spherical injection sites placed in tumor.

Figure 7.15 illustrates for 18 seconds, the maximum temperature achieved is at specific absorption rate of $1.95 \times 10^{9} W/m^{3}$. The spherical particles enriched region is placed uniformly in ellipsoid(tumor), in cylindrical healthy tissues.

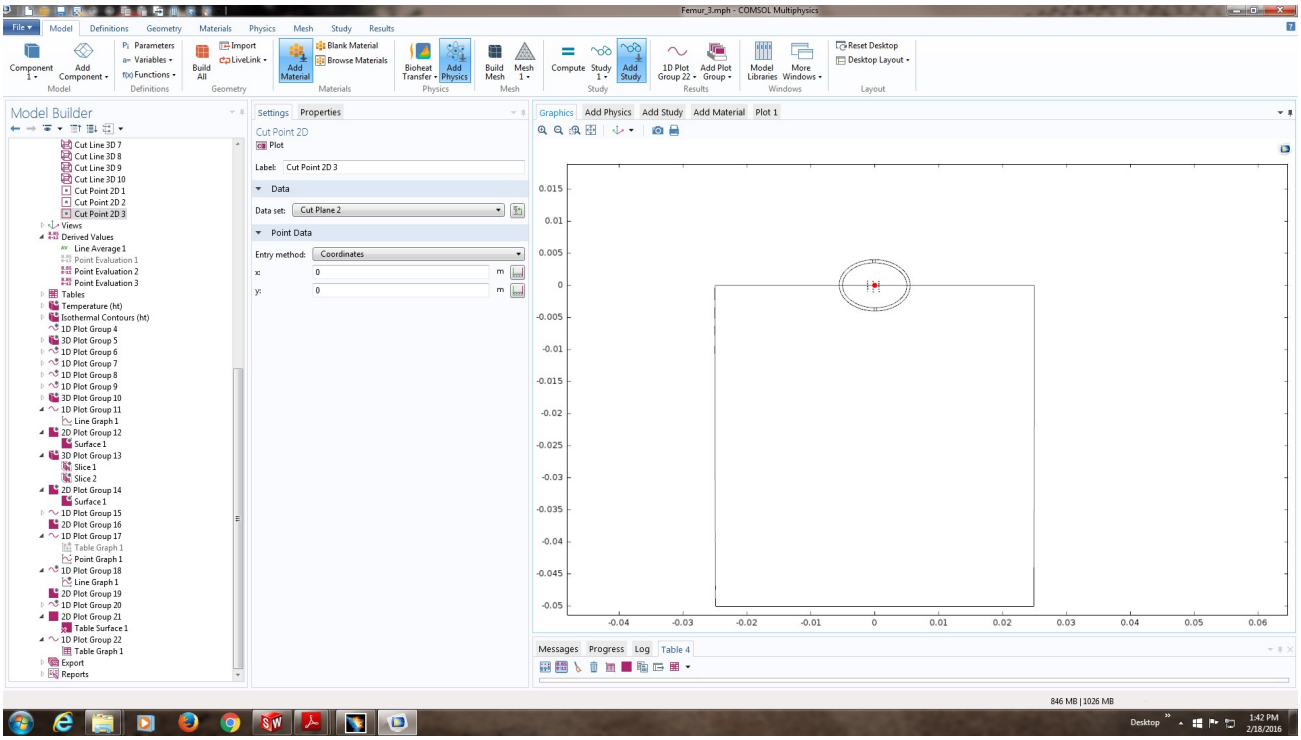

Figure 7.12:Demarcation point in center of tumor in two dimensional co-ordinates.

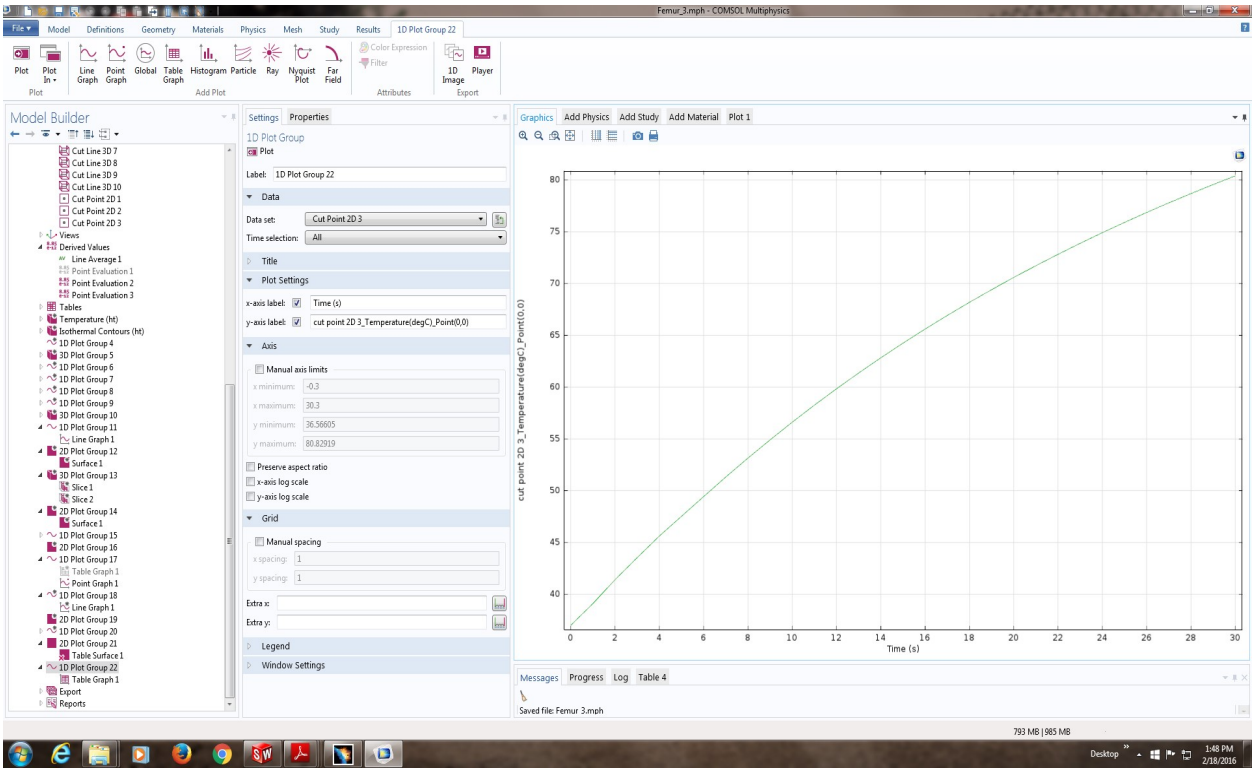

Figure 7.13: Temperature vs time curve representing the linear rise in temperature at space co-ordinates of tumor(0,0).

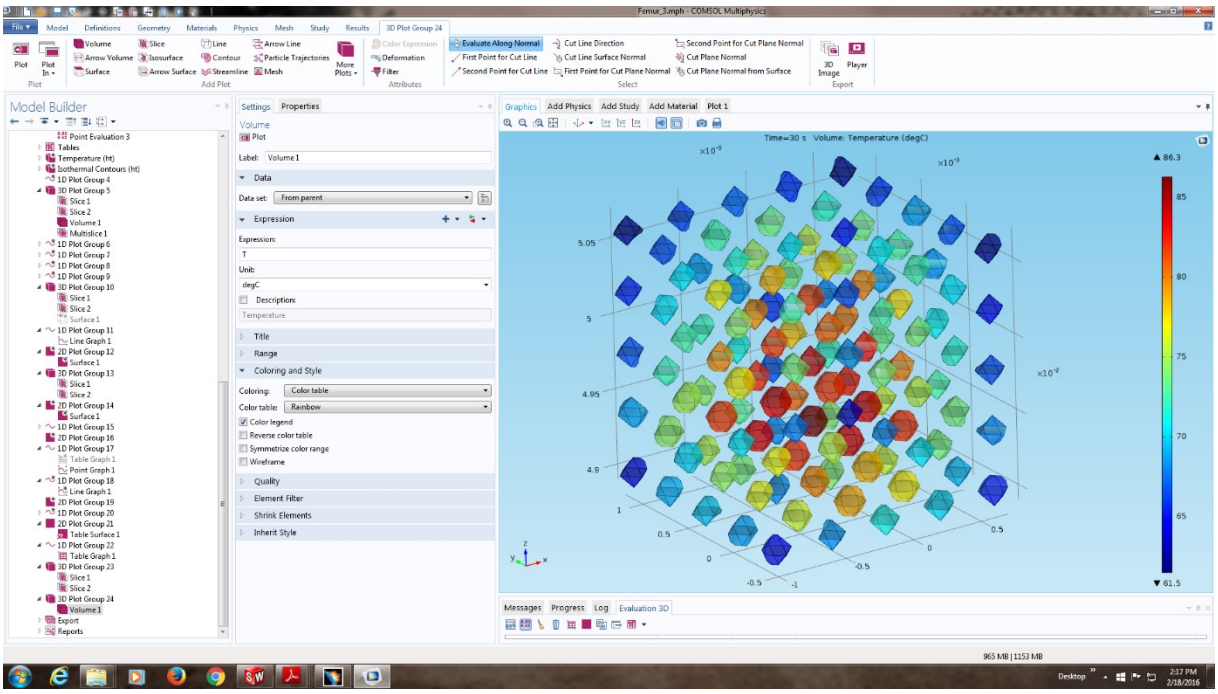

Figure 7.14 :Volumetric temperature representation of particle injection sites placed at core of tumor.

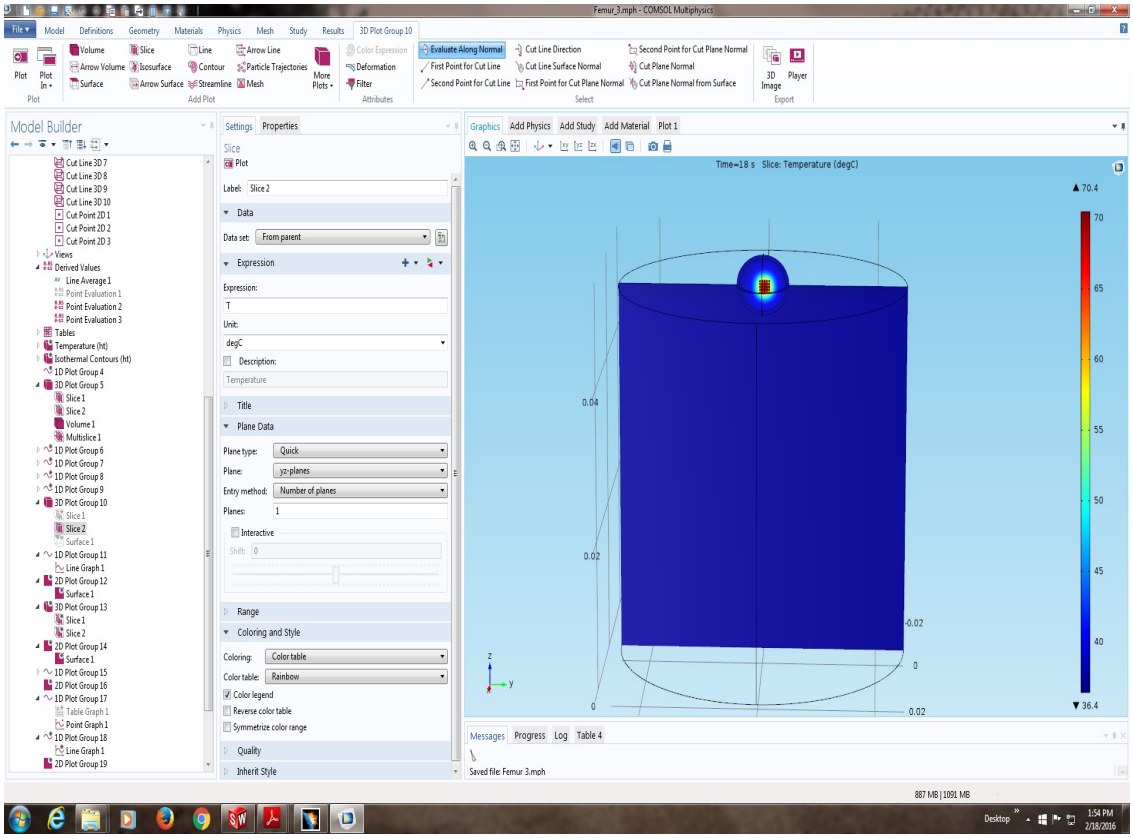

Figure 7.15:Representation of temperature at 18seconds in center of tumor at $1.95x10^{9}W/m^{3}$.

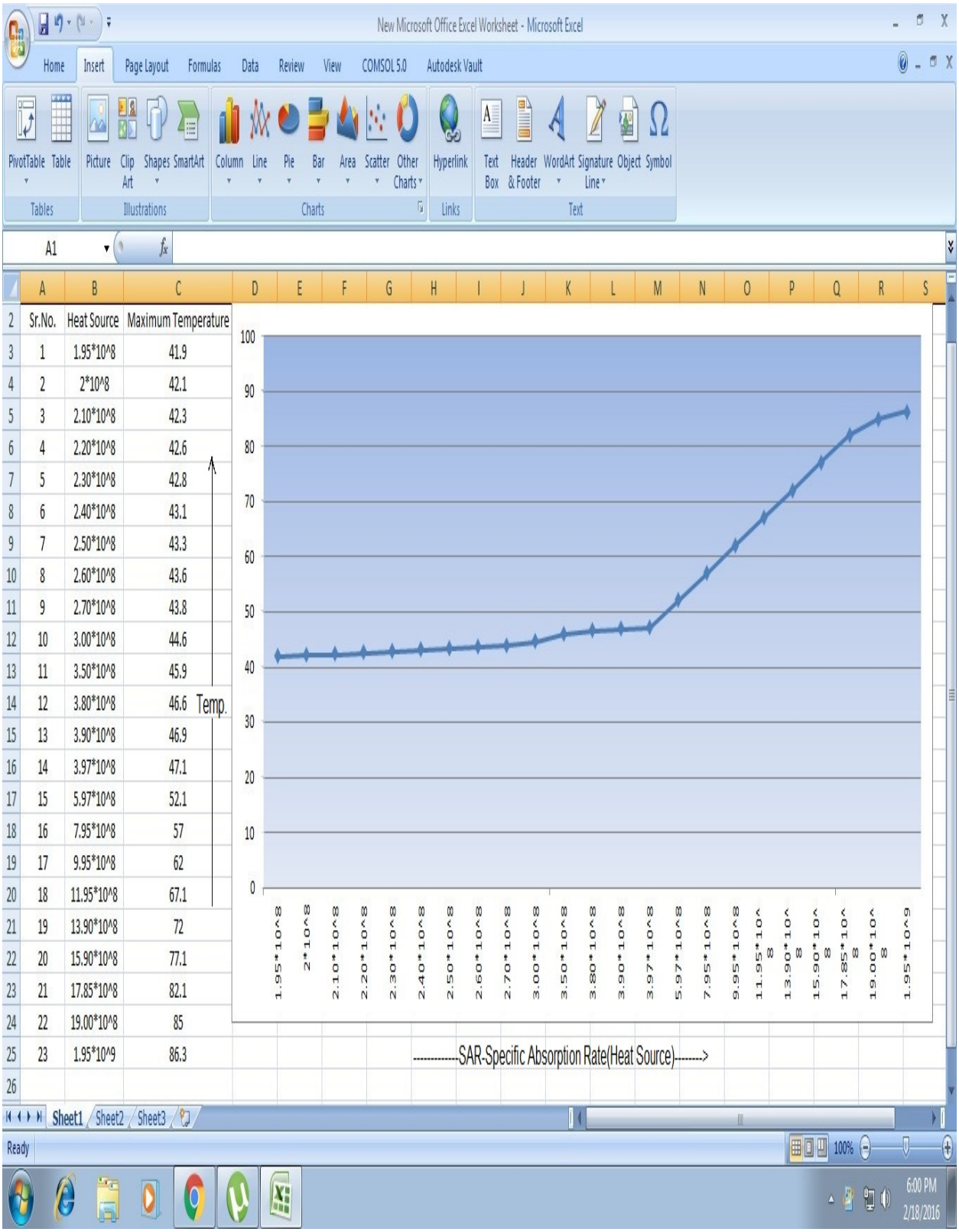

Figure 7.16:Representation of maximum volumetric temperature rise vs specific absorption rate(heat source of particles).

Figure 7.16: Representation of temperatures vs different heat inputs(SAR). The curve represents the very less increase till $3.50x10^8 W/m^3$, then shows a small linear increase till $3.97x10^8 W/m^3$; then a sudden increase is observed by increasing loss power till $19x10^8 W/m^3$.

In Figure 7.17;At $1.95x10^9 W/m^3$, the steady state is achieved and the maximum temperature of 86.3°C is achieved inside the domain.

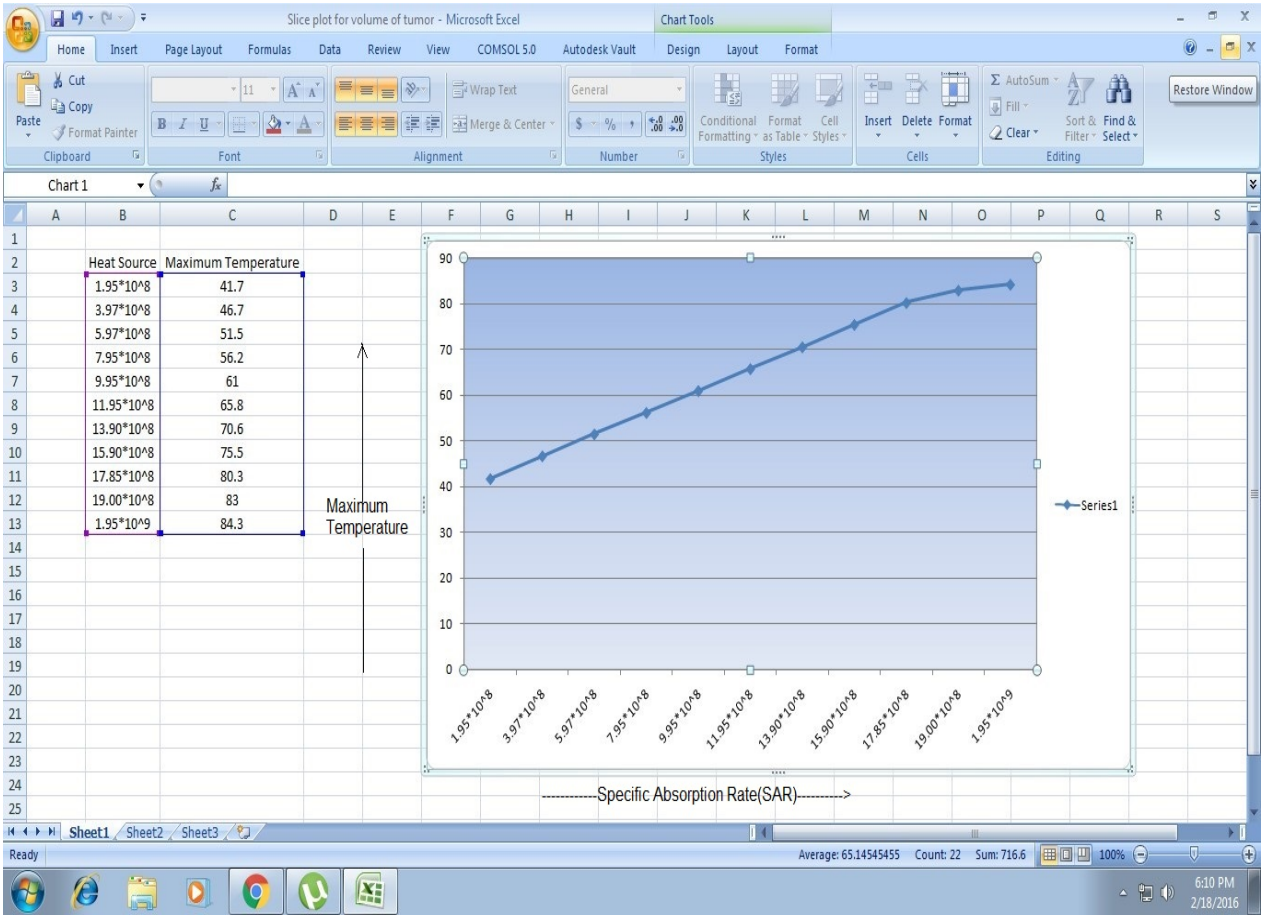

Figure7.17: Two slice plot of maximum temperature(°C) vs heat source(Specific absorption rate(W/m^3) for whole tumor part.

7.4 MAGNETIC FIELD CALCULATIONS

7.4.1 ANALYTICAL CALCULATIONS FOR MAGNETIC FIELD SOURCE

When the magnetic nanoparticles are place in the presence of magnetic field, due to relaxation mechansisms heat is induced inside the particles to produce therapeutic temperatures inside the tumors. Most of the experiments were performed in phantoms, agarose gels mostly studied, Animal models, and clinical trials on humans. In this work the analytical calculations are done to

calculate number of turns of copper wire around a circular insulated tube. The tissue under analysis to be put inside the domain to induce magnetic field induced heating. For solenoid the magnetic field is uniform. The current along with magnetic field strength are theinput parameters in which variation is performed. The results of analytical calculations are verified with simulations performed with Comsol-multiphysics. The physics used for the analysis is uncoupled AC-DC module(Magnetic fields with current).

The number of turns calculated for given geometrical considerations, the magnetic field is calculated via simulations is in very close relation. In context of hyperthermia, the model is extended by putting nanoparticles loaded tumor in healthy tissue and heating is induced by electromagnetic heating induced by current inputs to the coil. These are very important simulations since coupling between two different studies is not studied till date and in this study a novel idea is proposed.

The numerical formula used to calculate number of turns is stated as follows:

$$B = \frac{\mu_O NI}{\sqrt{4r_1^2 + L^2}} \tag{7.1}$$

Where,

N = Number of turns of wire ;

μ_O = Permeability of free space = $4\pi \times 10^{-7} \frac{N}{A^2}$;

B = Magnetic field ;

I = Current flowing in copper wire;

r_1 = Radius of hollow rod around which wires need to be wound and the hollow space where the tissue or sample containing gel need to be put in circular tube;

Magnetite and Maghemite are the most studied nanoparticles because of their bio-compatible nature. The other important parameters are quantized in magnetic parameters sheet reported in literature review for hyperthermia study.

The numerical values calculated are summarized in table 7.2.

Table 7.2: Analytical calculations performed to calculate number of turns for a coil(solenoid) to produce uniform magnetic field inside.

Magnetic Field Strength(B)	Current (I)	Number of turns of coil		Number of turns per cm of length		Diameter of Cylinder
		Length of coil		Length of coil per cm		
		5cm	10cm	5cm	10cm	
200mT(0.2T)	5A	2251	3559	450.2	355.9	50mm
200mT(0.2T)	10A	1126	1780	225.2	178	50mm
50mT(0.05T)	5A	464	830	92.8	83	30mm
50mT(0.05T)	10A	232	415	46.4	41.5	30mm
250mT(0.25T)	5A	2320	4154	464	415	30mm
250mT(0.25T)	10A	1160	2077	232	207	30mm

7.4.2 SIMULATION OF MAGNETIC FIELD GENERATION

Theoretical calculations of magnetic fields, must be matched with the similar conditions given in comsol. The number of turns given as input to comsol is 1126 turns with 10A current is flowing through coil along the direction been specified during simulations. The calculated magnetic field strength comes out to be 0.19T. The computed magnetic flux density is validated with analytical calculations of 0.20T. Magnetic flux densities are plotted along three directions in 1D plot group specified for points along the vertical axis, horizontal axis, and diagonal line passing through co-ordinate points specified for muscle tissue. The model is tumor inside muscle tissue placed in cylindrical coil (wound in circular fashion) and air region is specified as cube inside which the entire geometry is placed. Accordingly the number of turns can be adjusted to produce magnetic fields of higher intensities. The diameter of cylinder is also kept the same as 50mm as in theoretical calculations. The computational simulation and theoretical results are matched, hence, it can be stated that model is accurate to proceed with further refinement.

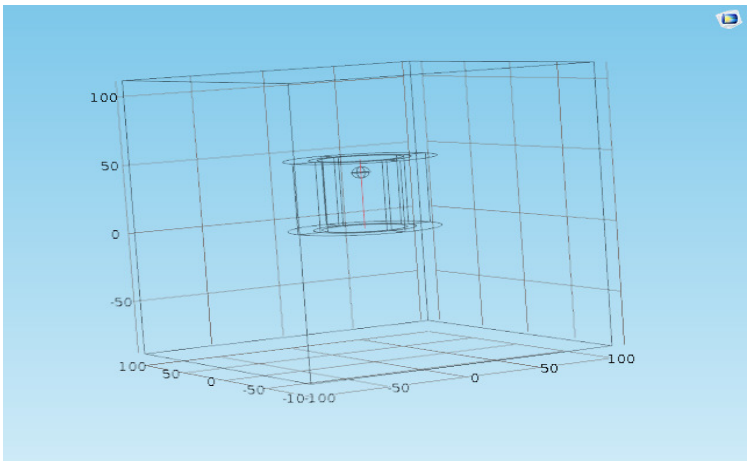

Figure 7.18: Representation of line(red in colour) passing through the centre of entire geometry

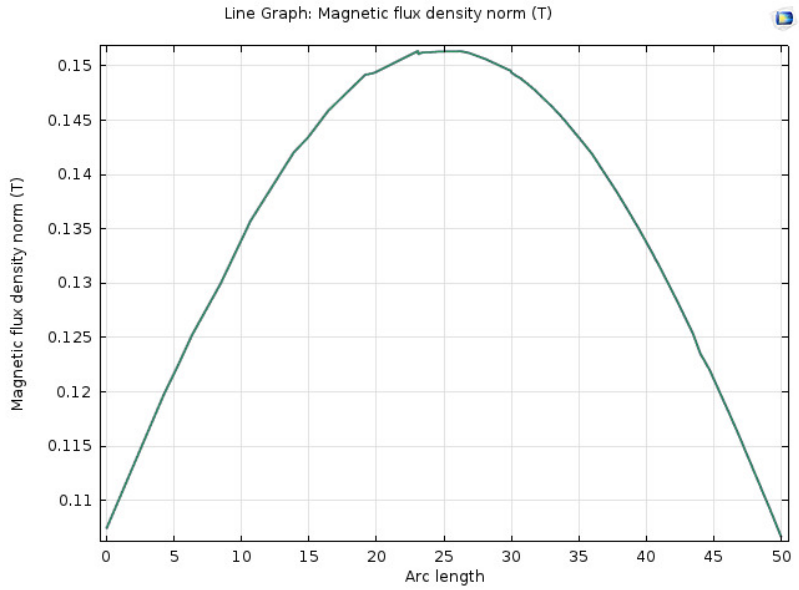

Figure 7.19: Representation of magnetic flux density for muscle tissue

Figure 7.18 represents the magnetic flux density maximum along the line of generation(line red in colour through vertical axis,Figure 7.19). The magnetic flux density achieved is around 0.19T(Figure 7.20;.7.22; 7.23)

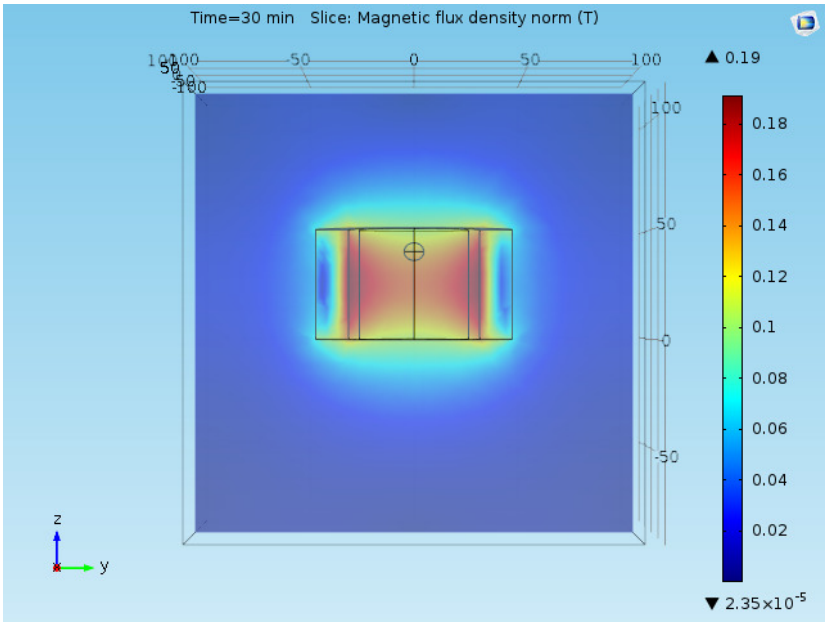

Figure 7.20: Representation of Magnetic flux density in y-z plane for muscle tissue(cylindrical in shape) and tumor (ellipsoid)with one slice plot

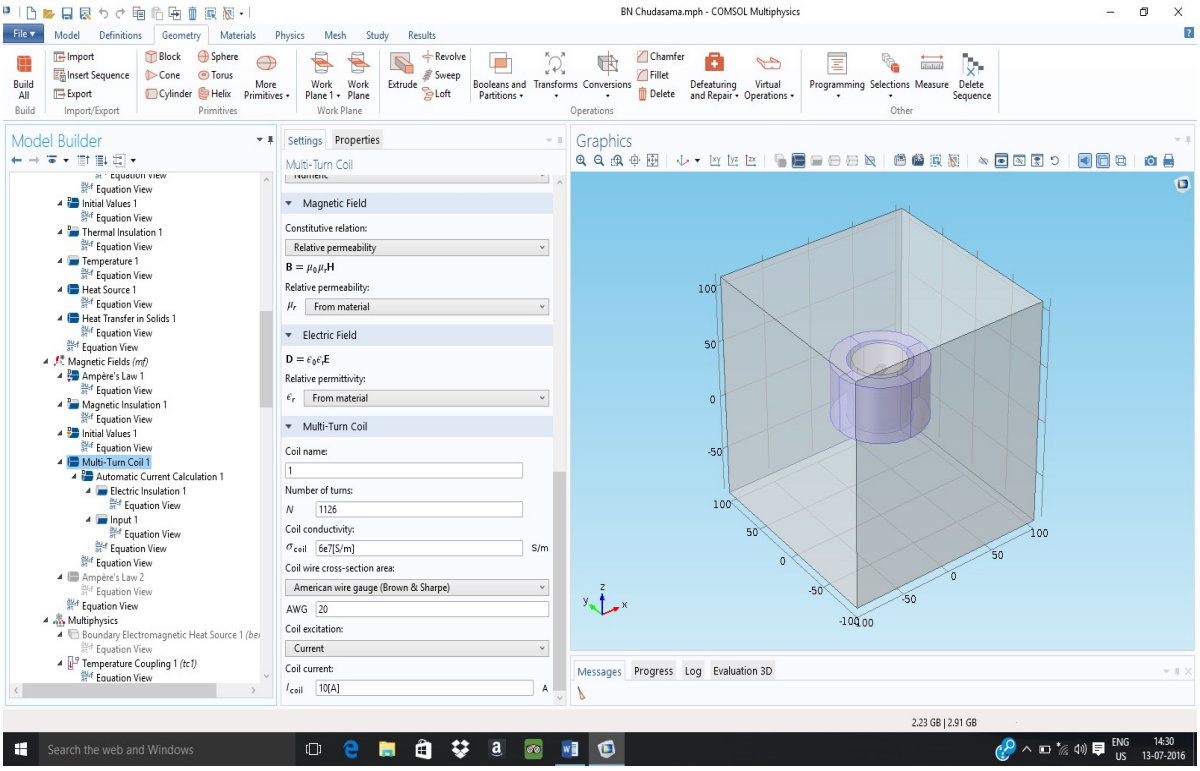

Figure 7.21: Representation of input of number of turns as 1126 to coil wound around the cylindrical space in circular fashion and current input as 10A.

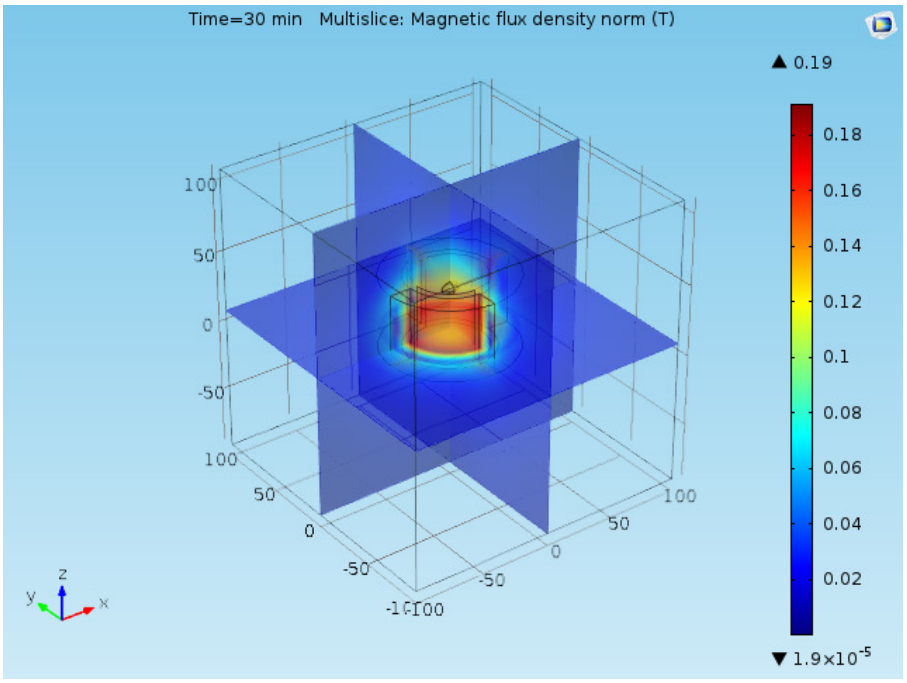

Figure7.22: Two slice plot for muscle(healthy tissue) and cancerous tissue in magnetic field

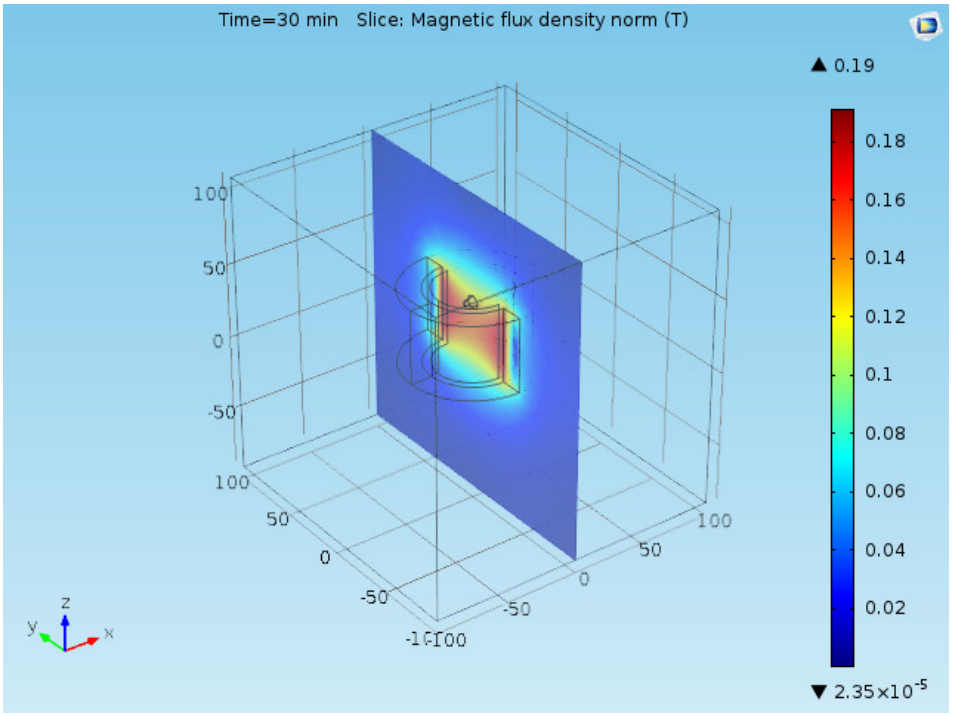

Figure 7.23: One slice plot for muscle tissue and cancerous tissue in magnetic field.

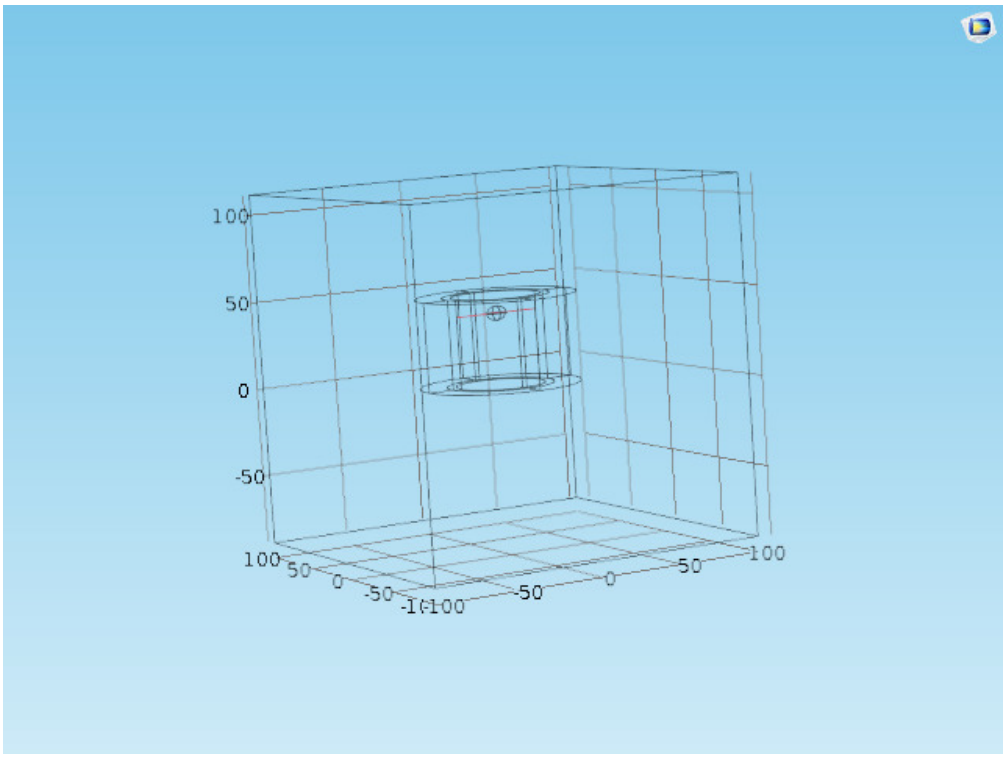

Figure 7.24: Representation of line(red in colour) passing through centre of tumor in horizontal direction

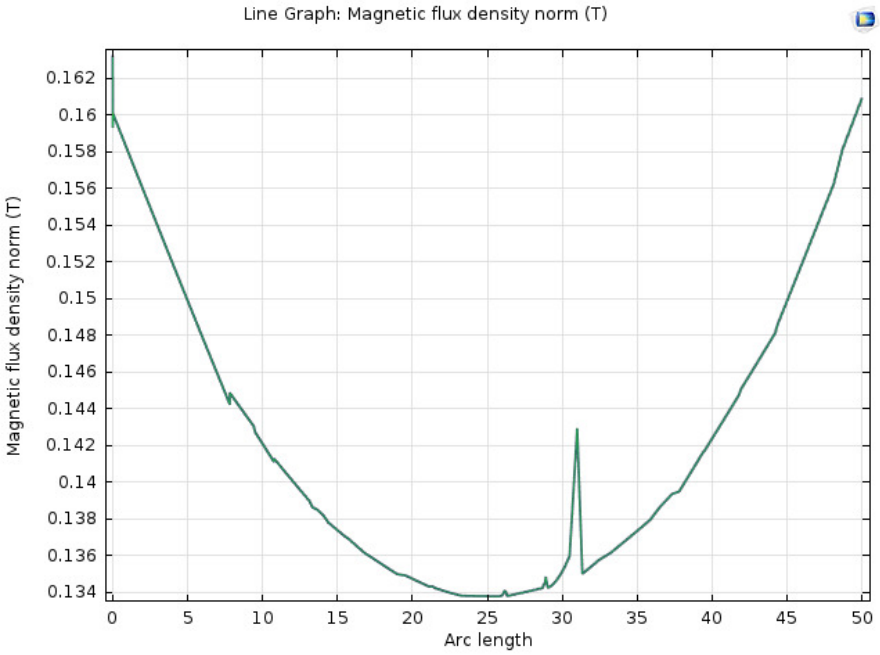

Figure 7.25: Representation of magnetic flux density in horizontal axis passing through center of tumor(diametrically).

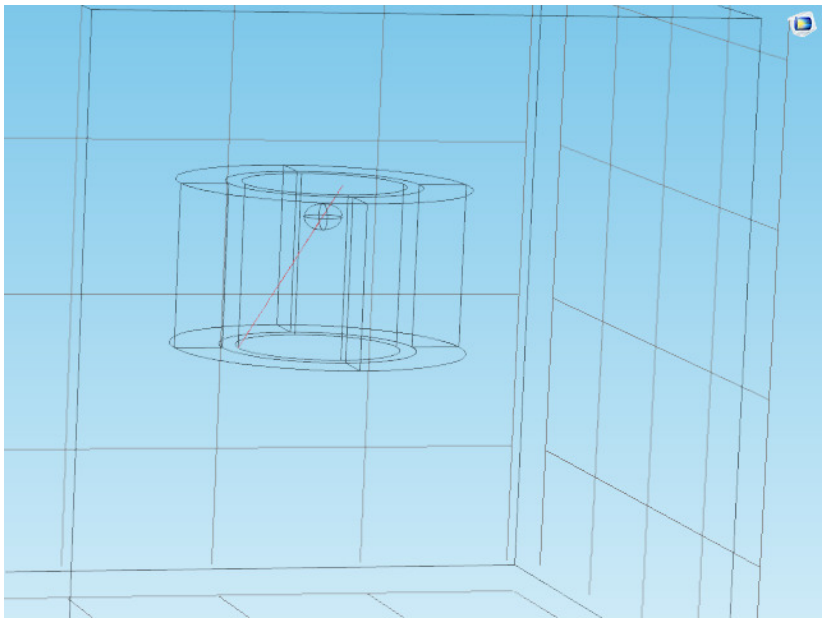

Figure 7.26: Representation of line(red in colour) passing through centre of tumor in diagonal direction

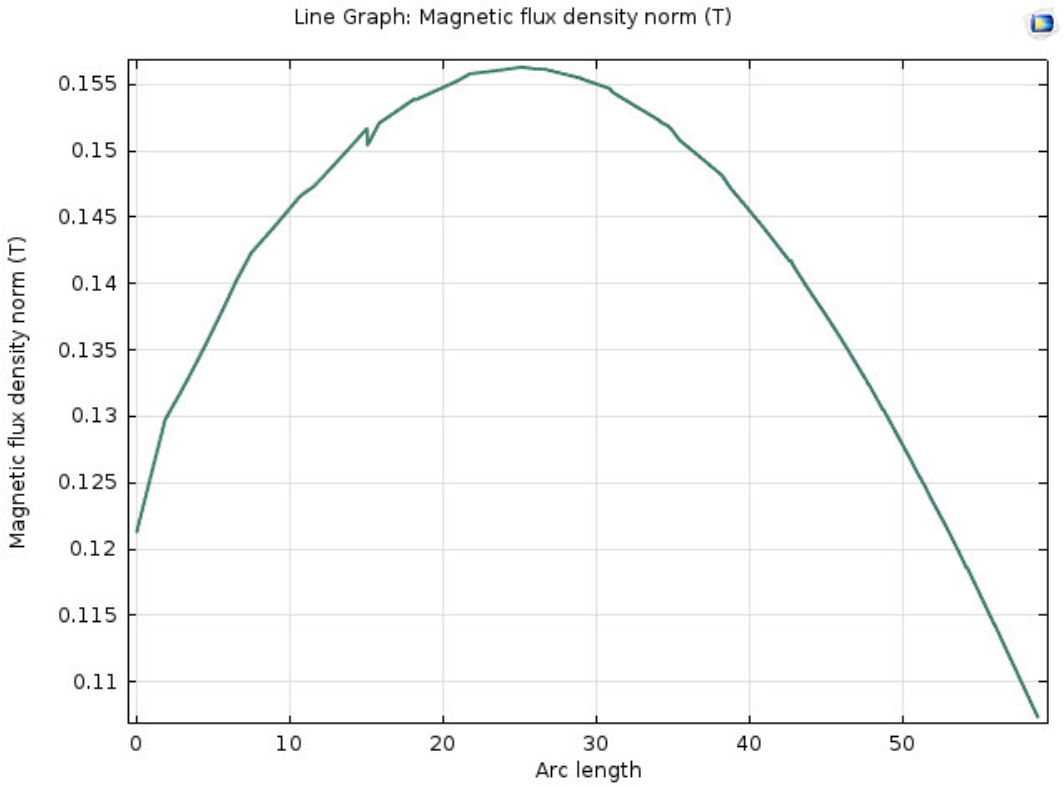

Figure 7.27: Representation of magnetic flux density in horizontal axis passing through center of tumor(diametrically).

7.5 COUPLING OF BIO-HEAT TRANSFER MODULE AND MAGNETIC FIELDS WITH CURRENTS

7.5.1 TEMPERATURE VARIATIONS FOR TISSUE ENRICHED WITH PARTICLES

In most of the simulations studies, the heat dissipation patterns are observed by applying Bio-heat transfer study only. Magnetic field parameters are kept into consideration as by correctly defining the heat input parameter into the Penne's Bioheat equation. As per literature survey, till date there is no coupling interface is studied which provides the heat input to pennes equation by coil defined heating. In this context an attempt is made to develop such simulation that provides insight to this electromagnetic heating principle. Two types of variations for three different sets of frequencies are studied along line(red in colour) passing through tumor centre vertically and horizontally. The variations performed are as follows:

1.Transient temperature variations for muscle tissue loaded with magnetic nanoparticles at undermentioned frequency range to study hyperthermia.

- Frequency of 400kHz
- Frequency of 500kHz
- Frequency of 600kHz

2.Spatial variations of magnetic field for muscle tissue for undermentioned frequency range

- Frequency of 400kHz
- Frequency of 500kHz
- Frequency of 600kHz

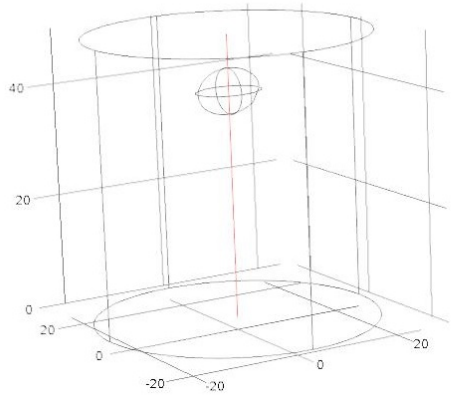

Figure 7.28: Illustration of plot generation line(red in colour) along the centre of tumor and healthy tissue.

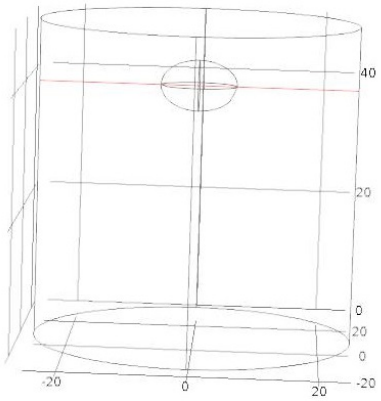

Figure 7.29: Illustration of plot generation line(red in colour) along the diameter of tumor and healthy tissue.

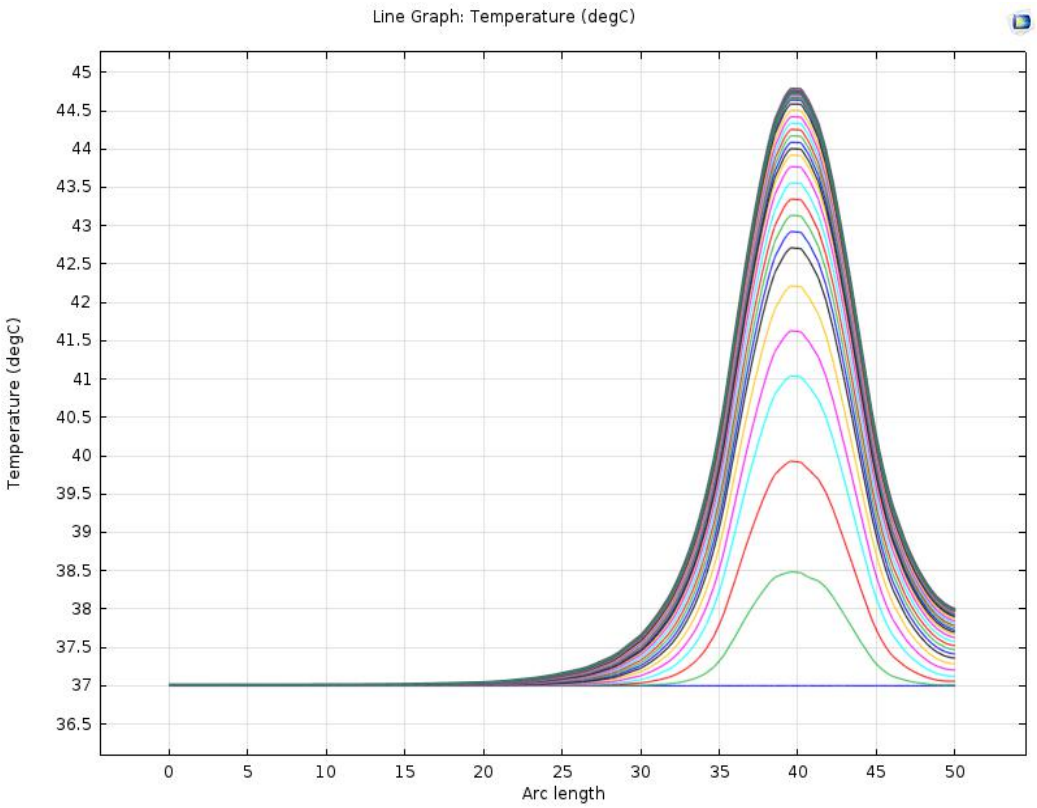

Figure 7.30: Temperature along centre of Muscle Tissue for 400kHz frequency passing through tumor.

In figure 7.30, Temperature variations are studied along the vertical axis passing through the tumor centre for muscle tissue. The curve depicts the temperature rise for the central tumor region due to the presence of magnetic nanoparticles. This sharp peak at centre accounts for proper heat dissipation at the central core of tumor and the temperature is between the permissible limits. The therapeutic window of hyperthermia is between 41.5°C and 48°C. The temperature is 44.8°C. The frequency of 400kHz can agitate the nanoparticles and is sufficient to cause the necrosis of tumor. The curve also depicts that the temperature rise is observed in tumor part of tissue and healthy tissues are not affected by the heat patterns induced by this frequency induced heating.

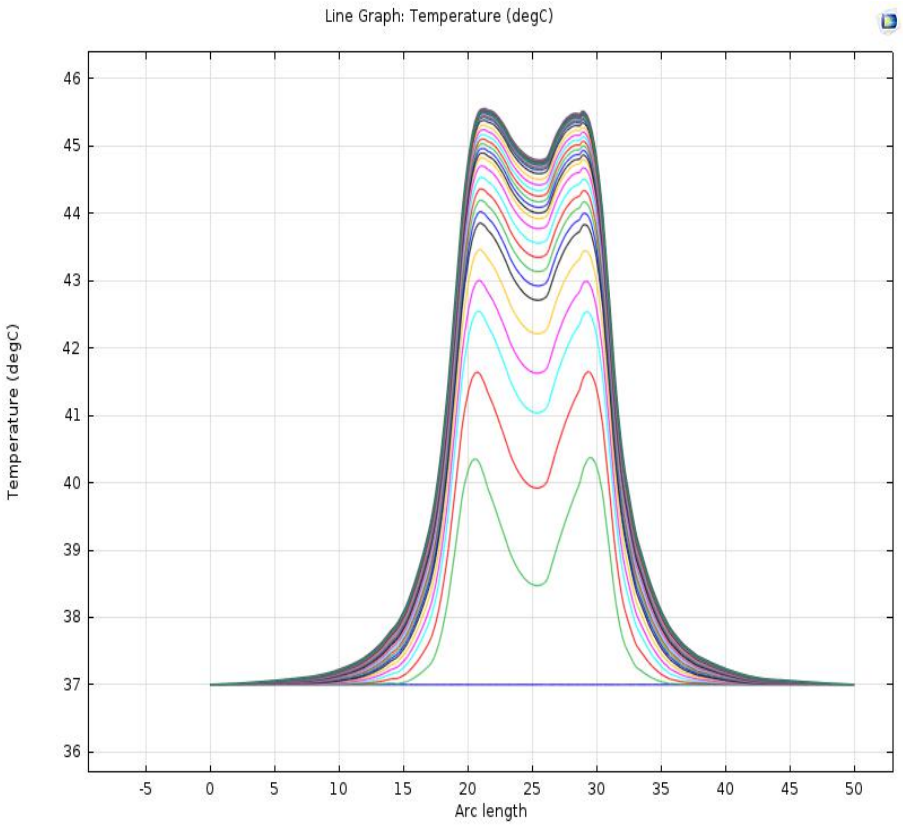

Figure 7.31: Temperature along diameter of Muscle Tissue passing through tumor for 400kHz frequency

The figure 7.31 is the representation of temperature variations along the diameter of tumor. The inverted bell shape curve is obtained which shows a sharp double peaks near to tumor border about 45.5°C. The depression observed inside the tumor is due to higher magnetic heating towards the portion of tumor near to surface of coils. As the distance from the coils decreases i.e maximum at centre, maximum depression curves are found. Again the higher temperature peaks are observed for tumor part and the healthy tissue region remains unaffected at 400kHz. The similar shape curve is obtained by Piotr GAS,2010[25], and also as shown for breast tissue in by Miaskowski et al.,2013[16] in his work. It is been mentioned in [16], that parameters of muscle tissue is generally assigned to cancer layer, which is a common methodology when cancerous tissues are considered or modeled as validated by Fear et al.,2002[118] and Shea et al.,2010[119] in their work. This also validates that the assumption of defining the tissue under consideration as muscle tissue is correct. This is also due to the fact that since the geometry is symmetrical, it considers it to show double peaks at extreme ends.

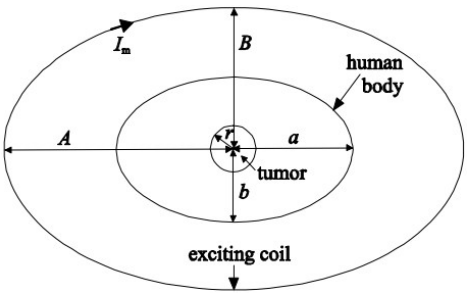

Figure 7.32: Illustration of similar geometrical domains considered in hyperthermia study as spherical tumor carrying human body is placed inside the exciting coil carrying current by Piotr GAS,2010[25].

Figure 7.32 describes the geometrical domain similar to the present work. In the present analysis, three-dimensional model is assumed by considering the ellipsoid(representing tumor) symmetrically put inside the cylinder(representing muscle tissue) and the whole geometrical domain is placed inside another cylinder(representing current carrying coil) which produces the uniform magnetic field inside the muscle tissue. Piotr GAS,2010[25] in his work considered spherical tumor symmetrically placed inside ellipse surrounded by another current carrying wire represented by ellipse. So, the geometries are similar in similarities except that the considered analysis is two-dimensional analysis.

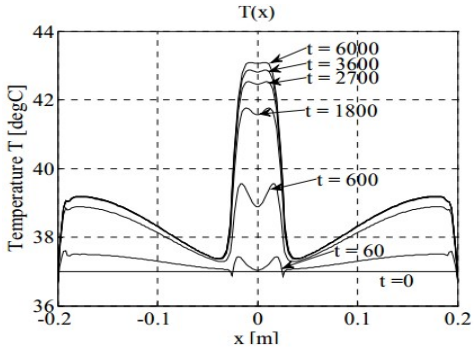

Figure 7.33: Illustration of Temperature distribution along the horizontal symmetry axis of human body for different time span showing inverted bell shaped curved at center of spherical tumor by Piotr GAS,2010[25].

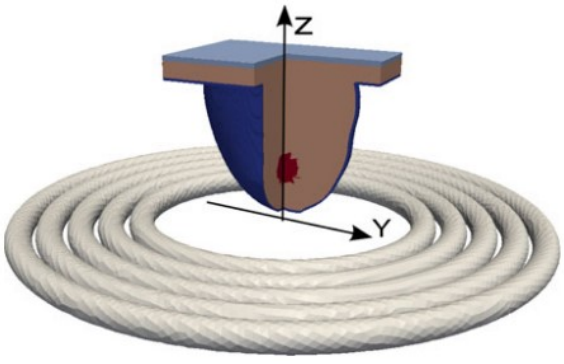

Figure 7.34: Illustration of tumor loaded with nanoparticles in breast tissue placed inside five turn exciting coil by Miaskowski et al.,2013[16].

Figure 7.34 describes the geometrical domain of breast model from phantom studies. Breast tumor inside the coil is heated by magnetic field imposed on nanoparticles. The mixture model is used to define the material properties to tumor enriched with nanoparticles. Corresponding to this model, the temperature plots are created in tumor Y co-ordinate which again validates the trends of plots received for current model for horizontal axis of tumor(i.e diameter variations).

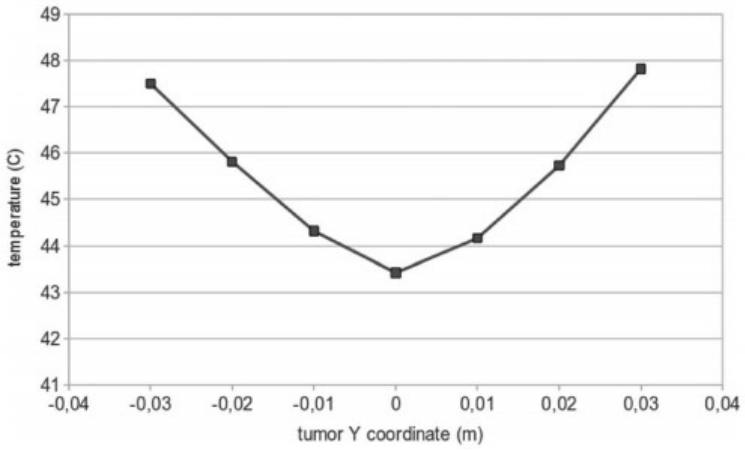

Figure 7.35: Illustration of temperature depression for tumor domain symmetrically placed inside the five turn-coil carrying current by Miaskowski et al.,2013[16].

Figure 7.35, describes the decreasing trend of temperature at centre or inverted bell shaped curved is obtained. The temperature is found maximum at the two extremes of tumor loaded with particles. This is attributed by the fact that the magnetic field is maximum towards the tumor part more inclined or close to coils. The higher temperature will be reached when the tumor is shifted to side rather than at center of coil. This is due to the fact that magnetic field goes higher when approaching the coil cables. Thus, the maximum stimulation will be given when the breast is positioned over the winding rather than in center of coil.

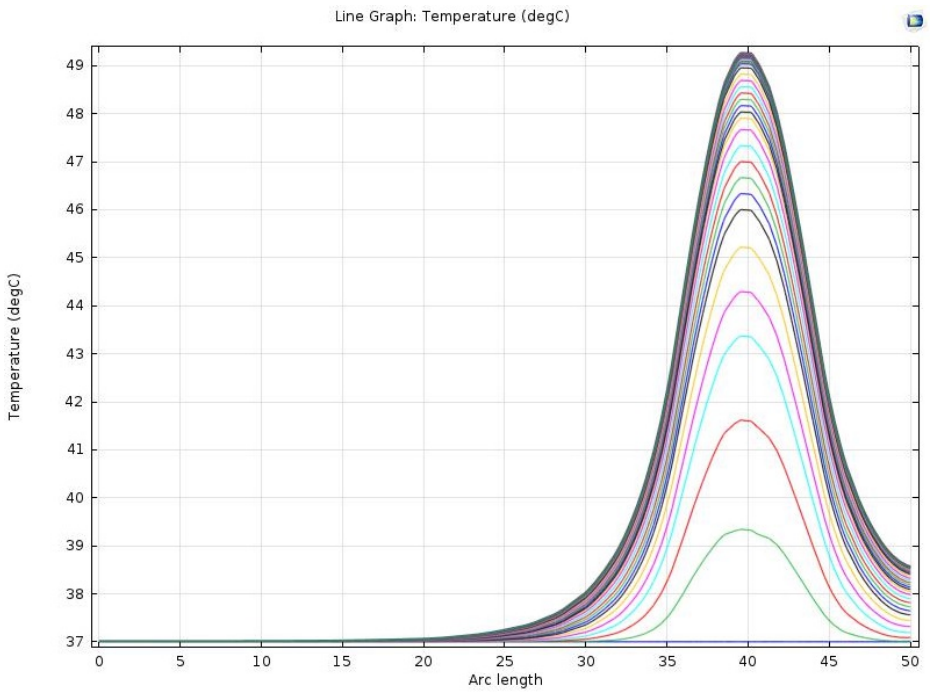

Figure 7.36: Temperature along centre of Muscle Tissue for 500kHz frequency passing through tumor

In figure 7.36, Temperature variations are studied along the vertical axis passing through the tumor centre for muscle tissue. The curve depicts the temperature rise for the central tumor region due to the presence of magnetic nanoparticles. The temperature is 49.4°C. The frequency of 500kHz can agitate the nanoparticles and is sufficient to cause the necrosis of tumor. The curve also depicts that the temperature rise is observed in tumor part of tissue and healthy tissues are not affected by the heat patterns induced by this frequency induced heating. At this frequency, hyperthermia can be used as monotherapy. The maximum temperature is at center and at this frequency, thermal ablation can be achieved starting from the basal temperatures of 37°C, the core body temperature condition been imposed as an important boundary condition on surface geometry of model.

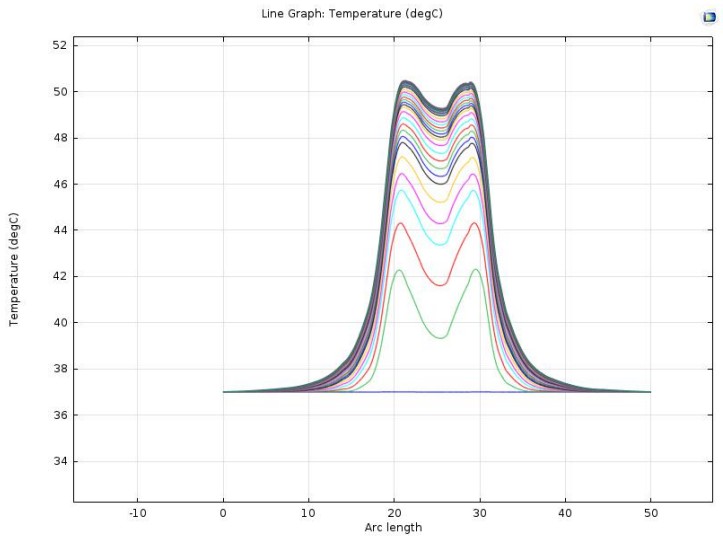

Figure 7.37: Temperature along diameter of Muscle Tissue passing through tumor for 500kHz frequency

The figure 7.37 is the representation of temperature variations along the diameter of tumor. The inverted bell shape curve is obtained which shows a sharp double peaks near to tumor border about 50.3°C. The depression observed inside the tumor is due to higher magnetic heating towards the portion of tumor near to surface of coils.

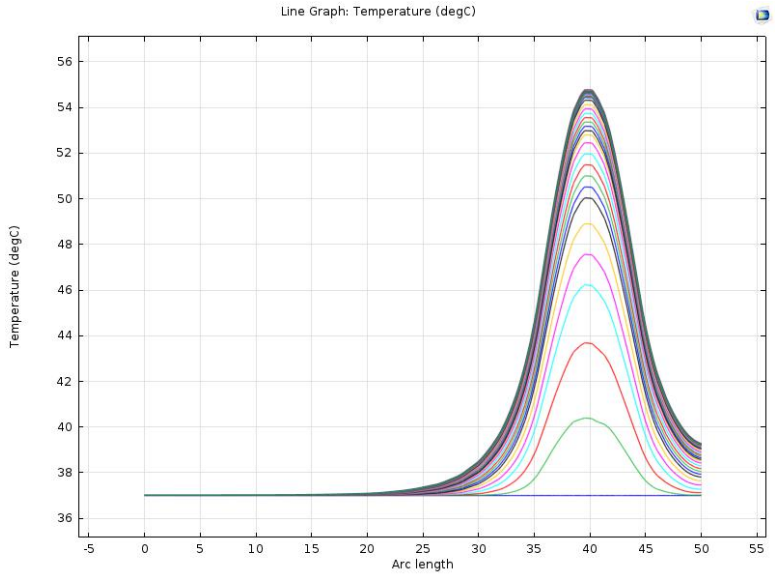

Figure 7.38: Temperature along centre of Muscle Tissue for 600kHz frequency passing through tumor.

At 600kHz operating frequency, the muscle tissue observes an increase of temperature and reaching upto maximum value of 55°C to operate the tumor with thermal ablation technique

of hyperthermia. The temperature again founds to be maximum in vertical axis passing through the tumor center.

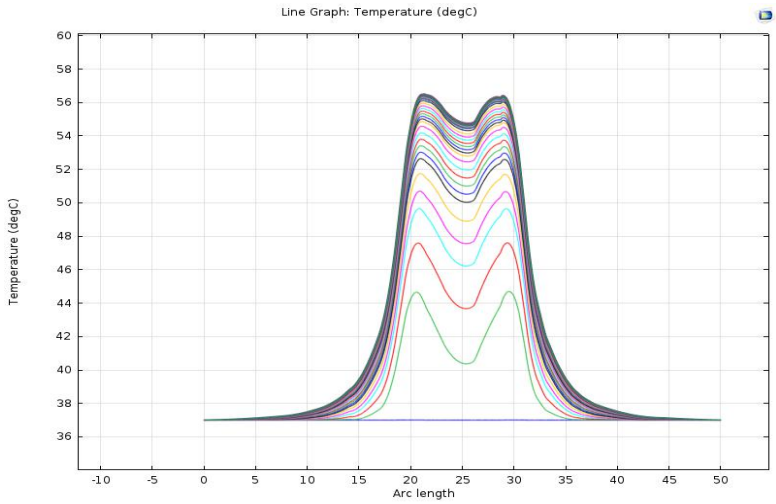

Figure 7.39: Temperature along diameter of Muscle Tissue passing through tumor for 600kHz frequency.

The inverted bell curve for different periods of time is observed in figure 7.39. The maximum temperature achieved at near corners of tumor founds a maximum value of 56.3°C. This depression at center is attributed by the distance effect of tumor from surface of coil. This temperature elevations can completely ablate the tumor region.

7.5.2 STUDY OF MAGNETIC FIELDS ALONG SPATIAL COORDINATES

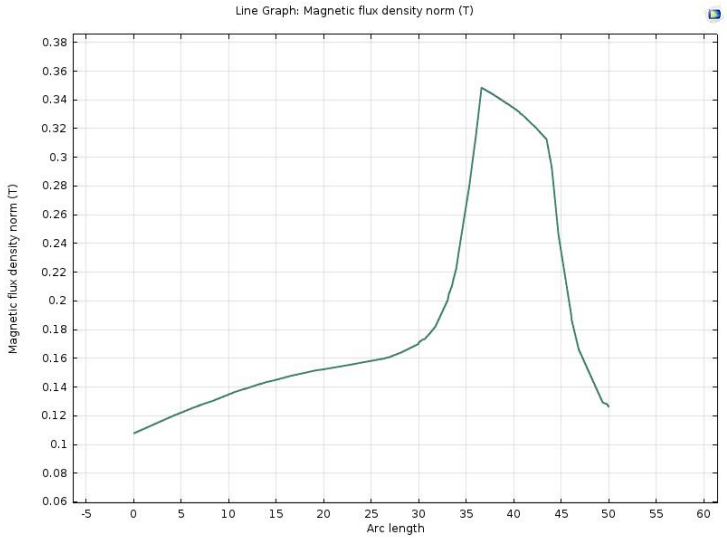

Figure 7.40: Magnetic flux density along vertical axis passing through tumor at 400kHz.

The maximum magnetic field is found near to the nanoparticles enriched region. The peak value is found to be 0.35T as found in figure 7.40.

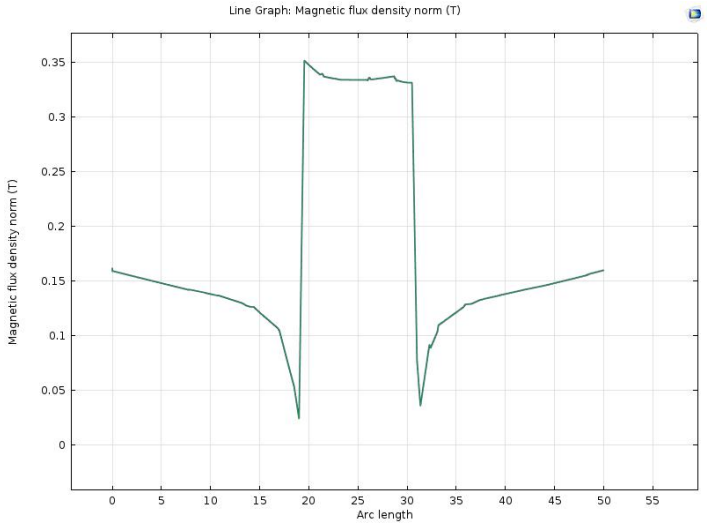

Figure 7.41: Magnetic Flux density variations along diameter(horizontal axis) of tumor at frequency of 400kHz.

Figure 7.41 illustrates that maximum magnetic flux density is about 0.35T and is around the tumor constituted region at frequency of 400kHz.

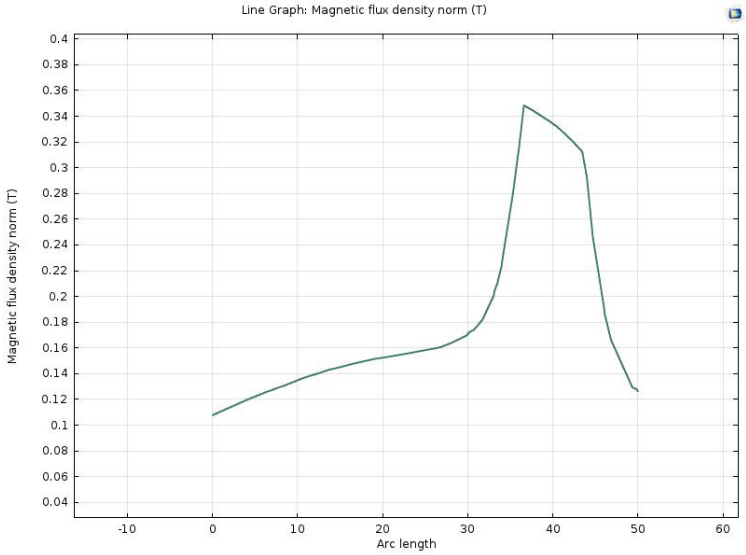

Figure 7.42: Magnetic flux density along vertical axis passing through tumor at 500kHz.

The maximum magnetic field is found near to the nanoparticles enriched region. The peak value is found to be 0.35T as found in figure 7.42.

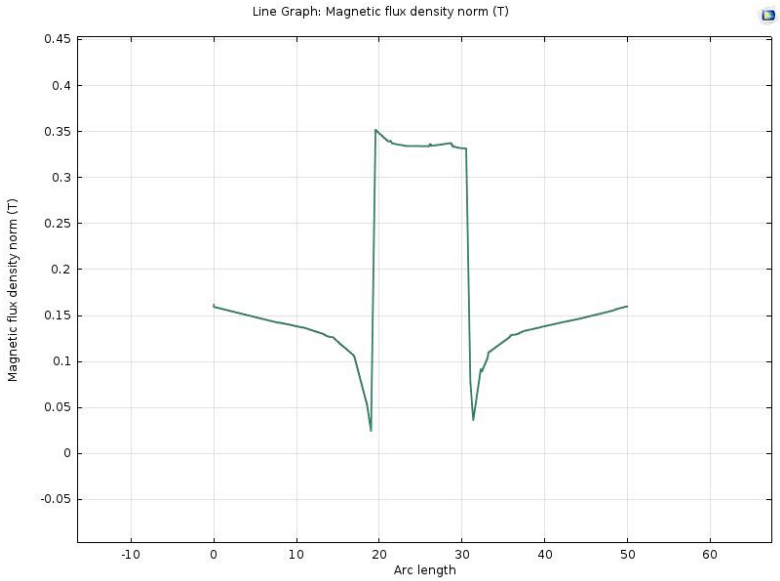

Figure 7.43: Magnetic Flux density variations along diameter(horizontal axis) of tumor at 500kHz.

Figure 7.43 illustrates that maximum magnetic flux density is about 0.35T and is around the tumor constituted region.

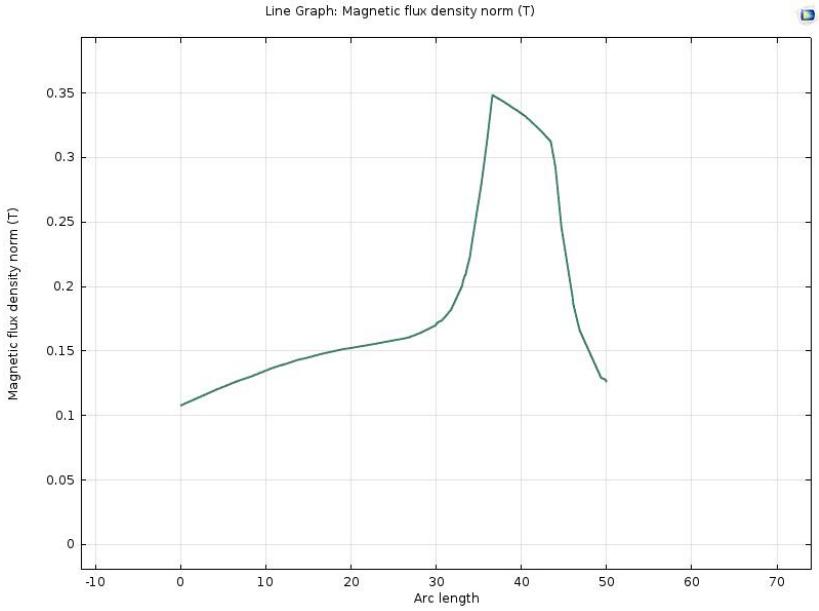

Figure 7.44: Magnetic flux density along vertical axis passing through tumor at 600kHz.

The maximum magnetic field is found near to the nanoparticles enriched region. The peak value is found to be 0.35T as found in figure 7.44.

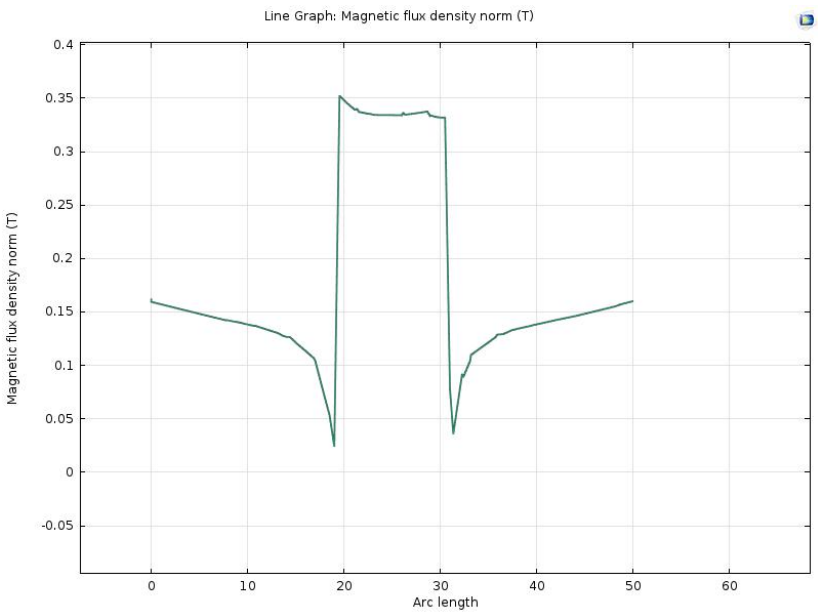

Figure 7.45: Magnetic Flux density variations along diameter(horizontal axis) of tumor at 500kHz.

Figure 7.45 illustrates that maximum magnetic flux density is about 0.35T and is around the tumor constituted region.

It is been concluded as per the results plots obtain in figures from figure 7.40 to figure 7.45 that the maximum flux density of 0.35T is obtained for fixed number of turns i.e 1126 turns. The further increase of magnetic field can be obtained with further increase of number of turns. The frequency increase is must to increase the rate at which the heating should be imposed in nanoparticles to induce the maximum damage to cancerous tissues. The frequency range chosen is from the extensive parameters limits reported in literature summary sheets for magnetic nanoparticles. It is been found that these are the operatable frequency range for hyperthermia studies.

7.6 TRANSIENT BIOHEAT TRANSFER ANALYSIS ON BREAST TISSUE

The therapeutic window of hyperthermia studies on cancer, involves different effective temperature ranges. The programmed cell death of cancerous cells starts with 41.5°C. As reported in literature, the definition of hyperthermia is defined for temperature range of 41.5°C-

46.5°C. But this range is not sufficient to completely necrose the tissue. It must be assisted with present on clinical modalities of chemotherapy and radiotherapy. These two assisting modalities themselves do tumor puncture and as found in literature survey many tumors regrow and again develops their own micro-environment. So, to overcome this problem and opens the horizons of hyperthermia to be used as monotherapy, the therapeutic window is refined and new term thermal ablation is proposed with quite high temperature ranges. At further high temperatures the coagulation necrosis occurs. In this study, all three aspects are tuned specifically for breast tissues in terms of temperatures variations in center of tumor, study of surface temperatures achieved in tumor tissues. These temperature elevations helps us predict the operating range for which maximum damage can be imposed with respect to size of tumor.

Surface and Volumetric plots are extensively obtained to observe the requisite temperature range to breast tumors. The heat source inputs are implemented via bio-heat transfer module of comsol-multiphysics. The F.E.A analysis on breast model is performed with finer mesh settings and the grid independency test is also performed illustrating the uniqueness of results. The results are validated with literature.Following heat inputs are given to the model to account for suitable operating range

- **Plot No.1: Heat Input(S.A.R)=1.95×105W/m3**

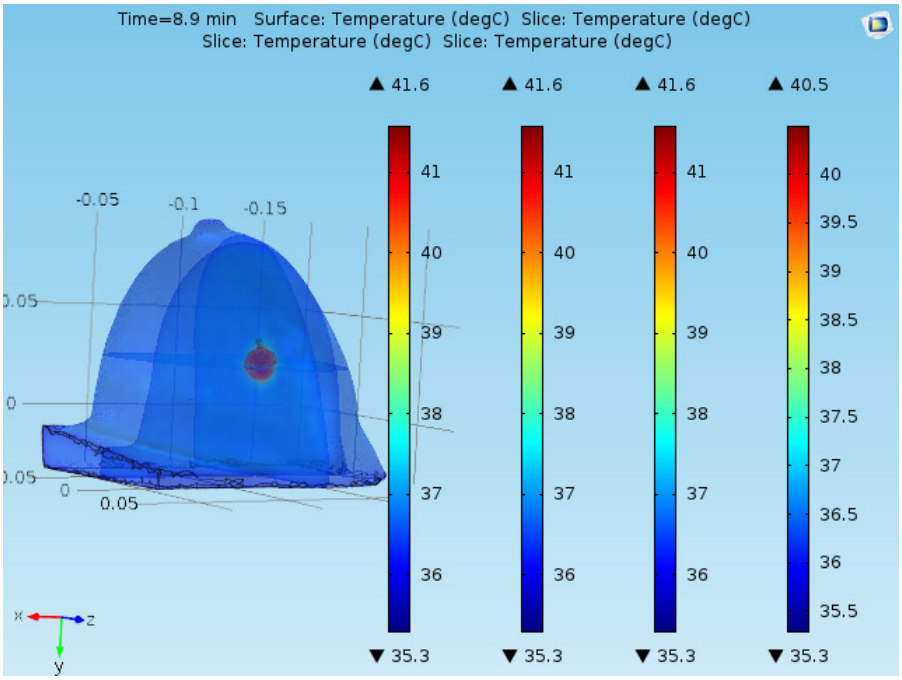

Figure 7.46: Surface-volume plot for breast model geometry at heat input of $1.95\times10^{5}W/m^{3}$

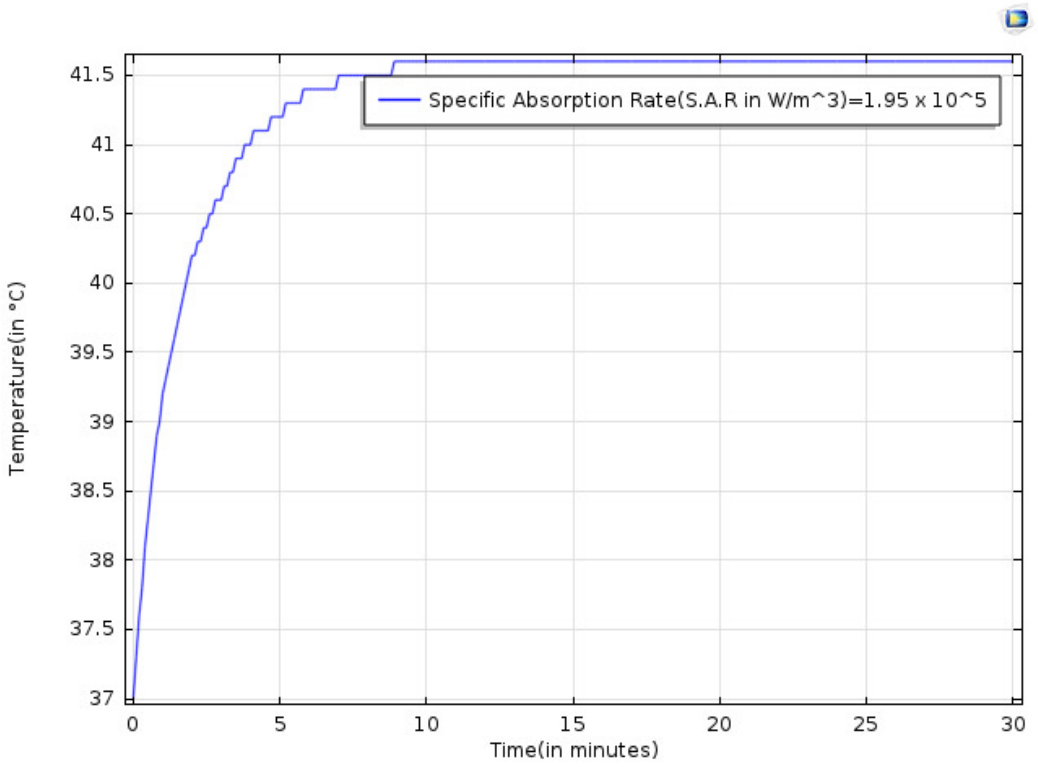

Figure 7.47:Temperature vs time variations for Specific Absorption Rate(S.A.R) of $1.95\times10^5 W/m^3$

❖ **Plot No.2:Heat Input(S.A.R)=$3\times10^5 W/m^3$**

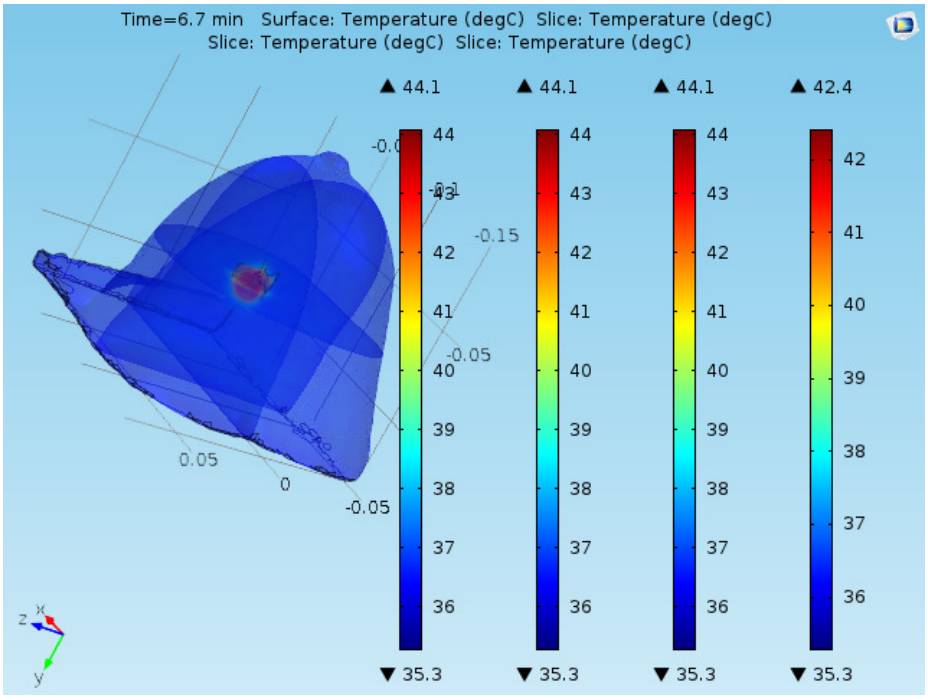

Figure 7.48: Surface-volume plot for breast model geometry at $3x10^5 W/m^3$

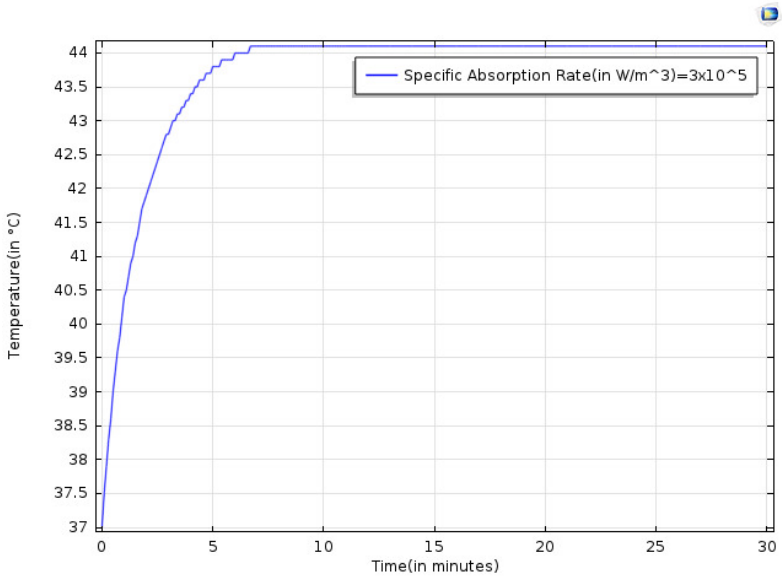

Figure 7.49:Temperature vs time variations for Specific Absorption Rate(S.A.R) of $3\times10^5 W/m^3$

❖ **Plot No.3: Heat Input(S.A.R)=$4\times10^5 W/m^3$**

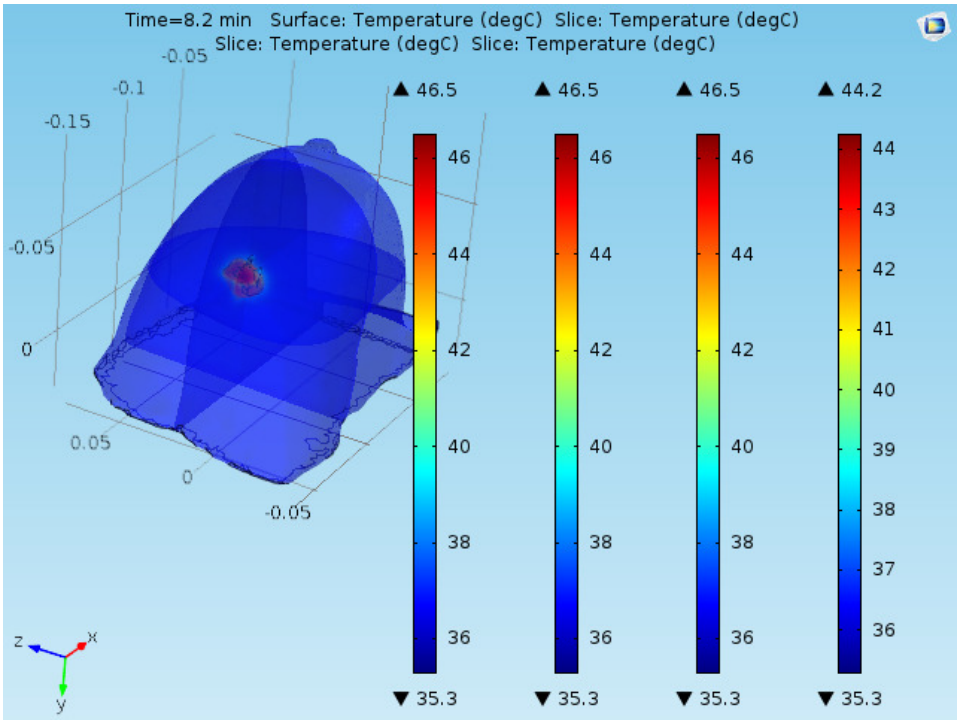

Figure 7.50 : Surface-volume plot for breast model geometry$4\times10^5 W/m^3$

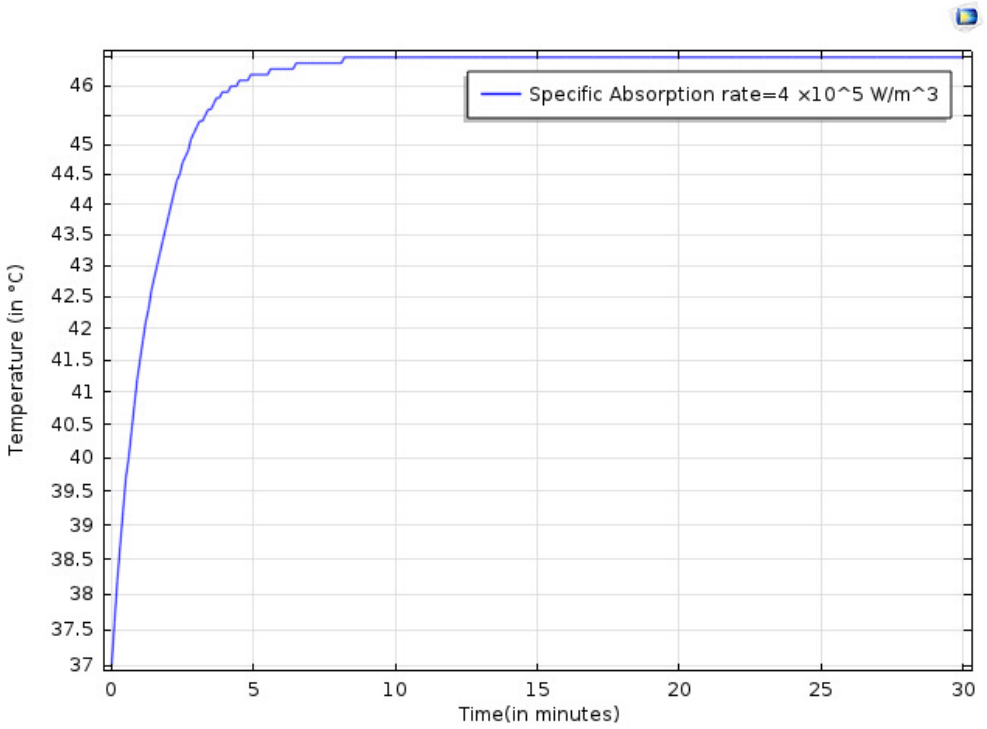

Figure 7.51:Temperature vs time variations for Specific Absorption Rate(S.A.R) of $4\times10^5 W/m^3$

❖ **Plot No.4: Heat Input(S.A.R)=$5\times10^5 W/m^3$**

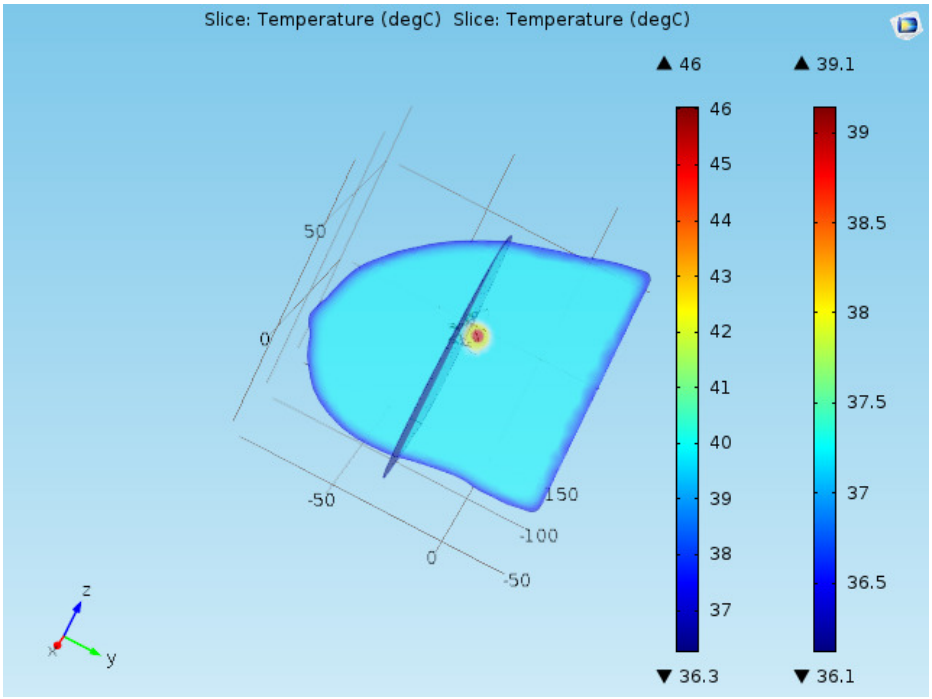

Figure 7.52: Volume two-slice temperature plot for Specific Absorption Rate(S.A.R) of $5\times10^5 W/m^3$

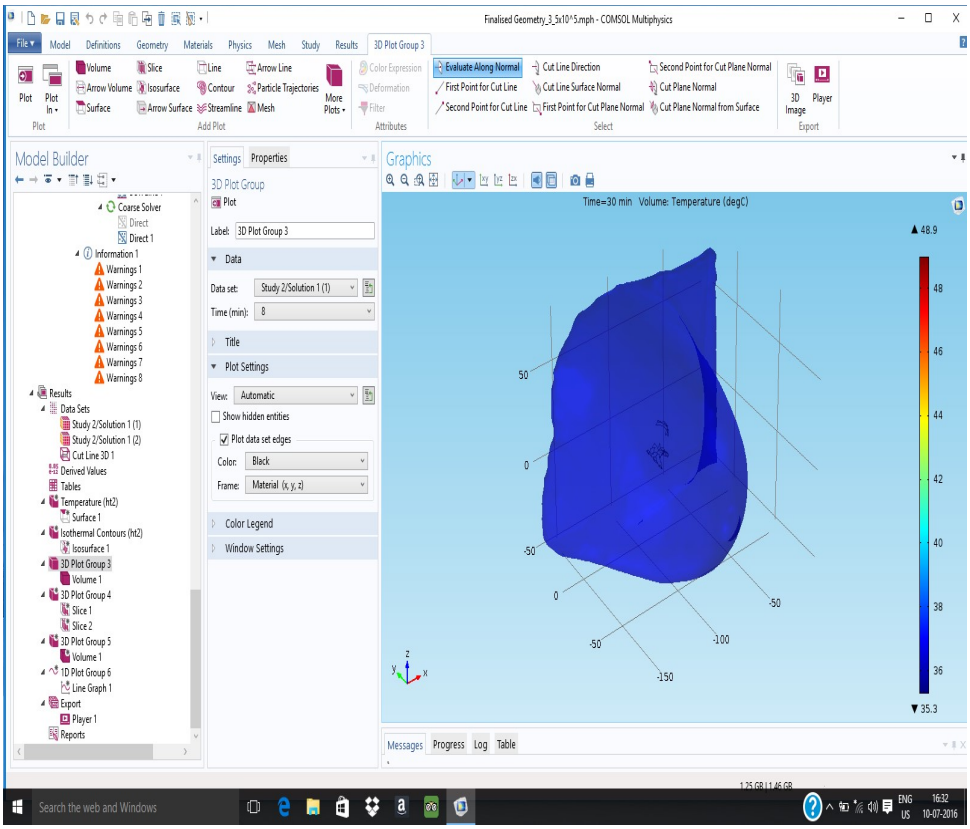

Figure 7.53: Volume temperature plot for breast model at Specific Absorption Rate(S.A.R) of $5 \times 10^5 W/m^3$

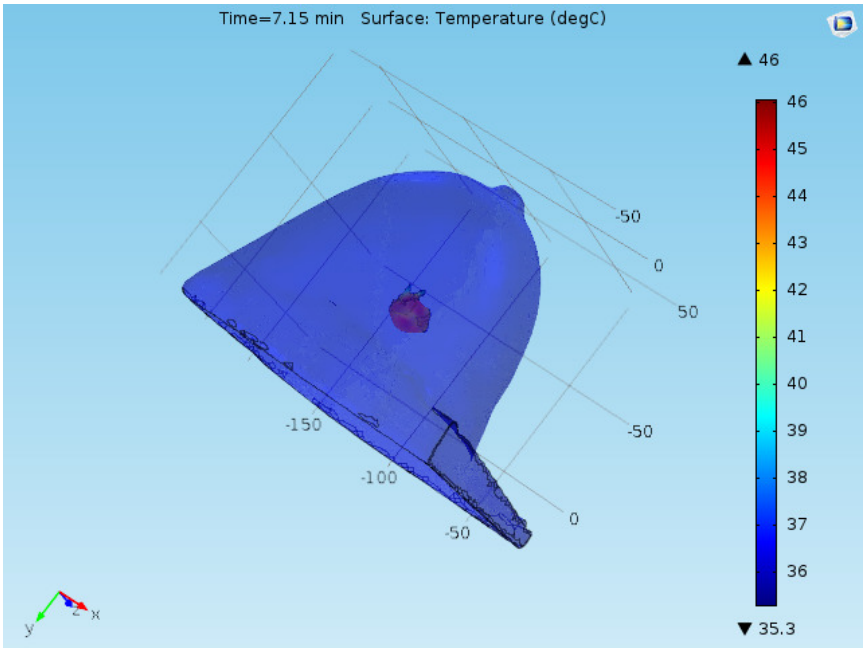

Figure 7.54: Surface temperature plot for breast model at Specific Absorption Rate(S.A.R) of $5\times10^5 W/m^3$

❖ **Plot No.5: Heat Input(S.A.R)=$6\times10^5 W/m^3$**

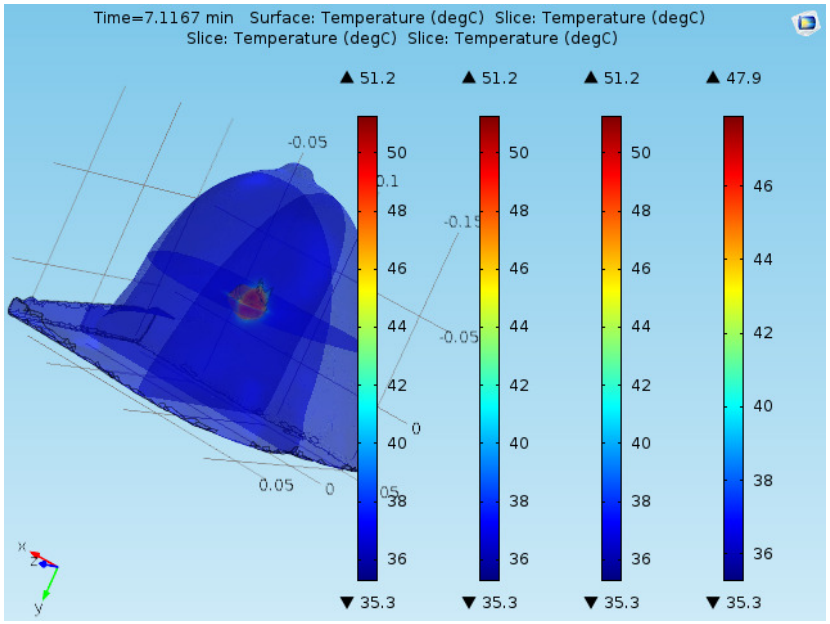

Figure 7.55: Surface-volume plot for breast model geometryat$6\times10^5 W/m^3$

❖ **Plot No.6: Heat Input(S.A.R)=$7\times10^5 W/m^3$**

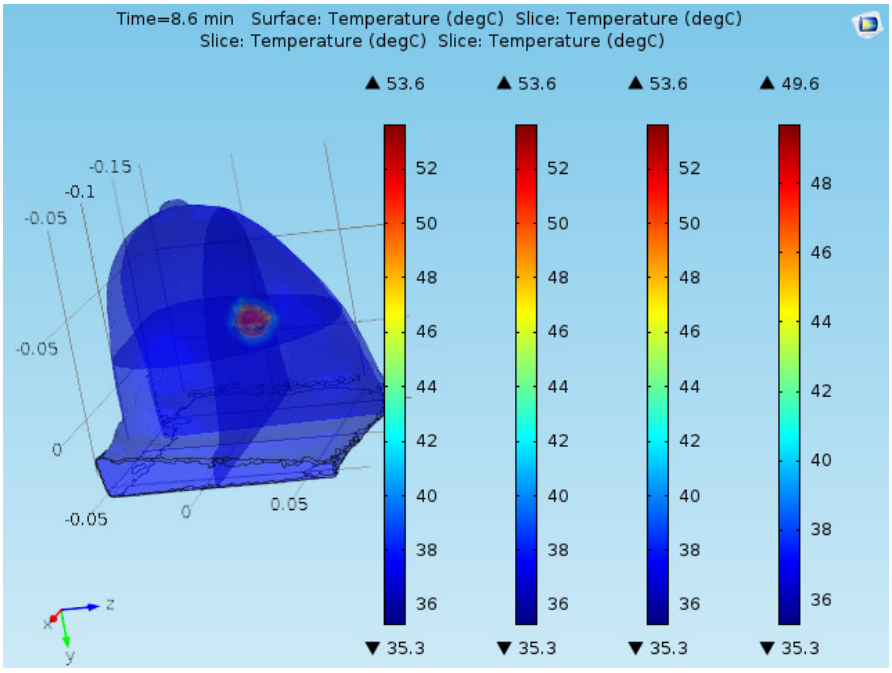

Figure 7.56: Surface-volume plot for breast model geometry at $7\times10^5 W/m^3$

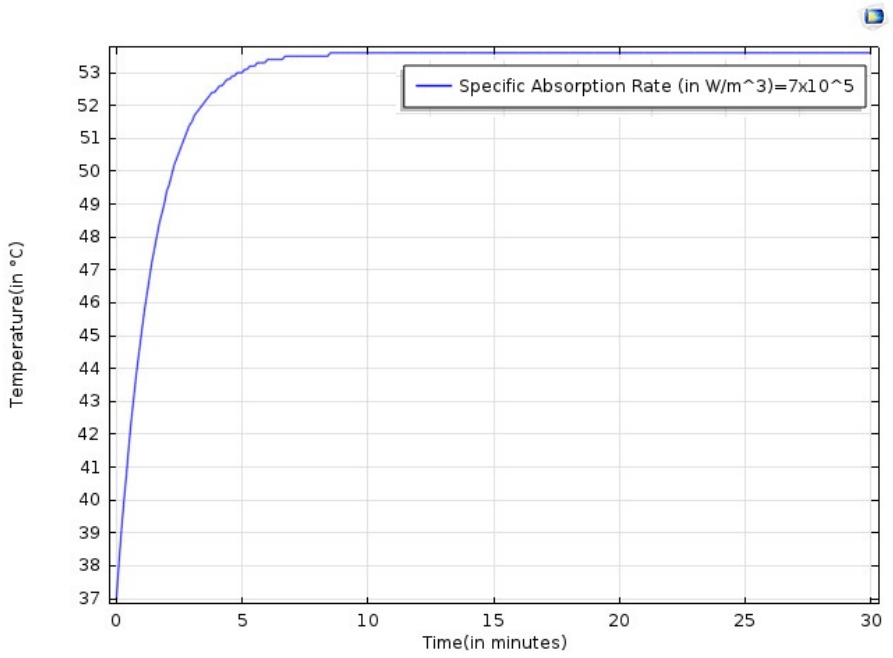

Figure 7.57:Temperature vs time variations for Specific Absorption Rate(S.A.R) of $7\times10^5 W/m^3$

❖ **Plot No.7: Heat Input(S.A.R)=$8\times10^5 W/m^3$**

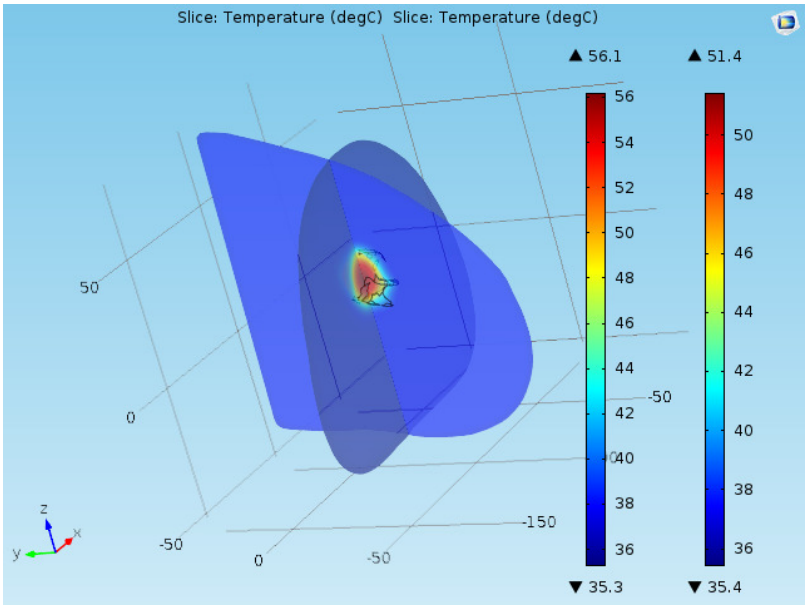

Figure 7.58: Volume plot for breast model geometry at $8\times10^5 W/m^3$

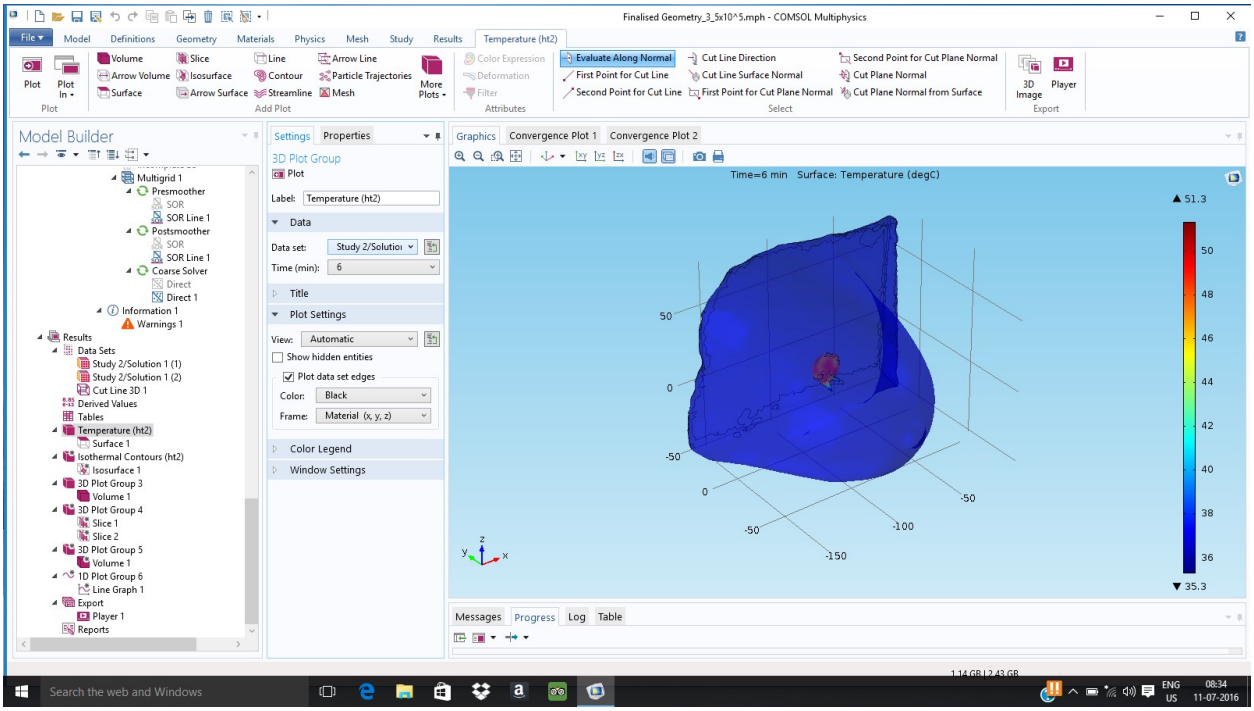

Figure 7.59 Surface temperature plot for breast model at Specific Absorption Rate(S.A.R) of $8\times10^5 W/m^3$

❖ Plot No.8: Heat Input(S.A.R)=$9\times10^5 W/m^3$

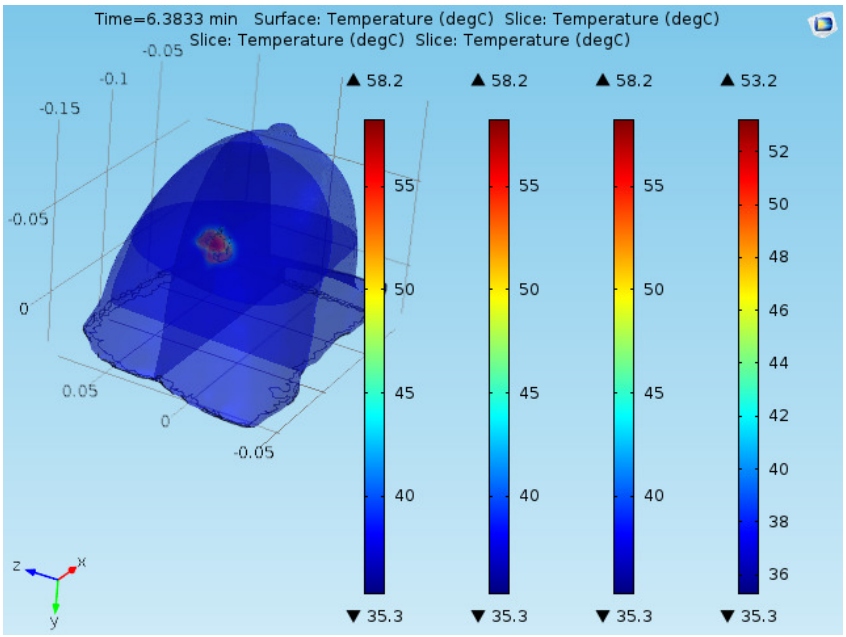

Figure 7.60: Surface-volume plot for breast model geometry at $9\times10^5 W/m^3$

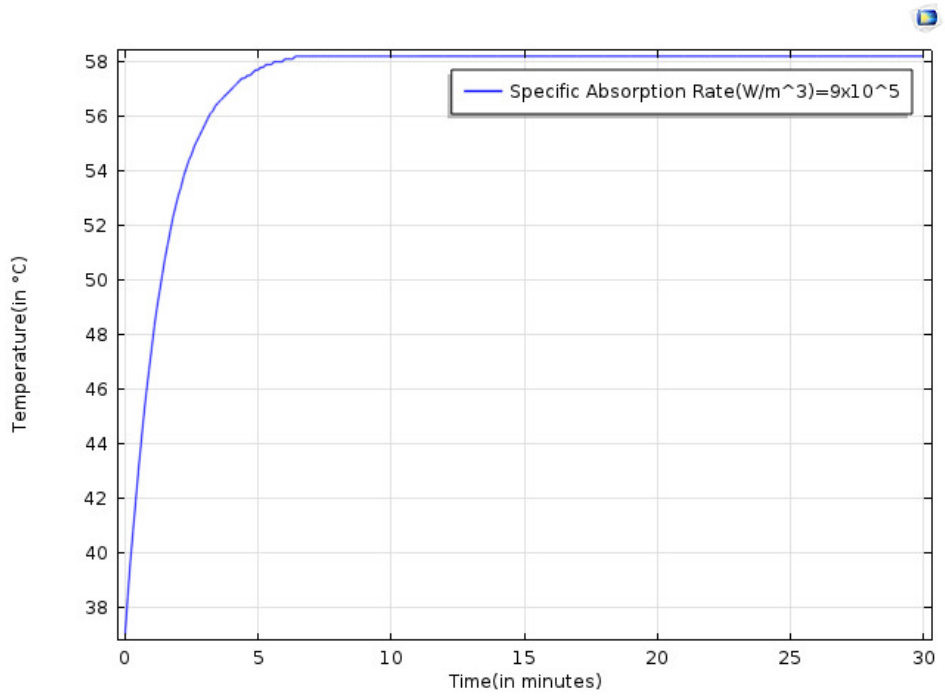

Figure 7.61:Temperature vs time variations for Specific Absorption Rate(S.A.R) of $9\times10^5 W/m^3$

❖ **Plot No.9: Heat Input(S.A.R)=$1.35\times10^6 W/m^3$**

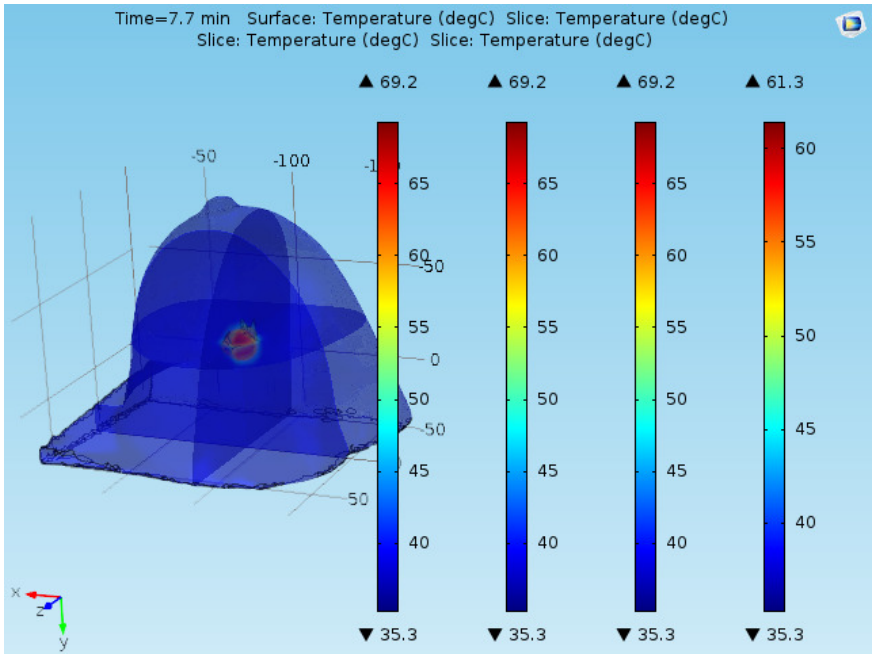

Figure 7.62: Surface-volume plot for breast model geometry at $1.35\times10^6 W/m^3$

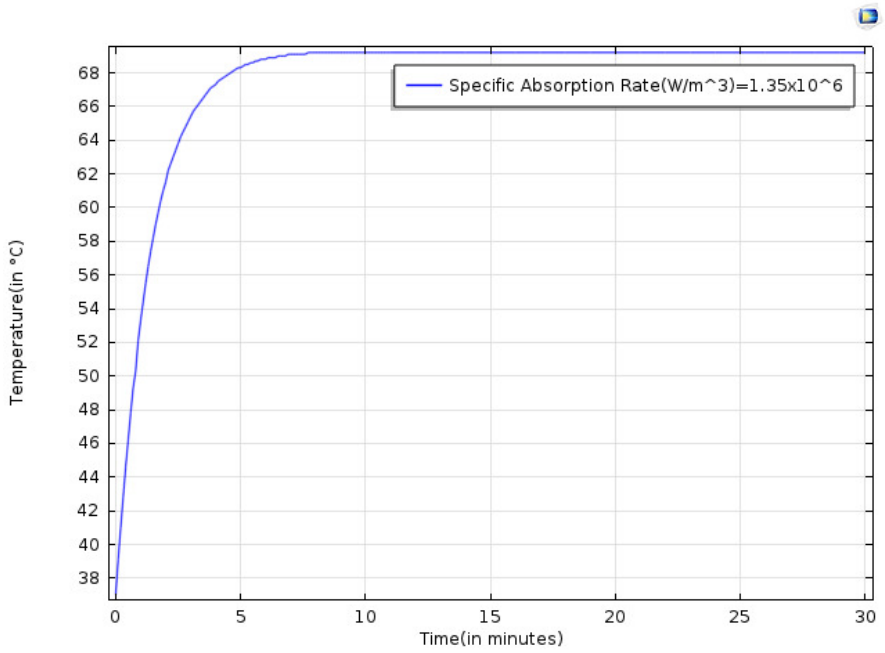

Figure 7.63:Temperature vs time variations for Specific Absorption Rate(S.A.R) of $1.35\times10^{6}W/m^{3}$

❖ **Plot No.10: Heat Input(S.A.R)=$1.35\times10^{6}W/m^{3}$**

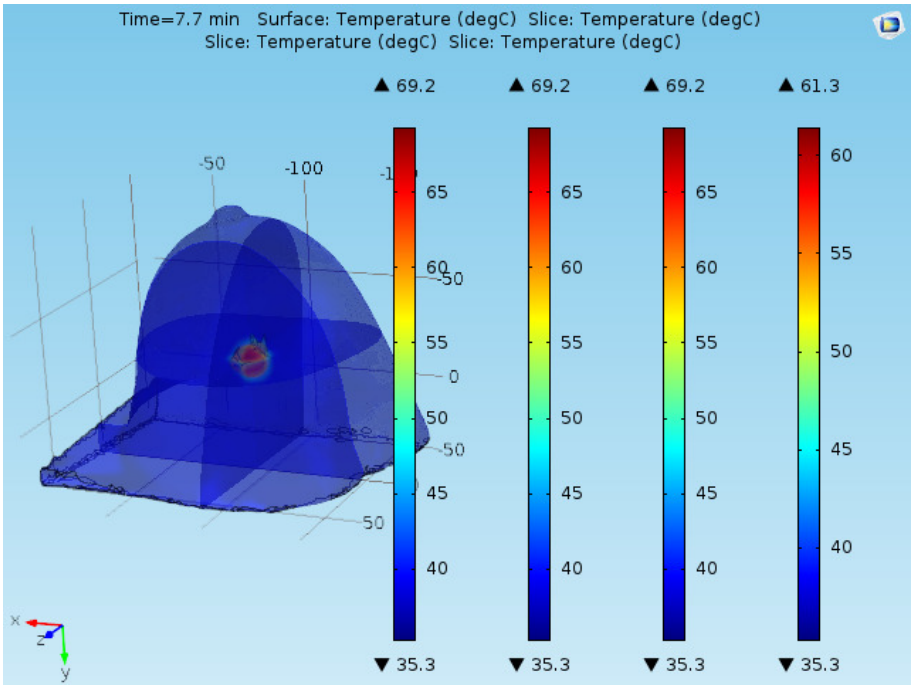

Figure 7.64: Surface-volume plot for breast model geometry at $1.35\times10^{6}W/m^{3}$

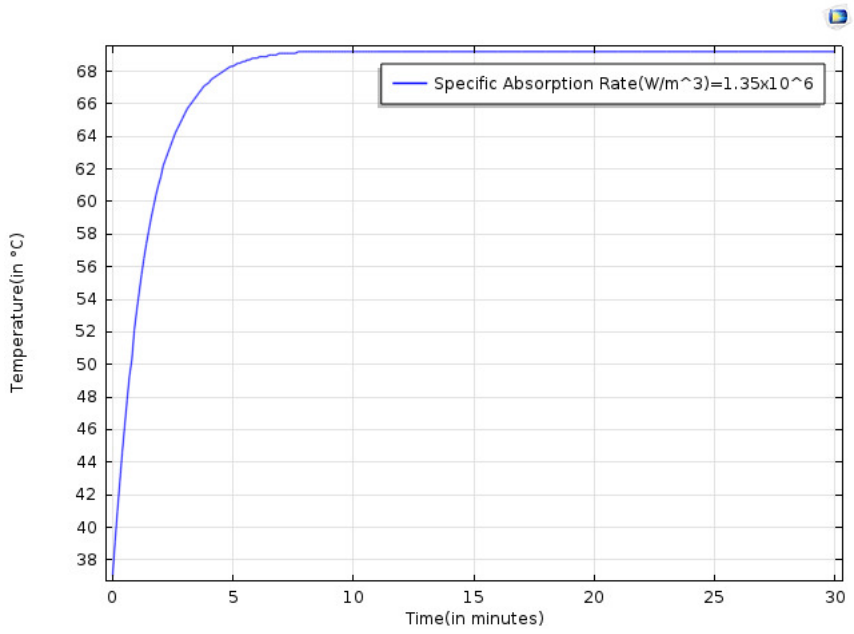

Figure 7.65:Temperature vs time variations for Specific Absorption Rate(S.A.R) of $1.35\times10^{6}W/m^{3}$

❖ **Plot No. 12: Heat Input(S.A.R)=$1.5\times10^{6}W/m^{3}$**

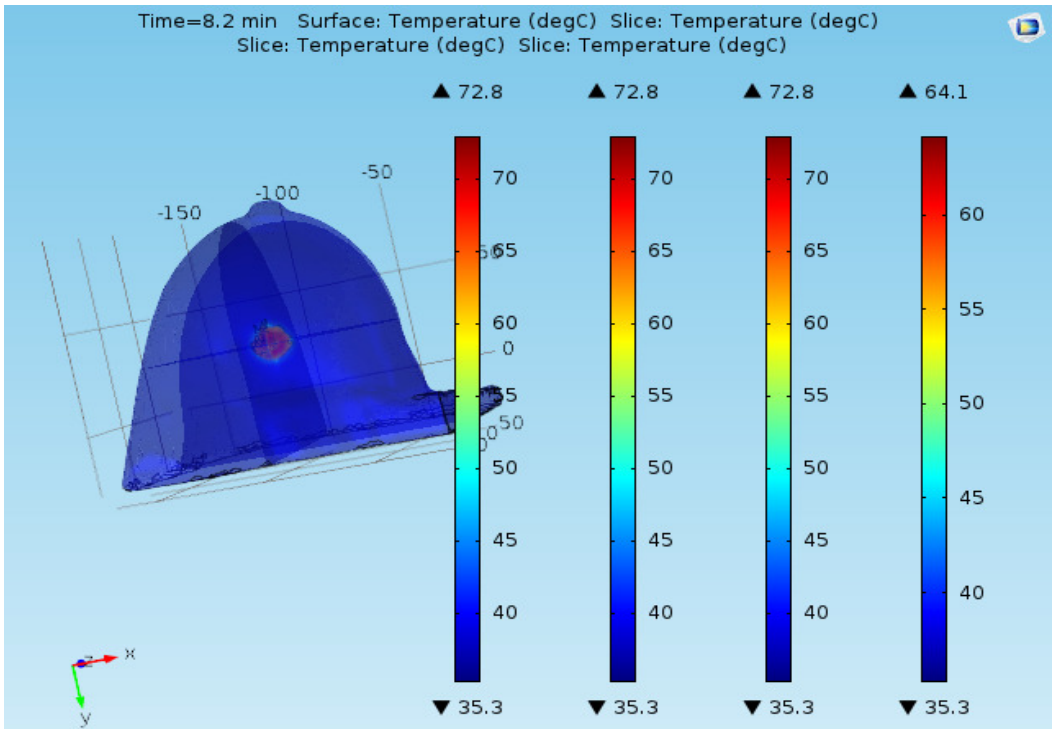

Figure 7.66: Surface-volume plot for breast model geometry at $1.5 \times 10^6 W/m^3$

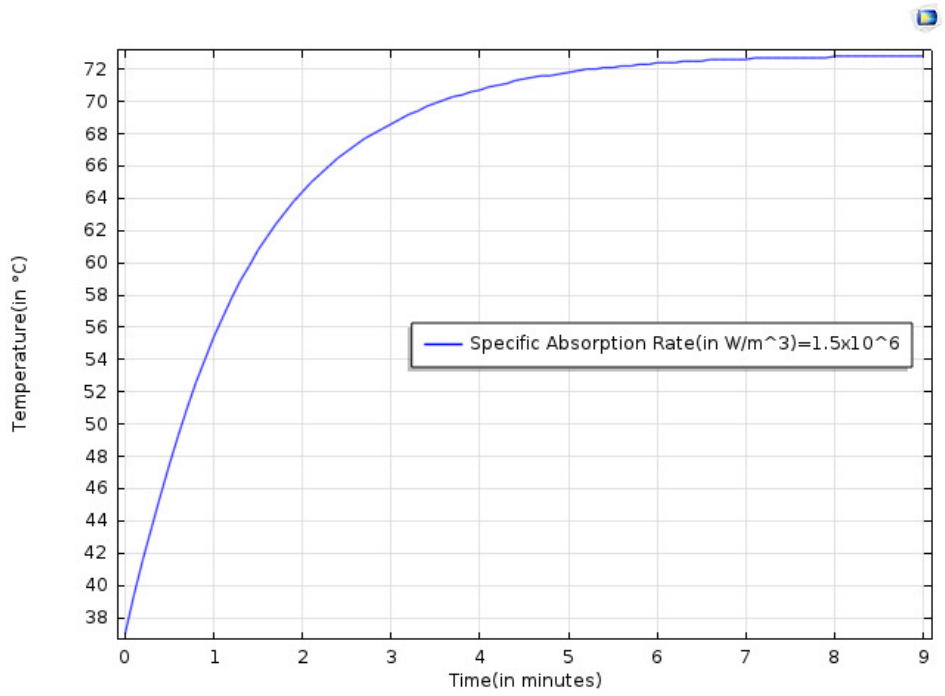

Figure 7.67:Temperature vs time variations for Specific Absorption Rate(S.A.R) of $1.5 \times 10^6 W/m^3$

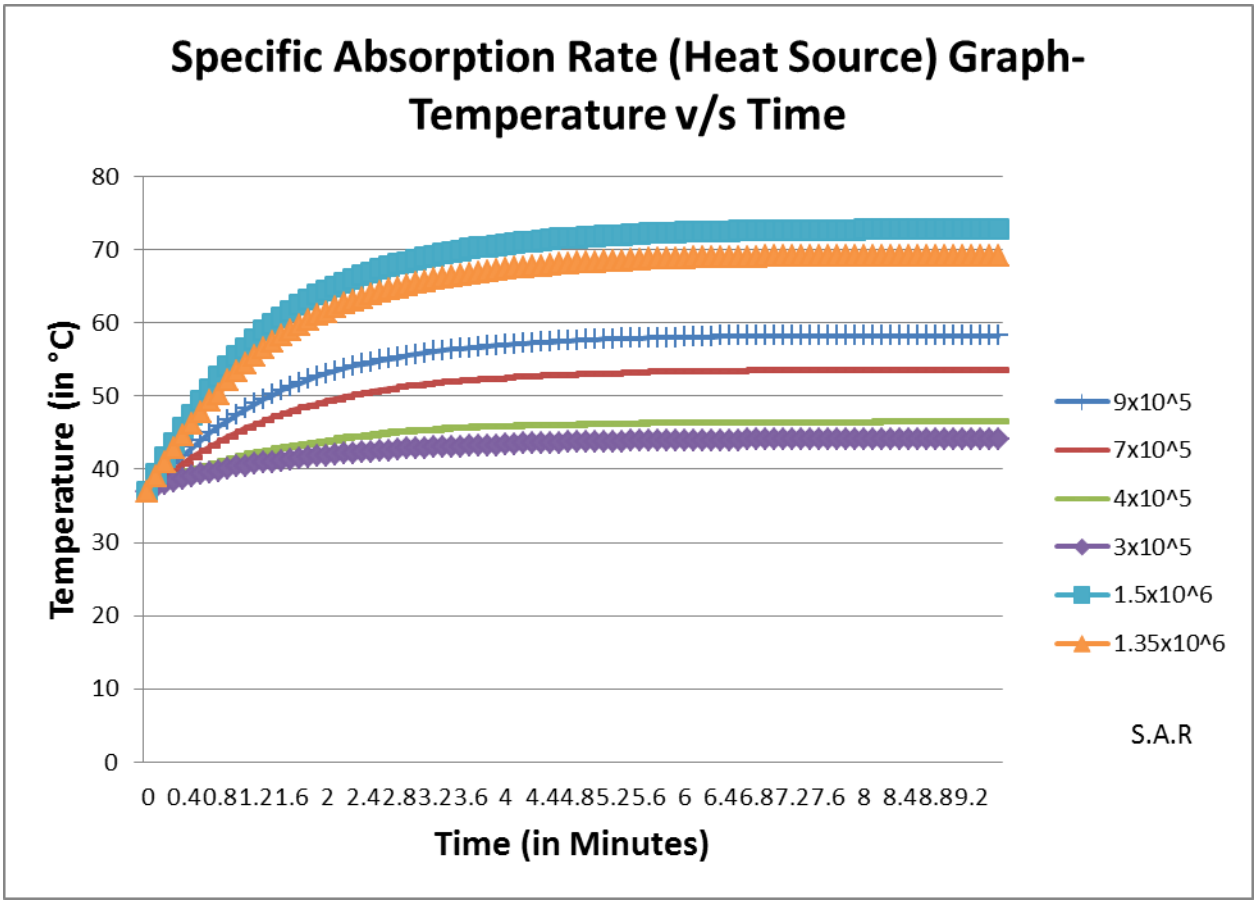

Figure 7.68: Temperature vs time variations for different heat inputs for breast tumor

The results are plotted for different heat input to breast tumors. The variations performed reveals that for successful hyperthermia to be achieved with different operating range of heat inputs to be used as monotherapy or as an assistive technology to chemotherapy or radiotherapy. Successful clinical trials performed by Hilger et al.,2001[28], similar peak temperature value is observed as reported in their work of 71.6°C±8 and minimum temperature as reported is 58°C. The results of figure 7.67 are in accordance with the results of Hilger and co-workers.(figure 7.69). So, to operate breast tumors having 2572mm^3 volume, a specific absorption rate of 1.5×10^6W/m^3 is sufficient enough to completely do the necrosis to the tissue. Based upon this Specific absorption rate; heat input parameter, the appropriate values of operating frequency and amplitude is selected. The results as reported in literature proposes 6.5kA/m amplitude and 400kHz frequency to produce maximum temperature till 71.6°C±8. So, our calculation of SAR is validated.

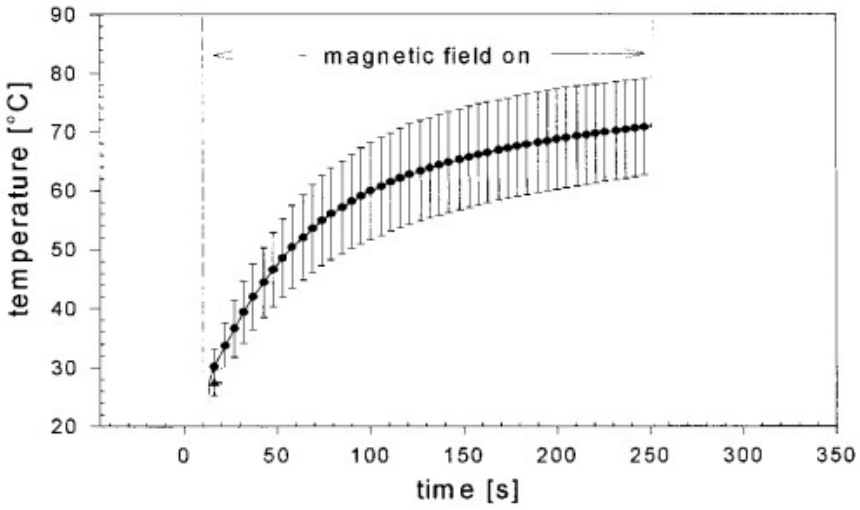

Figure 7.69:Variations of temperatures vs time for breast model in magnetic field exposure(Hilger et al.,2001[28])

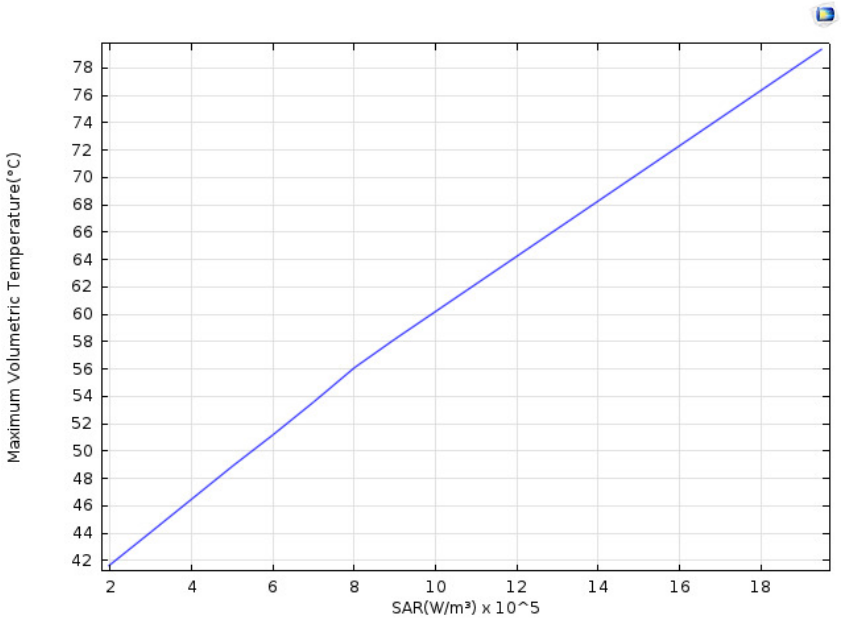

Figure 7.70: Representation of maximum volumetric temperature at core region of breast tumor for different S.A.R value range.

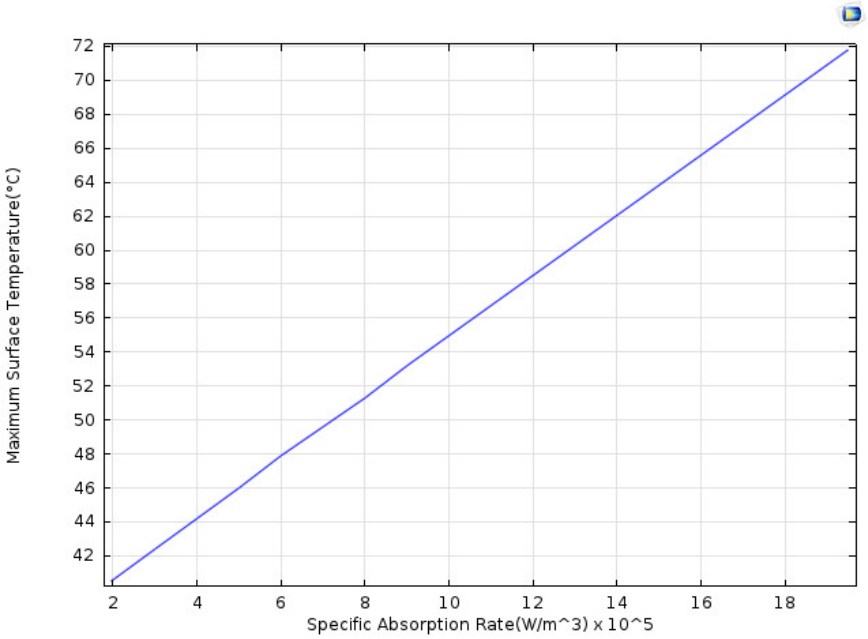

Figure 7.71: Representation of maximum surface temperature at core region of breast tumor for different S.A.R value range

RESULS FOR BREAST TISSUE PARAMETERS

Sr. No.	Heat Input (Q_{source})*or* Specific Absorption Rate(S.A.R in W/m^3)	S.A.R in (W)	Analysis Time in (min.)	Steady State Achievement in (min.)	Max. Surface Temp. in (°C)	Maximum Volumetric Temperature in (°C)
1	1.95×10^5	0.50154	30	8.9	40.5	41.6
2	3.00×10^5	0.7716	30	6.7	42.4	44.1
3	4.00×10^5	1.0288	30	8.2	44.2	46.5
4	5.00×10^5	1.286	30	7.15	46	48.9
5	6.00×10^5	1.5432	30	7.12	47.9	51.2
6	7.00×10^5	1.8004	30	8.5	49.6	53.6
7	8.00×10^5	2.0576	30	6.00	51.3	56.1
8	9.00×10^5	2.3148	30	6.38	53.2	58.2
9	1.35×10^6	3.4722	30	7.7	61.4	69.2
10	1.45×10^6	3.858	30	8.2	64.1	72.8
11	1.95×10^6	5.0154	30	7.05	71.8	79.4

CHAPTER 8

CONCLUSIONS, CLOSING REMARKS & FUTURE RESEARCH DIRECTIONS

8.1 OVERVIEW

The advent of non-invasive measurement strategies is expected to be strong stimulant for improving the accuracy of patient-specific simulations and also modeling the real-time treatment optimization strategies. There is a strong need of computational analysis related studies as it better controls the clinical work-flow for routine clinical use. It provides platform of discussion to doctors, engineers, researchers to think and rethink to upgrade the existing modalities and opens doors for new technologies to come forward and the existing ones to mature and develop understandability.

Thermal predictions are very sensitive to thermal parameters, and little data is available on these properties or their variations between patients and under heat stress. Therefore, an extensive uncertainty evaluation per application and treatment site is essential to quantify the accuracy of patient-specific predictions.

According to tedious literature review performed by the author of this dissertation, a novel approach is proposed and no part of such studies are represented in Hyperthermia on actual tumor models till date. This study can be enhanced by incorporating the effect of blood vessels in the near vicinity of tumor related tissues, and the flow of nanoparticles can also be studied in special relation to it. Considering the research scope of this thesis, constraints are evaluated on the principles of heat transfer (Nano-heat transfer) and to keep the principles of micro-fluidics for future studies. There can be near feasibility possible to incorporate both important thermal engineering principles(Bio-nanoheat transfer and micro-fluidics)into one single model. This study at most covers important aspects of Image processing, Magnetic field in Bio-medicine, and Hyperthermia (Thermal ablation , Tissue Necrosis). This is considered as an important bridge between “Bio-heat transfer” and “Bio-fluid dynamics(blood)”.

In this study, the pennes bioheat equation is used to evaluate the temperature distribution in tumor core region with tune able parameter S.A.R. This parameter is a heat input to pennes equation and based on this concentration of particles can also be proposed.

8.2 FUTURE RESEARCH DIRECTIONS

The monitoring of adequate temperatures at the tumor site is one of the unsolved problems. This problem can be solved by computational programs to calculate the values at each defined parts of tumor. the accuracy of the models describing the physical situation. The physiological parameters are individually varying to a significant amount, such models are subject to significant modeling errors.

The obtained dicom images are 104 in number which are acceptable to create shape of tumor but unable to visualize blood carrying vessels in and around tumor vasculature. The images were taken at 1.5 mm slice thickness and it should be acceptable to take it at lesser distance between slices i.e around 0.5mm thickness and number sets should be more i.e minimum 250 images. The current available data from PGIMER, is evaluated and only the tumors are visible and the vessels enhancement is missing. The effect of blood perfusion, nanoparticles flow inside the tumor vessels via intravenous injection can be evaluated in future work. Magnetic drug targeting is also an important extension of present work.

In the current work, nanoparticles are assumed spherical and only monodispersion is considered. The effect of polydispersion, and different shapes of particles can also be incorporated in future studies. This study evaluates transient temperature plots in core tumor region. The process of tissue necrosis via electromagnetic heating can also be inculcated in future research studies.

8.3 CHALLENGES

While hyperthermia is a treatment modality that holds a lot of promises for cancer therapy, the methods of attaining, maintaining, monitoring, and modeling; it may suffer from many inadequacies. Therefore, there is always a foremost need to continue efforts to provide more refinement to address this problem in a more efficient way. Hyperthermia has been well proved to be used as an adjunct to established oncological modalities but still it has not achieved the status of "*standard oncological therapy*".

The computational work done is very less for hyperthermia studies. The parameters which are given as an input to comsol-multiphysics are very limited in number. There is availability of selected resources to carry out the practical work. It was not an easy task to captulate the review of literature regarding this study. Collection of dicom format data is the biggest challenge. The data is obtained from P.G.I.M.E.R, Chandigarh. It was very tough challenge while consulting different hospitals to provide data related to breast cancer patients. Most of the hospitals do just the mammography(2D graphs) and facility of MRI scanning is available in very few hospitals. Each simulation on breast model needs around 16-24 hours for completion. Magnetic field simulations again takes very long time to process results. Author worked on 64GB RAM system i7 processor still the computational time was very long

REFERENCES

[1] M.Pavel and A.Stancu, "Ferromagnetic nanoparticles dose based on tumor size in magnetic fluid hyperthermia cancer therapy," *IEEE Transactions on Magnetics*, Vol. 45, No.11, (2009).

[2] M.Pavel, G.Gradinariu and A.Stancu, "A study of the interactions between ferromagnetic nanoparticles used in MFH," *IEEE ROMSC*, Iasi,Romania, (2007).

[3] M.Pavel, G.Gradinariu and A.Stancu, "Study of optimum dose of ferromagnetic nanoparticles suitable for cancer therapy using MFH," *IEEE Transactions on Magnetics*, Vol. 44, No.11, (2008).

[4] M.Pavel and A.Stancu, "Study of the optimum injection sites for a multiple metastases region in cancer therapy by using MFH," *IEEE Transactions on Magnetics*, Vol. 45, No.11, (2009).

[5] I.Astefanoaei, I.Dumitru, A.Stancu, and H.Chiriac, "A thermo-fluid analysis in magnetic hyperthermia," *Chinese Physics B*, Vol.23, No.4, (2014).

[6] L.Wu, J.Cheng, W.Liu, and X.Chen, "Numerical analysis of electromagnetically induced heating and bioheat transfer for magnetic fluid hyperthermia," *IEEE Transactions on Magnetics* , Vol. 51,No.2, (2015).

[7] S.Ghosh, D.Das Gupta, S.Chakraborty, and S.K.Das, "Superparamagnetic nanoparticle assisted hyperthermia and cooling protocol for optimum damage of internal carcinoma using computational predictive model," *Heat Mass Transfer*, (2013).

[8] H.Salarian, A.H.S.Garmabaki, M.Zakariapour, B.Ghorbani, and M.Amidpour, "A numerical study of heating effect of magnetic nanoparticles hyperthermia with alternating magnetic field," *Proceedings of International Conference on Advances in Mechanical Engineering*, (2011).

[9] Z.Wang, I.Aarya, M.Gueorguieva, D.Liu, H.Luo, L.Manfredi, L.Wang, D.McLean, S.Coleman, S.Brown, and A.Cuschieri, "Image-based 3D modeling and validation of radiofrequency interstitial tumor ablation using a tissue-mimicking breast phantom," *International Journal of Computer Assisted Radiology and Surgery*, Vol.7, pp.941-948, (2012).

[10] A.LeBrun, N.Manuchehrabadi, A.Attaluri, F.Wang, R.Ma, L.Zhu, "MicroCT image-generated tumour geometry and SAR distribution for tumour temperature elevation simulations in magnetic nanoparticle hyperthermia," *International Journal of Hyperthermia*, pp.1-9, (2013).

[11] J.F.Cepeda, S.Birla, J.Subbiah, and H.Thippareddi, "A practical method to model complex three-dimensional geometries with non-uniform material properties using image-based design and comsol multiphysics," *Proceedings of the COMSOL Conference in Boston*, (2013).

[12] Z.Li, M.Kawashita, N.Araki, M.Mistumori, and M.Hiraoka, "Effect of particle size of magnetite nanoparticles on heat generating ability under alternating magnetic field," *International Society for Ceramics in Medicine*, Vol.1, pp.1-4, (2011).

[13] Y.Arum, Y.Song, and J.Oh, "Controlling the optimum dose of AMPTS functionalized-magnetite nanoparticles for hyperthermia cancer therapy," *Applied Nanoscience*, Vol.1, pp.237-246, (2011).

[14] M.Javidi, M.Heydari, A.Karimi, M.Haghpanahi, M.Navidbakhsh, and A.Razmkon, "Evaluation of the effects of injection velocity and different gel concentrations on

nanoparticles in hyperthermia therapy," *Journal of Biomedical Physics and Engineering*, Vol.4, pp.151-162, (2014).

[15] S.Taloub, F.Hobar, I.Astefanoaei, I.Dumitru, O.F.Caltun, "FEM investigation of coated magnetic nanoparticles for hyperthermia," *Nanoscience and Nanotechnology*, Vol.6(1A), pp. 55-61,(2016).

[16] A.Miaskowski, and B.Sawicki, "Magnetic fluid hyperthermia modeling based on phantom measurements and realistic breast model," *IEEE Transactions on Biomedical* Engineering, Vol.60, No.7, pp.1806-1813, (2013).

[17] S.Maenosono, and S.Saita, "Theoretical assessment of FePt nanoparticles as heating elements for magnetic hyperthermia," *IEEE Transactions on Magnetics*, Vol.42, No.6, pp.1638-1642, (2006).

[18] F.Henrich, H.Rahn, and S.Odenbach, "Heat transition during magnetic heating treatment: Study with tissue models and simulation," *Journal of Magnetism and Magnetic Materials*, Vol.380, pp.353-359, (2015).

[19] C.Lin, and K.Liu, "Estimation for the heating effect of magnetic nanoparticles in perfused tissues," *International Communications in Heat and Mass Transfer*, Vol.36, pp.241-244, (2009).

[20] R.E.Rosensweig, "Heating magnetic fluid with alternating magnetic field," *Journal of Magnetism and Magnetic Materials*, Vol.252, pp.370-374,(2002)

[21] S.Purushotham, and R.V.Ramanujan, "Modeling the performance of magnetic nanoparticles in multimodal cancer therapy," *Journal of Applied Physics*, Vol.107, pp.114701-1 to 114701-8, (2010).

[22] R.Xu, Y.Zhang, M.Ma, J.Xia, J.Liu, Q.Guo, and N.Gu, "Measurement of specific absorption rate and thermal simulation for arterial embolization hyperthermia in the maghemite-gelled model," *IEEE Transactions on Magnetics*, Vol.43, No.3, pp.1078-1085,(2007)

[23] K.Balusu, S.S.Suganthi, and S.Ramakrishnan, "Modelling bio-heat transfer in breast cysts using finite element analysis," *Non-Invasive Imaging and Diagnostics Laboratory,Biomedical Engineering Group,Department of Applied Mechanics,IIT-Madras,India.*

[24] S.N.Tabatabaei, and S.Martel, "The concentration effect of magnetic iron oxide nanoparticles on temperature change for hyperthermic drug release applications via AC magnetic field," *Nanorobotics Laboratory,Department of Computer and Software Engineering, École Polytechnique de Montréal,Canada.*

[25] P.Gas, "Temperature inside tumor as time function in RF hyperthermia," *Przeglad Elektrotechniczny(Electrical Review) ISSN 0033-2097,R.86NR12,* pp.42-45, (2010).

[26] Manjunath N., Sanchu S., Sujith Kumar P.,and Praseetha K., "Tissue damage analysis and bioheat transfer simulation of radiofrequency ablation in hepatic tumor," *International Journal of Emerging Technology and Advanced Engineering*, Vol.4, pp.233-236, (2014).

[27] A.Cervadoro, C.Giverso, R.Pande, S.Sarangi, L.Preziosi, J.Wosik, A.Brazdeikis, and P.Decuzzi, "Design maps for the hyperthermic treatment of tumors with superparamagnetic nanoparticles," *PLOS ONE*, Vol.8, pp.1-14, (2013).

[28] I.Hilger, W.Andrä, R.Hergt, R.Hiergeist, H.Schubert, and W.A.Kaiser, "Electromagnetic heating of breast tumors in interventional radiology:In-vitro and in-vivo studies in human cadavers and mice," *Radiology,* Vol.218, No.2, pp.570-575,

(2001).
[29] I.Hilger, R.Hergt, and W.A.Kaiser, "Towards breast cancer treatment by magnetic heating," *Journal of Magnetism and Magnetic Materials,* Vol.293, pp.314-319, (2005).
[30] I.Hilger, R.Hergt, and W.A.Kaiser, "Use of magnetic nanoparticle heating in the treatment of breast cancer," *IEEE Proeedings on Nanobiotechnology*, Vol.152, No.1, pp.33-39, (2005).
[31] A.G.Roca, M.P.Morales, K.O'Grady and C.J.Serna, "Structural and magnetic properties of uniform magnetite nanoparticles prepared by high temperature decomposition of organic precursors," *Nanotechnology*, Vol.17, pp.2783-2788, (2006).
[32] P.Pradhan, J.Giri, G.Samanta, H.D.Sarma, K.P.Mishra, J.Bellare, R.Banerjee, and D.Bahadur, "Comparative evaluation of heating ability and biocompatibility of different ferrite-based magnetic fluids for hyperthermia application," *Journal of Biomedical Materials Research Part B:Applied Biomaterial*, Vol.30630, pp.12-22, (2006).
[33] S.Ghosh, T.Das, S.Chakraborty, and S.K.Das, "Predicting DNA-mediated drug delivery in interior carcinoma using electromagnetically excited nanoparticles," *Computers in Biology and Medicine*, Vol.41, pp.771-779, (2011).
[34] E.Gedik, H.Kurt, Z.Recebli, and C.Balan, "Two-dimensional CFD simulation of magnetorheological fluid between two fixed parallel plates applied external magnetic field," *Computers and Fluids*, Vol.63, pp.128-134, (2012).
[35] Q.A.Pankhurst, J.Connolly, S.K.Jones, and J.Dobson, "Applications of magnetic nanoparticles in biomedicine," *Journal of Physics D:Applied Physics*, Vol.36, pp.R167-R181, (2003).
[36] C.M.Chang, W.T.Cheng, W.J.Liu, H.W.Cheng, C.E.Huang, and S.W.Du, "Thermal flow of fluid with magnetic particles in the presence of magnetic field," *International Communications in Heat and Mass Transfer*, Vol.37, pp.801-808, (2010).
[37] H.Aminfar, M.Mohammadpourfard, and F.Ghaderi, "Two-phase simulation of non-uniform magnetic field effects on biofluid(blood) with magnetic nanoparticles through a collapsible tube," *Journal of Magnetism and Magnetic Materials,* Vol.332, pp.172-179, (2013).
[38] M.R.Habibi, M.Ghassemi, M.H.Hamedi, "Analysis of high gradient magnetic field effects on distribution of nanoparticles injected into pulsatile blood stream," *Journal of Magnetism and Magnetic Materials*, Vol.324, pp.1473-1482, (2012).
[39] M.Ashtiani, S.H.Hashemabadi, A.Ghaffari, "A review on magnetorheological fluid preparation and stabilization," *Journal of Magnetism and Magnetic Materials*, Vol.374, pp.716-730, (2015).
[40] S.Kenjeres, "Numerical analysis of blood flow in realistic arteries subjected to strong non-uniform magnetic fields," *International Journal of Heat and Fluid Flow*, Vol.29, pp.752-764, (2008).
[41] M.Gonzales-Weimuller, M.Zeisberger, and K.M.Krishnan, "Size-dependent heating rates of iron oxide nanoparticles for magnetic fluid hyperthermia," *Journal of Magnetism and Magnetic Materials*, Vol.321, pp.1947-1950, (2009).
[42] X.L.Liu, H.M.Fan, J.B.Yi, Y.Yang, E.S.G.Choo, J.M.Xue, D.D.Fan, and J.Ding, "Optimization of surface coating on Fe_3O_4 nanoparticles for high performance magnetic hyperthermia agents," *Journal of Materials Chemistry*, Vol.22, pp.8235-8244, (2012).
[43] M.R.Barati, C.Selomulya, and K.Suzuki, "Particle size dependence of heating power in $MgFe_2O_4$ nanoparticles for hyperthermia therapy application," *Journal of Applied*

Physics, Vol.115, No.17B522, pp.1-3, (2014).

[44] P.de la Presa, Y.Luengo, M.Multigner, R.Costo, M.P.Morales, G.Rivero, and A.Hernando, "Study of heating efficiency as a function of concentration, size, and applied field in γ-Fe_2O_3 nanoparticles," *Journal of Physical Chemistry C*, Vol.116, pp.25602-25610, (2012).

[45] M.Song, Y.Zhang, S.Hu, L.Song, J.Dong, Z.Chen, and N.Gu, "Influence of morphology and surface exchange reaction on magnetic properties of monodisperse magnetite nanoparticles," *Colloids Surface A.*,Vol.408, pp.114-121, (2012).

[46] P.Hugounenq, M.Levy, D.Alloyeau, L.Lartigue, E.Dubois, V.Cabuil, C.Ricolleau, S.Roux, C.Wilhelm, F.Gazeau, and R.Bazzi, "Iron oxide monocrystalline nanoflowers for highly efficient magnetic hyperthermia," *Journal of Physical Chemistry C.*, Vol.116, pp.15702-15712, (2012).

[47] P.B.Shete, R.M.Patil, N.D.Thorat, A.Prasad, R.S.Ningthoujam, S.J.Ghosh, and S.H.Pawar, "Magnetic chitosan nanocomposite for hyperthermia therapy application: Preparation, characterization and in vitro experiments," *Applied Surface Science*, Vol.288, pp.149-157, (2014).

[48] N.D.Thorat, V.M.Khot, A.B.Salunkhe, A.I.Prasad, R.S.Ningthoujam, and S.H.Pawar, "Surface functionalized LSMO nanoparticles with improved colloidal stability for hyperthermia applications," *Journal of Physics D: Applied Physics*, Vol.46, No.10, pp.105003, (2013).

[49] N.D.Thorat, V.M.Khot, A.B.Salunkhe, R.S.Ningthoujam, and S.H.Pawar, "Functionalization of $La_{0.7}Sr_{0.3}MnO_3$ nanoparticles with polymer: Studies on enhanced hyperthermia and biocompatibility properties for biomedical applications," *Colloids and Surfaces B:Biointerfaces*, Vol.104, pp.40-47, (2013).

[50] R.Kappiyoor, M.Liangruksa,R.Ganguly, and I.K.Puri,"The effects of magnetic nanoparticle properties on magnetic fluid hyperthermia," *Journal of Applied Physics*, Vol.108, pp.-094702-1 to 094702-8 , (2010).

[51] A.Jordan, P.Wust, H.Fähling, W.John, A.Hinz, and R.Felix, "Inductive heating of ferromagnetic particles and magnetic fluids:physical evaluation of their potential for hyperthermia," *International Journal of Hyperthermia,* Vol.25, No.7, pp.499-511, (1993).

[52] C.CF, others, "Synthesis and evaluation of colloidal magnetic iron oxides for the site-specific radiofrequency-induced hyperthermia of cancer," *Journal of Magnetism and Magnetic Materials*, Vol.122, No.1-3, pp.374-378, (1993).

[53] M.Kallumadil, M.Tada, T.Nakagawa, M.Abe, P.Southern, and Q.A.Pankhurst, "Suitability of commercial colloids for magnetic hyperthermia," *Journal of Magnetism and Magnetic Materials*, Vol.321, No.10, pp.1509-1513, (2009).

[54] V.S.Kalambur, B.Han, B.E.Hammer, T.W.Shield, and J.C.Bischof, "In-vitro characterization of movement, heating, and visualization of magnetic nanoparticles for biomedical applications," *Nanotechnology*, Vol.16, pp.1221, (2005).

[55] I.Hilger, K.Frühauf, W.Andrä, R.Hiergeist, R.Hergt, and W.A,Kaiser, "Heating potential of iron oxides for therapeutic purposes in interventional radiology," *Academic Radiology*, Vol.9, No.2, pp.198-202, (2002).

[56] M.Ma, Y.Wu, J.Zhou, Y.Sun, Y.Zhang, and N.Gu, "Size dependence of specific power absorption of Fe_3O_4 particles in AC magnetic field," *Journal of Magnetism and Magnetic Materials*, Vol.268, No.1-2, pp.33-39, (2004).

[57] R.Hergt, W.Andrä, C.G.d'Ambly, I.Hilger, W.A.Kaiser, U.Richter, and H.G.Schmidt, "Physical limits of hyperthermia using magnetite fine particles," *IEEE Transactions on Magnetics*, Vol.34, No.5, pp.3745-3754, (1998).

[58] N.A.Brusentsov, V.V.Gogosov, T.N.Brusentsova, A.V.Sergeev, N.Y.Jurchenko, A.A.Kuznetsov, O.A.Kuznetsov, and L.I.Shumakov, "Evaluation of ferromagnetic fluids and suspensions for the site-specific radiofrequency-induced hyperthermia of MX11 sarcoma cells in vitro," *Journal of Magnetism and Magnetic Materials*, Vol.225, No.1-2, pp.113-117, (2001).

[59] R.C.O'Handley, "Modern magnetic materials:principles and applications," *Publisher Wiley.*

[60] T.L.Kline, Y.H.Xu, Y.Jing, and J.P.Wang, "Biocompatible high-moment FeCo-Au magnetic nanoparticles for magnetic hyperthermia treatment optimization," *Journal of Magnetism and Magnetic Materials*,Vol.321, No.10, pp.1525-1528, (2009).

[61] Z.Li, M.Kawashita, N.Araki, M.Mitsumori, and M.Hiraoka et al., "Magnetic nanoparticles with high heating efficiencies for application in the hyperthermia of cancer," *Materials Science and Engineering C.*, Vol.30, pp.990-996, (2010).

[62] I.dos Santos, D.Haemmerich, C.Pinheiro, and A.da Rocha, "Effect of variable heat transfer coefficient on tissue temperature next to a large vessel during radiofrequency tumor ablation," *Biomedical Engineering* Online 7:21, (2008).

[63] AL van de Ven, P.Kim, O.Haley, J.R.Fakhoury, G.Adriani, et al., "Rapid tumoritropic accumulation of systematically injected plateloid particles and their biodistribution," *Journal of Control Release*, Vol.158, pp.148-155, (2012).

[64] J.P.Fortin, C.Wilhelm, J.Servais, C.Ménager, J.C.Bacri, and F.Gazeau, "Size-sorted anionic iron-oxide nanomagnets as colloidal mediators for magnetic hyperthermia," *Journal of the American Chemical Society*, Vol.129, No.9, pp.2628-2635, (2007).

[65] J.P.Fortin, F.Gazeau, and C.Wilhelm, "Intracellular heating of living cells through Néel relaxation of magnetic nanoparticles," *European Biophysics Journal*, Vol.37, No.2, pp.223-228, (2008).

[66] M.Johannsen, U.Gneveckow, L.Eckelt, A.Feussner, N.Waldöfner, R.Scholz, S.Deger, P.Wust, S.A.Loening, and A.Jordan, "Clinical hyperthermia of prostate cancer using magnetic nanoparticles:Presentation of a new interstitial technique," *International Journal of Hyperthermia*, Vol.21, pp.637-647, (2005).

[67] M.Johannsen, U.Gneveckow, B.Thiesen, K.Taymoorian, C.H.Cho, N.Waldöfner, R.Scholz, A.Jordan, S.A.Loening, and P.Wust, "Thermotherapy of prostate cancer using magnetic nanoparticles: Feasibility, imaging, and three-dimensional temperature distribution," *European Urology*, Vol.52, No.6, pp.1653-1661, (2007).

[68] P.Wust, U.Gneveckow, M.Johannsen, D.Bohmer, T.Henkel, F.Kahmann, J.Sehouli, R.Felix, J.Ricke, and A.Jordan, "Magnetic nanoparticles for interstitial thermotherapy feasibility, tolerance, and achieved temperature" *International Journal of Hyperthermia*, Vol.22, No.8, pp.673-685, (2006).

[69] X.Wang, H.Gu, and Z.Yang, "The heating effect of magnetic fluids in an alternating magnetic field," *Journal of Magnetism and Magnetic Materials*, Vol.293, No.1, pp.334-340, (2005).

[70] I. Hilger, R.Hergt, W.A.Kaiser, "Effects of magnetic thermoablation in muscle tissue using iron oxide particles," *Invest Radiology*, Vol.35, No.3, pp.170-179, (2000).

[71] A.Jordan, P.Wust, H.Fähling, W.John, A.Hinz, and R.Felix, "Inductive heating of

ferromagnetic particles and magnetic fluids:Physical evaluation of their potential for hyperthermia," *International Journal of Hyperthermia*, Vol.9, No.1, pp.51-68, (1993).

[72] A.Jordan, R.Scholz, P.Wust, H.Fähling, J.Krause, W.Wlodarczyk, B.Sander, T.Vogl, and R.Felix, "Effects of magnetic fluid hyperthermia (MFH) on C3H mammary carcinoma in vivo," *International Journal of Hyperthermia*, Vol.13, No.6, pp.587-605, (1997).

[73] C.L.Dennis, A.J.Jackson, J.A.Borchers, P.J.Hoopes, R.Strawbridge, A.R.Foreman, J.van Lierop, C.Grüttner, and R.Ivkov,"Nearly complete regression of tumors via collective behavior of magnetic nanoparticles in hyperthermia," *Nanotechnology,* Vol.20, No.395103, (2009).

[74] R.K.Gilchrist, R.Medal, W.D.Shorey, R.C.Hanselman, J.C.Parrott, and C. B.Taylor, "Selective inductive heating of lymph nodes," *Annals of Surgery*, Vol.146, No.596, (1957).

[75] R.T.Gordon, J.R.Hines, and D.Gordon,"Intracellular hyperthermia: A biophysical approach to cancer treatment via intracellular temperature and biophysical alterations" *Medical Hypotheses*, Vol.5, pp.83–102, (1979).

[76] A.Ito, K.Tanaka, K.Kondo, M.Shinkai, H.Honda, K.Matsumoto, T.Saida, and T.Kobayashi, "Tumor regression by combined immunotherapy and hyperthermia using magnetic nanoparticles in an experimental subcutaneous murine melanoma," *Cancer Science*, Vol.94, pp.308–313, (2003).

[77] M.Johannsen, B.Thiesen, U.Gneveckow, K.Taymoorian, N.Waldöfner, R.Scholz, S.Deger, K.Jung, S.A.Loening, and A.Jordan, "Thermotherapy using magnetic nanoparticles combined with external radiation in an orthotopic rat model of prostate cancer," *The Prostate*, Vol.66, pp.97–104, (2006).

[78] M.Johannsen, B.Thiesen, A.Jordan, K.Taymoorian, U.Gneveckow, N.Waldöfner, R.Scholz, M.Koch, M.Lein, K.Jung, and S.Loening, "Magnetic fluid hyperthermia (MFH) reduces prostate cancer growth in the orthotopic dunning R3327 rat model," *The Prostate*, Vol.64, pp.283–292, (2005).

[79] A.Jordan, R.Scholz, P.Wust, H.Fähling, J.Krause, W.Wlodarczyk, B. Sander, T.Vogl, and R.Felix, "Effects of magnetic fluid hyperthermia (MFH) on C3H mammary carcinoma in vivo," *International Journal of Hyperthermia*, Vol.13, pp.587–605, (1997).

[80] N.Kawai, A.Ito, Y.Nakahara, M.Futakuchi, T.Shirai, H.Honda, T.Kobayashi, and K.Kohri, "Anticancer effect of hyperthermia on prostate cancer mediated by magnetite cationic liposomes and immune-response induction in transplanted syngeneic rats," *The Prostate*, Vol. 64, pp.373–381, (2005).

[81] B.Le, M.Shinkai, T.Kitade, H.Honda, J.Yoshida, T.Wakabayashi, and T.Kobayashi, "Preparation of tumor-specific magnetoliposomes and their application for hyperthermia," *Journal of Chemical Engineering of Japan*, Vol. 34, pp.66–72, (2001).

[82] J.Motoyama, N.Yamashita, T.Morino, M.Tanaka, T.Kobayashi, and H.Honda, "Hyperthermic treatment of DMBA-induced rat mammary cancer using magnetic nanoparticles," *BioMagnetic Research and Technology*, Vol.6, No.2, (2008).

[83] A.Natarajan, C.Gruettner, R.Ivkov, G.L.DeNardo, G.Mirick, A.Yuan, A. Foreman, and S.J.DeNardo, "NanoFerrite particle based radioimmuno- nanoparticles: Binding affinity and in vivo pharmacokinetics," *Bioconjugate Chemistry*, Vol.19, pp.1211–1218, (2008).

[84] T.Ohno, T.Wakabayashi, A.Takemura, J.Yoshida, A.Ito, M.Shinkai, H.Honda, and T.Kobayashi, "Effective solitary hyperthermia treatment of malignant glioma using stick type CMC-magnetite:In vivo study," *Journal of Neuro-Oncology*, Vol.56, pp.233–239, (2002).

[85] K.Tanaka, A.Ito, T.Kobayashi, T.Kawamura, S.Shimada, K.Matsumoto, T.Saida, and H.Honda, "Intratumoral injection of immature dendritic cells enhances antitumor effect of hyperthermia using magnetic nanoparticles," *The International Journal of Cancer*, Vol.116, pp.624–633, (2005).

[86] M.Yanase, M.Shinkai, H.Honda, T.Wakabayashi, J.Yoshida, and T.Kobayashi, "Antitumor immunity induction by intracellular hyperthermia using magnetite cationic liposomes," *Cancer Science*, Vol.89, pp.775–782, (1998).

[87] M.Shinkai, M.Yanase, M.Suzuki, H.Honda, T.Wakabayahi, J.Yoshida, and T.Kobayahi, "Intracellular hyperthermia for cancer using magnetite cationic liposomes," *Journal of Magnetism and Magnetic Materials*, Vol.194, pp.176–184, (1999).

[88] I.Hilger, R.Hiergeist, R.Hergt, K.Winnefeld, H.Schubert, and W.A.Kaiser, "Thermal ablation of tumors using magnetic nanoparticles: an in vivo feasibility study," *Investigative Radiology*, Vol.37, pp.580, (2002).

[89] K.R.Sharma, "Transport phenomena in biomedical engineering," *McGraw-Hill*,*ISBN 978-0-07-166398-4*,*New York*,*USA*, (2010).

[90] Y.G.Lv, and J.Liu, "Effect of transient temperature on thermoreceptor response and thermal sensation," *Building and Environment*, Vol.42, pp.656-664, (2007).

[91] M.Malekigorji, A.DM.Curtis, and C.Hoskins "The use of iron oxide nanoparticles for pancreatic cancer therapy," *Journal of Nanomedicine Research*, Vol.1, No.1, pp.1-12, (2014).

[92] W.J.Atkinson, I.A.Brezovich, and D.P.Chakraborty, "Useable frequencies in hyperthermia with thermal seeds," *IEEE Transactions on Biomedical Engineering*, Vol.1, pp.70-75, (2007).

[93] A.Hervault, and N.T.Kim Thanh, "Magnetic nanoparticle-based therapeutic agents for thermo-chemotherapy treatment of cancer," *Nanoscale*, Vol.6, pp.11553-11573, (2014).

[94] J.H.Park, G.Saravanakumar, K.Kim, and I.C.Kwon, "Targeted delivery of low molecular drugs using chitosan and its derivatives," *Advanced Drug Delivery Reviews*, Vol.62, pp.28–41, (2010).

[95] V.V.Mody, A.Cox, S.Shah, A.Singh, W.Bevins and H.Parihar, "Magnetic nanoparticle drug delivery systems for targeting tumor," *Applied Nanoscience,* Vol.4, pp.385-392, (2014).

[96] Akira Ito, Masashige Shinkai, Hiroyuki Honda, and Takeshi Kobayashi, "Review on Medical Application of Functionalized Magnetic Nanoparticles," *Journal of Bioscience and Bioengineering*, Vol.100, (2005).

[97] Challa S.S.R.Kumar, J. H., *Nanofabrication: Towards Biomedical Applications*, Germany: Wiley-VCH, Weinheim, (2005).

[98] Arruebo Manuel, R.F.-P., "Magnetic nanoparticles for drug delivery," *Nanotoday*, pp. 22-32, (2007).

[99] P.Kaur, M.L.Aliru, A.S.Chadha, A.Asea, and S.Krishnan, Review Article, "Hyperthermia using nanoparticles- Promises and pitfalls," *International Journal of Hyperthermia*, Vol.32, No.1, (2016).

[100] I.Hilger, "In-vivo applications of magnetic nanoparticle hyperthermia," *International*

Journal of Hyperthermia, Vol.29, No.8, pp.828-834, (2013).

[101] Suzanne C.Smeltzer, and B.Bare, *Textbook on Medical Surgical Nursing*, *ch-48*, *pp.1453*, (2001).

[102] J.J.W.Lagendijk, P.M.Van den Berg, J.Bach Anderson, J.W.Hand, F.Bardati, N.K.Uzunoglu et al., editors, "Treatment Planning and Modelling in Hyperthermia:A Task Group Report, ,"Tor Vergata, Rome, *Postgraduate School of Medical Physics*, II *University of Rome*, (1992).

[103] R.K.Gilchrist, R.Medal, W.D.Shorey, R.C.Hanselman, J.C.Parrott, and C.B.Taylor, "Selective inductive heating of lymph nodes," *The Annals of Surgery*, Vol.146, pp.596-606, (1957).

[104] B.Kozissnik, A.C.Bohorquez, J.Dobson, and C.Rinaldi, Review Article, "Magnetic fluid hyperthermia: Advances, challenges, and opportunity," *International Journal of Hyperthermia*, Vol.29, No.8, pp.706-714, (2013).

[105] I.A.Brezovich and R.F.Meredith, "Practical aspects of ferromagnetic thermoseed hyperthermia," *Radiologic Clinics of North America*, Vol.27, pp.589-602, (1989).

[106] Q.A.Pankhurst, J.Connolly, S.K.Jones, and J.Dobson, "Applications of magnetic nanoparticles in biomedicine," *Journal of Physics D: Applied Physics*, Vol.36, pp.R167-R181, (2003).

[107] R. Hergt, and S.Dutz, "Magnetic particle hyperthermia-Biophysical limits of a visionary tumour therapy," *Journal of Magnetism and Magnetic Materials*, Vol.311, pp.187-192, (2007).

[108] B.W.Raaymakers, A.N.T.J Kotte, and J.J.W Lagendijk, "Discrete vasculature(DIVA) model simulating the thermal impact of individual blood vessels for In-vivo heat transfer," *Advances in Numerical Heat Transfer*, Vol.3, pp.121-148, (2009).

[109] J.D.Overgaard, M.C.C.Hulshof, G.Arcangeli, O.Dahl, O.Mella, S.M.Bentzen, "Hyperthermia as an adjuvant to radiation therapy of recurrent or metastatic malignant melanoma," A multi centre randomized trial by European Society for Hyperthermic Oncology, *International Journal of Hyperthermia*, Vol.25, pp.323-334, (2009).

[110] S.A.Sapareto, A.C.Perez, "Thermal dose expression in clinical hyperthermia and correlation with tumor response/control," *Cancer Research*, Vol.44, pp.4818-4825, (1984).

[111] E.Jones, "A randomized trial of hyperthermia and radiation for superficial tumors," *Journal of Clinical Oncology*, Vol.23, No.13, pp.3079-3085, (2005).

[112] D.Caruntu, G.Caruntu, O'Connor, and C.J.J, "Magnetic properties of variable- sized Fe_3O_4 nanoparticles synthesized from non-aqueous homogeneous solutions of polyols," *Journal of Physics D: Applied Physics*,Vol.40, pp.5801-5809, (2007).

[113] P.Guardia, A.Labarta, and X.Batlle, "Tuning the size, the shape, and the magnetic properties of iron-oxide nanoparticles," *Journal of Physical Chemistry C*, Vol.115, pp.390-396, (2011).

[114] C.Pereira, A.M.Pereira, C.Fernandes, M.Rocha, R.Mendes, M.Fernandez-Garcia, A.Guedes, P.B.Tavares, J.M.Greneche, J.P.Araujo, and C.Freire, "Superparamagnetic MFe_2O_4 (M=Fe,Co,Mn) nanoparticles:Tuning the particles size and magnetic properties through a novel one-step co-precipitation route," *Chemistry of Materials*, Vol.24, pp.1496-1504, (2012).

[115] S.Mornet, S.Vasseur, F.Grasset, and E.Duguet, "Magnetic nanoparticle design for medical diagnosis and therapy," *Journal of Materials Chemistry*, Vol.14, pp.2161-2175,

(2004).
[116] M.Jeun, S.Lee, J.Kang, A.Tomitaka, K.Kang, Y.Kim, Y.Takemura, K.Chung, J.Kwak, and S.Bae, "Physical limits of pure superparamagnetic Fe_3O_4 nanoparticles for a local hyperthermia agent in nanomedicine," *Applied Physics Letters*, Vol.100, pp.092406:1-092406:4, (2012).
[117] R.Muller, S.Dutz, A.Neeb, A.Cato, and M.Zeisberger, "Magnetic heating effect of nanoparticles with different sizes and size distribution," *Journal of Magnetism and Magnetic Materials*,Vol.328, pp.80-85, (2013).
[118] E.C.Fear, X.Li, S.C.Hagness, and M.A.Stuchly, "Confocal microwave imaging for breast cancer detection: Localization of tumors in three dimensions," *IEEE Transactions on Biomedical Engineering*, Vol.49, No.8, pp.812-822, (2002).
[119] J.D.Shea, P.Kosmas, B.D.V.Veen, and S.C.Hagness, "Contrast enhanced microwave imaging of breast tumors: A Computational study using 3-D realistic numerical phantoms," *Inverse Problems,* Vol.26, pp.1-22, (2010).
[120] M.Lahonian, A.A.Golneshan, "Numerical study of temperature distribution in a spherical tissue in magnetic fluid hyperthermia using lattice Boltzmann method," *IEEE Trans Nanobio*, Vol.10, No.4, pp.262-268, (2011).

WEB/ONLINE REFERENCES

[W.1] D.Sardari, and N.Verga, Book Title- "Current cancer treatment-Novel beyond conventional approaches," Chapter-21," *Cancer treatment with hyperthermia,*" pp.455-474, (2011), Available from: http://www.intechopen.com/books/current-cancer-treatment-novel-beyond-conventional-approaches/cancer-treatment-with-hyperthermia, [Accessed as on 16/08/2015].

[W.2] A.Zolfaghari, and M.Maerefat, Book Title-"Developments in heat transfer," Chapter-9,"*Bioheat transfer,*" pp.153-170, (2011), Available from: http://www.intechopen.com/books/developments-in-heat-transfer/bioheat-transfer, [Accessed as on 26/02/2015].

[W.3] M.L.Etheridge, N.Manucherabadi, R.Franklin, and J.C.Bischof, Book Title-"," Chapter-20,"*Superparamagnetic iron oxide nanoparticle heating: A basic tutorial*," pp.1-23, (2013), Available from: http://nebula.wsimg.com/d8257f0acc9e9ed1281280fc2674a0d3?AccessKeyId=7DFAEE857476F4D911D3&disposition=0., [Accessed as on 16/08/2015].

[W.4] M.Lahonian, Book title-"Hyperthermia," Chapter-4,"*Diffusion of magnetic nanoparticles within a biological tissue during magnetic fluid hyperthermia*," pp.129-144, (2012), Available from: http://www.intechopen.com/books/hyperthermia/diffusion-of-magnetic-nanoparticles-within-a-biological-tissue-during-magnetic-fluid-hyperthermia ,or http://dx.doi.org/10.5772/52305,[Accessed as on 5/02/2016].

[W.5] American Cancer Society, "*Cancer Facts & Figures 2016,"* Atlanta: American Cancer Society, Inc.(2016)

[W.6] American Cancer Society, "*Breast Cancer Facts & Figures 2015-2016,"* Atlanta: American Cancer Society, Inc.(2015).

[W.7] Availablefrom:http://www.hopkinsmedicine.org/healthlibrary/test_procedures/gynecology/breast_magnetic_resonance_imaging_mri_92,p09110/, [Accessed as on 26/02/2016].

[W.8] Anatomical Planes,http://www.youmedicine.arduanet.it/it/youmedicine-flash/876-basic-terms-in-topographic-anatomy-anatomic-planes-and-directions,[Accessed as on 17/02/2016].

[W.9] 78 Steps Health Journal-Plasma Membrane also Human Physiology by R.F.Schmidt and G.Thews, Available from: http://www.78stepshealth.us/skeletal-muscle-2/body-temperatures-and-heat-transfer-in-the-body.html[Accessed as on 18/03/2016].

[W.10] Isotherms of human body, Available from: https://books.google.co.in/books?id=8WrmCAAAQBAJ&pg=PA534&lpg=PA534&dq=Isotherms+of+human+body&source=bl&ots=9ZcBwfz8Dy&sig=vhniQ4A1Rb9CfbPSZFun5RBB2Mo&hl=en&sa=X&ved=0ahUKEwiOs8jk9bHMAhUOG44KHXxaBEAQ6AEIGzAA#v=onepage&q=Isotherms%20of%20human%20body&f=false[Accessed as on 14/04/2016].

APPENDIX-A

PERMISSION CERTIFICATE

THAPAR UNIVERSITY
(Declared as Deemed-to-be-University u/s 3 of the UGC Act, 1956)
Thapar Technology Campus, Post Box No. 32
Patiala 147 004 Punjab India
Fax : +91-175-2364498, 2393005
URL : www.thapar.edu

The Head of Department,
Radio-diagnosis Department,
P.G.I.M.E.R,Sector-12,
Chandigarh.

Subject:-For providing CT Scan/micro-CT Scan dicom format data of "Breast Cancer Patient" for doing the analysis in COMSOL-MULTIPHYSICS Software by new technique of "Magnetic Nano-Particle Induced Hyperthermia" likely to be helpful as an additional healing treatment assisted with Chemotherapy or Radiotherapy.

Dear Concerned,

I am hereby sending one of our ME-Research Scholar Mr. Manpreet Singh who is been a regular student of ME-THERMAL ENGINEERING specialisation been offered by Mechanical Engineering Department.He is been doing research in field of Bio-Heat Transfer.His area of Thesis Dissertation is "BIO-HEAT TRANSFER ANALYSIS USING MAGNETIC-NANOPARTICLES INDUCED HYPERTHERMIA".Since, large number of female cancer patients die every year because of this noble cause.Since till date treatments available are chemotherapy or radiotherapy or at last surgically removing the breasts of cancer patients. "Bio-heat transfer analysis using Magnetic Nano-particles(MNP's) induced Hyperthermia" is an innovative field to do Magnetic Drug Targeting and to specially cure CARCINOMA(cancerous cells) or specifically to Tumors.This is an interdisciplinary study which will involve Heat-transfer/Fluid Mechanics in Biological Tissues and is a part of Bio-medical Engineering/Bio-mechanical Engineering/Tissue engineering.

As a part of this initiative been receiving enormous help earlier at various levels by various departments, hereby Mechanical Engineering Department with a ray of hope been requesting you to provide the CT Scan/Micro-CT Scan data in dicom format or other necessary information that would help our student in the best possible way. We are sure you will come forward to help the candidate.
Moreover,the student is been associated with

1. Dr.Saroj Kumar Mohapatra(Supervisor)
   Sr. Professor & Head, MED, Thapar University, Patiala
2. Dr.SanjeevSoni(Co-Supervisor)
   Senior Scientist,Biomedical Instrumentation
   CSIR -Central Scientific Instruments Organisation, Sector 30C-Chandigarh
3. Dr.Satbir Sehgal (Co-Supervisor)
   Professor & Dean Research, Mechanical Engineering Department,
   Chandigarh University, Gharuan(Punjab)

Yours Sincerely,

With warm regards,

(S.K.Mohapatra)
Sr. Professor& Head

Sr. Professor & Head
Mechanical Engineering Deptt.
Thapar University,
PATIALA-147004

17.2.11

डॉ० एन० खण्डेलवाल
DR. N. KHANDELWAL
प्राचार्य एवं अध्यक्ष
Professor & Head
रेडियोनिदान विभाग
Deptt. of Radiodiagnosis
पी० जी० आई०, चण्डीगढ़
P.G.I CHANDIGARH

APPENDIX-B

CONFLICT OF INTERESTS

The Authors don’t have any conflict of Ineterst with any one or any institution. The Authors alone are responsible for the content and writing.

APPENDIX-C

HYPERTHERMIA POSTER PRESENTATION

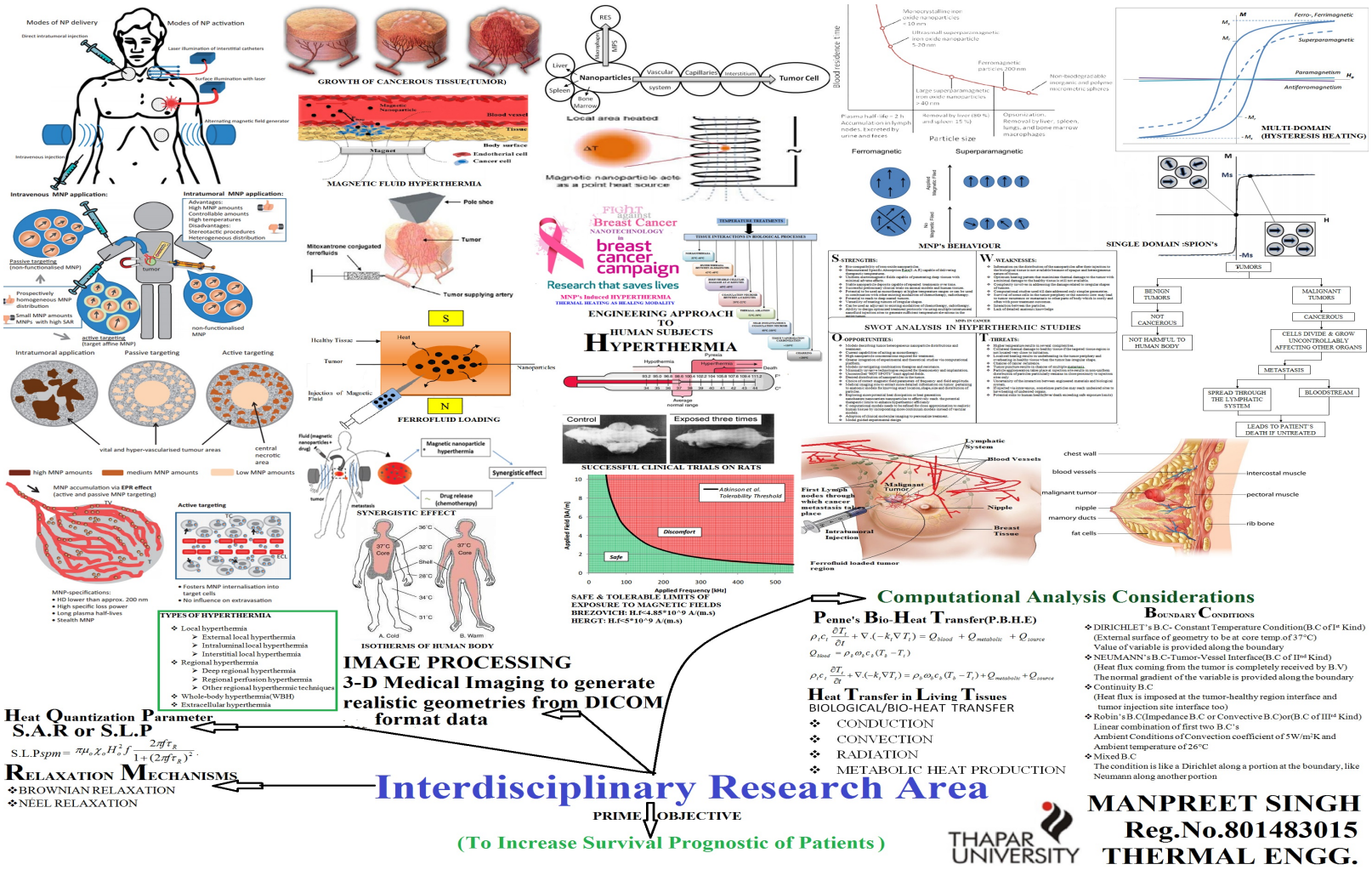

APPENDIX-D

DICOM DATA PROCESSING

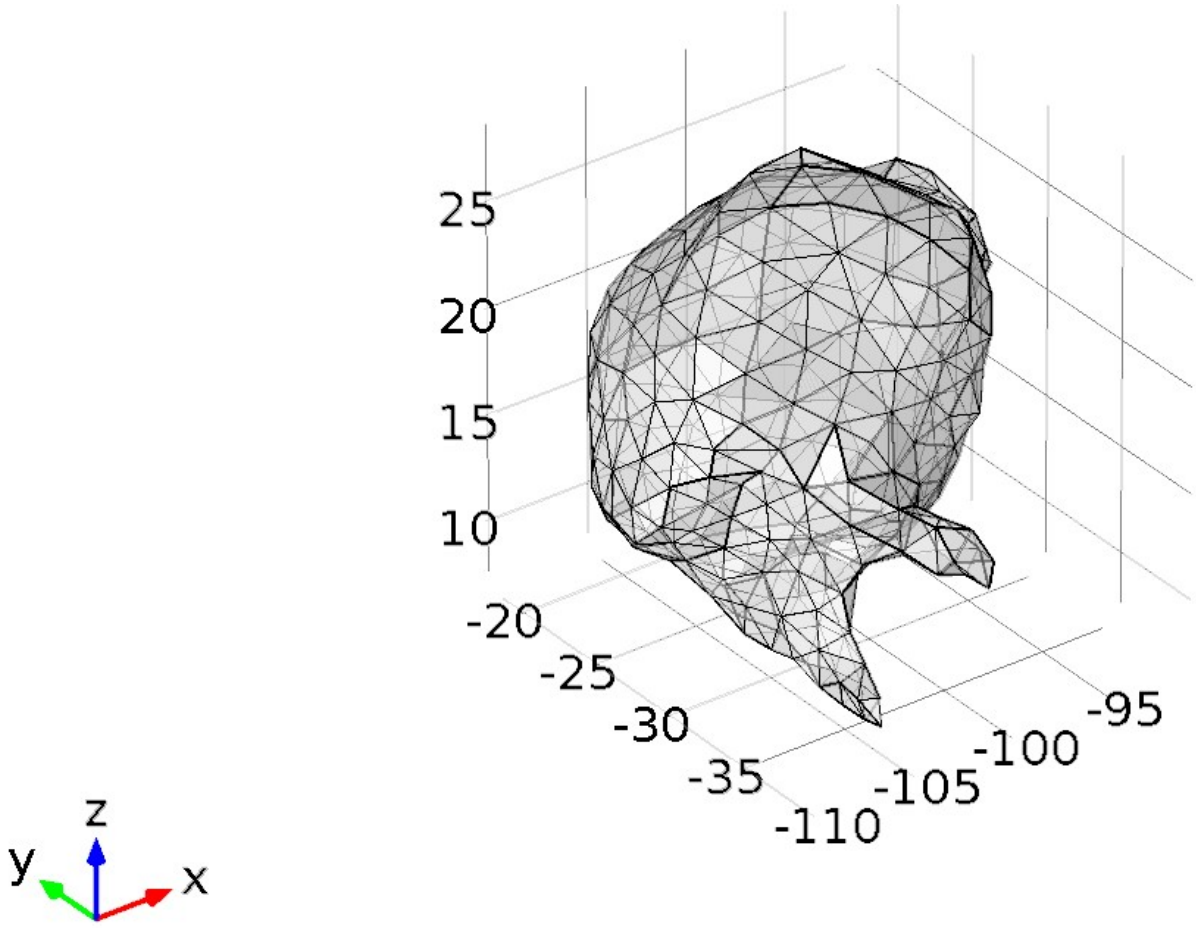

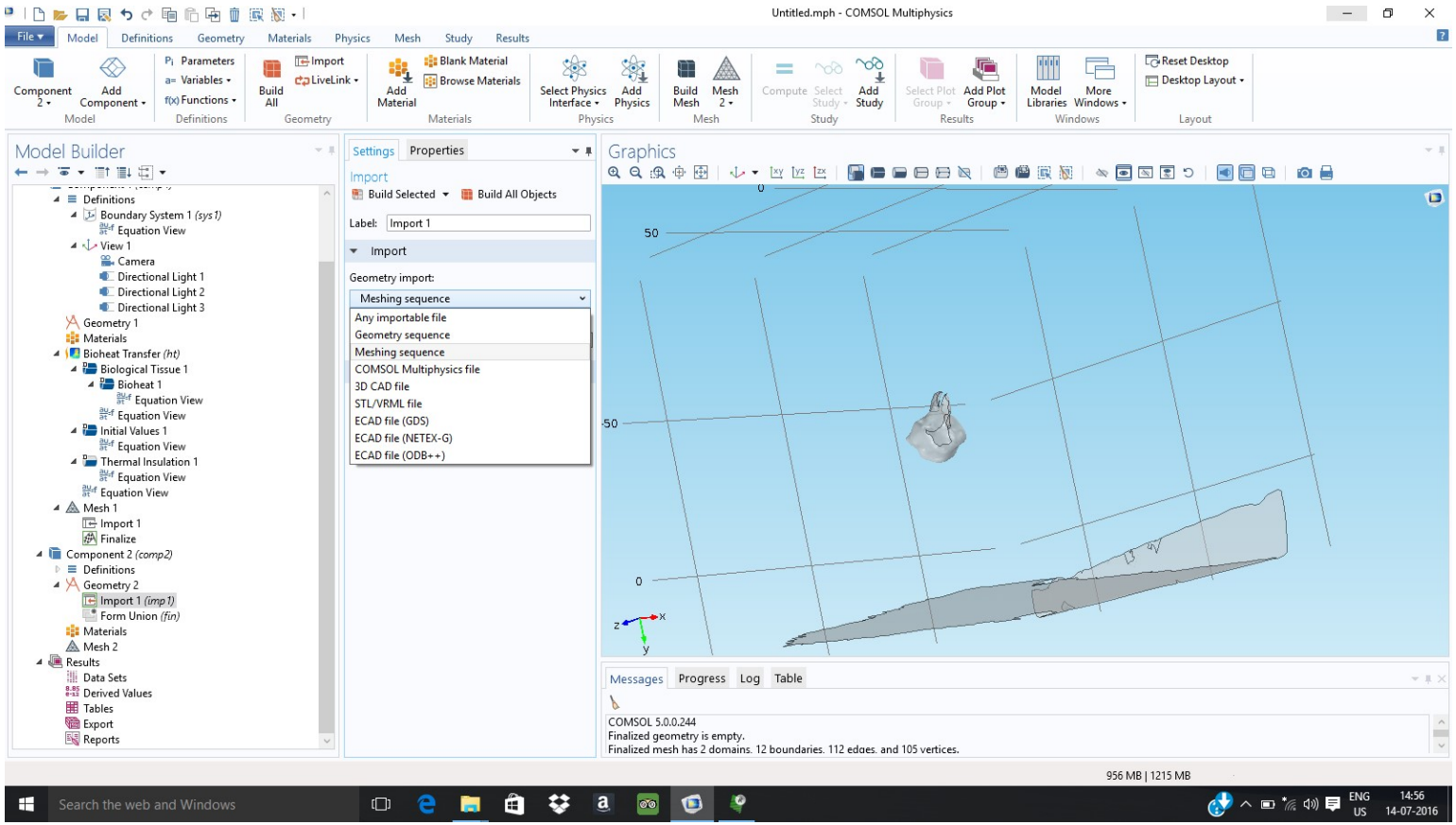
Untitled.mph - COMSOL Multiphysics
File
Model
Definitions
Geometry
Materials
Physics
Mesh
Study
Results
Component 2
Add Component
Parameters
Variables
Functions
Build All
Import
LiveLink
Add Material
Blank Material
Browse Materials
Select Physics Interface
Add Physics
Build Mesh
Mesh 2
Compute
Select Study
Add Study
Select Plot Group
Add Plot Group
Model Libraries
More Windows
Reset Desktop
Desktop Layout
Model Builder
Definitions
Boundary System 1 (sys1)
Equation View
View 1
Camera
Directional Light 1
Directional Light 2
Directional Light 3
Geometry 1
Materials
Bioheat Transfer (ht)
Biological Tissue 1
Bioheat 1
Initial Values 1
Thermal Insulation 1
Mesh 1
Import 1
Finalize
Component 2 (comp2)
Geometry 2
Import 1 (imp1)
Form Union (fin)
Mesh 2
Results
Data Sets
Derived Values
Tables
Export
Reports
Settings
Properties
Import
Build Selected
Build All Objects
Label:
Import 1
Geometry import:
Meshing sequence
Any importable file
Geometry sequence
Meshing sequence
COMSOL Multiphysics file
3D CAD file
STL/VRML file
ECAD file (GDS)
ECAD file (NETEX-G)
ECAD file (ODB++)
Graphics
Messages
Progress
Log
Table
COMSOL 5.0.0.244
Finalized geometry is empty.
Finalized mesh has 2 domains, 12 boundaries, 112 edges, and 105 vertices.
956 MB | 1215 MB
Search the web and Windows
ENG
US
14:56
14-07-2016

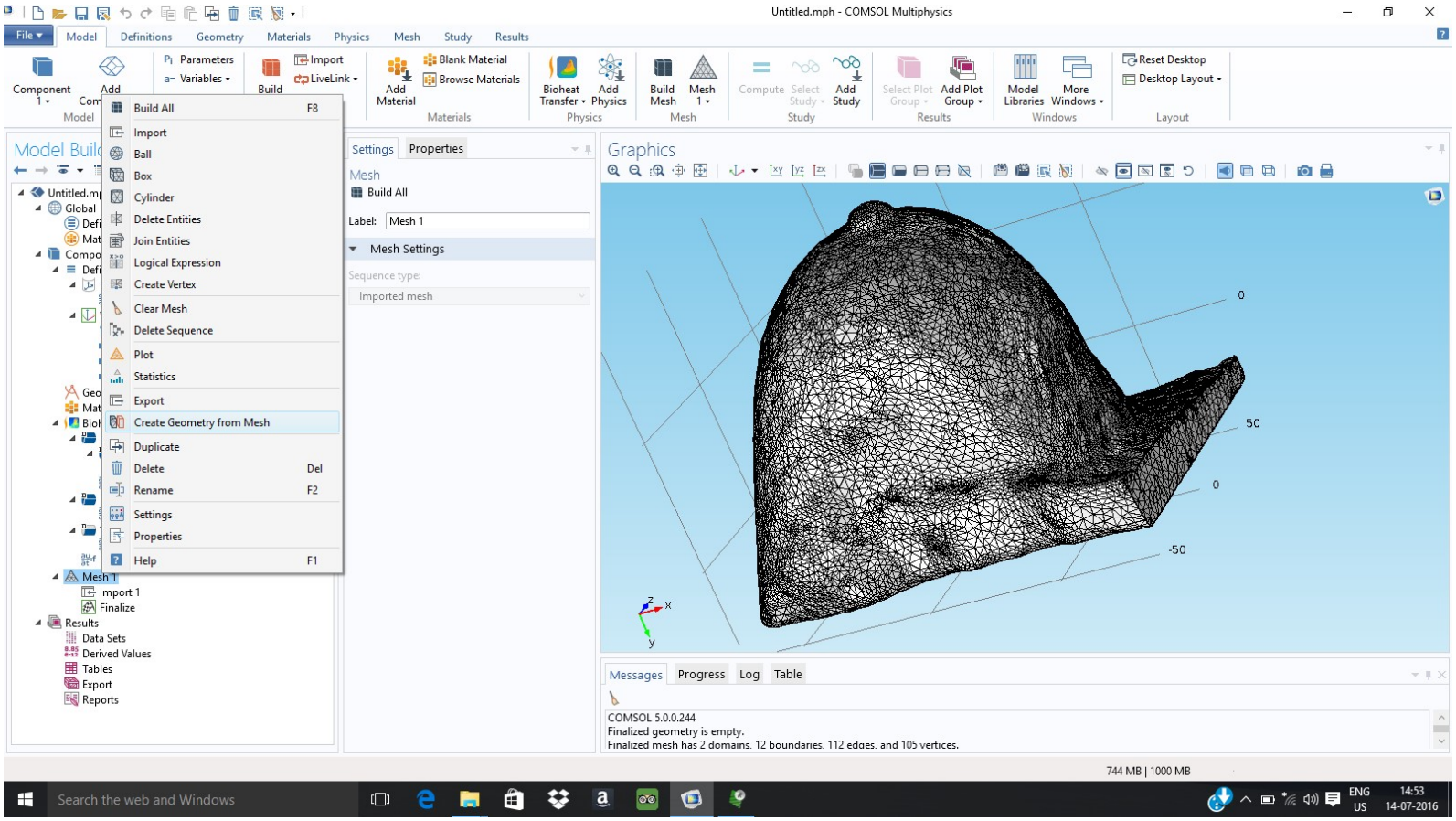
Untitled.mph - COMSOL Multiphysics
File
Model
Definitions
Geometry
Materials
Physics
Mesh
Study
Results
Component 1
Add
Parameters
Variables
Build
Import
LiveLink
Add Material
Blank Material
Browse Materials
Bioheat Transfer
Add Physics
Build Mesh
Mesh 1
Compute
Select Study
Add Study
Select Plot Group
Add Plot Group
Model Libraries
More Windows
Reset Desktop
Desktop Layout
Model Builder
Build All F8
Import
Ball
Box
Cylinder
Delete Entities
Join Entities
Logical Expression
Create Vertex
Clear Mesh
Delete Sequence
Plot
Statistics
Export
Create Geometry from Mesh
Duplicate
Delete Del
Rename F2
Settings
Properties
Help F1
Mesh 1
Import 1
Finalize
Results
Data Sets
Derived Values
Tables
Export
Reports
Settings
Properties
Mesh
Build All
Label: Mesh 1
Mesh Settings
Sequence type:
Imported mesh
Graphics
0
50
0
-50
Messages
Progress
Log
Table
COMSOL 5.0.0.244
Finalized geometry is empty.
Finalized mesh has 2 domains, 12 boundaries, 112 edges, and 105 vertices.
744 MB | 1000 MB
Search the web and Windows
ENG
US
14:53
14-07-2016

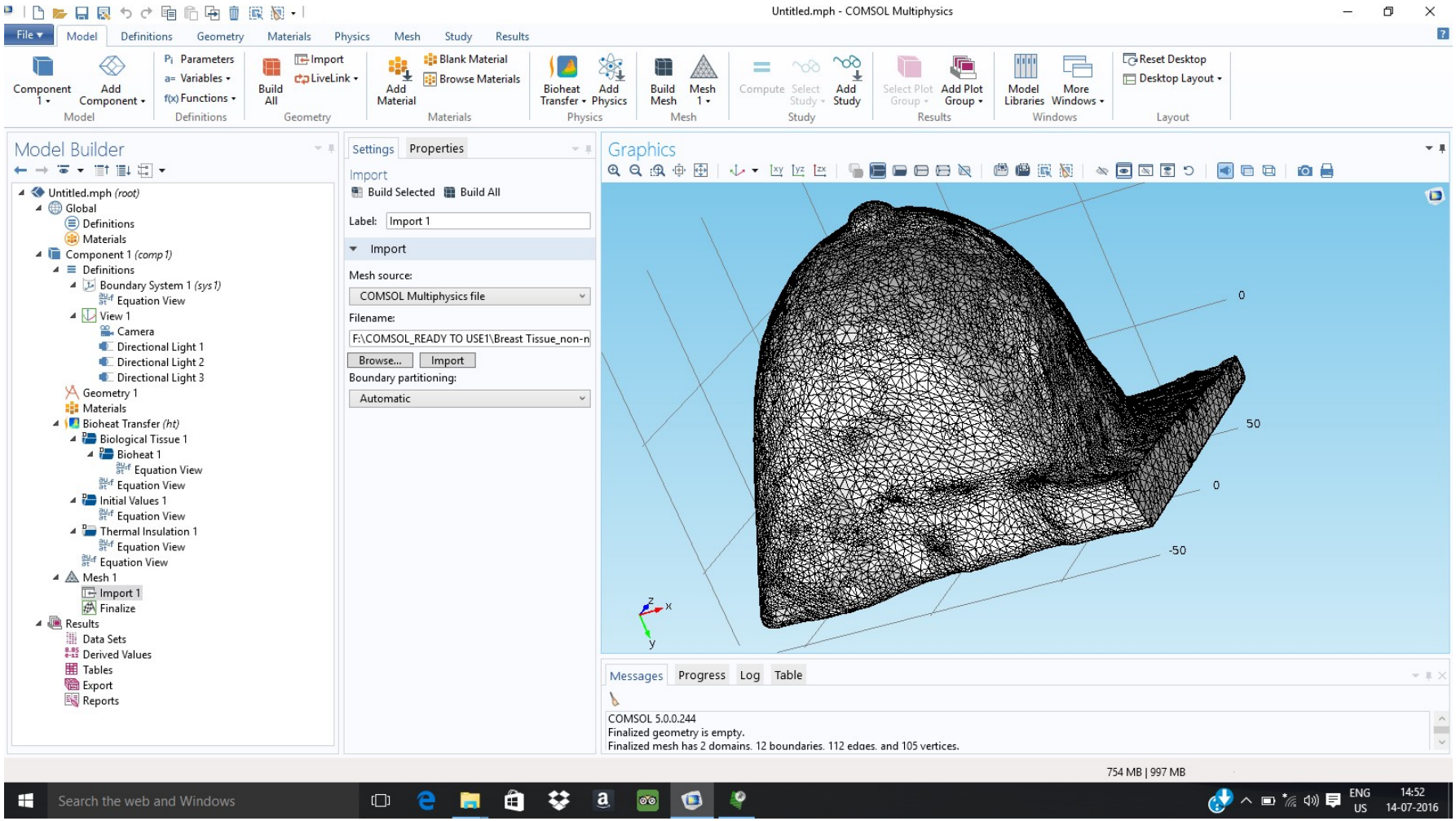
Untitled.mph - COMSOL Multiphysics
File
Model
Definitions
Geometry
Materials
Physics
Mesh
Study
Results
Component 1
Add Component
Parameters
Variables
Functions
Build All
Import
LiveLink
Add Material
Blank Material
Browse Materials
Bioheat Transfer
Add Physics
Build Mesh
Mesh 1
Compute
Select Study
Add Study
Select Plot Group
Add Plot Group
Model Libraries
More Windows
Reset Desktop
Desktop Layout
Model Builder
Untitled.mph (root)
Global
Definitions
Materials
Component 1 (comp 1)
Definitions
Boundary System 1 (sys1)
Equation View
View 1
Camera
Directional Light 1
Directional Light 2
Directional Light 3
Geometry 1
Materials
Bioheat Transfer (ht)
Biological Tissue 1
Bioheat 1
Equation View
Equation View
Initial Values 1
Equation View
Thermal Insulation 1
Equation View
Equation View
Mesh 1
Import 1
Finalize
Results
Data Sets
Derived Values
Tables
Export
Reports
Settings
Properties
Import
Build Selected
Build All
Label: Import 1
Import
Mesh source:
COMSOL Multiphysics file
Filename:
F:\COMSOL_READY TO USE1\Breast Tissue_non-n
Browse...
Import
Boundary partitioning:
Automatic
Graphics
0
50
0
-50
Messages
Progress
Log
Table
COMSOL 5.0.0.244
Finalized geometry is empty.
Finalized mesh has 2 domains, 12 boundaries, 112 edges, and 105 vertices.
754 MB | 997 MB
Search the web and Windows
ENG
US
14:52
14-07-2016

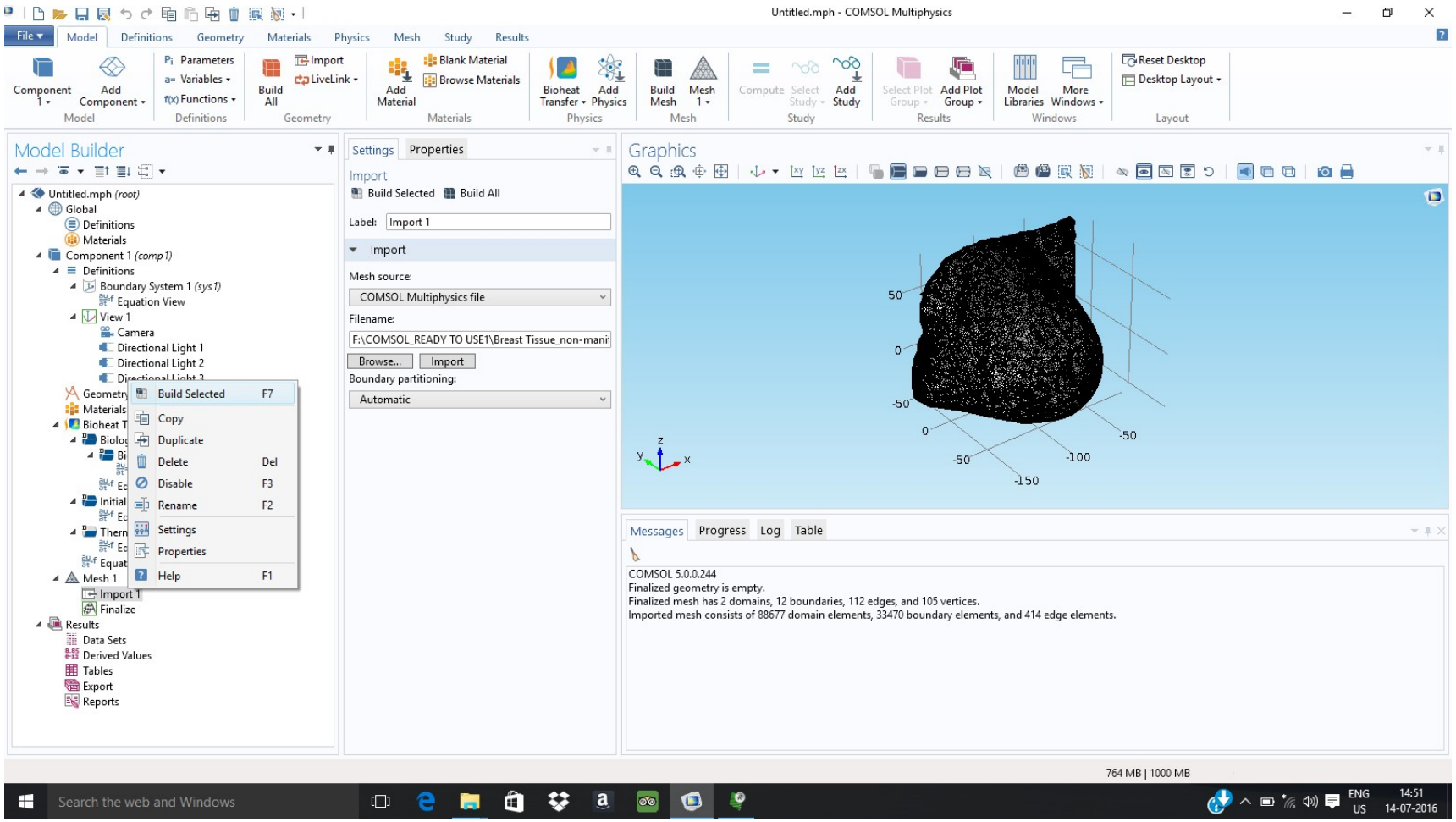
Untitled.mph - COMSOL Multiphysics
File
Model
Definitions
Geometry
Materials
Physics
Mesh
Study
Results
Component 1
Add Component
Parameters
Variables
Functions
Build All
Import
LiveLink
Add Material
Blank Material
Browse Materials
Bioheat Transfer
Add Physics
Build Mesh
Mesh 1
Compute
Select Study
Add Study
Select Plot Group
Add Plot Group
Model Libraries
More Windows
Reset Desktop
Desktop Layout
Model Builder
Untitled.mph (root)
Global
Definitions
Materials
Component 1 (comp 1)
Definitions
Boundary System 1 (sys 1)
Equation View
View 1
Camera
Directional Light 1
Directional Light 2
Geometry
Materials
Mesh 1
Import 1
Finalize
Results
Data Sets
Derived Values
Tables
Export
Reports
Build Selected F7
Copy
Duplicate
Delete Del
Disable F3
Rename F2
Settings
Properties
Help F1
Settings
Properties
Import
Build Selected
Build All
Label: Import 1
Import
Mesh source:
COMSOL Multiphysics file
Filename:
F:\COMSOL_READY TO USE1\Breast Tissue_non-manif
Browse...
Import
Boundary partitioning:
Automatic
Graphics
Messages
Progress
Log
Table
COMSOL 5.0.0.244
Finalized geometry is empty.
Finalized mesh has 2 domains, 12 boundaries, 112 edges, and 105 vertices.
Imported mesh consists of 88677 domain elements, 33470 boundary elements, and 414 edge elements.
764 MB | 1000 MB
Search the web and Windows
ENG US
14:51
14-07-2016

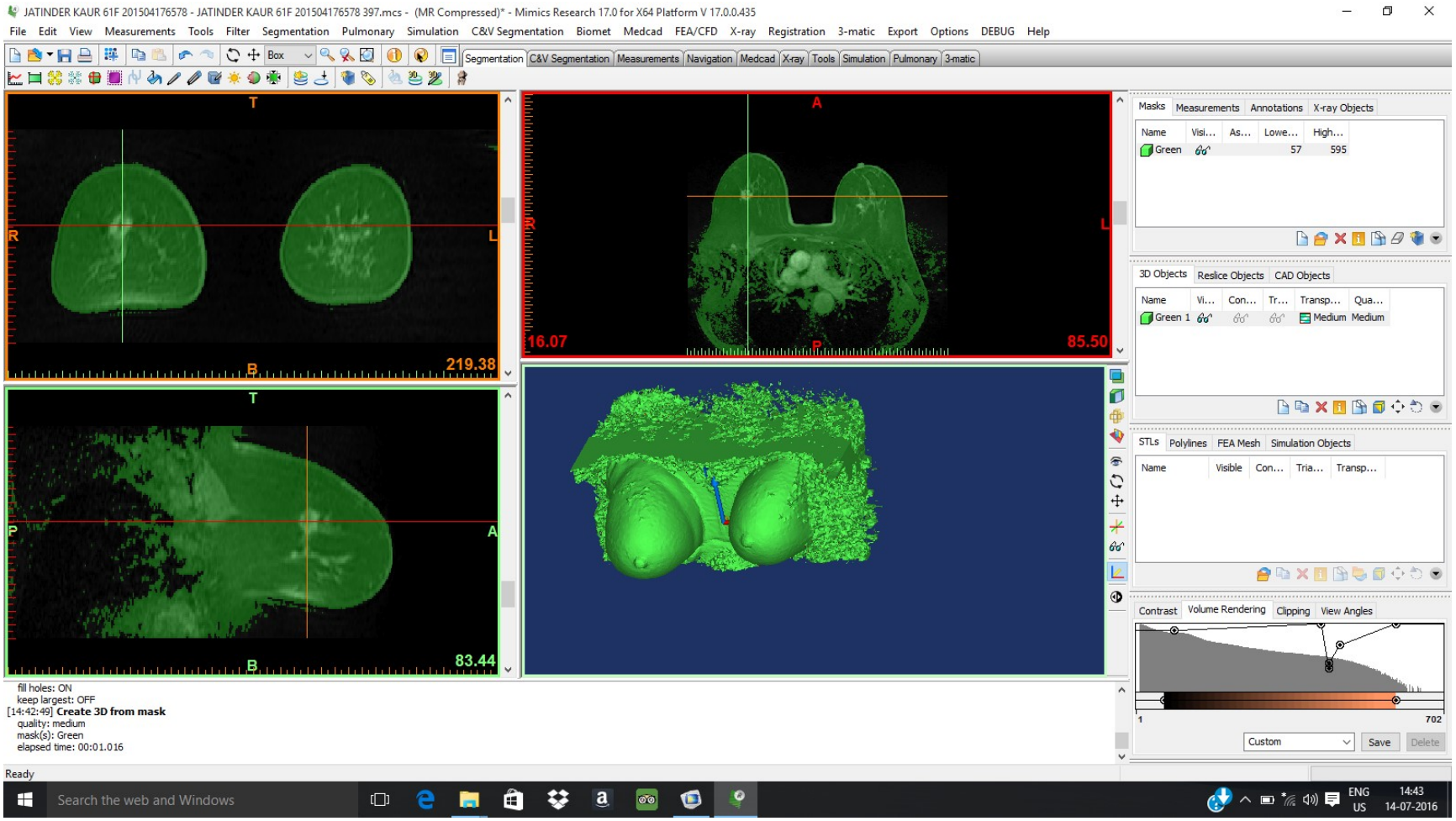
JATINDER KAUR 61F 201504176578 - JATINDER KAUR 61F 201504176578 397.mcs - (MR Compressed)* - Mimics Research 17.0 for X64 Platform V 17.0.0.435
File Edit View Measurements Tools Filter Segmentation Pulmonary Simulation C&V Segmentation Biomet Medcad FEA/CFD X-ray Registration 3-matic Export Options DEBUG Help
Segmentation C&V Segmentation Measurements Navigation Medcad X-ray Tools Simulation Pulmonary 3-matic
T
R
L
B
219.38
A
R
L
16.07
P
85.50
T
P
A
B
83.44
Masks Measurements Annotations X-ray Objects
Name Visi... As... Lowe... High...
Green 57 595
3D Objects Reslice Objects CAD Objects
Name Vi... Con... Tr... Transp... Qua...
Green 1 Medium Medium
STLs Polylines FEA Mesh Simulation Objects
Name Visible Con... Tria... Transp...
Contrast Volume Rendering Clipping View Angles
1
702
Custom
Save
Delete
fill holes: ON
keep largest: OFF
[14:42:49] Create 3D from mask
quality: medium
mask(s): Green
elapsed time: 00:01.016
Ready
Search the web and Windows
ENG
US
14:43
14-07-2016

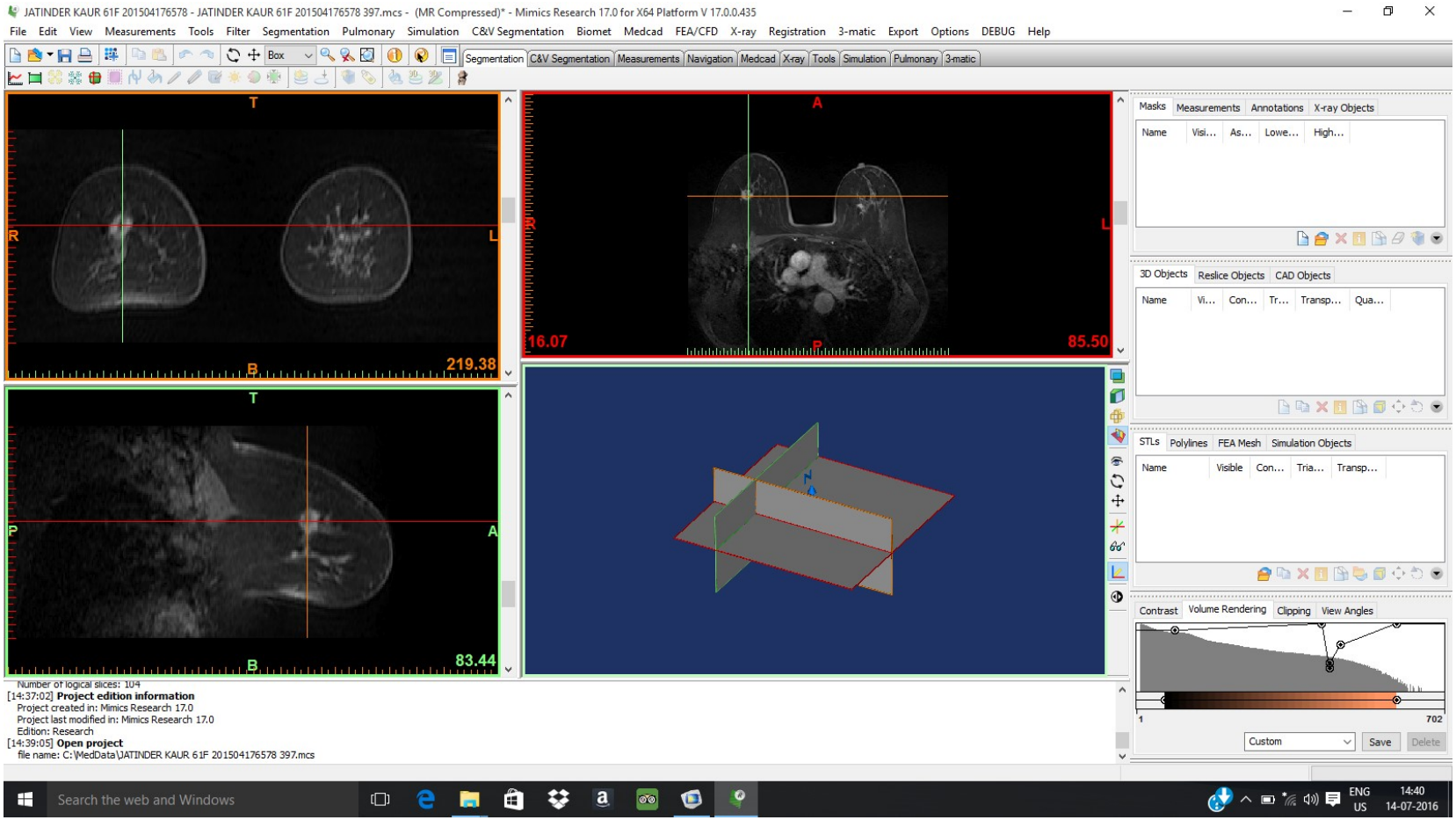
JATINDER KAUR 61F 201504176578 - JATINDER KAUR 61F 201504176578 397.mcs - (MR Compressed)* - Mimics Research 17.0 for X64 Platform V 17.0.0.435
File Edit View Measurements Tools Filter Segmentation Pulmonary Simulation C&V Segmentation Biomet Medcad FEA/CFD X-ray Registration 3-matic Export Options DEBUG Help
Segmentation C&V Segmentation Measurements Navigation Medcad X-ray Tools Simulation Pulmonary 3-matic
T
R
L
B
219.38
A
16.07
P
85.50
T
P
A
B
83.44
Masks Measurements Annotations X-ray Objects
Name Visi... As... Lowe... High...
3D Objects Reslice Objects CAD Objects
Name Vi... Con... Tr... Transp... Qua...
STLs Polylines FEA Mesh Simulation Objects
Name Visible Con... Tria... Transp...
Contrast Volume Rendering Clipping View Angles
1
702
Custom
Save
Delete
Number of logical slices: 104
[14:37:02] Project edition information
Project created in: Mimics Research 17.0
Project last modified in: Mimics Research 17.0
Edition: Research
[14:39:05] Open project
file name: C:\MedData\JATINDER KAUR 61F 201504176578 397.mcs
Search the web and Windows
ENG
US
14:40
14-07-2016

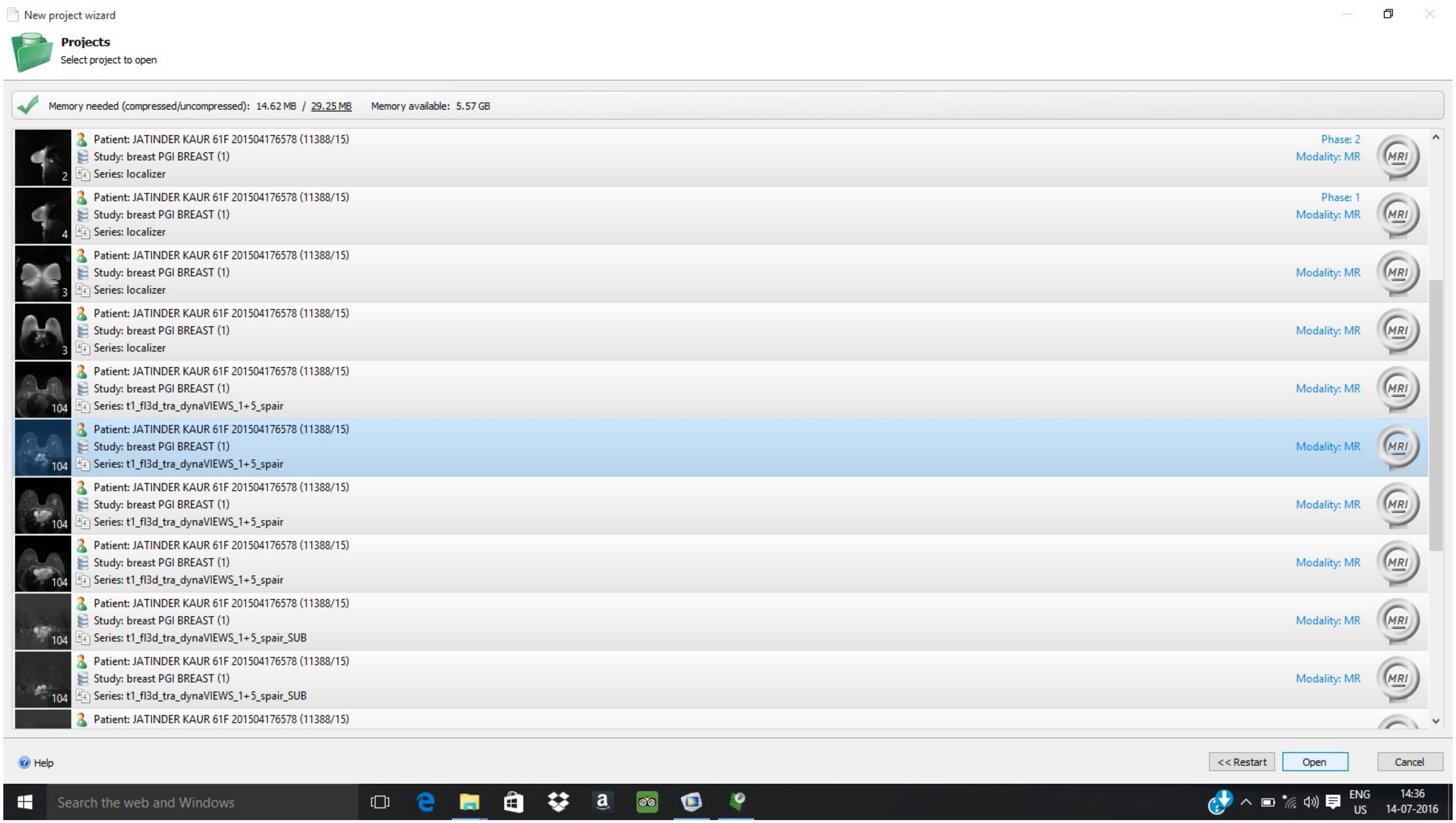
New project wizard
Projects
Select project to open
Memory needed (compressed/uncompressed): 14.62 MB / 29.25 MB
Memory available: 5.57 GB
Patient: JATINDER KAUR 61F 201504176578 (11388/15)
Study: breast PGI BREAST (1)
Series: localizer
Phase: 2
Modality: MR
Patient: JATINDER KAUR 61F 201504176578 (11388/15)
Study: breast PGI BREAST (1)
Series: localizer
Phase: 1
Modality: MR
Patient: JATINDER KAUR 61F 201504176578 (11388/15)
Study: breast PGI BREAST (1)
Series: localizer
Modality: MR
Patient: JATINDER KAUR 61F 201504176578 (11388/15)
Study: breast PGI BREAST (1)
Series: localizer
Modality: MR
Patient: JATINDER KAUR 61F 201504176578 (11388/15)
Study: breast PGI BREAST (1)
Series: t1_fl3d_tra_dynaVIEWS_1+5_spair
Modality: MR
Patient: JATINDER KAUR 61F 201504176578 (11388/15)
Study: breast PGI BREAST (1)
Series: t1_fl3d_tra_dynaVIEWS_1+5_spair
Modality: MR
Patient: JATINDER KAUR 61F 201504176578 (11388/15)
Study: breast PGI BREAST (1)
Series: t1_fl3d_tra_dynaVIEWS_1+5_spair
Modality: MR
Patient: JATINDER KAUR 61F 201504176578 (11388/15)
Study: breast PGI BREAST (1)
Series: t1_fl3d_tra_dynaVIEWS_1+5_spair
Modality: MR
Patient: JATINDER KAUR 61F 201504176578 (11388/15)
Study: breast PGI BREAST (1)
Series: t1_fl3d_tra_dynaVIEWS_1+5_spair_SUB
Modality: MR
Patient: JATINDER KAUR 61F 201504176578 (11388/15)
Study: breast PGI BREAST (1)
Series: t1_fl3d_tra_dynaVIEWS_1+5_spair_SUB
Modality: MR
Patient: JATINDER KAUR 61F 201504176578 (11388/15)
Help
<< Restart
Open
Cancel
Search the web and Windows
ENG
US
14:36
14-07-2016

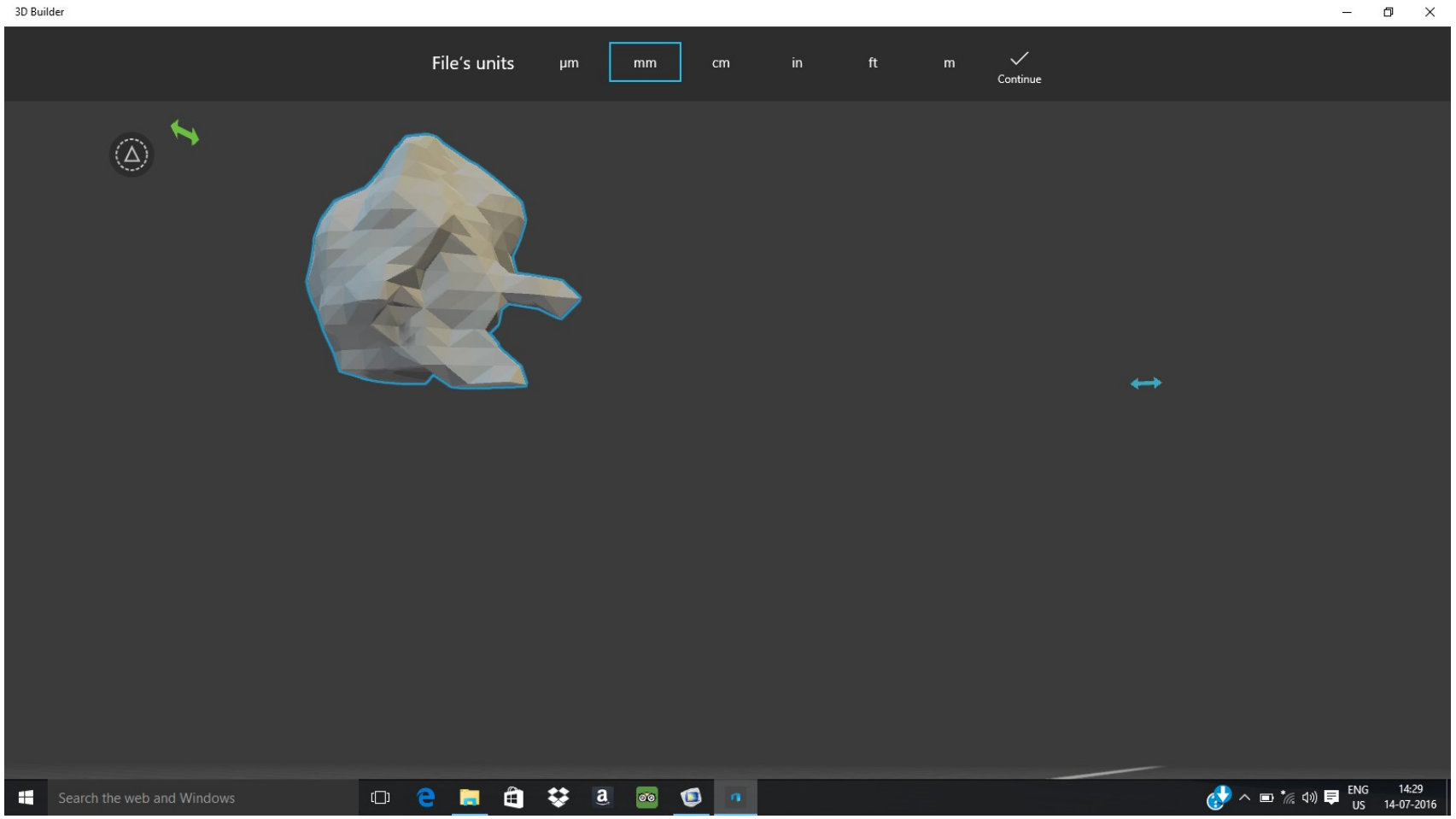
3D Builder
File's units
µm
mm
cm
in
ft
m
Continue
Search the web and Windows
ENG
US
14:29
14-07-2016

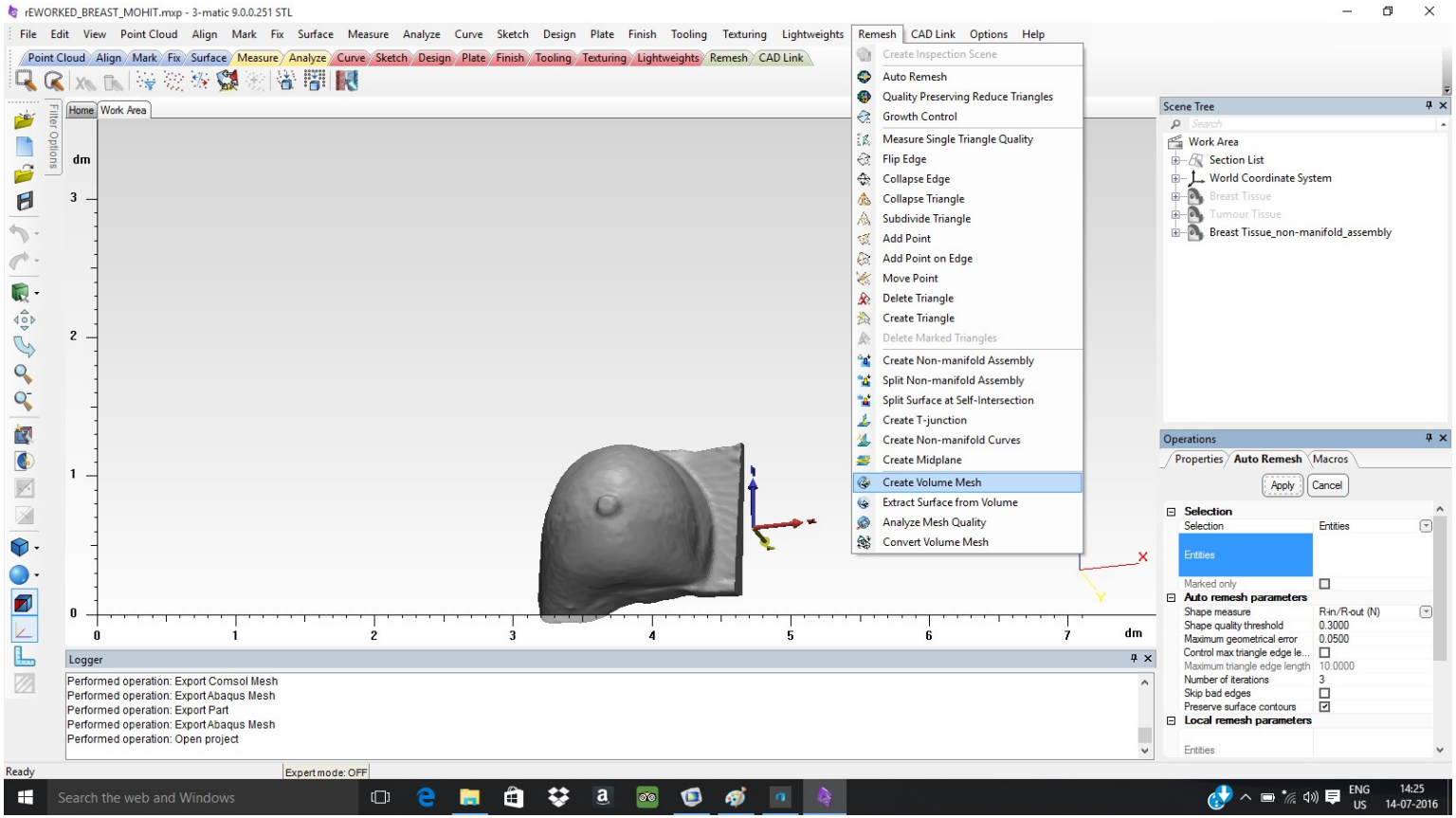
rEWORKED_BREAST_MOHIT.mxp - 3-matic 9.0.0.251 STL
File Edit View Point Cloud Align Mark Fix Surface Measure Analyze Curve Sketch Design Plate Finish Tooling Texturing Lightweights Remesh CAD Link Options Help
Create Inspection Scene
Auto Remesh
Quality Preserving Reduce Triangles
Growth Control
Measure Single Triangle Quality
Flip Edge
Collapse Edge
Collapse Triangle
Subdivide Triangle
Add Point
Add Point on Edge
Move Point
Delete Triangle
Create Triangle
Delete Marked Triangles
Create Non-manifold Assembly
Split Non-manifold Assembly
Split Surface at Self-Intersection
Create T-junction
Create Non-manifold Curves
Create Midplane
Create Volume Mesh
Extract Surface from Volume
Analyze Mesh Quality
Convert Volume Mesh
Scene Tree
Work Area
Section List
World Coordinate System
Breast Tissue
Tumour Tissue
Breast Tissue_non-manifold_assembly
Operations
Properties Auto Remesh Macros
Apply Cancel
Selection
Auto remesh parameters
Local remesh parameters
Logger
Performed operation: Export Comsol Mesh
Performed operation: Export Abaqus Mesh
Performed operation: Export Part
Performed operation: Export Abaqus Mesh
Performed operation: Open project
Ready
Expert mode: OFF
Search the web and Windows
ENG US
14:25
14-07-2016

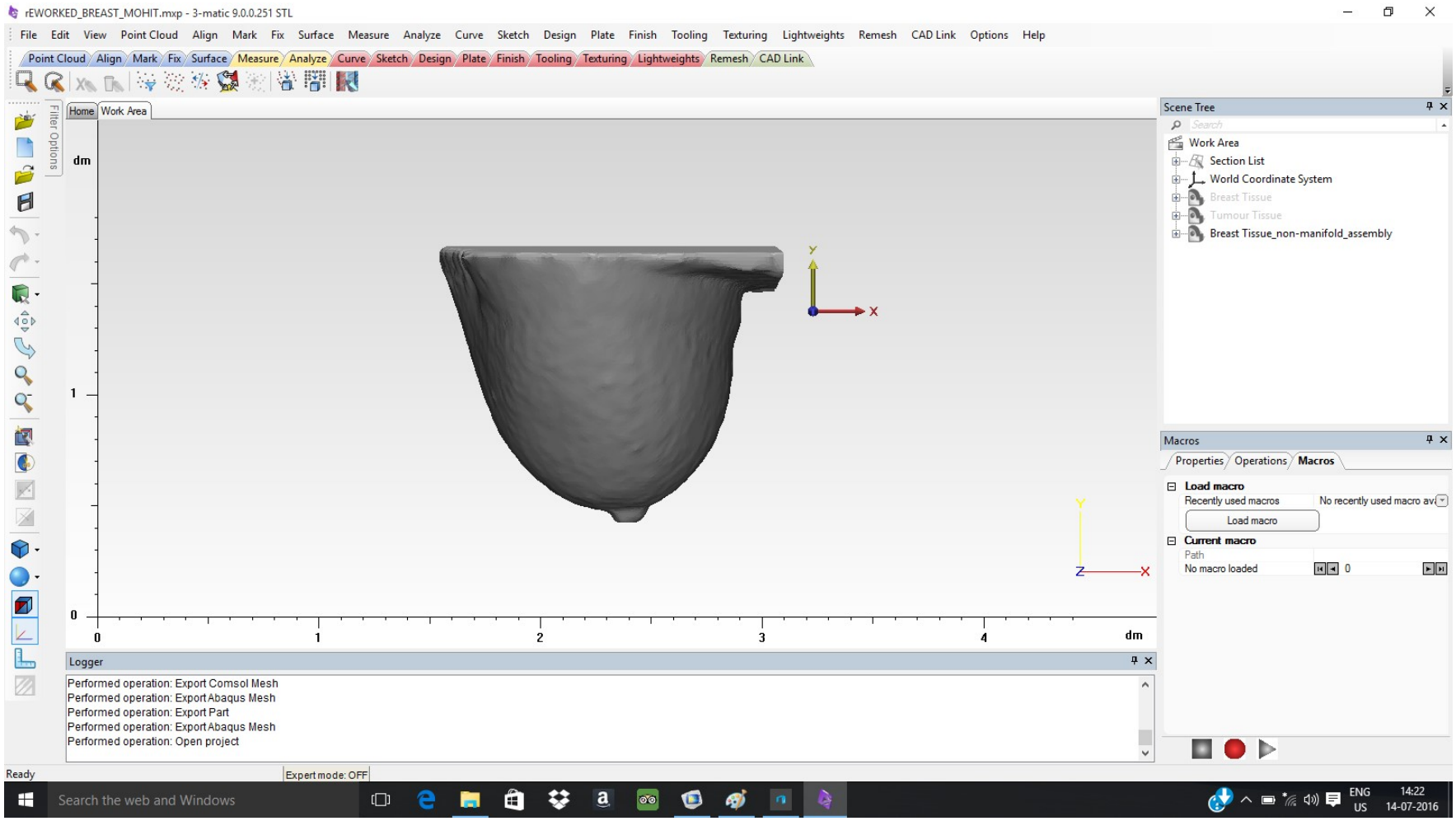
rEWORKED_BREAST_MOHIT.mxp - 3-matic 9.0.0.251 STL
File Edit View Point Cloud Align Mark Fix Surface Measure Analyze Curve Sketch Design Plate Finish Tooling Texturing Lightweights Remesh CAD Link Options Help
Point Cloud Align Mark Fix Surface Measure Analyze Curve Sketch Design Plate Finish Tooling Texturing Lightweights Remesh CAD Link
Home Work Area
Filter Options
dm
1
0
0 1 2 3 4 dm
Scene Tree
Search
Work Area
Section List
World Coordinate System
Breast Tissue
Tumour Tissue
Breast Tissue_non-manifold_assembly
Macros
Properties Operations Macros
Load macro
Recently used macros
No recently used macro av
Load macro
Current macro
Path
No macro loaded
0
Logger
Performed operation: Export Comsol Mesh
Performed operation: Export Abaqus Mesh
Performed operation: Export Part
Performed operation: Export Abaqus Mesh
Performed operation: Open project
Ready
Expert mode: OFF
Search the web and Windows
ENG
US
14:22
14-07-2016

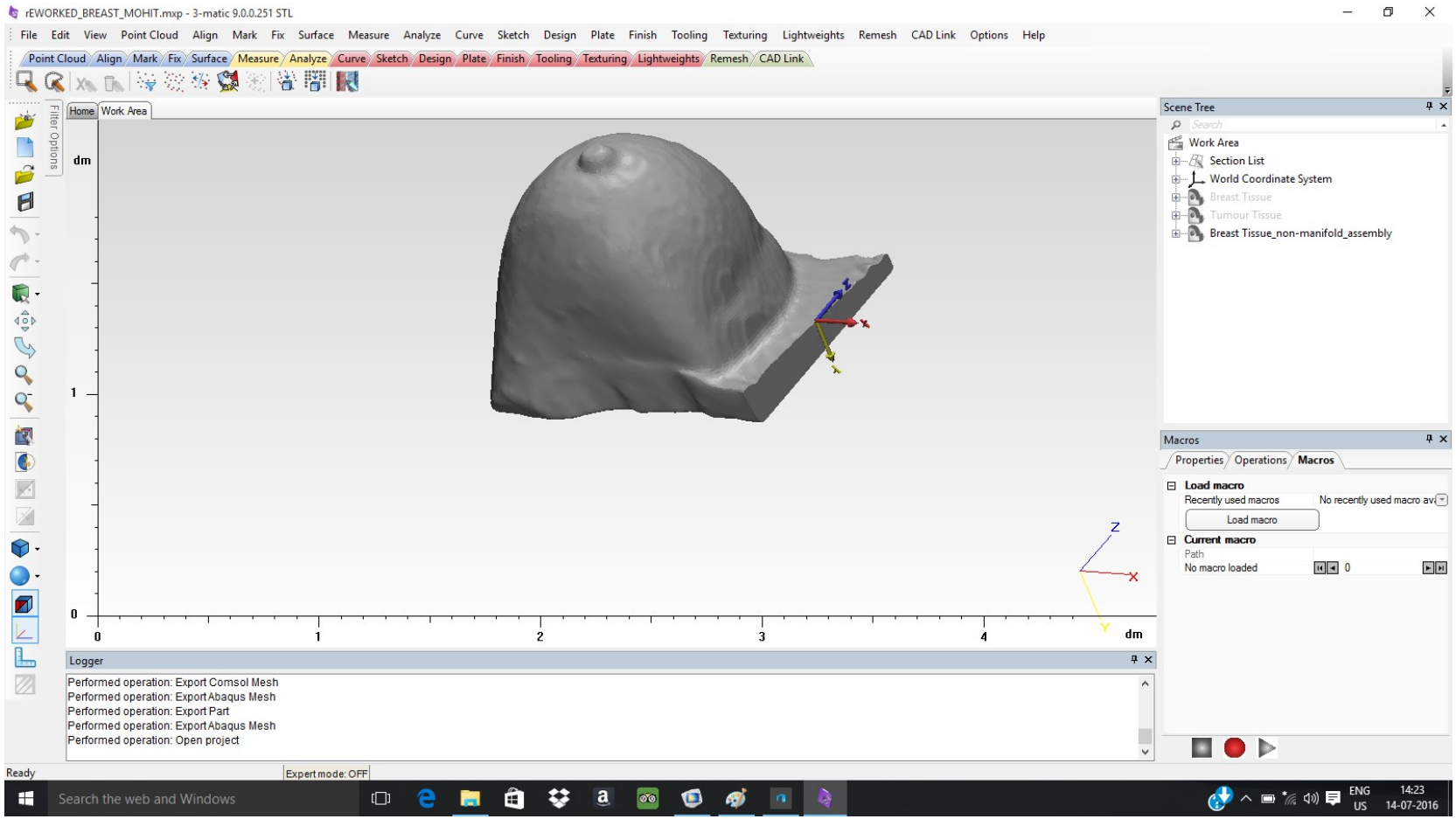
rEWORKED_BREAST_MOHIT.mxp - 3-matic 9.0.0.251 STL
File Edit View Point Cloud Align Mark Fix Surface Measure Analyze Curve Sketch Design Plate Finish Tooling Texturing Lightweights Remesh CAD Link Options Help
Point Cloud Align Mark Fix Surface Measure Analyze Curve Sketch Design Plate Finish Tooling Texturing Lightweights Remesh CAD Link
Home Work Area
Filter Options
dm
1
0
0 1 2 3 4 dm
Z
X
Y
Scene Tree
Search
Work Area
Section List
World Coordinate System
Breast Tissue
Tumour Tissue
Breast Tissue_non-manifold_assembly
Macros
Properties Operations Macros
Load macro
Recently used macros
No recently used macro av
Load macro
Current macro
Path
No macro loaded
0
Logger
Performed operation: Export Comsol Mesh
Performed operation: Export Abaqus Mesh
Performed operation: Export Part
Performed operation: Export Abaqus Mesh
Performed operation: Open project
Ready
Expert mode: OFF
Search the web and Windows
ENG
US
14:23
14-07-2016

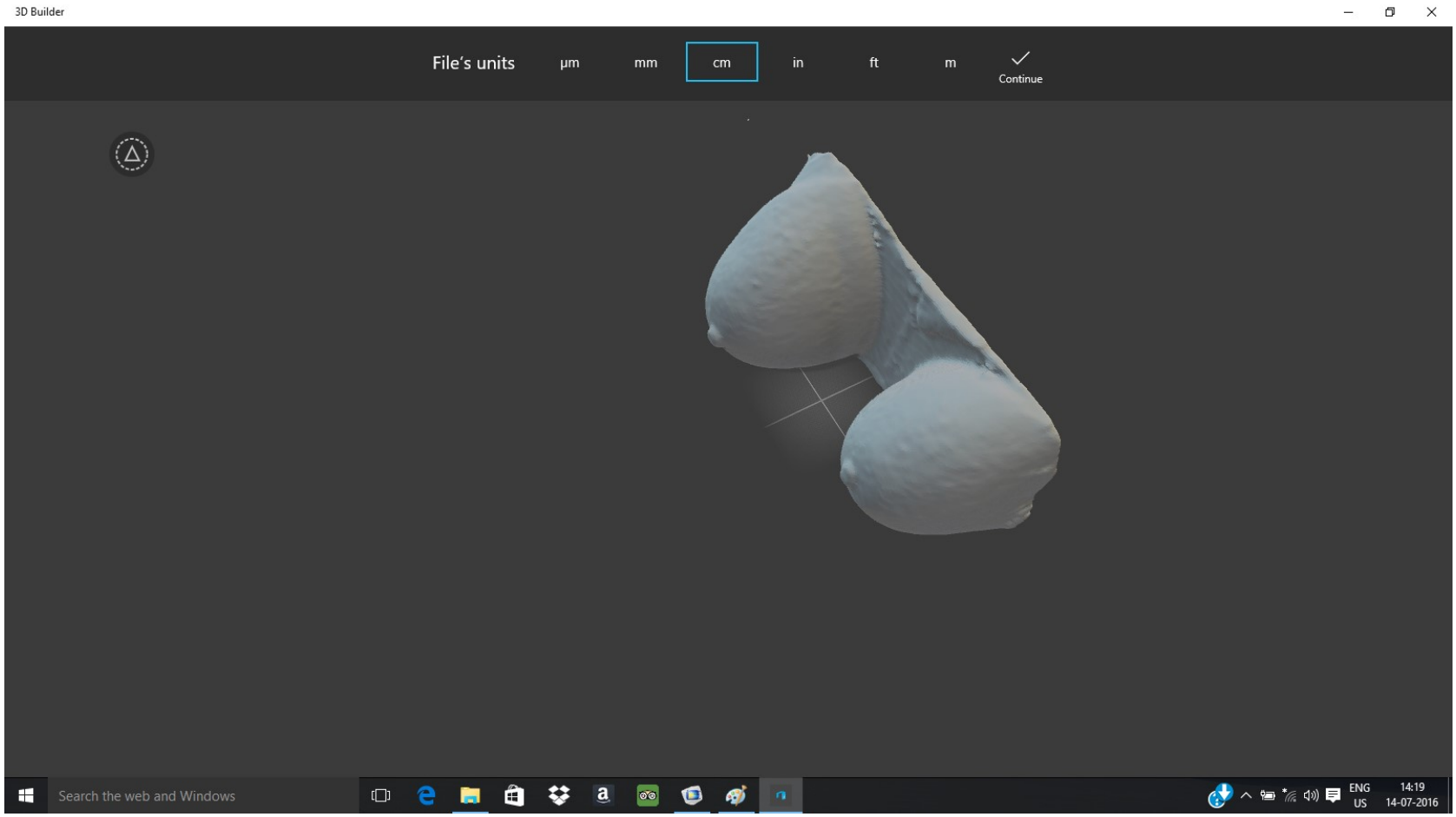
3D Builder
File's units
µm
mm
cm
in
ft
m
Continue
Search the web and Windows
ENG
US
14:19
14-07-2016

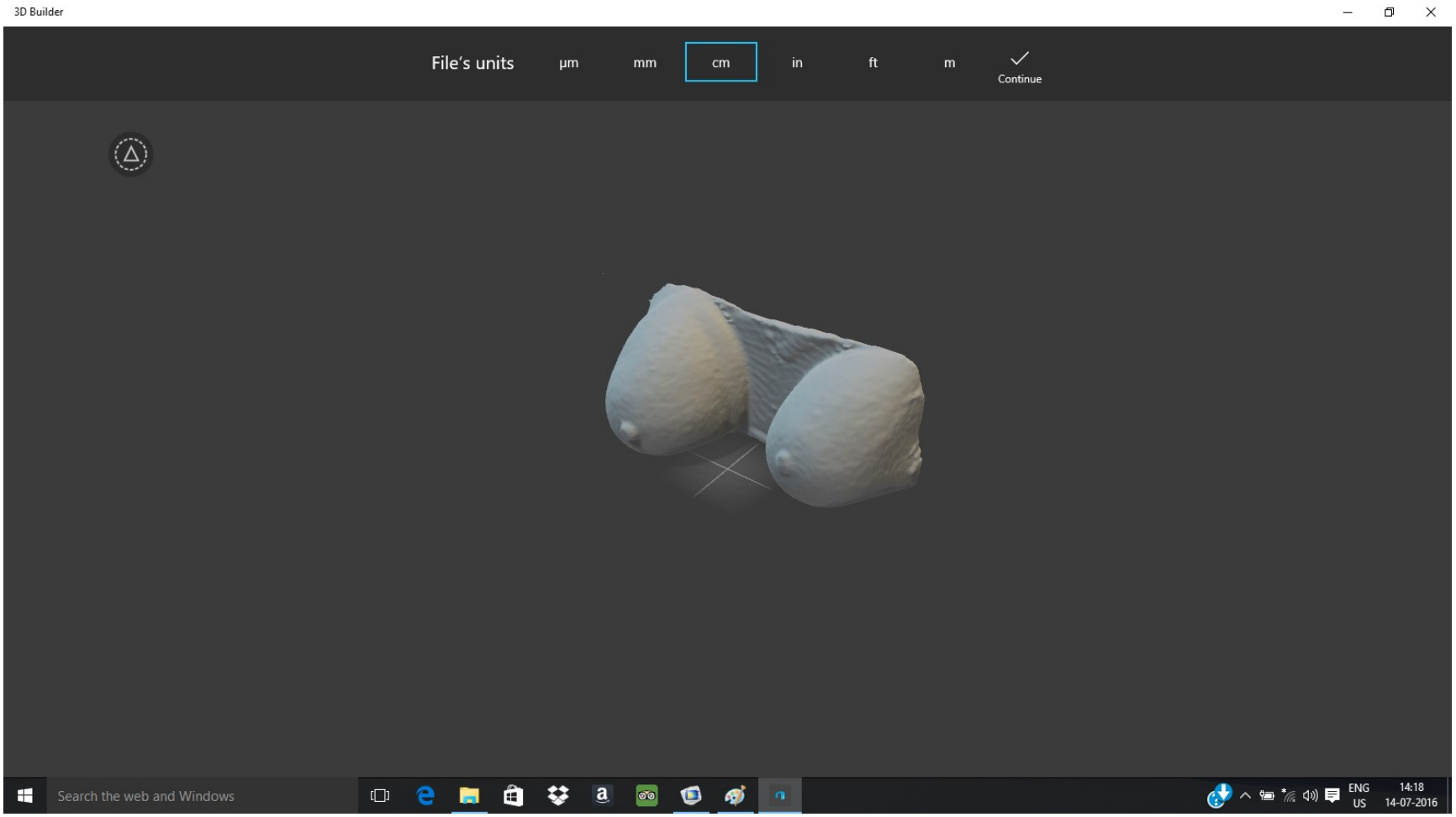
3D Builder
File's units
µm
mm
cm
in
ft
m
Continue
Search the web and Windows
ENG
US
14:18
14-07-2016

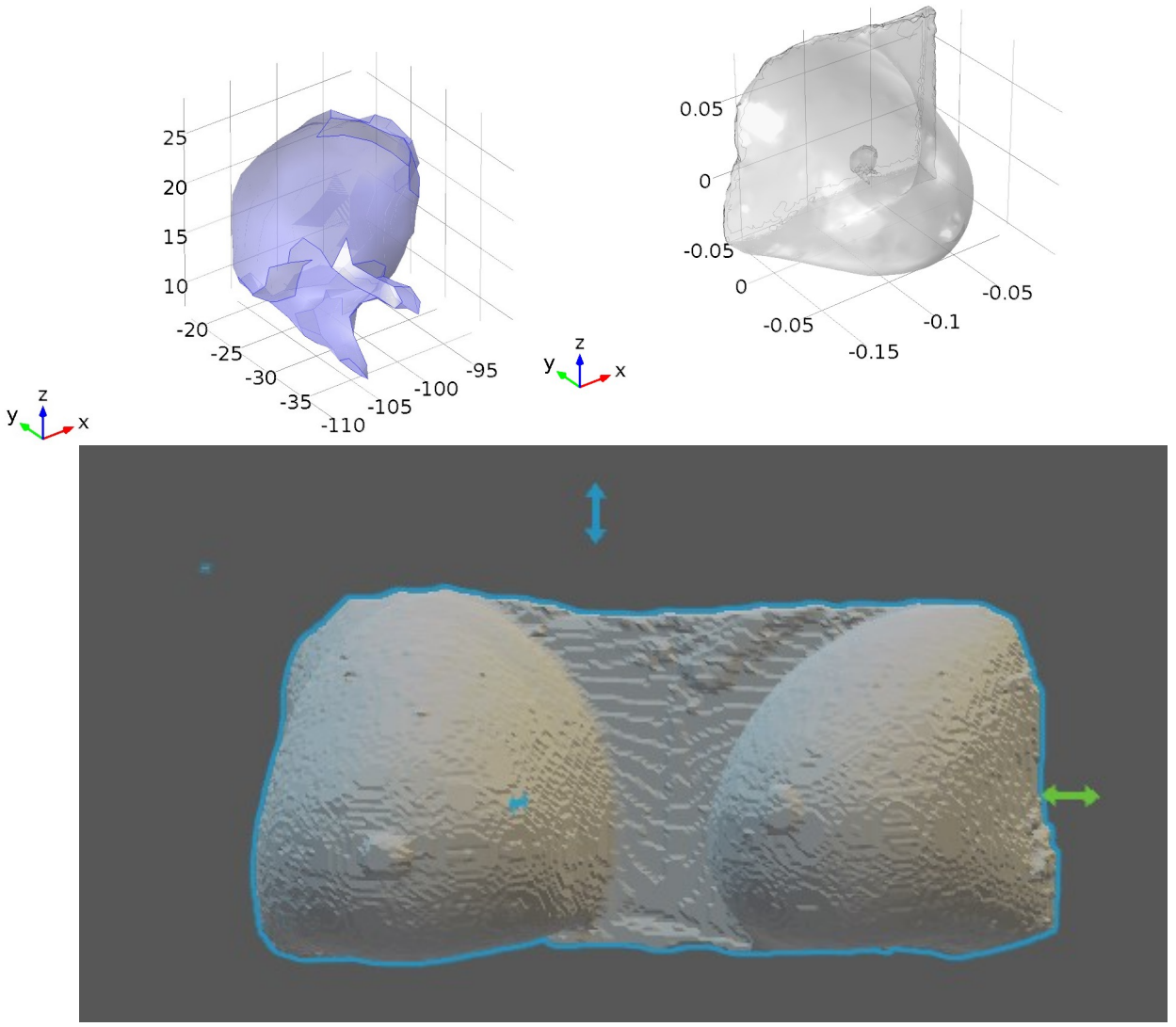
25
20
15
10
-20
-25
-30
-35
-110
-105
-100
-95
z
y
x
0.05
0
-0.05
0
-0.05
-0.15
-0.1
-0.05
z
y
x